Characterisation and modulation of the gelatinase system of human Bruch's membrane

Lee, Yunhee

Awarding institution:
King's College London

CHARACTERISATION AND MODULATION

OF THE GELATINASE SYSTEM OF HUMAN BRUCH'S MEMBRANE

YUNHEE LEE
MSc

A Thesis Submitted for the Degree of Doctor of Philosophy
at King's College London, University of London

June 2011

ACKNOWLEDGMENTS

This project was generously funded by Fight for Sight. I am deeply grateful to them.

I would like to thank my supervisor, Professor John Marshall, for his help and all the opportunities he has provided. He has given me fantastic memories and experiences I could never have dreamed of.

This thesis would not have been possible without the guidance and help of brilliant biochemist, Dr. Ali Hussain. I owe my deepest gratitude to him and will never forget his inspiring guidance and advice for research.

I am heartily thankful to Dr. Jinjun Zhang, my colleague and good friend, for her kindness and sharing good moments with me. I want to thank Ms. Ann Patmore for her support and help.

I am greatly indebted to my parents, Dong Sung Lee and In Sug Oh, for endless love and prayers to overcome all the obstacles throughout my life and this study. There are no enough words to express my gratitude for their unconditional support. I am deeply grateful to my younger brother, Myeong Jin Lee, for valuable comments on research and encouragement for the completion of this thesis.

Last but not the least, I thank the one above all of us, my Lord, for answering my prayers for giving me strength and all blessings.

DEDICATION…

…All my work is dedicated to my family and Jesus Christ.

“What you decide on will be done, and light will shine on your ways. (Job 22:28)”

ABSTRACT

Ageing of Bruch's membrane is associated with structural and functional deterioration. Accumulation of normal and abnormal collagen in ageing Bruch's has led to the hypothesis of diminished matrix degradation mediated normally by a family of protease enzymes called the matrix metalloproteinases (MMPs). Underlying mechanisms leading to diminished MMP activity in ageing Bruch's remain unknown but functional changes of diminished transport are well documented. Ageing remains the biggest risk factor in AMD with nearly 30% of all individuals reaching the age of 85 years showing some loss of central vision.

In the present thesis, the gelatinase system (constituting MMPs 2&9) has been examined resulting in the identification and characterisation of three additional high molecular weight species termed HMW 1&2 and a large macromolecular weight MMP complex (LMMC). HMW1&2 were shown to be covalently bonded homo- and/or hetero- polymers of pro-MMPs 2&9. HMW species in effect sequester pro-MMPs 2&9 reducing the pool available for activation and the age-related increase in HMW species is expected to augment this reduction.

In Bruch's membrane from donors with AMD, levels of HMW1&2 were considerably elevated ($p<0.05$) with a concomitant reduction in the amount of active MMPs 2&9 ($p<0.05$). The reduction in activated MMP species therefore underlies the reduced degradative capacity of Bruch's in these patients.

Elution studies demonstrated the existence of a free-bound equilibrium for the gelatinases with the bound forms being retained by hydrophobic, ionic or metal mediated interactions. Since divalent metal ions are deposited in Bruch's of AMD

donors, metal chelation was assessed as a possible means of inducing MMP release. Metal chelation with EGTA resulted in the release of active forms of MMP2 and significantly improved the fluid transport properties of the membrane ($p<0.005$). This finding would suggest that zinc supplementation in AMD is an inappropriate form of therapy.

TABLE OF CONTENTS

LIST OF FIGURES

LIST OF TABLES

LIST OF ABBREVIATIONS

A2-E	N-retinylidene-N-retinylethanolamine
AGE	advanced glycation end products
AMD	age related macular degeneration
APMA	aminophenyl mercuric acetate
Aβ	amyloid beta protein
BM	Bruch's membrane
CA	cytosine-adenine
CC	Choriocapillaris
CETP	cholesterylester transfer protein
CFB	complement factor B
CFH	complement factor H
CML	Carboxymethyllysine
Cp	Ceruloplasmin
CRBP	cellular retinol binding protein
CS	chondroitin sulphate
DMT	divalent metal transporter
DS	dermatan sulphate
DTT	Dithiothreitol
ECM	extracellular matrix
EFEMP1	epidermal fibulin-like extracellular matrix protein
EGF	epithelial growth factor
EGTA	ethylene glycol tetraacetic acid
EL	elastin layer
F	Ferritin
FCS	foetal calf serum
FP	Ferriportin

FRD	fibronectin repeat domain
GAG	Glycosaminoglycan
HC	hydraulic conductivity
Heph	Hephaestin
HMW	high molecular weight
HPLC	high performance liquid chromatography
HS	heparan sulphate
Htra	heat shock serine protease
IAA	Iodoacetate
ICL	inner collagenous layer
IL	Interleukin
IPM	interphotoreceptor matrix
IRBP	interphotoreceptor retinol binding protein
LIF	leukemia inhibitory factor
LIPC	hepatic lipase
LMMC	large macromolecular weight MMP complex
LPS	Lipopolysaccharide
LSC	long spaced collagen
M	muller cell
MMP	matrix metalloproteinases
MtF	mitochondrial ferritin
MT-MMP	membrane-type MMP
MW	molecular weight standards
OCL	outer collagenous layer
OG	O-glycosylation
PAI	plasminogen activator inhibitor
PDGF	platelet derived growth factor
PG	Proteoglycan
PMA	phorbol esters
RAGE	advanced glycation end products receptor

RB	resistance barrier
RBP	retinol binding protein
RIO	rod inner segment
ROS	rod outer segment
ROS	reactive oxygen species
RPE	retinal pigment epithelium
SDS	sodium dodecyl sulphate
SFD	Sorsby's fundus dystrophy
Tf	Transferrin
TGF	transforming growth factor
TIMP	tissue inhibitor of MMP
TNF	tumor necrosis factor
TTR	Transthyretin
uPA	urokinase plasminogen activator
VEGF	vascular endothelial growth factor
WBC	white blood cell

CHAPTER 1

INTRODUCTION

1 INTRODUCTION

Bruch's membrane is an acellular pentalaminated extracellular matrix (ECM) located between the retinal pigment epithelium (RPE) and the fenestrated capillaries of the choroidal circulation. It therefore mediates the passive bi-directional transport processes for the exchange of nutrients and waste products between the RPE/photoreceptor complex and the choroidal circulation. The high metabolic activity of photoreceptor cells requires similarly high metabolic exchange rates across Bruch's and the RPE. The structural and functional integrity of Bruch's membrane is maintained by tightly coupled processes of continuous synthesis and degradation, the latter mediated by a family of zinc-containing, calcium dependent proteolytic enzymes called the matrix metalloproteinases (MMPs). Despite the presence of this rejuvenation cycle, ageing of Bruch's results in structural and functional deterioration with considerably compromised transport capacities across the membrane. In the very elderly, signs of diminished vitamin A transport are often detected clinically as diminished scotopic thresholds. More severe reductions in fluid and macromolecular traffic across Bruch's have been observed in the advanced ageing associated with age related macular degeneration (AMD).

1.1 Transport systems in the outer retina

The neural retina maintains one of the highest rates of oxidative metabolism of any tissue in the body and as such requires a rapid and uninterrupted supply of blood-borne metabolic substrates (Ahmed *et al.*, 1993; Bui *et al.*, 2003; Cohen *et al.*,

1960; Cringle *et al.*, 2002; Warburg, 1927; Winkler, 1983). The transport pathways for both nutritional supply and waste removal are therefore of paramount importance in maintaining the structural and functional integrity of the neural retina. Rate-limiting sites for transport are provided across two anatomically distinct blood retinal barriers formed between the endothelium cells of retinal capillaries in the inner retina and by RPE cells in the outer retina (Cunha-Vaz *et al.*, 1966; Foulds, 1990; Marshall, 1998).

In the inner retinal capillaries, blood-borne metabolites are selectively transported across the endothelium cells and then traverse a basement membrane prior to uptake by retinal neurones. In the outer retina, blood-borne constituents are readily released from the fenestrated choroidal capillaries onto Bruch's and are sieved by the membrane according to size prior to presentation at the basal surface of the RPE cell for eventual transport to photoreceptor cells.

From measurements of blood flow and oxygen extraction, it has been shown that in those regions of the fundus with a dual supply, the choroidal contribution accounts for over 90% of the metabolic requirements of photoreceptor cells (Bill, 1970; Tornquist *et al.*, 1979; Wilson *et al.*, 1973). In the foveolar region of the human fundus, the absence of inner retinal capillaries means that the choroidal circulation must provide metabolic support to the whole retina. The importance of the choroidal circulation in the macular area is emphasised by the nearly 8-fold higher blood flow in this region compared with the peripheral fundus (Alm *et al.*, 1973).

1.1.1 Inward transport pathway: Nutritional maintenance

The numerous endothelium fenestrations of the choriocapillary network allow easy passage out of most blood constituents including large carrier proteins and lipoprotein species for presentation to the outer aspects of Bruch's membrane (Burns *et al.*, 1980; Cunha-Vaz *et al.*, 1966; Hazlett *et al.*, 1974; Pino *et al.*, 1981). The spectrum of substances presented to Bruch's membrane for transport will therefore range from simple sugars and amino acids to carrier bound species such as those for vitamin A, fatty acids, heavy metals and finally the supramolecular complexes associated with the plasma lipoproteins.

If the diameter of the traversing molecules (such as glucose, amino acids) is considerably small in comparison to the inter-fibre spaces within Bruch's membrane, then their diffusion fluxes would only be governed by their free diffusion coefficients (D):

$$J = -D \left(d¢/dx\right)$$

where J is the experimental flux ($mol/m^2/s$), ¢ is the concentration of traversing molecule (mol/m^3), and x is the thickness of Bruch's membrane. Thus the flux would be directly proportional to the concentration gradient across the membrane.

For larger molecules, such as carrier proteins, the degree of resistance encountered during transit will be governed by their size, charge distribution, hydrophobic/hydrophilic nature, and the likelihood of collisions with structural parameters of the conducting pathway. Transport schemes across Bruch's membrane for small and larger molecules are given in Figure 1.1.

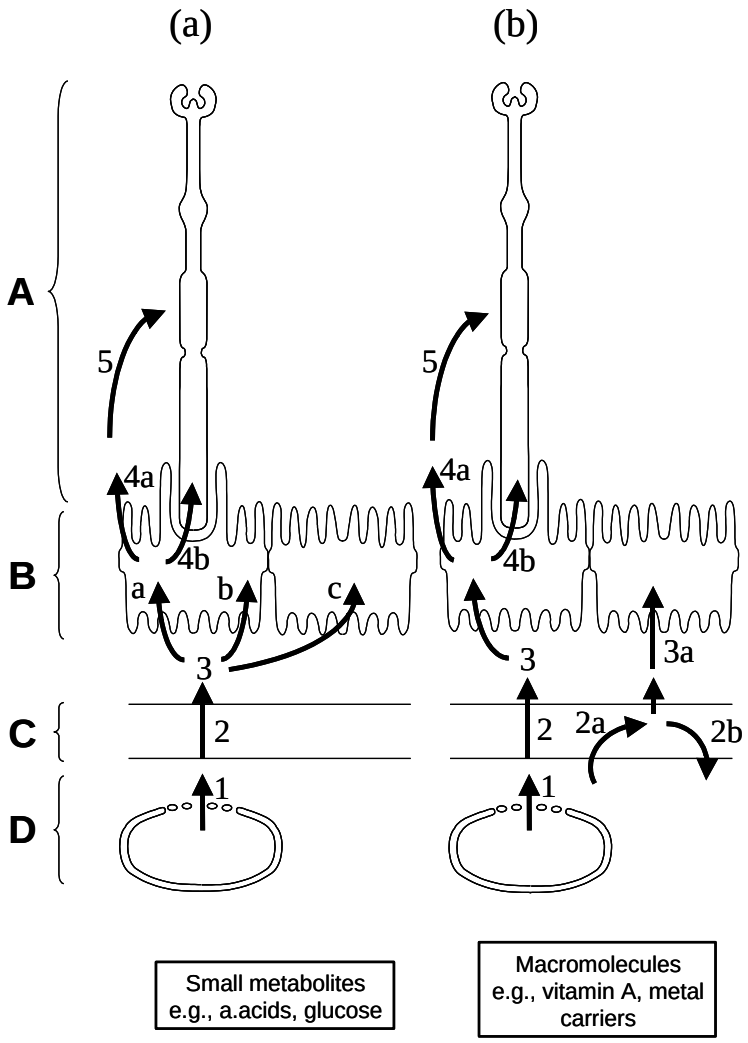

Figure 1.1 Transport pathways for delivery of blood-borne metabolites to photoreceptor cells.

[a] Small metabolites. After release from the choriocapillaris [1], metabolites diffuse passively across Bruch's membrane [2] to be presented at the basal convoluted surface of the RPE [3]. The basal membrane is traversed by free diffusion or carrier mediated translocation, the latter involving active or passive transporters. Having negotiated the cytoplasmic space, metabolites are released into the interphotoreceptor matrix (IPM) by undefined mechanisms at the apical surface [4a,b]. Following diffusion down concentration gradients across the IPM, metabolites are finally taken up by the inner segment regions of the photoreceptor layer [5]. Rapid uptake into outer segments may be possible at sites of microvillus ensheathment [4b]. A, photoreceptor layer; B, RPE layer; C, Bruch's membrane; D, choriocapillaris.

[b] Macromolecules. Large molecules including ligand-carrier complexes are released by the fenestrated endothelium of the choriocapillaris [1]. Depending on their size, these species may either diffuse across Bruch's [2] or partially penetrate the membrane to release their payloads [2a]. The ligand-free complex can then return to the choroidal circulation [2b]. Interaction with specific receptors at the basal surface of the RPE leads to internalisation of the ligand [3]. Ligands may then cross the cytoplasmic space either in free form or bound to specific carriers, but again, the release mechanism at the apical surface is poorly understood. Carriers may again facilitate diffusion across the IPM for final delivery to the photoreceptor cell [5]. (After Hussain & Marshall, 2004).

For smaller molecules, their passage through Bruch's is sustained by passive transport down concentration gradients with rates being subject to Fick's laws of diffusion (Pappenheimer, 1953; Pappenheimer *et al.*, 1951). Larger proteins such as the broad spectrum albumin, ceruloplasmin, transferrin, retinol binding protein and various species of ferritin can cross Bruch's membrane. Interestingly, immunohistochemical techniques have shown that some proteins were capable of entering Bruch's but were unable to traverse it (Pino *et al.*, 1983). The size of protein or proteo-lipid complex that can enter Bruch's will be determined by the inter-fibrillar spacing within Bruch's membrane.

Several studies have now shown that this spacing is not uniform across the thickness of Bruch's membrane. Both excimer ablation studies and morphometric analyses of sub-layers have shown tight packing of collagenous fibres in the so-called 'resistance barrier' in the inner collagenous zone in juxtaposition to the elastin layer of the membrane (Hussain *et al.*, 2004; Marshall, 1998; Starita *et al.*, 1997). This region, with an anatomically determined spacing between fibres of about 10-14nm will therefore determine the size exclusivity of macromolecules that can be transported. Outside this region of the resistance barrier, the spacing is much larger allowing the entry of much larger molecules but blocking their translocation across Bruch's membrane. A schematic of the variation in fibrillar spacing across the thickness of Bruch's membrane is depicted in Figure 1.2.

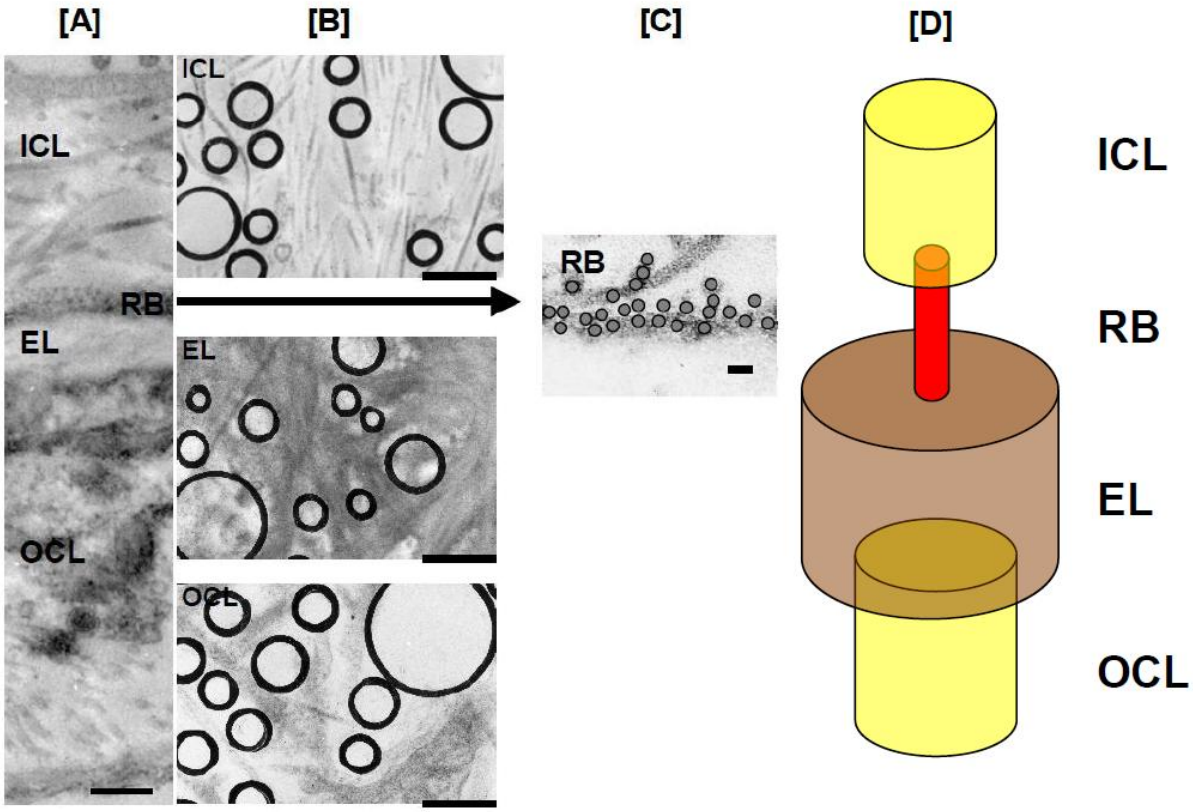

Figure 1.2 Collagenous fibre spacing within Bruch's membrane: Topography of the conducting pathway.

Panel [A]: Transverse electron micrograph of Bruch's membrane from a donor aged 38 years. ICL, inner collagenous layer; EL, elastin layer; OCL, outer collagenous layer; RB, resistance barrier, site assigned on the basis of excimer laser ablation experiments (see Starita et al., 1997). Bar = 0.25μm.

Panel [B]: Tangential electron micrographs through the inner collagenous, elastin and outer collagenous layers of Bruch's membrane showing the construction of potential pores for fluid transport. The presence of debris was not taken into account during assignment of pores. Bar = 0.5μm.

Panel [C]: High magnification micrograph of the resistance region allowing visualisation of the tight 'weave' of 10nm filaments that constitute the barrier. These filaments have been highlighted in the micrograph. The average distance between the fibres taken from many micrographs was determined to be about 14nm, suggesting a pore radii of 7nm for passage of molecules. Bar = 30 nm.

Panel [D]: Data from the morphometric analysis together with experiments to localise the resistance barrier (Starita et al., 1997) allowed the construction of the pore model to describe the transport pathways through human Bruch's membrane. (Modified from Hussain & Marshall, 2004)

The topography of the conducting channels shows that species larger than the confines of the 'resistance' barrier can enter the much wider crevices in the outer collagenous layer but cannot traverse the membrane. This aspect may be very important in allowing large ligand-bound carriers to enter Bruch's and the subsequent interaction, with perhaps localised charged regions, may lead to disassociation of their payloads which then continue through the remainder of the membrane. The possible interaction of carrier molecules with the hydrophobic and hydrophilic domains within the microenvironment of Bruch's membrane has received little attention and yet may be a key mechanism in the transport of lipids.

The likely effect of the constrained topography of the conducting channel on diffusion will be dependent on the size of the traversing molecules. Small molecules such as amino acids and glucose possess a hydrated radii that is infinitesimal compared to the radii at the pore constriction and such species will therefore be oblivious to the presence of the barrier. Since the microviscosity of fluid within a barrier of similar dimensions has been shown to be the same as in bulk solution, the rate of diffusion of small molecules will be dictated simply by the trans-membrane concentration gradients (Pappenheimer, 1953; Pappenheimer *et al.*, 1951). Larger molecules will interact with the barrier boundaries and in addition to steric hindrance may also undergo hydrophilic and hydrophobic interactions. Excellent studies have delineated the effect of steric hindrance on the diffusion of biological molecules through artificial membranes (Curry, 1984). It has been shown that flux rates were reduced to about 60% of those expected from free diffusion when the solute radius was about 10% of pore radius (Beck *et al.*, 1972; Renkin, 1954; Wendt *et al.*, 1979).

Having traversed Bruch's, blood-borne metabolites are then presented at the basolateral surface of the RPE. Adjacent RPE cells are coupled by extensive junctional complexes called 'zonulae occludentes' and these constitute the anatomical site of the outer blood-retinal barrier (Shakib *et al.*, 1972; Taniquchi, 1976). All metabolites must therefore gain access to the interior of the RPE cell for further translocation. Small molecules (including the dissolved gases oxygen and carbon dioxide) can diffuse rapidly across the basal membrane of the RPE and move down their concentration gradients. Larger species require the assistance of membrane carriers and these fall into two categories. Passive carriers bind the ligand on the outer surface and then diffuse across the membrane to release their load down a concentration gradient. Active transporters often utilise the inward sodium gradient and can thereby actively transport ligands against their concentration gradients. Detailed characteristics of carriers have been presented for glucose, retinol, taurine and glutamate (Heller *et al.*, 1976; Kundaiker *et al.*, 1996; Miyamoto *et al.*, 1994; To *et al.*, 1998). Large transport molecules such as the retinol-retinal binding protein-transthyretin complex and lipoproteins interact with specific receptors on the RPE to unload their ligands (Bavik *et al.*, 1992; Hayes *et al.*, 1989).

The basolateral aspect of the RPE cell rests in intimate contact with Bruch's membrane and thereby minimises the diffusional distance allowing rapid movement of released metabolites. More importantly, the convolutions in the membrane greatly increase the surface area over which exchange can occur.

Most metabolites will move across the cytoplasmic space of the RPE down their concentration gradients. Some potentially toxic substances such as the

retinoids are transported across bound to specific carriers such as the cellular retinol binding protein (CRBP). Little is known of the release processes at the apical surface of the RPE cell but it is assumed that metabolites leave by passive diffusion.

Metabolites released into the IPM are taken up by photoreceptors by a combination of active and passive processes. Two routes are possible for delivery to photoreceptor cells. Firstly, released metabolites may either diffuse freely or diffuse attached to carrier proteins for uptake by the inner segment compartment. Secondly, the intimate relationship between the RPE cytoplasmic extensions (microvilli) and the distal part of the outer segment may promote rapid uptake by minimising the diffusional distance.

The mechanism for delivery of lipids is poorly understood. Fatty acids could be transported in the IPM bound to albumin. But the possible synthesis and release of lipoprotein-type molecules as delivery vehicles by the RPE needs investigation. A recent study has detected apo B and apo B mRNA in human RPE but its role in the inner loop recycling of lipids and/or in the deposition of lipids beneath the RPE requires clarification (Malek *et al.*, 2003).

1.1.1.1 Size selectivity of transported molecules

The spacing between the collagenous fibres in the resistance barrier provides a rough estimation of 10-14nm as the maximum diameter of traversing macromolecules. A more quantitative study has been undertaken by investigating the diffusional flux of FITC-labelled dextran molecules in the molecular weight range 4.2-500 kDa (Hussain *et al.*, 2010). As the molecular weight of the dextran species

increases, its diffusional constant D decreases. Thus a plot of diffusional flux versus molecular weight of species would be expected to show a decreasing relationship whether or not there was any interaction of the diffusing species with the structural elements of the matrix of Bruch's membrane. Normalisation of these experimental fluxes with respect to their free diffusion coefficients (D/Do) would be expected to produce horizontal lines on the D/Do vs. MW plots (Michel *et al.*, 1999; Pappenheimer *et al.*, 1951; Renkin *et al.*, 1988). However, if the dextran molecules were large enough to interact with the fibre-matrix of the membrane, then downward deviations would be expected on the plots.

As shown in Figure 1.3, the D/Do plots for transport across Bruch's membrane deviated downwards, providing evidence for dextran-membrane interactions. The relationship was biphasic, with a rapid decrease between 4.4 and 77 kDa followed by a much shallower change between 77 and 500 kDa dextrans. The latter region may well represent 'reptation' behaviour whereby a much larger linear molecule can get through a smaller opening by 'snaking' through it (Pluen *et al.*, 1999). Thus the larger dextran molecules (because of the nature of their long flexible chains) could traverse membranes by the process of 'reptation' whereas similarly sized globular proteins would be restricted. The 'reptation' behaviour is displayed by mRNA molecules as they 'snake' their way through the small openings (pores) in the nuclear membrane.

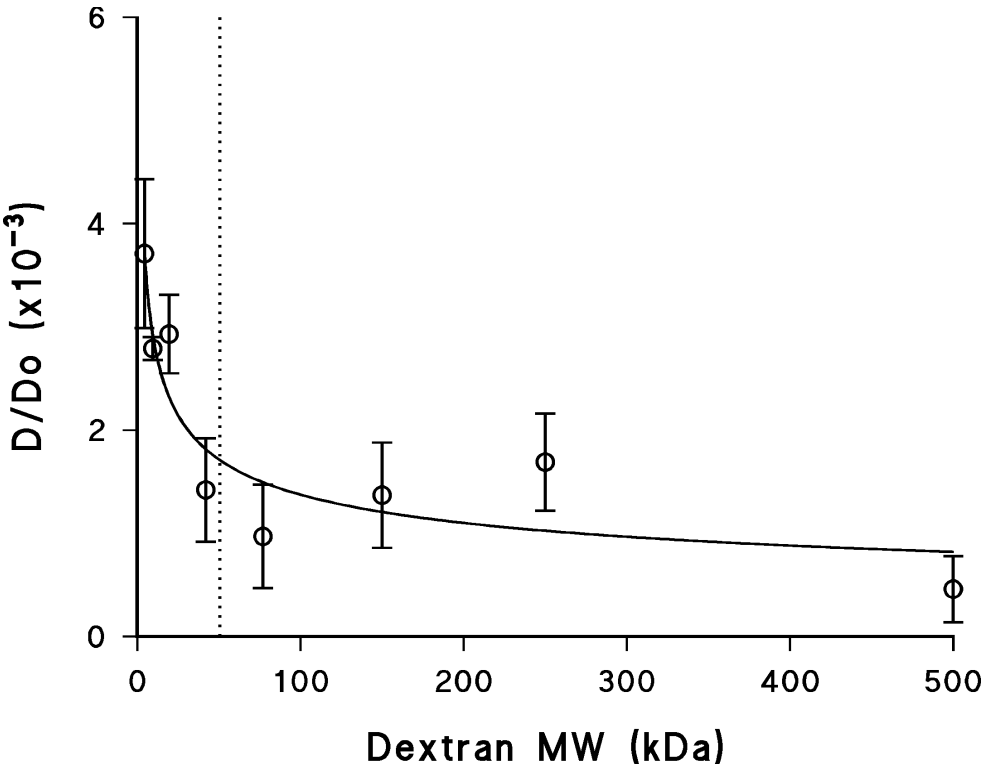

Figure 1.3 Dextran diffusion across macular regions in six donors aged 77-87 years over a large molecular weight range of 4.4 – 500 kD.

The plot shows normalised D/Do ratios as a function of dextran molecular weight. Continuous line is the non-linear regression fits to the equation $y=a*MW^b$.

If the region between 4.4 and 77 kDa dextran (non-reptation behaviour) is extrapolated, the exclusion limit for dextran molecules can be calculated as 71 kDa. This limit approximates to a Stokes-Einstein radius of about 6.0nm. However, (Refojo, 1982) has highlighted the inaccuracy of this conversion since the normally determined Stokes radius (r_s ,from diffusional work) does not reflect the effective radius of the hydrated molecule but rather that of a hard sphere that diffuses at the same rate as the molecule. This is particularly important in the case of dextran molecules that are non-spheroidal as the randomly coiled linear polymers in the

study of Hussain et al., 2010. An alternative method for determining molecular radius is by calibration with protein standards using size exclusion chromatography (r_{sec}) and this determination is thought to reflect the functional size of dextrans (Williams *et al.*, 1998). Using this conversion, the radius of a traversing molecule at the exclusion limit would be 5.6nm. Thus proteins such as catalase (radius 5.2nm & MW 240kDa), and ferritin (radius 5.5nm & MW 440-500kDa) would be expected to diffuse across Bruch's membrane. Plasma proteins ranging in size of 40-200 kDa have been shown to cross Bruch's membrane (Moore *et al.*, 2001). However, it is difficult to explain how the much larger lipoprotein complexes comprising LDL (radius 11.5nm) can also cross Bruch's membrane (Gordiyenko *et al.*, 2004; Tserentsoodol *et al.*, 2006). They can certainly enter Bruch's because of the larger open spaces outside the resistance barrier and therefore it is very likely that they may undergo some processing prior to transfer of the core across Bruch's.

1.1.1.2 Mechanism of transport: Metals and retinoids (vitamin A)

Carrier proteins are often used in the transport of important metabolites. Often, hydrophobic regions within the carrier allow binding of hydrophobic substrates thereby effectively increasing the 'solubility' of these compounds in the aqueous environment of blood. Binding and stabilisation also tends to prolong the half-lives of many unstable compounds. The carrier protein can also be used to regulate delivery to target tissues that express specific receptors for the protein. More importantly, binding of potentially harmful entities protects tissues from cytotoxicity due to high local concentrations of these substances. These principles are explained in detail for the transport of metals and vitamin A.

1.1.1.2.1 Divalent metals

Heavy metals are essential cofactors for metabolic, physiological, antioxidant, and drug detoxification processes. In the retina, they further participate in the highly specialised processes of visual function. The fatty acid desaturase is an iron-containing enzyme that provides unsaturated fatty acids for the continuous synthesis of outer segment disc membranes (Shichi, 1969). Photoreceptor specific guanylate cyclase is an iron-containing enzyme that plays a pivotal role in the phototransduction cascade of vision (Yau *et al.*, 1989). RPE65 is also an iron-dependent isomerohydrolase catalyzing the conversion of all-trans-retinyl ester to 11-cis-retinol in the visual cycle and essential for normal vision (Moiseyev et al., 2005). Zinc, another heavy metal, is also widely distributed in biological systems. It is an essential constituent of about 300 enzymes (including the anti-oxidant enzymes catalase and superoxide dismutase) and plays a structural role in over 400 nuclear regulatory elements and has specific roles in vision associated with both the turnover of Bruch's membrane and in the operation of the visual cycle (Berg *et al.*, 1996; Grahn *et al.*, 2001; Kimura *et al.*, 2000; Ugarte *et al.*, 2001).

Free iron (Fe^{2+}) is toxic and is therefore incorporated into haem or non-haem proteins. It can react with hydrogen peroxide in the Fenton reaction to generate hydroxyl radicals that are extremely damaging to cellular elements (Chevion, 1988). Rapid sequestration of free iron is essential to protect against free-radical damage. Thus, extracellular iron overload from sub-retinal haemorrhages can cause photoreceptor degeneration if not treated urgently by metal chelation therapy(Glatt *et al.*, 1982).

Because of its toxicity, iron is transported in the bloodstream in its ferric state ((Fe^{3+}) bound to the transport protein, transferrin. Since delivery to photoreceptors requires the crossing of several barriers, many transport proteins are involved in the transport of iron as shown schematically in Figure 1.4:

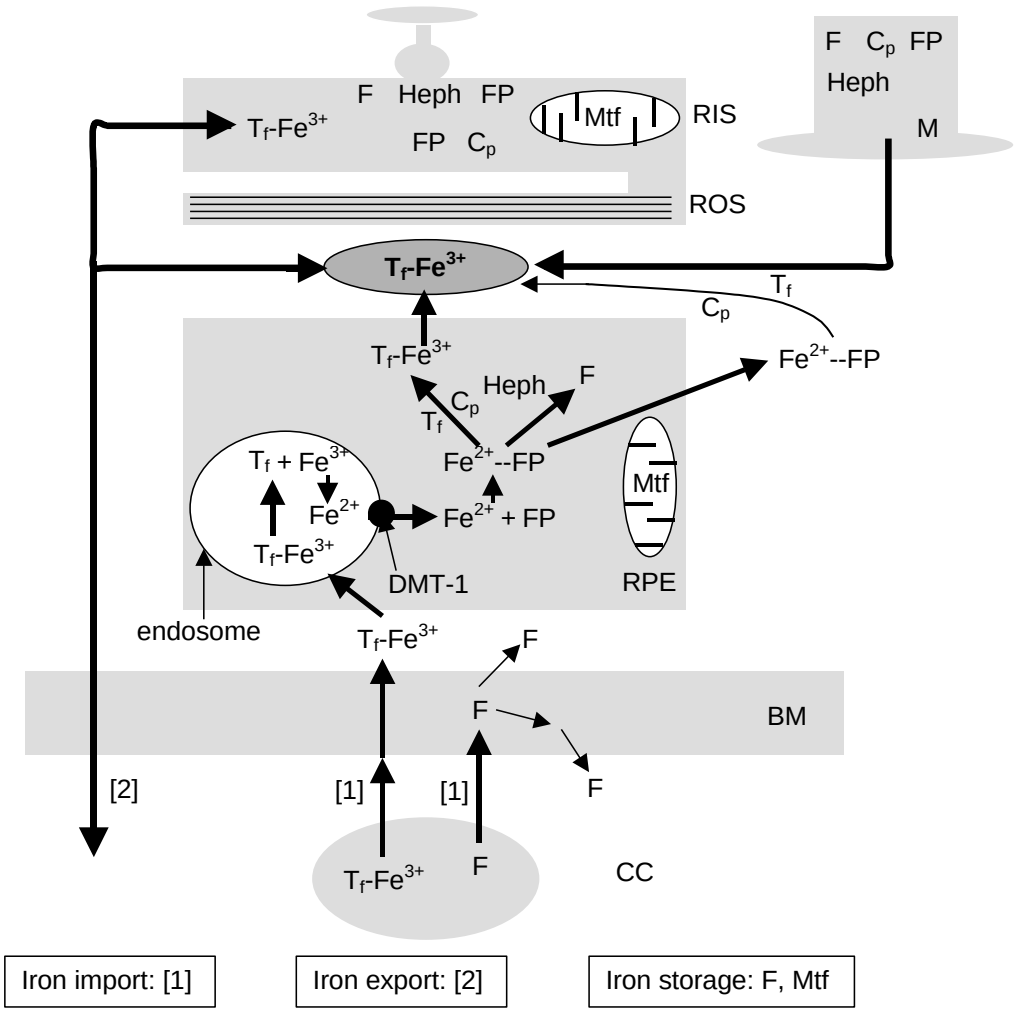

Figure 1.4 Iron mobilisation pathways in the outer retina.

Circulating transferrin (Tf) is released from the choriocapillaris (CC), traverses Bruch's membrane (BM) and is taken up by the RPE. Intracellular ferrous iron (Fe2+) is bound to ferriportin (FP), converted to the ferric form by either ceruloplasmin (Cp)/hephaestin (Heph) and loaded onto transferrin for subsequent release and either intercompartmental mobilisation or export via the choroidal circulation. Some of this iron is stored as ferritin (F). Mitochondrial ferritin (Mtf) binds the toxic Fe2+, converts it to Fe3+ and is then stored. M, Muller cell; RIS & ROS, rod inner and outer segment; DMT-1, divalent metal transporter. The above scheme was constructed from references (Chowers *et al.*, 2006; Dunaief, 2006; Hahn *et al.*, 2004a; Hahn *et al.*, 2004b).

Transferrin mRNA levels in the retina are 6-fold higher than those in the liver or brain indicating high rates of retinal iron transport (Farkas et al., 2004; Yefimova et al., 2000). Transferrin released from the choriocapillaries diffuses across Bruch's membrane and is endocytosed by RPE following binding to the cell surface transferrin receptor (Hunt et al., 1989). The low pH in the endosome leads to disassociation of iron from ferritin. Divalent metal transporter 1 (DMT1) transports iron from the endosome into the cytoplasm (He et al., 2007) .

Iron export from the RPE is mediated by ferroportin (Fp) that binds free ferrous iron preferentially (Donovan et al., 2000). Free ferrous iron (Fe^{2+}) must be oxidised to its inert ferric form (Fe^{3+}) before it can be loaded onto transferrin. This can be achieved by the ferroxidases ceruloplasmin (Cp) and hephaestin (Heph). Cp facilitates iron export by oxidizing iron from Fe^{2+} to Fe^{3+}. Fp is localized on the basolateral surface of RPE cells suggesting cooperation of Fp with the Cp/Heph system to release iron from the RPE (Hahn *et al.*, 2004a).

Iron storage is mediated by cytoplasmic ferritin, each ferritin molecule can hold 4,500 iron molecules in the ferric state. Most of the metabolically active iron is processed in the mitochondria, which has own iron storage protein, mitochondrial ferritin (MtF) (Levi et al., 2001). MtF displays ferroxidase activity such that released toxic ferrous iron can be converted into the inert ferric state and stored. In the rat retina, highest iron levels were found to be in the RPE, choroid, and the inner segments of photoreceptor cells (Yefimova et al., 2000).

Zinc is another important divalent metal ion with a deficiency being linked to ageing, changes in dark adaptation, and night blindness (Evans, 1986; Grahn et al., 2001). Lack of zinc can affect important antioxidants such as catalase and

superoxide dismutase, retinol dehydrogenase in the visual cycle, and matrix metalloproteinases which play a central role in the turnover and remodelling of Bruch's membrane (Ugarte et al., 2001). Zinc is transported across Bruch's bound to specific protein carriers (Leung *et al.*, 2008; Redenti *et al.*, 2004).

1.1.1.2.2 Vitamin A transport

Photoisomerisation of 11-cis retinal in the rhodopsin molecule leads to its release as all-trans retinal. This is then reduced to retinol and transported to the RPE cell where in a series of enzymatic reactions, it is reconverted to 11-cis-retinal and transported back to the photoreceptor cell culminating in the vitamin A cycle shown schematically in Figure 1.5. Retinoids have a very low solubility in aqueous media, high susceptibility for oxidation and are toxic in high concentrations. They are therefore always bound to carrier molecules. In the extracellular environment, they are bound to retinol binding protein (RBP), albumin and interphotoreceptor retinol binding protein (IRBP). Intracellularly, they are bound to cellular retinol and retinal binding proteins (CRBP, CRALBP). Although retinol is recycled between the photoreceptor and the RPE, losses occur due to oxidative damage of the chromophore and thus a continuous supply is required from the choroidal circulation.

In the blood, retinol is carried bound to a 21kDa carrier, the retinol binding protein (RBP) (Cowan *et al.*, 1990). This 1:1 retinol-RBP complex is in turn bound in 1:1 ratio to transthyretin (TTR), a homotetramer composed of 14-kDa subunits (Bellovino *et al.*, 1996; Melhus *et al.*, 1991). The combined molecular weight of the retinol-RBP-TTR complex is about 75 kDa (Bok, 1985).

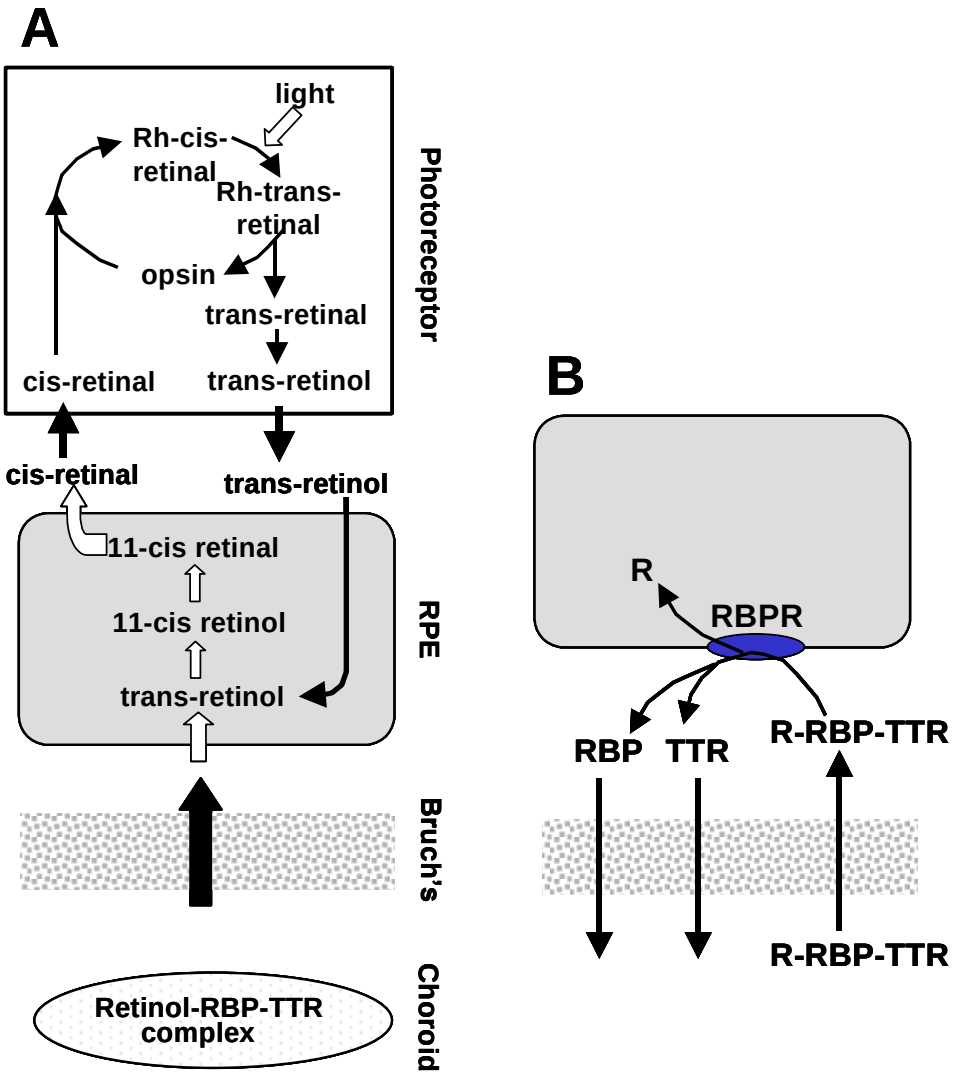

Figure 1.5 The vitamin A cycle and blood-borne delivery of retinol.

A: The vitamin A cycle. Photoisomerised all-trans retinal is recycled by the RPE and transported back to the photoreceptor cell for incorporation into rhodopsin. Endogenous stores of the retinoid are supplemented by supply from the choroidal circulation via Bruch's membrane.

B: Blood-borne delivery of retinol. The retinol-retinol binding protein-transthyretin complex (R-RBP-TTR) crosses Bruch's and following interaction with the RBP receptor on the basal surfaces of the RPE, the retinol is internalised and RBP and TTR are released back into the circulation.

The retinol-RBP-TTR complex crosses Bruch's membrane to interact with the RBP receptor on the basolateral surface of the RPE. The subsequent mechanism that delivers retinol to the RPE is not clear. The RBP does not appear to enter the RPE cell (Heller *et al.*, 1976). Current data suggests that retinol bound RBP has a higher affinity for the receptor than free RBP (Heller, 1975). Thus free RBP, having released its load is easily displaced by retinol bound RBP. It is suggested that the interaction of RBP with its receptor on the RPE leads to the dissociation of RBP and TTR leading to the release of retinol for uptake (Paci *et al.*, 2005). Released RBP and TTR then diffuse out across Bruch's membrane into the choroidal circulation.

1.1.2 Outward transport: waste disposal

The waste disposal pathway, operating in the opposite direction to nutritional transport serves to remove metabolic waste, degradation products of phagocytosed outer segment material, and fluids (Figure 1.6). Metabolic waste products are generally small soluble species that can diffuse freely down their concentration gradients across the RPE and Bruch's membrane for final removal into the choriocapillary network. The bulk of the fluid originating in the retina is actively transported by the RPE onto Bruch's membrane for passive movement into the choroid.

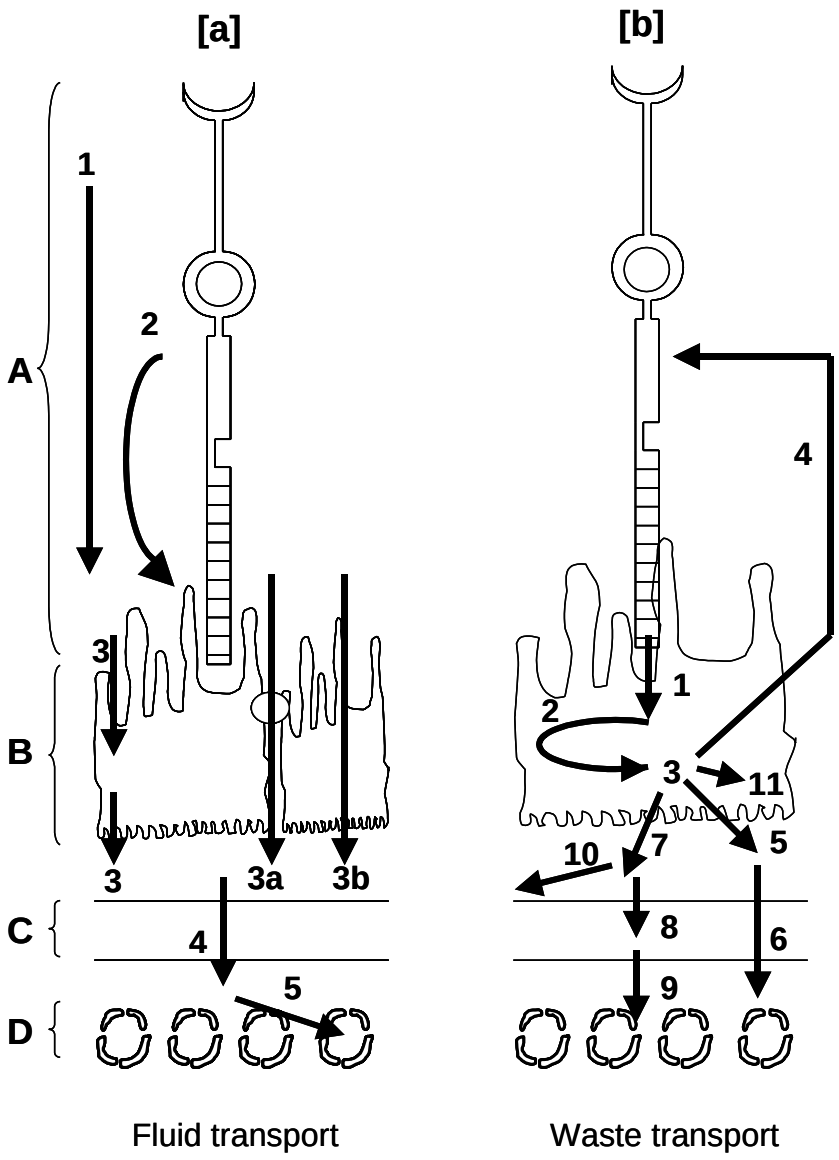

Figure 1.6 Transport pathways for removal of waste products.

[a] Fluid transport. Fluid arising from the inner retina [1], and from photoreceptor metabolism [2] is presented at the apical surface of the RPE. In a healthy RPE, the major proportion (about 70%) is removed by an active process mediated by solute-coupled water transport [3]. The remaining 30% is transported by hydrostatic and osmotic processes (3a and 3b respectively).

[b] Waste transport. Metabolic waste products (including urea and carbon dioxide) are removed by simple diffusion down their concentration gradients. Phagocytosis [1] and phagolysosomal degradation of outer segment portions [2] constitutes the major source of waste material. The fate of the phagolysosomal contents [3] is dependent on the degree of degradation. Fatty acids, retinoids, essential metals and vitamins for example can be recycled to the photoreceptor by the inner loop of transport [4]. Small soluble/insoluble products are voided onto Bruch's membrane [5] for clearance into the choroidal circulation [6]. Particulate matter is also voided onto Bruch's [7]. Some of this material will enter the inner layer of Bruch's where it may become trapped [8] or if sufficiently small, traverse the membrane [9]. The larger fragments will be deposited on the surface of Bruch's membrane [10] and may become focal centres for generalised lipid or drusen formation. The complex, non-degradable macromolecular complexes within the phagolysosome give rise to lipofuscin which is normally deposited as granules in clearly discernable sacs within the cytoplasm of the RPE cell [11].

1.1.2.1 Fluid transport

Fluid originating in the retina (from inner retinal capillary bed and retinal metabolism) is transported out by the RPE. Net outward fluid movement has been demonstrated both in-vivo (Frambach *et al.*, 1982; Marmor *et al.*, 1980; Negi *et al.*, 1986b) and in-vitro (Tsuboi, 1987; Tsuboi *et al.*, 1988).

Nearly 70% of outward fluid movement by the RPE is mediated by an active process, driven by transport of ions from apical to basal compartments (Negi *et al.*, 1986b; Quinn *et al.*, 1992). Excellent work in several laboratories has elucidated the ionic mechanism for fluid transport across the RPE (Adorante *et al.*, 1990; Bialek *et al.*, 1994; Joseph *et al.*, 1991; Quinn *et al.*, 1992). Briefly, the Na+,K+,2Cl- co-transporter on the apical surface mediates the entry of ions into the RPE cell and the increase in intracellular osmolarity in the locality will allow passive entry of water at that site. Extrusion of K+ and Cl- at the basal surface leads to outward water flow and the coupling in these ionic movements at the two surfaces provides the basis for net fluid transport across the RPE. The other 30% is thought to be due to passive means, driven mainly by the hydrostatic and osmotic gradients between the subretinal space and the extravascular choroid. Osmotic gradients arise from the high molecular weight species that are normally excluded from Bruch's membrane (see earlier). In addition, it has been estimated that albumin is present in the extravascular compartment at a concentration of about 10% of plasma and this will additionally contribute a small osmotic gradient pulling water out of Bruch's membrane (Toris *et al.*, 1990).

Quantitative measurements of fluid transport by the human RPE are few and have often been derived from pathological situations and therefore may be open to over-estimation. In one study, fluid transport for the entire RPE area of approximately 10 cm^2 was estimated to be between 1-2mls per day (0.04-0.08 μl / hour / mm^2) (Pederson, 1994). Another clinical study examined the rate of regression of a retinal bleb in a non-rhegamatous detachment using B-scan ultrasonography and assuming that fluid was cleared by the RPE calculated the rate of transport to be of the order of 0.11 μl / hour / mm^2 (Chihara *et al.*, 1985).

Several animal studies incorporating both induced retinal blebs and in-vitro Ussing chambers have determined the rate of fluid transport by the RPE to be about 0.1248 ±0.11 μl / hour / mm^2, a value similar to that in the human studies given above (Frambach *et al.*, 1982; Hughes *et al.*, 1984; Negi *et al.*, 1986a; Negi *et al.*, 1986b; Tsuboi, 1987; Tsuboi *et al.*, 1988).

Fluid pumped out by the RPE is then transported across Bruch's due to a hydrostatic pressure head. The hydraulic conductivity (HC) of Bruch's membrane required to transport the output from the RPE can be calculated from:

$$HC = \text{flow} / \text{pressure}$$

However, the hydrostatic pressure differential across human Bruch's has not been determined due primarily to technical difficulties. In monkeys, the pressure differential across the vitreous and suprachoroidal space was estimated to be about 4 mm Hg (equivalent to 534 Pa) (Emi *et al.*, 1989). Since a pressure differential was not detected across the neural retina (Maurice *et al.*, 1971), the 4mm Hg gradient must fall across the RPE-Bruch's complex. There is no doubt that some of this pressure head must fall across the RPE. Thus, at best, the driving pressure gradient

across Bruch's can be no more than 4mmHg but in all probability would be expected to be lower. Using a value of 4mmHg, the hydraulic conductivity of Bruch's required to transport fluid deposited onto its surface by the RPE (0.13 μl / hour / mm^2) can therefore be calculated as 0.65 x 10^{-10} m/sec/Pa.

1.1.2.2 Transport of phagocytic by-products

Retinal photoreceptors maintain one of the highest rates of oxidative metabolism of any cell type in the body and it has been estimated that during normal metabolism, the mitochondrial electron transport chain converts 1-5% of consumed oxygen to reactive oxygen species (ROS: superoxide, $\circ O^-_2$ and hydrogen peroxide, H_2O_2) (Ahmed *et al.*, 1993; Bui *et al.*, 2003; Korshunov *et al.*, 1997). Furthermore, these receptors operate in an environment rich in highly unsaturated fatty acids, high oxygen tension and light, an 'explosive' mixture for generation and propagation of free-radical mediated damage pathways (Bicknell *et al.*, 2002; Boulton *et al.*, 2001). This highly oxidative environment of the retina leads to oxidation of outer segment lipids such as docosahexonoic acid (Esterbauer *et al.*, 1991; Miceli *et al.*, 1994). Free radical mediated attack will lead to chain propagation reactions and despite the presence of blockers of this ravagenous process (e.g., vitamin E, superoxide dismutase, catalase), considerable damage is sustained. Such oxidative reactions lead to the formation of reactive aldehydes that can cross-link proteins leading to the formation of large macromolecular complexes (Witz, 1989).

The sustained photoreceptor damage, noticeably in the lipid rich membrane discs of outer segments, is transferred en masse to the RPE cells by the process of daily disc shedding and phagocytosis by the RPE (Bok *et al.*, 1979; Young, 1976). It

has been estimated that in humans, each RPE cell ingests about 6000-8000 discs daily (Bok, 1994; Feeney-Burns, 1980; Young, 1982). Complete digestion within the RPE cell reduces the complex structures to their basic building blocks of fatty acids, amino acids, vitamins including the retinoids and essential metals. These are normally recycled back to the photoreceptor using the pathways described earlier and assist in the re-synthesis of new discs (Bok, 1990). This short pathway is often termed the inner loop of nutrient transport compared to the outer loop involving transport of blood-borne nutrients.

Phagosomes containing discs with minimal damage can fuse with lysosomes and the major degradation products can be recycled with the minor small non-degradable material being voided out of the cell for clearance by Bruch's membrane.

1.2 Ageing of transport systems

1.2.1 Structural and compositional alterations of ageing Bruch's membrane

Bruch's membrane undergoes age-related morphological and compositional alterations with its thickness increasing 2-3 fold over the life-span of an individual (Newsome *et al.*, 1987; Okubo *et al.*, 1999; Ramrattan *et al.*, 1994; Sarks, 1976; van der Schaft *et al.*, 1992). Despite the overall increase in thickness, the elastin layer of the membrane at both macular and peripheral locations was not observed to thicken to any significant level (Chong *et al.*, 2005). Compositional alterations include the deposition of lipids (Curcio *et al.*, 2001; Holz *et al.*, 1994; Pauleikhoff *et al.*, 1990; Sheraidah *et al.*, 1993), proteins (Hageman *et al.*, 1999; Kliffen *et al.*, 1995) and

carbohydrate associated moieties such as glycolipids, glycoproteins and proteoglycans (Farkas *et al.*, 1971; Mullins *et al.*, 1997).

1.2.1.1 Lipid accumulation

Very early histochemical studies showed an age-related accumulation of lipids in Bruch's membrane leading to the concept of a 'lipid barrier' that was postulated to undermine metabolic exchange processes between the choroidal blood supply and the light sensitive receptor cells (Bird *et al.*, 1986; Grindle *et al.*, 1978). This concept was particularly useful in explaining the occurrence of RPE detachments in patients with AMD where the 'hydrophobicity' of ageing Bruch's blocked the exit pathways for fluids and the continuing pumping by RPE cells led to fluid accumulation and eventual detachment (Bird *et al.*, 1986).

Subsequent quantitative studies showed little or no deposition of lipids prior to the age of 40-50 years followed by an exponential increase thereafter (Holz *et al.*, 1994; Sheraidah *et al.*, 1993). More recent studies have examined filipin fluorescence due to the presence of free and esterified cholesterol and suggest an earlier onset of accumulation of these species (Curcio *et al.*, 2001; Ruberti *et al.*, 2003). In samples from aged donors (>60 years), 80-100nm particles enriched in esterified and free cholesterol were observed to occupy a third of the inner collagenous layer and to exist as a discreet sublayer in between the RPE basal lamina and Bruch's membrane. All of the above studies confirm the greater accumulation of various lipids in macular regions compared to the periphery.

1.2.1.2 Collagen content and age

The collagen content of Bruch's increases throughout life and two forms can be recognised morphologically (Bird *et al.*, 1986; Loffler *et al.*, 1986; Sarks, 1976; van der Schaft *et al.*, 1992). Collagen with a 64nm periodicity is intrinsic to the membrane and accumulates throughout life. Another form with a banding periodicity of 100-140nm, termed long spaced collagen (LSC) becomes prominent after the age of 40 years. The presence of LSC in the outer collagenous layer of most young eyes suggests it to be a normal feature of collagen turnover. Its increased presence in the basal laminar deposits (between the plasma and basement membrane of the RPE) and in the outer collagenous layer of Bruch's is thought to be a response of distressed cells (Guymer *et al.*, 1999; Marshall *et al.*, 1994; Sarks, 1976; van der Schaft *et al.*, 1991).

Ageing also results in a change in the properties of the collagen molecule. The insoluble collagen content of Bruch's membrane was shown to increase linearly with age (Karwatowski *et al.*, 1995) and over a 10-decade period accounted for nearly 50% of membrane collagen. The insolubility is indicative of denaturation and subsequent chemical modification including greater cross-linking and formation of advanced glycation end-products (AGE's).

1.2.1.3 Advanced glycosylation and lipid end-products (AGEs and ALEs)

Pentosidine and carboxymethyllysine (CML), two of the most studied collagen AGE products were shown to be present in ageing Bruch's membrane, basal laminar and linear deposits and in soft macular drusen (Handa *et al.*, 1999; Ishibashi *et al.*, 1998). Quantitative studies have shown an age-dependent increase in the level of

pentosidine in Bruch's membrane (Handa *et al.*, 1999). AGE's are strong promoters of protein cross-linking (Krishnamurti *et al.*, 1997; Tian *et al.*, 1996) and can thus reduce the porosity of an ECM with dire consequence for transport pathways. More importantly, AGE's reduce protein susceptibility to enzymatic proteolysis and will uncouple the tightly regulated matrix metalloproteinase (MMP) synthetic/degradation system for normal membrane rejuvenation leading to increased deposition of matrix components (Haas *et al.*, 1998; Howard *et al.*, 1996; Rittie *et al.*, 1999; Scott *et al.*, 1998), a situation present in ageing Bruch's membrane. Interestingly, ARPE-19 cells grown on AGE modified matrigel showed altered expression of plasminogen-activator-inhibitor-1 (PAI-1) leading to decreased plasmin activation resulting in reduced MMP activation (Bobbink *et al.*, 1997; Corcoran *et al.*, 1996; Honda *et al.*, 2001). Other workers have previously observed a marked absence of active MMPs 2&9 in macular regions of human Bruch's membrane whereas their presence in the periphery was routinely demonstrated (Guo *et al.*, 1999). This AGE mediated alteration could therefore contribute to the expansion of ageing human Bruch's membrane in the macular region.

1.2.1.4 Accumulation of phagocytic debris

As indicated earlier, the highly oxidative environment of the retina leads to free-radical mediated damage of outer segment lipids such as docosahexonoic acid and formation of reactive aldehydes that can cross-link proteins leading to the formation of large macromolecular complexes (Esterbauer *et al.*, 1991; Sayre *et al.*, 1996; Witz, 1989). Phagocytosis of outer segment tips simply transfers this reactive system to the interior of the RPE, which like the retina, is situated in a highly

oxidative environment. This material can therefore undergo further oxidative damage whilst in the RPE cell. The reactive species within the engulfed disc material may damage the phagosomal membrane leading to problems of fusion with lysosomes so that further processing is inhibited (Hoppe *et al.*, 2001).

Phagolysosomes containing damaged outer segment material could theoretically degrade the accessible material with the remainder being packaged as lipofuscin granules. However, current evidence suggests this to be unlikely. A major fluorophore of lipofuscin has been shown to be a bis-retinoid called N-retinylidene-N-retinylethanolamine (A2-E) (Reinboth *et al.*, 1997; Sakai *et al.*, 1996). Although the mechanism remains unknown, A2-E has been shown to inhibit lysosomal proteolysis in RPE cells (Holz *et al.*, 1999; Sundelin *et al.*, 1998). A2-E also inhibits the phagolysosomal degradation of phospholipids and may therefore influence the natural history of lipid deposits of Bruch's membrane (Finnemann *et al.*, 2002). The toxic environment within the phagolysosomes containing such damaged material is expected to result in incomplete degradation of contents. Furthermore, the phagolysosomal membrane may itself undergo damage with the possibility of leakage of destructive contents into the cytoplasm. Products of incomplete digestion will include soluble components that are likely to be recycled, 'normal' membraneous aggregates, and insoluble particulate material containing lipofuscin.

Lipofuscin granules are discernable by the age of 10 years and occupy nearly 20% of cytoplasmic volume by the age of 80 years (Feeney-Burns *et al.*, 1984). Decreased cytoplasmic volume may have ramifications for the storage potential for diffusible metabolites. Furthermore, increasing levels of melanolipofuscin complexes result in removal of an important free-radical scavenger from the anti-oxidant

machinery of RPE cells (Feeney-Burns *et al.*, 1984; Schmidt *et al.*, 1986). There is also some evidence that increased lipofuscin can compromise the phagocytic degradation potential of the cell resulting in increased levels of partially digested material that must be removed from the cell. Several reports have now demonstrated an age-related decline in the activity of lysosomal enzymes and this will result in greater accumulation of lipofuscin (Boulton *et al.*, 1989; Kennedy *et al.*, 1995; Liles *et al.*, 1991; Wilcox, 1988).

Increased lipofuscin within the RPE is an indicator of increased production of 'undigested' debris. Thus ageing results in greater amounts of membraneous derived waste products being extruded onto Bruch's membrane. The smaller fraction may pass through Bruch's membrane or coalesce to produce larger species that may be trapped in the membrane. Peroxidised PUFA's have been demonstrated in Bruch's membrane and particles containing these species may cross-link with proteins to become trapped in the membrane (Hicks *et al.*, 1989; Kikugawa *et al.*, 1987; Wiegand *et al.*, 1983). Larger particles may only penetrate the inner collagenous layer whereas even larger species may be deposited onto the surface of Bruch's membrane progressing to the formation of drusen (Feeney-Burns *et al.*, 1985; Ishibashi *et al.*, 1986).

It is also likely that free lipids could aggregate leading to 'free-energy' driven growth, stabilisation and deposition. High resolution morphometric studies have shown the presence of 100 nm particles enriched in esterified and free cholesterol (Curcio *et al.*, 2001; Ruberti *et al.*, 2003). The latter studies showed these particles to occupy >30% of the inner collagenous layer in eyes from donors aged over 60 years.

Further incorporation is likely to lead to fusion of these particles resulting in sheets of soft drusen.

The deposition and growth of this lipid rich component under the basal aspects of the RPE is expected to considerably increase the diffusional distance for transport of nutrients.

1.2.2 Hydrodynamics and ageing of Bruch's membrane

Previously (section: 1.1.2.1) the hydraulic conductivity of Bruch's required to deal with fluid output from the RPE was calculated as 0.65×10^{-10} m/sec/Pa. This threshold value may be appropriate at peripheral locations but at macular sites, high photoreceptor densities would be expected to produce higher fluid output. Thus, for comparative purposes, threshold values in the macular region should be higher than calculated.

Several studies have now documented on the hydraulic conductivity of ageing human Bruch's membrane. (Fisher, 1987) showed the hydraulic conductivity of Bruch's to halve between the ages of 22 and 71 years. Subsequent and more detailed studies showed an exponential reduction in hydraulic conductivity at both macular and peripheral locations (Moore *et al.*, 1995; Starita *et al.*, 1996). A more extensive analysis of transport across Bruch's, including samples from donors with age-related macular degeneration (AMD) is presented in Figure 1.7 and Figure 1.8 (Hussain *et al.*, 2004).

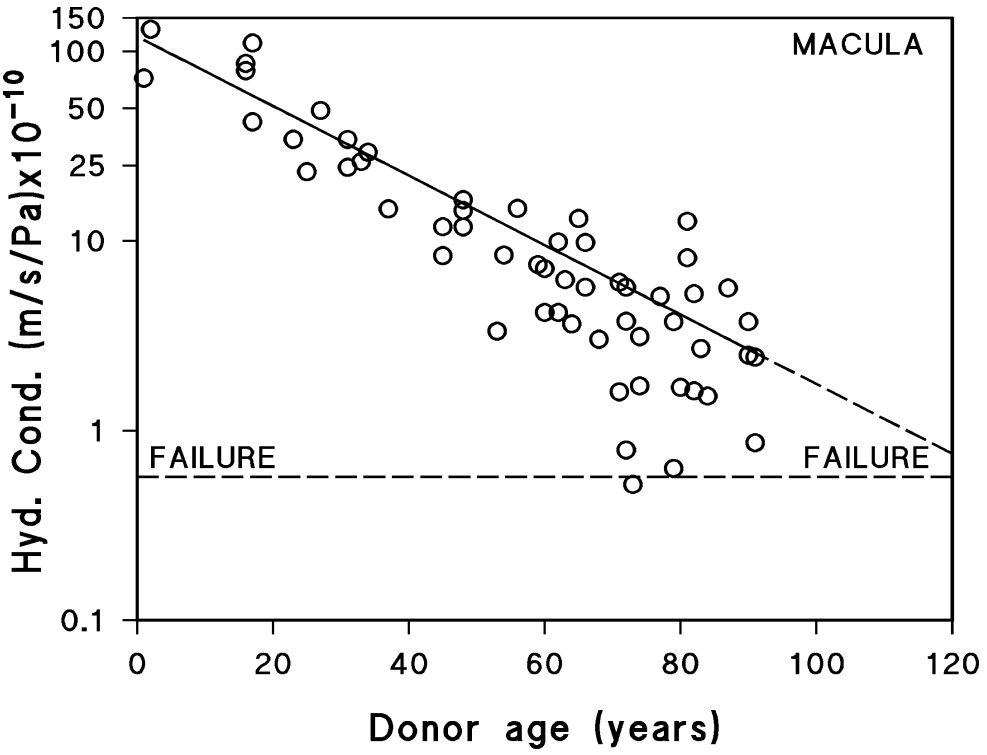

Figure 1.7 Age-dependent variation in the hydraulic conductivity of human Bruch's membrane: macular region.

The semi-logarithmic plot shows an exponential decay in the hydraulic conductivity of Bruch's membrane.The failure threshold for fluid transport was calculated from the minimum hydraulic conductivity of Bruch's required to transport fluid pumped out by human and animal RPE as described in the text. In this control donor population, the likelihood of the decay curve meeting the failure threshold lies outside the normal human life span. Data from 56 donors, age range 1-91 years. Modified from Hussain et al., 2004.

In macular regions, hydraulic conductivity was observed to decrease exponentially (linear line in the log transform of Figure 1.7). The rate of change in hydraulic conductivity with age remains unaltered throughout the life of an individual and is depicted by the linear regression fit on the logarithmic plots. In an exponential relationship, the rate of decay is often characterised by the half-life of the process and can be calculated as ln(2) / k, where k is the decay constant obtained from the

non-linear regression fit to the data. In macular regions, the half-life for the age-related decline in hydraulic conductivity was calculated as 16 years, i.e., the capacity for transport of fluids is halved for every 16 years of life. The regression line of Figure 1.7 can be extrapolated to cut the failure threshold and this would represent a finite period of viable function for transport of fluids through Bruch's membrane. In the case of the macular data, the age at which Bruch's would be expected to fail is about 127 years, well outside the normal human life span. In a given individual, environmental factors, smoking habits or genetics may influence the rate of decline and this secondary modulation may be reflected in the scatter of Figure 1.7. Since the data of Figure 1.7 was accrued from a 'control' donor population, it might be argued that although the demise in hydraulic conductivity is rather precipitous, it nevertheless has very little effect on the underlying physiology. Thus Bruch's has rather an excess capacity for dealing with fluid output from the RPE. On the other hand, the declining exponential curves may be indicative of the increasing risk in the elderly of developing transport problems that may progress to pathology.

Hydraulic conductivity at peripheral locations also showed an exponential decrease with age but the decay constant was lower with a half-life of 23 years (Figure 1.8). Thus ageing in non-macular regions occurs at a much slower rate. Extrapolating the non-linear regression transform to meet the failure threshold provided a shelf-life of Bruch's in the periphery of about 174 years, again the capacity for transport across Bruch's appears to be far in excess of that required for routine daily transport of fluids. The similarities in the exponential graphs between macular and peripheral regions suggests that in the normal eye, measurement of

hydraulic conductivity in one region can provide a good estimate of the situation in the other.

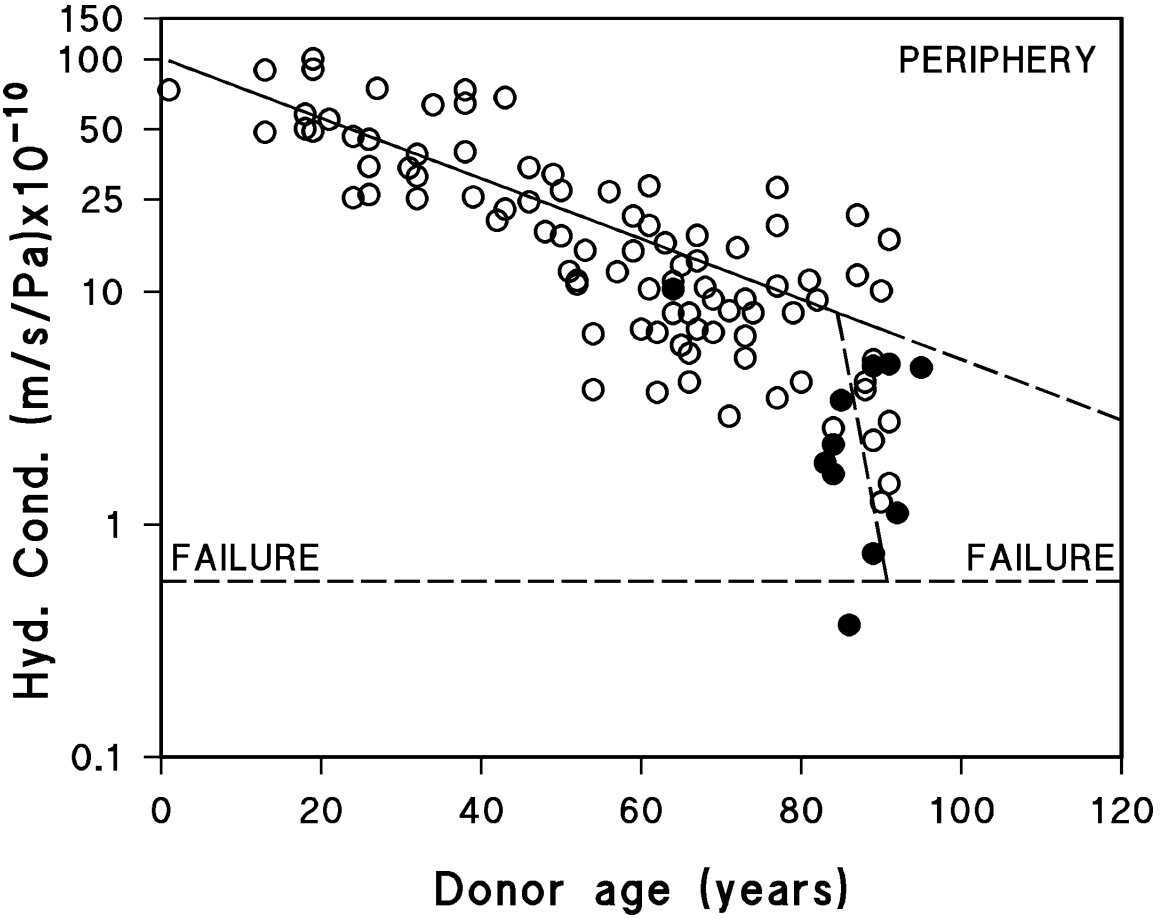

Figure 1.8 Age-dependent variation in the hydraulic conductivity of human Bruch's membrane: peripheral region.

A similar exponential decay in hydraulic conductivity was also observed in the peripheral region of the human fundus but with a slower half-life of 23 years (open circles, n=90; age range 1-90 years). Hydraulic conductivities of AMD donors (n=12; age range 64-95 years, filled circles) were all below the mean regression line of the control samples and showed a drift towards failure thresholds.
Modified from Hussain et al., 2004.

In AMD, the ultrastructural changes in Bruch's membrane are best described as advanced ageing (Green *et al.*, 1993; Green *et al.*, 1977; Sarks, 1976). Since eyes from aged AMD donors often show the very late stage of the disease, macular scarring prevents isolation of this region but peripheral regions were examined and resulting hydraulic conductivities are presented in Figure 1.8.

Interestingly, all twelve AMD samples showed conductivities that fell beneath the regression line for control donors. Of these twelve samples, two (16.7%) were on or below the demarcation line of minimum hydraulic conductivity. If a parallel can be drawn between hydraulic conductivities of macular and peripheral regions in control with those in AMD, then it can be predicted that in the latter, the fluid transportation system of Bruch's must be under severe strain and more likely to fail leading to accumulation of fluid under the RPE. It is therefore not surprising that 12-20% of AMD sufferers show RPE detachments as the continued pumping by the RPE leads to fluid accumulation and subsequent detachment (Bird *et al.*, 1986).

1.2.3 Macromolecular transport and ageing of Bruch's membrane

Carrier mediated delivery of metabolites across Bruch's is essential for both RPE and photoreceptor survival. Their payload includes important ligands such as vitamin A (retinol binding protein), the heavy metals iron and copper (transferrin, ceruloplasmin), and lipids (lipoproteins). Albumin can also carry a variety of metabolites including fatty acids.

Some evidence already exists to suggest that this transportation function may be impaired in elderly patients with ageing changes in Bruch's membrane (Chen *et*

al., 1992; Pauleikhoff *et al.*, 1990; Steinmetz *et al.*, 1993; Sunness *et al.*, 1988). These patients displayed good visual acuity but on fluorescein angiography there was evidence of delayed choroidal perfusion in other areas of the fundus. Functional analysis of these regions showed elevated dark adaptation thresholds similar to changes observed in vitamin A deficiency. Similar changes were observed in Sorsby's fundus dystrophy (SFD), a disease with many clinical associations with AMD together with the presence of a 30 μm thick lipid rich deposit in Bruch's membrane (Steinmetz *et al.*, 1992). The conclusion has been that ageing changes in Bruch's membrane lead to a diminution in the transport of macromolecules such as vitamin A-RBP.

Traversing protein carriers such as albumin, transferrin, and ceruloplasmin display Stokes-Einstein radii of 3.58nm, 4.3nm and 4.68nm respectively. The diffusional status of ageing Bruch's was previously assessed using a quasi-spherical FITC-labelled dextran of molecular weight 21.2 kDa and Stokes-Einstein radius of 3.28nm (Hussain *et al.*, 2010). The diffusional studies for macular and peripheral Bruch's are presented in Figure 1.9: Diffusional transport of the FITC-labelled test probe declined linearly with ageing at both macular and peripheral locations. As with hydraulic conductivity, the decline in the non-macular fundus was much slower. At macular locations, there was a nearly 80% reduction in diffusional transport between the first and ninth decade of life.

Another study, using serum proteins as markers showed a 10-fold decline in diffusion rate between the first and ninth decade of life in macular regions of the human fundus (Moore *et al.*, 2001). Thus macromolecular traffic through macular Bruch's membrane undergoes considerable attenuation with ageing of donor and

supports the earlier conclusions derived from clinical studies of elevated dark adaptation thresholds.

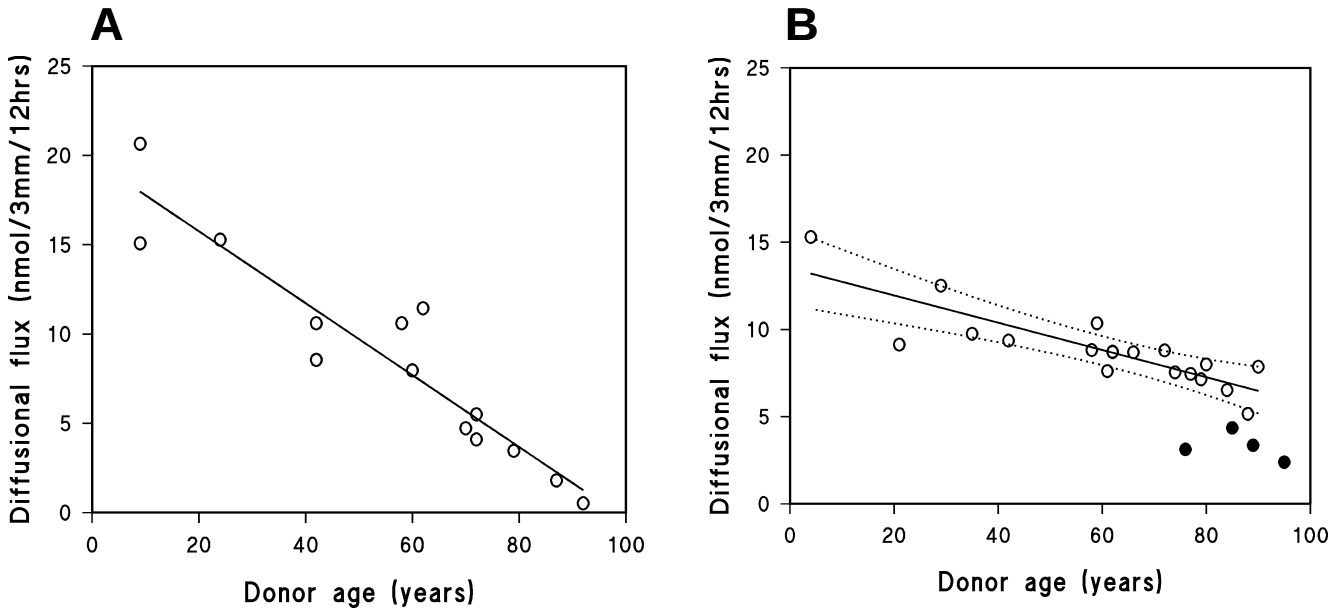

Figure 1.9 Age related variation in the diffusional flux of a 21.2 kDa dextran through Bruch's membrane from macular (A) and peripheral (B) locations.

Diffusional fluxes were measured (over a period of 12 hours) in response to a 0.412mM concentration gradient of the FITC-dextran across the preparation. Ageing of the donor was associated with a highly significant decline in the rate of diffusion across Bruch's membrane, $p < 0.001$. In (B), the 99% confidence limits for the normal donor population are shown as dotted lines. Diffusional levels in Bruch's membrane from peripheral samples of AMD donors (filled circles) were much lower lying outside the 99% confidence limits of the 'normal' population (From Hussain et al., 2010).

As with hydraulic conductivity, the diffusional pathways appear to maintain a capacity that is far in excess of that required for supplying the neural retina. However, some elderly patients do show signs of reduced supply of vitamin A and thus in these subjects, the transport rates must have been operating at close to minimal

rates of supply for retinal maintenance. Nonetheless, the capacity to withstand an additional insult may be compromised. Thus in four AMD donors, peripheral rates of diffusion of the test probe were considerably reduced (Figure 1.9B) with values lying outside the 95% confidence limits of the control population. As with hydraulic conductivity, the diffusional situation at macular locations is likely to be much more severe in these patients. The reduction in the diffusional transport of this test probe means that all carriers transporting essential vitamins, lipids, and heavy metals that are of vital importance to both metabolic and enzymic protection systems (such as catalase and superoxide dismutase) will be severely compromised. The initial impact of a reduction in macromolecular transport may place the homeostatic protective systems (both in the RPE and photoreceptors) under considerable stress increasing the likelihood of a pathological insult.

1.2.4 Advanced changes in age-related macular degeneration

The ageing changes in structure and composition of Bruch's membrane have already been discussed. Associated changes in functional parameters of transport were also shown to decline and in the control aged, problems associated with carrier proteins for vitamin A were apparent. The morphologically advanced ageing in AMD is therefore expected to exacerbate the functional decline in transport properties (Hammes et al., 1999). Although macular regions have not yet been assessed, peripheral locations in donor AMD eyes showed considerable compromise in fluid and macromolecular transport (Hussain *et al.*, 2010; Hussain *et al.*, 2004).

Restricted transport of carrier proteins not only reduces the delivery of retinoids, vitamins and metals to overlying RPE and retina, it can also lead to the deposition of these materials in the matrix of Bruch's membrane. For example, the increased thickness of Bruch's, cross-linking of collagen fibres, increased rigidity of the membrane and reduced porosity can considerably increase the 'dwell' times for traversing molecules. Increased dwell times can increase the risk of oxidative damage and entrapment of carrier proteins within Bruch's. Released payloads such as iron, zinc, copper can then complex with the debris leading to increased levels in the membrane. The presence of toxic levels of these metals poses further risk of damage to the membrane.

Iron levels are higher in aged control subjects, but AMD donors display much elevated levels in the retina, RPE, and Bruch's-choroid (Dentchev et al., 2005; Dunaief, 2006). If the entry of iron via transferrin and ferritin is curtailed, the raised levels in RPE and retina must occur via additional pathways such as the inner retinal circulation and possibly the vitreous. It is also likely that with reduced capability of exit pathways, iron storage of ferritin becomes more important leading to its accumulation in the retina and RPE. Elevated levels of iron in Bruch's could also be due to entrapment and stabilisation of plasma-derived transferrin and ferritin within the reduced porosity of aging Bruch's and by complexation of divalent metals to amorphous debris within the membrane.

Increased levels of iron in photoreceptors, RPE and Bruch's risk additional damage from released free iron (Fe^{2+}) since the free radical pathway in the presence of high levels of unsaturated lipids, light, and oxygen will exacerbate the underlying pathological mechanism (Organisciak et al., 1998).

Metabolic insufficiency leads to a highly stressed RPE cell that may undergo apoptosis discharging its contents onto Bruch's membrane. Histopathological investigations have often underlined the presence of such a 'stressed' situation in the RPE-Bruch's complex of donor AMD eyes (Sarks *et al.*, 1999). Complement activation and local inflammatory processes have been implicated in the formation of drusen as these deposits contain both cascade proteins and immune system components and terminal immune complexes (Donoso *et al.*, 2006; Hageman *et al.*, 2001; Johnson *et al.*, 2001; Mullins *et al.*, 2001). Since extensive druse formation is a hallmark of AMD, inappropriate complement activation due to the CFH polymorphisms may well contribute to the development of AMD.

Several single nucleotide polymorphisms have been identified in the complement factor H (CFH) gene that were strongly associated with AMD (Edwards *et al.*, 2005; Hageman *et al.*, 2005; Haines *et al.*, 2005; Klein *et al.*, 2005). Some of these polymorphisms were located in the functional domains of the CFH gene and immunohistochemical analyses have shown increased presence of CFH expression in macular areas of AMD donors compared to controls (Hageman *et al.*, 2005). Other single nucleotide polymorphisms with even greater association with AMD have been found in both coding and non-coding flanking regions of the CFH gene (Li *et al.*, 2006; Maller *et al.*, 2006). The list of AMD-associative sites in members of the complement system is further enlarged by the presence of polymorphisms in the complement factor B (CFB) and complement C2 cascades (Gold *et al.*, 2006; Maller *et al.*, 2006).

Release of vascular endothelial growth factor (VEGF) is an early event in the angiogenic process. It is thought that AGEs and ALEs stimulate the AGE-receptor

(RAGE) on RPE cells that culminates in the release of VEGF from highly stressed cells. Although neovascular episodes occur in only about 10%-20% of all AMD cases, they are nevertheless responsible for nearly 90% of cases of visual loss.

Anatomical variations in the elastin layer of Bruch's between macular and extra-macular regions are thought to underlie the greater susceptibility of the former region to choroidal neovascularisation (Chong *et al.*, 2005). This study showed that the elastin layer in the macular region was three to six times thinner and two to five times more porous than at peripheral locations, changes that are more likely to compromise barrier function against potential neovascularisation at the macula. The elastin layer in the macular region of AMD donors was shown to be much thinner and more porous compared to age-matched controls. Furthermore, endogenous inhibitors of angiogenesis such as endostatin, pigment epithelium-derived factor and thrombospondin 1, normally present in Bruch's membrane, were shown to be significantly lowered in AMD thereby increasing the vulnerability for choroidal neovascularisation (Bhutto *et al.*, 2008).

The advanced ageing changes in Bruch's membrane associated with AMD and the potential for inflicting degenerative insults are shown in schematic form in Figure 1.10.

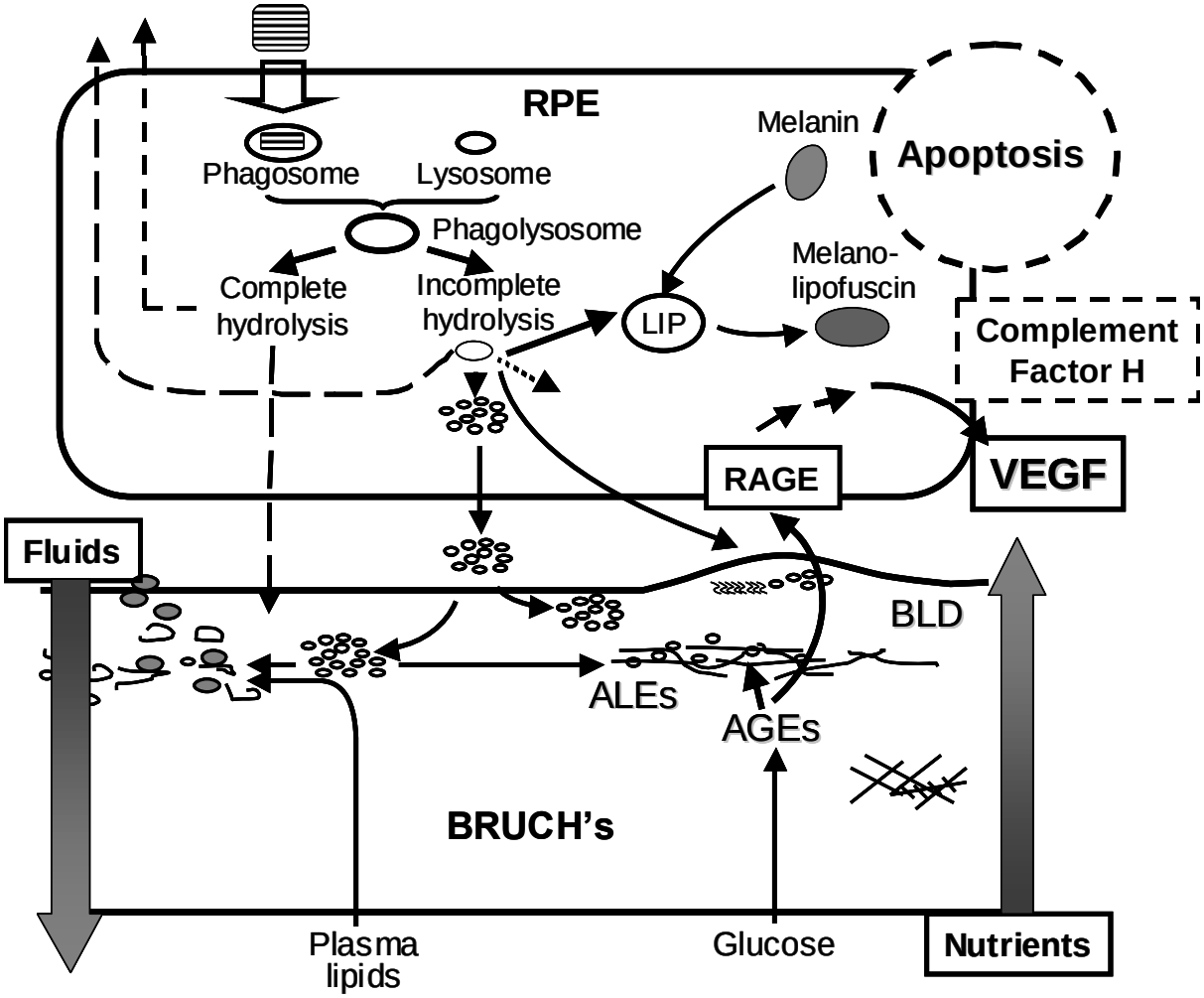

Figure 1.10 Summary of advanced ageing changes in the RPE-Bruch's complex and the potential for transition to pathology.

In AMD, an exaggeration of the various ageing mechanisms described in the text leads to severe structural and functional compromise of Bruch's membrane. The resulting diminished metabolic support increases 'stress' on the RPE cell that may then proceed to pathological alterations via apoptosis or the recruitment of additional inflammatory or neovascular episodes.

1.3 Extracellular matrix turnover and Bruch's membrane

1.3.1 Structural elements of Bruch's membrane

In addition to acting as a scaffold for adhesion of RPE cells, the matrix of Bruch's also serves as a reservoir of factors that promote cell proliferation, activation, and migration (Aumailley *et al.*, 1998; Labat-Robert *et al.*, 1990; Vaday *et al.*, 2000). In common with other ECMs, Bruch's contains four major classes of structural components: (i) collagens, (ii) elastin(s), (iii) proteoglycans and (iv) structural glycoproteins (Labat-Robert *et al.*, 1990).

The collagen molecule contains high levels of proline and glycine and exists as a triple helix by the inter-twining of three α-chains to form a rope-like structure. Nineteen types of collagen molecules have been identified and it is the relative mix of these that determines the physical characteristics of a given matrix (Aumailley *et al.*, 1998). The fibrillar collagens (types I, II, III, V and XI) are relatively inextensible and therefore determine the rigidity of a matrix (Scott, 1995). Types IX and XII can cross-link with other collagen fibres and to non-collagenous components of the matrix. Network-forming collagens are represented by types IV and VII and of these type IV spontaneously aggregates into meshworks to form the major skeletal backbone of basement membranes (Grant *et al.*, 1981). Type VII molecules form dimers that assemble into specialized structures called anchoring fibrils and function to attach epithelium cells to their basement membrane (Aumailley *et al.*, 1998).

The elastin protein is also rich in proline and glycine but unlike collagen, it is not glycosylated. Elastin molecules assemble into elastic fibres that become highly

cross-linked to form extensive networks of fibres and sheets. Hydrophobic regions within the molecule are thought to impart elastic properties with an alanine-lysine rich α helical segment being responsible for cross-linking adjacent molecules (Robert *et al.*, 1980). These elastic fibres are enmeshed with microfibrils comprising glycoproteins and can interact directly with cellular membranes (Hornebeck *et al.*, 1986; Robert *et al.*, 1986).

Proteoglycans (PGs) consist of glycosaminoglycan (GAG) chains covalently linked normally to a core glycoprotein. The presence of GAGs allows proteoglycans to form gels of varying 'pore' size and therefore can serve as size and charge sieves regulating molecular traffic through the matrix (Wight *et al.*, 1987). Proteoglycans bind growth factors and by shifting the equilibrium between bound and free, can regulate cell proliferation (Schmidt *et al.*, 1987). They also bind proteolytic enzymes and their inhibitors and therefore by immobilising the enzymes at local sites can regulate enzymic activity (Alberts *et al.*, 1994).

Fibronectin is a disulfide-bonded dimer and multiple forms exist due to variations in the nature of the side chains. Soluble plasma fibronectin plays a role in enhancing blood clotting, wound healing and phagocytosis. Highly insoluble fibronectin molecules are found assembled at cell surfaces and within extracellular matrices and can interact with integrin cell membrane receptors to play a role in cell adhesion (Birdwell *et al.*, 1978). Other glycoproteins include the laminin family of ECM components.

The molecular composition of Bruch's membrane has been shown to be similar to that of most extracellular matrices and includes collagens of type I, III, IV, V and VI, proteoglycans such as heparan and chondroitin sulphate, and glycoproteins

such as laminin and fibronectin (Campochiaro *et al.*, 1986; Das *et al.*, 1990; Lin, 1989; Marshall *et al.*, 1994; Newsome *et al.*, 1987). However, the distribution of the individual components varies between layers of Bruch's membrane and is shown schematically in Figure 1.11.

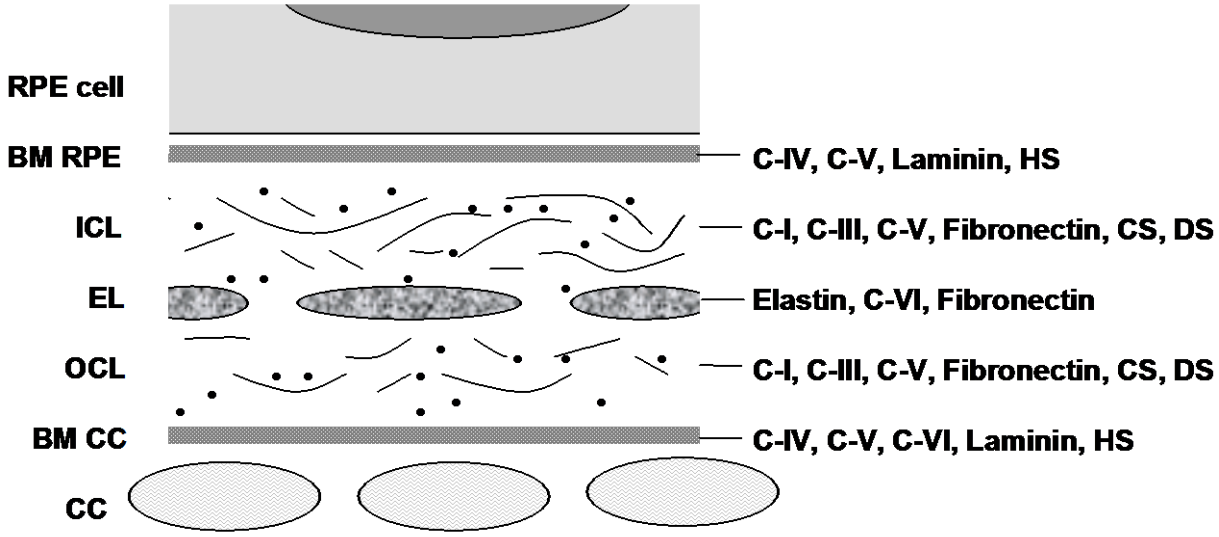

Figure 1.11 Schematic representation of Bruch's membrane with location of its ultrastructural components.

Abbreviations: BM, basement membrane; ICL, inner collageous layer; EL, elastin layer; OCL, outer collagenous layer; CC, choriocapillaris; C, collagen, HS, heparan sulphate; CS, chondroitin sulphate; DS, dermatan sulphate. After (Campochiaro *et al.*, 1986; Das *et al.*, 1990; Marshall *et al.*, 1993; Marshall *et al.*, 1994; Marshall *et al.*, 1992).

1.3.2 Homeostatic turnover of Bruch's membrane

To maintain the structural and functional properties of Bruch's, homeostatic ECM turnover of the membrane is a critical requirement. A tightly controlled balance

of coupled synthesis and degradation processes regulate the turnover of Bruch's. The degradation pathway is mediated by a family of proteolytic enzymes called the matrix metalloproteinases (MMPs) (Birkedal-Hansen et al., 1993; Woessner, 1991). Secretion of MMPs 1, 2, 3 and 9 by the RPE and choroidal endothelium cells has been shown and their presence in Bruch's has been demonstrated (Alexander et al., 1990; Guo et al., 1999; Hunt et al., 1993; Vranka et al., 1997). The proteolytic activity of MMPs is controlled by the presence of tissue inhibitors of MMPs (TIMPs), which are represented by four gene products. TIMP2 and TIMP3 has been localised in Bruch's membrane. Among the TIMPs, TIMP3 is unique in that that it exists bound to the matrix of Bruch's membrane (Fariss et al., 1997; Vranka et al., 1997). A disturbance of the synthesis and degradation pathways for matrix turnover and renewal can cause severe dysfunction in Bruch's membrane. Mutations in the TIMP-3 gene leads to an early-onset form of macular degeneration called Sorsby's fundus dystrophy, characterised by a thick (~30μm) deposition of lipid-rich material on top of Bruch's (Fariss *et al.*, 1998; Weber *et al.*, 1994). Although mutations in the TIMP3 gene are not associated with AMD (De La Paz *et al.*, 1997), strong associations for higher risk of AMD have been reported near the TIMP3 locus (Chen *et al.*, 2010; Neale *et al.*, 2010). Mutations in molecules that normally interact with the MMP system can also lead to abnormal ECM turnover (Klenotic *et al.*, 2004). Thus a mutation in the TIMP-3 binding epidermal fibulin-like extracellular matrix protein 1 (EFEMP1) is responsible for the hereditary macular degenerative disease, Malattia Leventinese (Marmorstein *et al.*, 2002).

1.3.3 The matrix metalloproteinase family

1.3.3.1 Structure of MMPs

The first member of MMP family, collagenase, was identified in 1962 in tadpole tails and could degrade fibrillar collagen. A family of structurally related collagenases, 23 members in humans (24 members in mice) has now been documented and referred to as the MMP family. MMPs belong to the metzincin superfamily of proteases, named after the presence of a zinc ion and a methionine residue at the active site.

Other high molecular weight gelatinases (representing dimers and polymers) have been identified. In human and dog brain, a 280 kDa gelatinase species that reacted with antibodies to MMP9 has been documented (Lim *et al.*, 1997). Similarly, in human Bruch's membrane, two high molecular weight forms (130 and 225 kDa) were identified and suggested to be mono- and hetero-dimers of MMPs 2&9 (Guo *et al.*, 1999).

Most MMPs share conserved domain structure containing an invariant Cys residue at the active site, the catalytic domain with active site zinc ion, a hinge region, and a C-terminal hemopexin-like domain which attaches to the catalytic domain by a flexible hinge (Figure 1.12).

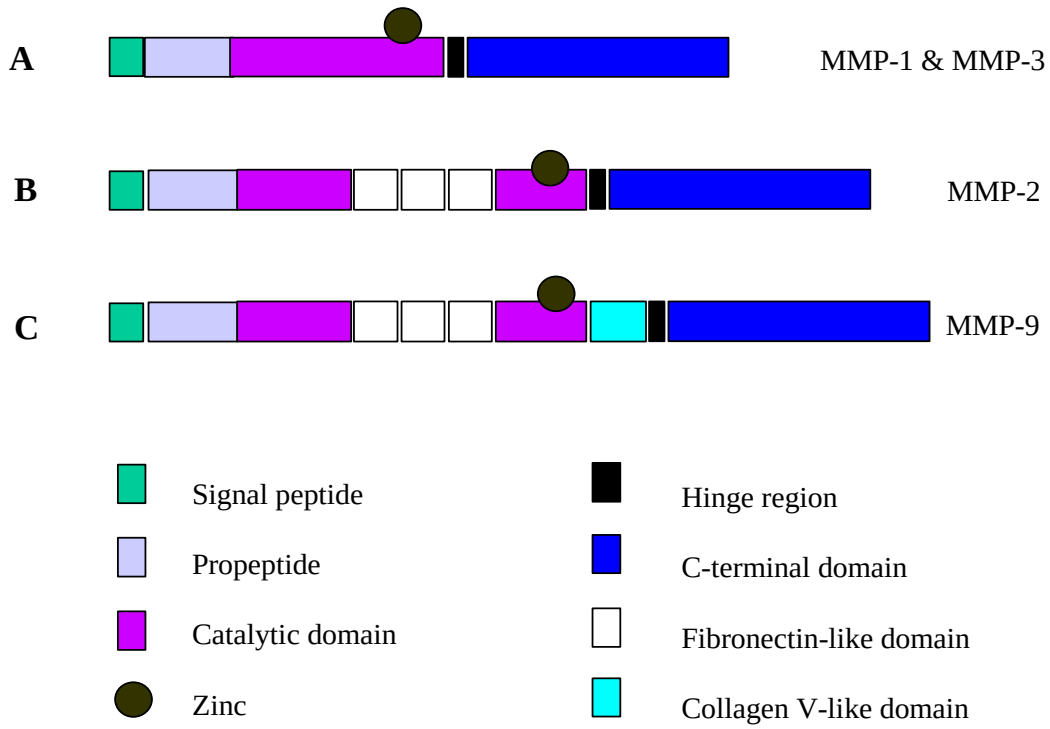

Figure 1.12 Protein structure of MMPs.

Panel A, domain structure of majority of members of MMP family including MMP-1 and MMP-3. Four domains are signal peptide, propeptide, catalytic domain with Zn++ binding site, and C-terminal hemopexin domain. Panel B, MMP-2 domain structure, the catalytic domain is separated by the 'fibronectin' domain. Panel C, MMP-9 domain structure, a 'collagen V' is inserted between catalytic domain and C-terminal domain. After (Matrisian, 1992; Sato *et al.*, 1994; Woessner, 1991)

The pro-peptide

Most of the MMPs are released as inactive zymogens with a pro-peptide domain that needs to be cleaved for activation of the enzyme, referred to as the "cysteine switch" activation mechanism (Van Wart et al., 1990). The pro-peptide domain contains an invariant Cys residue that ligates the active site zinc ion to prevent catalysis, keeping the enzyme in an inactive state.

The catalytic domain

The active site of MMPs is formed in the catalytic domain, and the catalytically important Zn^{2+} ion is bound to three histidine residues in the HEXGHXXGXXH zinc-binding motif. The gelatinases (MMP2 and MMP9) have three fibronectin type repeats (which mediate binding to collagens) encoded in their catalytic domain.

The hinge region

The catalytic domain links to C-terminal domain by a hinge region.

The hemopexin-like C-terminal domain

The hemopexin domain has a four bladed β propeller structure that provides a flat surface and mediates protein-protein interaction such as substrate recognition, enzyme activation, and protease localization (Overall, 2002). This domain interacts with tissue inhibitors of matrix metalloproteinases (TIMPs).

The gelatinases (MMP2 and MMP9) contain an additional fibronectin-like domain that is believed to facilitate binding to their gelatin substrates. The 'collagen V' domain has homology to type V collagen and is found only in MMP9 (Matrisian, 1992; Matrisian, 1990; Woessner, 1991).

The five members of the MT-MMP family have three additional insertions. The first one is inserted in the pro and catalytic domains, the second in the catalytic domain, and the third in the C-terminal domain (Basset *et al.*, 1990; Sato *et al.*, 1994).

1.3.3.2 Substrate specificity of MMPs

The members of the MMP family are divided into several groups. The three major groups, based on substrate preferences comprise collagenases, gelatinases and the stromelysins (Murphy *et al.*, 1991). Another group comprises the membrane-type MMPs (MT-MMPs) and these are not secreted but are an integral part of the plasma membrane (Sato *et al.*, 1994). The substrate specificity of these various MMPs is given in Table 1.1. From the composition of structural elements and the broad substrate specificities of the proteolytic enzymes, it is clearly discernable that activated MMPs can degrade nearly all components of the matrix of Bruch's membrane.

The members of the MMP family are listed in Table 2. However, additional species also occur from dimerization and polymerisation processes (Guo *et al.*, 1999; Lim *et al.*, 1997). MMP9 can also exist in dimeric or polymeric latent and active forms but the biological significance of these transitions is not known (Goldberg *et al.*, 1992). However, dimerization is known to significantly reduce the rate of activation of pro-MMP9 by MMP3 (Olson *et al.*, 2000). Since dimerization/polymerisation is sensitive to thiol reduction, the interaction is thought to be disulphide mediated but the origin of the participating cysteines is not known (Goldberg *et al.*, 1992; Olson *et al.*, 2000). Interestingly, deletion mutants of MMP9 lacking the O-glycosylation (OG) domain were only observed as monomers (Van den Steen *et al.*, 2006). There is evidence that the hemopexin domain in MMP9 can participate in dimerization/polymerization via non-covalent and mainly hydrophobic interactions (Bjorklund *et al.*, 2004; Cha *et al.*, 2002)

Group	Name	MMP Number	Molecular Mass (kDa) Latent	Molecular Mass (kDa) Active	Substrate	Activator	Inducers*
Collagenases	Interstitial collagenase	MMP-1	55	52	Collagen I, II, III, VII, X Gelatin, proteoglycans	Plasma, MMP-3, MMP-7, MMP-10	TNFα, IL-1β. PDGF, phorbol
	Neutrophil collagenase	MMP-8	75	58	Collagen I, II, III, proteoglycans	MMP-3, -7, -10	TNFα, IL-1β.
	Collagenase 3	MMP-13	65	55	Collagen I, II, III, IV, gelatin, PCP, fibronectin	MT-MMP	LIF, TNFα, IL-1β.
Gelatinases	Gelatinase A	MMP-2	65/72#	58/66#	Gelatin, laminin, Collagen I, IV, V, VII, XI, fibronectin, elastin	MT-MMP	TGFβ
	Gelatinase B	MMP-9	92	84	Gelatin, Collagen IV, V, VII, fibronectin, elastin	Plasmin, MMP-2	TGFβ, TNFα, IL-1β, phorbol
Stromelysins	Stromelysin 1	MMP-3	57	46	Collagen II, III, IV, V, IX, X, XI, laminin, fibronectin, elastin, gelatin, proteoglycans, procollagen,		TNFα, EGF, IL-1β,, phorbol
	Stromelysin 2	MMP-10	57	46	Similar to stromelysin 1		
	Stromelysin 3	MMP-11	51	44	Gelatin, fibronectin, proteoglycans, α1 protease inhibitor		
	Uterine (PUMP-1)	MMP-7	28	19	Gelatin, fibronectin, laminin, Collagen IV, procollagenase, proteoglycans		LPS
MT-MMPs	MT1-MMP	MMP-14	64	54	ProMMP-2, proMMP-13, collagens, PCP, fibronectin, tenascin		TNFα, EGF, IL-1β,, phorbol
	MT2-MMP	MMP-15	72	61	Similar to MT1-MMP		
	MT3-MMP	MMP-16	66	55	ProMMP-2		
	MT4-MMP	MMP-17	?	54	ProMMP-2		
	MT5-MMP	MMP-24	63	62	ProMMP2		
Others	Matrilysin	MMP-7	28	20	Collagen IV, PCP, fibronectin, gelatin		
	Metalloelastase	MMP-12	54	45	Elastin		

∗TGFβ=transforming growth factor β; TNFα=tunor necrosis factor α; IL-1β=interleukin-1β; LPS=lipopolysaccharide; EGF=epithelial growth factor; PDGF=platelet derived growth factor; LIF=leukemia inhibitory factor; WBC=white blood cell; # Reduced

Ref. 1. Woessner, 1991; 2. Matrisian, 1992 ; 3. Dollery *et al.*, 1995; 4. Sato et al, 1997; 5. Li et al, 2000; 6. Sethi et al, 2000

Table 1.1 Characteristics of the members of the MMP family.

1.3.3.3 Control and regulation of MMP activity

Regulatory control of MMP function is complex and occurs at three levels of transcription, activation of latent proenzymes, and inhibition of proteolytic activity. A number of cytokines and growth factors have been shown to stimulate the synthesis of MMPs including interleukin-1 (IL-1), platelet-derived growth factor (PDGF), and tumor necrosis factor-α (TNF-α), whereas others, such as transforming growth factor-β (TGF-β), heparin, and corticosteroids, have an inhibitory effect (Table 1.1) (Nagase, 1996; Sethi *et al.*, 2000). In addition, cell-matrix and cell-cell interactions are also involved in MMP gene expression (Biswas *et al.*, 1995; Malik *et al.*, 1996; Tremble *et al.*, 1994).

1.3.3.3.1 General activation of MMPs

MMPs are secreted as latent pro-enzymes and are activated by the loss of a N-terminal pro-peptide sequence of about 80 amino acids (Bode *et al.*, 2003). A cysteine in the pro-domain coordinates with the zinc ion at the catalytic site and thereby occludes the active site (Elkins *et al.*, 2002; Morgunova *et al.*, 1999). The catalytic zinc is situated in a shallow cleft and accessibility (after removal of the pro-peptide) will determine substrate specificity for proteolysis (Solomon *et al.*, 2007).

Pro-MMPs are normally activated in vivo by other proteases such as tissue kallikrein, trypsin, and other MMPs (Ra *et al.*, 2007). As stated earlier, activation involves the dissociation of the cystein from the active site zinc ion followed by sequential removal of the pro-peptide. Pro-MMPs can also be activated in-vitro by

aminophenyl mercuric acetate (APMA) and other S-reactive reagents and with reactive oxygen species and detergents. In the case of APMA, activation proceeds to the removal of the pro-peptide whereas sodium dodecyl sulphate (SDS) exposure leads to enhanced proteolytic activity without loss of the pro-peptide.

Latent pro-MMPs can be activated by plasmin in the urokinase-plasminogen cascade (Murphy *et al.*, 1992; Nagase *et al.*, 1990; Sperti *et al.*, 1992). The role of urokinase plasminogen activator (uPA) and its specific receptor (uPA-r) and inhibitors (PAI) has been studied in relation to tissue invasion and cell surface proteolysis (Liotta *et al.*, 1991). The binding and activation of uPA on its receptor appears to provide a mechanism for localizing proteolytic activity at the leading edge of the invading cell (Kirchheimer *et al.*, 1989). Urokinase converts plasminogen, a component of plasma and interstitial fluids, into the active enzyme plasmin. Plasmin can recognize and cleave basic resides in the 'pro' domain of both collagenase and stromelysin enzymes resulting in activation of the enzymes. Activated stromelysin is autoproteolytic and cleaves itself at the phenylalanine residue at position 98, removing the entire 'pro' domain and resulting in a permanently active, low molecular weight form of the enzyme. Plasmin activation of collagenase makes this enzyme more susceptible to proteolytic cleavage by stromelysin (Nagase *et al.*, 1991).

1.3.3.3.2 Allosteric control of MMP activity

The activity of MMPs can also be regulated by allosteric control. Allosteric control means the ability to modify the activity of an enzyme by protein and ligand interactions at sites away from the catalytic site. The modular construction of pro-MMPs appears to be ideal for exercising such control. In pro-MMP9, the molecule is

thought to possess an elongated structure consisting of two globular domains separated by an unstructured and flexible 3nm long O-glycosylated (OG) domain (Rosenblum *et al.*, 2010). This flexibility allows varied conformational states that may be important in its activation and proteolytic function. The flexibility of the OG region means that the terminal domains have independent movement allowing protein-substrate interactions such as enzyme translocation on collagen fibrils (Overall *et al.*, 2007; Rosenblum *et al.*, 2010). The allosteric control is also thought to underlie the dimerization of MMP9 via the hemopexin and linker domains (Van den Steen *et al.*, 2006).

In the proteolytic cleavage of pro-MMP9 by kallikrein, the binding of kallikrein results in the disruption of the cystein mediated complexation of the active site zinc ion followed by proteolysis (Rosenblum *et al.*, 2010). Similarly, allosteric interaction by β-hematin with the hemopexin region of MMP9 destabilises the enzyme through conformational changes progressing to autocatalysis (Geurts *et al.*, 2008).

1.3.3.3.3 Activation of pro-MMP2

Triple helical collagens are resistant to proteolysis by most proteases but MMP2 is one of five collagenases capable of attacking such structures. Triple helices are generally broken into 3/4 and 1/4 fragments that can then be degraded by other MMPs. MMP2 contains a fibronectin repeat domain (FRD) for binding to collagen and gelatin and results in unwinding of the triple helix (Gioia *et al.*, 2007; Tam *et al.*, 2004). The catalytic and hemopexin domains work together to unwind triple-helical structure of collagen prior to cleavage (Chung *et al.*, 2004).

The activation mechanism of pro-MMP2 on the basolateral surface of the RPE has been investigated. Activation requires, in addition to membrane bound MT14, free and mobile levels of TIMP2 and pro-MMP2 (Butler *et al.*, 1998; Strongin *et al.*, 1995). The mechanism requires two molecules of MMP14; the first MMP14 molecule binds TIMP2 and this enables the formation of the ternary complex with pro-MMP2. A second MMP14 molecule then cleaves the pro-form to release active MMP2. Thus, efficient activation requires the presence of MMPs and TIMPs in optimum concentrations near the basolateral surface of the RPE. Age related alterations that reduce the free level of MMPs are therefore likely to compromise the activation of the MMP degradation system.

1.3.3.3.4 Tissue inhibitors of matrix metalloproteinases (TIMPs)

The proteolytic activity of MMPs can be inhibited by a 1:1 noncovalent binding to a family of protein inhibitors called TIMPs. TIMPS inhibit MMPs by inserting a conserved anchor into the active site of the target MMP. It should be noted that in plasma, inhibition of MMPs can also occur on binding to several proteins such as a_2-macroglobulin (Birkedal-Hansen *et al.*, 1993; Woessner, 1991). TIMP1, TIMP2, and TIMP4 are present in soluble forms, but TIMP3 is unique in that it is insoluble and bound to the extracellular matrix (Leco *et al.*, 1994).

Members of the TIMP family show about 40% sequence homology (Murate *et al.*, 1999; Murphy *et al.*, 1995). All TIMP's possess 12 cysteine residues in conserved regions of the molecule, forming six disulfide bonds that are essential for

maintaining the correct tertiary structure of the molecule. They also contain an amino terminal group that is responsible for inhibiting MMP activity and a C-terminal that controls autocatalytic activation (DeClerck *et al.*, 1993; Gomez *et al.*, 1997; Murphy *et al.*, 1991). TIMPs consist of between 184 (TIMP1, MW 25-36 kDa) and 194 amino acid residues (TIMP2) and apart from TIMP1 that is heavily glycosylated, the other members have been isolated in unglycosylated forms (TIMPs 2, -3; MW 21 kDa) (De Clerck *et al.*, 1989; Goldberg *et al.*, 1989; Pavloff *et al.*, 1992; Stricklin *et al.*, 1983).

TIMPs can also be regulated at the transcriptional level. For example, interleukin-1ß (IL-1 ß) and phorbol esters (PMA) stimulate TIMP-1 expression in cultured human fibroblasts (Overall, 1994), whereas TGF-1ß and retinoids downregulate the expression of TIMP1 (Clark *et al.*, 1987; Overall *et al.*, 1991). In RPE cells, expression of MMP's and TIMP's is upregulated by phorbol (Alexander *et al.*, 1990).

The TIMP1 gene has a TATA-less promoter which contains multiple responsive elements that respond to cytokines and many other agents (Campbell *et al.*, 1991; Edwards *et al.*, 1992). In contrast to the highly stimulus-responsive TIMP1 promoter, the TIMP2 promoter is unresponsive to cytokines (Shapiro *et al.*, 1992). Like TIMP1, TIMP3 can be regulated in vitro by an array of stimuli that influence ECM remodelling, including a tumor promoter, growth factors, cytokines and anti-inflammatory agents, and show that the on/off transcription kinetics are faster for TIMP3 than for TIMP1 (Leco *et al.*, 1994).

In summary, there are three situations where the regulation of MMPs is required. Firstly, MMPs are required at the leading edge of an invasive cell so that the ECM in front can be disassembled allowing the transit of the cell. Localised

transcriptional activation can then furnish large quantities of activated MMPs at the site of required action. Excessive MMPs at the locality can thus overcome the low endogenous presence of TIMPs. The potential for damage from the leakage of active MMPs away from the site of action is then combated by presence of TIMPs and other plasma inhibitory factors such as a_2-macroglobulin (Birkedal-Hansen *et al.*, 1993; Woessner, 1991). Secondly, activated MMPs may be released continuously to maintain a tightly coupled cycle of synthesis and degradation in order to continually renew the ECM despite the presence/absence of damaged elements. The basal release and activation of MMP2 has often been thought of contributing to this constitutive process in Bruch's membrane. Thirdly, MMPs may be released in response to damaging stimuli generated from the ageing process but very little is known of the mechanisms involved.

1.3.4 MMPs and TIMPs in ageing and retinal degeneration

In vitro serial subcultivation (mimicking ageing) of human fibroblasts has shown that basal levels of mRNAs encoding collagenase and stromelysin enzymes increase (Millis *et al.*, 1992). Similarly, synthesis and secretion rates of pro-collagenase and pro-stromelysin proteins are elevated in the late-passage (senescent) compared to early-passage (young) cells (Bauer *et al.*, 1985; Bauer *et al.*, 1986; Millis *et al.*, 1992). However, the expression of TIMP1 mRNA was lower in aged compared to younger cells. Interestingly, the changes in MMPs and TIMP1 associated with ageing cells were also observed in Werner syndrome, a condition of premature senescence (Millis *et al.*, 1992; Sottile *et al.*, 1989). In contrast to TIMP1, TIMP2 mRNA and protein levels increased in aging fibroblast cells and were

accompanied by an increase in levels of newly synthesized MMP2-TIMP2 complexes (Zeng *et al.*, 1994). Cultured human RPE cells also exhibit an age-related increase of MMP2 in late-passage (Padgett *et al.*, 1997).

Ageing of Bruch's membrane was associated with an increase in the level of proMMPs 2&9 (Guo *et al.*, 1999). Levels of active MMP2 were frequently observed in the periphery but rarely at macular locations. This may reflect slower ageing in the periphery similar to the slower decline in transport functions mentioned earlier.

Both levels of TIMP3 protein and MMP-inhibitory activity showed an age-dependent increase in the human RPE-choroid complex (Kamei *et al.*, 1999). In addition, immunoreactivity for TIMP3 was intense across Bruch's membrane in AMD and other retinal degenerative diseases such as retinitis pigmentosa and Sorsby's fundus dystrophy (SFD) (Fariss *et al.*, 1998; Kamei *et al.*, 1999).

1.3.4.1 Altered expression of TIMP3 in Sorsby's

Sorsby's fundus dystrophy (SFD) is an early-onset, inherited retinal degeneration. The clinical features are similar to AMD but with earlier onset of symptoms leading to loss of central vision. Mutations in the TIMP3 gene of patients with this rare disorder associated with accumulation of lipid-rich extracellular deposits and characterized by thickening of Bruch's membrane (Fariss et al., 1998; Weber et al., 1994). TIMP3 is synthesized and secreted by the RPE and is present in normal Bruch's membrane. Sorsby's patients showed extensive accumulation of TIMP3 in thickened Bruch's (Fariss et al., 1998). Overexpression of TIMP3 may affect degradative processes for matrix turnover and cause lipid-rich deposition in

SFD. This rare hereditary disorder demonstrates the importance of tightly regulated homeostatic turnover of the ECM for maintaining the integrity of Bruch's membrane.

1.3.4.2 MMP9 polymorphisms in AMD

Previous reports have shown reduced levels of active MMP2 and MMP9 in macular regions of human Bruch's membrane in comparison to peripheral regions (Guo et al., 1999). Pro-MMP enzymes need activation for catalytic function and reduction of active forms in aging Bruch's implies dysfunctional turnover of the membrane. Although active MMPs were reduced, their pro-forms showed an age-dependent increase (Guo et al., 1999).

Transcriptional levels of MMP9 are regulated by polymorphisms in the promoter region of the MMP9 gene (Peters et al., 1999; Shimajiri et al., 1999; Ye, 2000). The polymorphisms are in the microsatellite region with variations in the number of Cytosine-Adenine (CA) repeats. In animal models, the number of CA repeats correlates with level of gene expression. MMP9 activities were reduced to 50% when the number of CA repeats was shortened from 21 to 14 (Shimajiri et al., 1999). Furthermore, in mesangial cells, MMP promoter carrying 24 CA repeats showed more than 20 times higher expression compared to 20 repeats (Fornoni et al., 2002). An association between exudative AMD and number of CA repeats in the MMP9 promoter region has been reported. Longer microsatellites with 22 repeats or more CA repeats were associated with exudative AMD patients (Fiotti et al., 2005). This association between the higher CA repeats and AMD could explain the raised levels of plasma MMP9 in these patients (Chau *et al.*, 2008).

1.4 Problems prior to the commencement of this thesis

Although previous studies had identified the importance of two MMP species in the age-related modulation of the structure of Bruch's membrane, an understanding of age related changes in such molecules and consequences for transport mechanisms were effectively unknown. Specifically the following problems required empirical studies in order to elucidate their relative importance.

1. Previous work had shown the presence of high molecular weight species (HMW1&2) in human Bruch's but their monomeric composition and physiological significance to the remodeling process of the membrane was not known.

2. The existence of a dynamic equilibrium between free and bound MMP species, crucial in determining the level of pro-MMPs available for activation was unknown. Therefore the likely impact of age-related alterations in these compartments on the operation of the MMP system could not be ascertained.

3. Despite the presence of micro-satellite polymorphisms in the promoter region of the MMP9 gene and elevated levels of plasma pro-MMP9 levels in AMD patients, corresponding alterations in and likely effects on the MMP system of Bruch’s membrane had not previously been addressed.

4. The inter-relationships between the various gelatinase species in normal and AMD Bruch's were unknown.

5. The relevance of excessive deposition of divalent metals in Bruch's and choroid of elderly and AMD donors on the structural and functional characteristics of the membrane was unclear. A better understanding is a prerequisite for contemplating metal chelation therapy.

1.5 AIMS of the thesis

The overall aim of this thesis was to explore the major enzymatic frame work involved in the processes that maintain Bruch's membrane as a functional entity over a human life span. In order to facilitate such an understanding, it was deemed important to identify age-related changes in the level of individual MMP species and their inter-compartmental distribution together with the degree of sequestration that would be expected to impact on the activation of MMPs and therefore on the transportation properties of Bruch's membrane. An understanding of the MMP pathway and its alteration due to the advanced ageing process in AMD is an essential prerequisite for developing strategies for therapeutic intervention. Specific aims were as follows:

To understand the gelatinase system of Bruch's so as to allow therapeutic modulation to address the age-related failure in the transport properties of the membrane.

- To quantify age-related changes in the spectrum of gelatinases within human Bruch's membrane by utilising gelatin zymography
- To determine the equilibrium between bound and free level of individual gelatinase species using perfusion techniques
- To determine the gelatinase composition of the high molecular weight (HMW1 and HMW2) species by fragment analyses
- To determine the gelatinase composition of the high molecular weight (HMW1 and HMW2) species by Western blots with antibodies for MMP2 and MMP9

To quantify changes in the gelatinase system of Bruch's in both normal ageing and in AMD.

- Using the above, to construct the gelatinase pathway of Bruch's membrane to describe the age-related changes in individual components of the MMP system
- To evaluate the role of the gelatinase pathway, if any, in the pathophysiology of age-related macular degeneration (AMD)

To assess the potential for modulating the gelatinase system of Bruch's membrane in an effort to delay the ageing process.

- To assess the possibility of disturbing the free-bound equilibrium to cause the release of monomeric (pro and active) MMP species using a divalent metal chelator in order to improve transport through the membrane
- To assess the potential of enhancing the hydraulic conductivity of Bruch's following chelator mediated release of and/or conversion to active forms of MMPs

CHAPTER 2

GELATINASE SYSTEM OF HUMAN BRUCH'S MEMBRANE

2 GELATINASE SYSTEM OF HUMAN BRUCH'S MEMBRANE

2.1 INTRODUCTION

The matrix metalloproteinase (MMP) system plays an important role as the degradation arm of a continuously remodelling process that renews the extracellular matrix of Bruch's membrane. The gelatinase component of the MMP system, comprising pro-MMPs 2 & 9, has been shown to be secreted by both RPE and choroidal endothelium cells and its presence in Bruch's has been demonstrated (Alexander *et al.*, 1990; Guo *et al.*, 1999; Hunt *et al.*, 1993; Vranka *et al.*, 1997).

The pro-MMPs are inactive or latent enzymes that are normally activated physiologically by removal of an inhibitory pro-peptide of about 10 kDa (Ahir *et al.*, 2002; Matrisian, 1992; Murphy *et al.*, 1997). However, on exposure to sodium dodecyl sulphate (SDS), the enzymes undergo conformational changes leading to partial activation without loss of the inhibitory pro-peptide. Thus on gelatin zymography, these pro-MMPs 2 & 9 can be detected by their proteolytic action on the gelatin substrate and display molecular weights of 92 and 65 kDa respectively (Guo *et al.*, 1999). In the laboratory, the pro-peptide can also be removed with thiol reacting agents such as aminophenyl mercuric acetate (APMA) leading to full activation (Brown *et al.*, 1994; Woessner, 1991).

Transition to activated forms occurs via a series of intermediate structures. Thus for pro-MMP9 (MW 92 kDa), a transitory 88 kDa active form is observed

followed by its conversion to the fully activated 84 kDa enzyme. The 65 kDa pro-MMP2 enzyme is converted to the fully activated 58 kDa form, with the occasional presence of the partially activated 61kDa species (Ahir *et al.*, 2002; Guo *et al.*, 1999).

In aqueous solutions, MMPs can undergo dimerisation and polymerisation by non-covalent interactions but the physiological significance of this conversion is not known (Goldberg *et al.*, 1992; Guo *et al.*, 1999; Lim *et al.*, 1997). There is some evidence that dimerisation can significantly reduce the rate of activation of pro-MMP9 by MMP3 (Olson *et al.*, 2000). Because of the non-covalent nature of the interaction, such polymeric species are reduced to their monomeric states during preparation and processing for zymography. Thus these loosely associated polymeric forms cannot be detected as intact complexes by zymography.

Presence of additional gelatinase species, of much higher molecular weight than the pro-MMPs 2 & 9, have been shown on zymographic gels. Their existence in zymographic gels shows that the dimeric or polymeric forms must be stabilised by covalent bonding. In canine brain specimens, an additional gelatinase was characterised by a molecular weight 280 kDa. In human brain specimens from donors with Alzheimers disease, the presence of two high molecular weight species, 130 and 280 kDa has also been documented. The 280 kDa species was shown to react positively to MMP9 antibodies but the likelihood of the additional presence of MMP2 was not investigated. Interestingly, APMA activation resulted in reduction of molecular weight to 270 kDa (Lim *et al.*, 1997). Thus it would appear that only one MMP9 or MMP2 molecule in this complex was accessible to activation. This result suggests that the other molecules in this complex were protected from activation and may have implications for physiological activation.

Human Bruch's-choroid has also been shown to house two high molecular weight MMP species running at 225 and 130 kDa (Guo *et al.*, 1999). APMA activation resulted in a reduction in molecular weight in both species. The combination of APMA activation and reduction and alkylation resulted in loss of high molecular weight species with an increase in the amount of activated MMP9 indicating the presence of this monomer in the intact complex.

The gelatinase system has been implicated in the structural and functional demise of ageing human Bruch's membrane. This largely arose from the demonstration of accumulation of altered and denatured collagen in ageing Bruch's suggestive of a dysfunctional MMP system (Karwatowski *et al.*, 1995). The concept was further supported by the observation that active forms of MMP2 were frequently present in peripheral locations but only occasionally in macular regions (Guo *et al.*, 1999). Similarly, levels of TIMP3 and AGEs were elevated in ageing Bruch's, the former being a natural inhibitor and the latter known to compromise the proteolytic activity of MMPs (Haas *et al.*, 1998; Kamei *et al.*, 1999; Rittie *et al.*, 1999; Scott *et al.*, 1998).

An understanding of the mechanisms that compromise the activity of the gelatinase system requires a knowledge of the participating species, their interactions such as monomer to polymer formation (and hence sequestration of activity), and their compartmentalisation between bound and free states since this will control the amount of pro-enzyme available for activation. A previous study has reported that the levels of both pro-MMPs 2&9 increased with age. But in this study, only MMPs that could be extracted with Tris-HCl buffer containing 0.25% Triton X-

100 were quantified without any evaluation of the amount in the bound form (Guo *et al.*, 1999).

The present study was designed to characterise all the gelatinase species in human Bruch's-choroid with respect to their molecular weights, to determine the level of bound and free enzymes as a function of age, and to analyze the composition of the high molecular weight species with respect to their monomeric constitution.

ELISA techniques are normally used to quantify the level of specific proteins in a tissue extract but these are not applicable for the determination of gelatinase species for the following reasons. Firstly, the antibodies often cross-react and secondly they cannot differentiate between pro- and active forms of the gelatinases. Thirdly, antibodies specific to the high molecular weight forms have not yet been manufactured. Quantitative zymography is the only technique currently available that can separate all the gelatinase species. Complications that can arise from instability of MMPs under SDS denaturing conditions, and from variations in background staining and gel-to-gel variation were first addressed followed by quantification of specific species present in human Bruch's membrane.

2.2 METHODS

2.2.1 Tissue preparation

Human donor eyes were obtained from Bristol Eye Bank (Bristol, UK). Eyes with corneas removed for transplantation surgery were delivered in saline filled containers packed in ice, within 72 hours post-mortem time. Previous studies had shown structural and functional integrity of Bruch's and RPE for a period of up to 72 hours post-mortem (Hussain *et al.*, 1985; Moore *et al.*, 1995). Of the 29 donor eyes used in the ageing study (age range 21-99 years), post-mortem times were 36 hours for two donors, 57 hours for one donor, and the remainder were within the 37 to 50 hours.

A circumferential incision was made to remove the remaining anterior portion of the globe. The fundus was examined with a dissecting microscope to ensure that it was free from gross handling artefacts. An eight millimetre full thickness trephine, centred on the fovea, was removed for other on-going studies. A similar full thickness trephine was obtained from the peripheral region along an imaginary line lying on the meridian joining the fovea, optic disc, and the cut edges of the globe and used in the ageing study.

The isolated tissue discs were transferred to a Petri dish containing PBS with an antibiotic / antimycotic mixture (Sigma-Aldrich, Poole, UK). Retinal tissue was removed from the tissue button with fine forceps and the RPE cells were gently brushed away with a camel's hair brush. The Bruch's-choroid preparation was gently isolated from the underlying sclera with blunt forceps. The remaining globe was cut

into quadrants and peripheral Bruch's choroid isolated in a similar fashion and stored at –70ºC.

2.2.2 Zymographic analyses

The zymographic gels used in this study were 10 % SDS PAGE (1mm thick) containing a 4 % stacking layer and 0.1 % gelatin in the separating layer. Samples prepared in non-reducing SDS sample buffer were applied to the gel lanes together with prestained protein molecular weight markers (Invitrogen, Paisley, UK) and 20 % fetal calf serum (FCS, Sigma-Aldrich) acting as an internal standard to correct for gel-to-gel variation in background staining. Electrophoresis was performed with the X-Cell SureLock Mini-Cell system (Invitrogen, UK).

After electrophoresis (150 V, 1 hour), gel cassettes were removed from the electrophoretic apparatus, gels carefully removed and following a quick rinse in distilled water, incubated for two half hour periods in 2.5 % Triton X-100 solution to remove SDS and re-nature the enzymes. Gels were then transferred to reaction buffer (50 mM Tris-HCL, 10 mM $CaCl_2$, 75 mM NaCl, and 0.02 % NaN_3, pH 7.4) and incubated at 37 ºC for 18 hours to allow digestion of the gelatin substrate. After incubation, gels were rinsed in distilled water and stained with SimplyBlue SafeStain (Invitrogen, UK) containing Coomassie G-250 for three hours. Destaining was carried out in distilled water for 1.5 hours.

Proteolytic activity of gelatinases was observed as clear bands on a blue background. The gels were scanned at a resolution of 2400 dpi (Epsom 3490 scanner; Surrey, UK) and stored in JPEG format. The scanned colour files were

uploaded into the gel analysis software package in greyscale format (Quantiscan, version 3.0; Biosoft, Cambridge, UK). Before analysis, colours were inverted and MMPs were then visualised as dark bands against a whitish background. Following software mediated background subtraction, the area under individual gelatinase bands was quantified. The pro-MMP9 band of the foetal calf serum sample was used as a reference for normalization, because the MMP2 band was often distorted and skewed. Areas representing individual gelatinase bands were normalized with respect to the area of the control FCS pro-MMP9 band and further corrected for dilution, and MMP activities calculated as densitometric area per 8-mm disc of tissue.

2.2.2.1 Variable parameters in quantitative zymography

Key parameters influencing the observed activity of gelatinases in zymographic gels are (i) stability of enzyme in the presence of SDS buffers, (ii) incubation time for hydrolysis of gel-embedded gelatin, (iii) variation in gel-to-gel running times during electrophoresis and (iv) variations in background and band staining between gels.

Tissue samples used for the assessment of these variables utilised quadrants from one or several eyes. Pooled tissue samples were macerated using a pestle and mortar in Tris-HCl buffer (100mM Tris, 0.15M NaCl, 10mM $CaCl_2$, 0.02% sodium azide, pH 7.5). The extract was centrifuged at 10,000g for five minutes and the supernatant removed for analysis. Depending on the number of eyes used, the volume of the tissue extract varied between 1.0 and 3.0 mls.

2.2.2.1.1 Stability of MMP activity in SDS buffers

MMP extracts mixed with SDS sample buffer and left overnight (at 4ºC) were found to have lost all proteolytic activity (data not shown). Thus time-dependency of exposure to SDS is a factor that should be considered during zymographic runs. Generally, extracts mixed with non-reducing SDS sample buffers are loaded onto zymographic gels immediately or within 5-10 minutes. With a large number of samples for analysis and the need for loading several gels, this period could vary up to 30 minutes. Furthermore, the electrophoretic run itself would take about 1 hour during which time the enzymes would also be exposed to SDS.

Thus stability of MMPs was assessed covering an exposure period to SDS sample buffer of 0-2 hours. For this study, the MMP extract was obtained from one eye (donor aged 67 years). After the relevant incubation period, samples were loaded into gel lanes for zymography.

2.2.2.1.2 Use of foetal calf serum to control for gel-to-gel variation

Gel-to-gel variation in expressed proteolytic activity can be controlled by incorporating known amounts of purified enzyme on each gel. However, commercially available gelatinases show variable ratios for active/inactive species and activities deteriorate considerably on storage. Foetal calf serum (FCS) on the other hand only contains inactive pro-MMPs 2&9 and has therefore been utilised as an internal control in zymographic runs. FCS also deteriorates on storage with aged samples showing broadening and skewing of pro-MMP2 bands and the emergence of high molecular weight species. There is also batch-to-batch variation. Once thawed and aliquotted, a new FCS batch nevertheless maintains the band intensity

for pro-MMP9 for about a month. Thus, FCS working solutions need to be renewed each month.

For standard zymographic estimations, gels after electrophoresis are incubated for 18 hours to allow proteolytic digestion of gelatin. Slight variations in the thickness of the gels, temperature fluctuations over the 18-hour incubation period, and variations in destaining time resulting in background alterations all lead to complications in quantitative zymography.

To assess the effectiveness of incorporating an internal FCS control to normalise for these variations, four identical gels were prepared incorporating FCS and tissue extracts but each gel was incubated for different times and staining and destaining periods were also varied randomly. Extracts were obtained from three donor eyes (age range 56 – 67 years), mixed with an equal volume of SDS sample buffer, and after electrophoresis, individual gels were incubated for 13, 16, 18 and 22 hours. The stained gels were scanned and the Quantiscan software used to subtract background and calculate the areas under individual gelatinase bands. The effectiveness of using FCS as an internal standard to correct for variations in gel band intensities was assessed.

2.2.2.1.3 Linearity between enzyme activity and band area

For quantitative work it is important to establish a relationship between amount of enzyme and corresponding area under the gelatinase band. A linear relationship is ideal but a non-linear relationship can also be used for quantitative purposes. Serial dilutions of both FCS and a tissue extract were run on zymographic

gels and the relationship between the amount of enzyme within each lane and the resulting area under individual gelatinase bands investigated.

2.2.3 Gelatinase species of human Bruch's-choroid

A tissue extract was obtained from two pairs of donor eyes (ages 75 & 83) and after mixing with an equal volume of SDS sample buffer, 10, 15, and 20ul aliquots were applied to lanes. A high range multicoloured molecular weight standard (71-500 kDa, Invitrogen) was also incorporated. After electrophoresis, the gel was photographed to obtain a record of the positions of the molecular weight standards. The gel was then developed in incubation buffer and after staining and scanning, the migratory distances of individual gelatinase species were obtained. Migratory distances of the standard molecular weights were also obtained. Logarithmic plots were then constructed to calculate the molecular weights of the individual gelatinase species.

2.2.4 Fragment analyses of high molecular weight gelatinase species

Previous studies had shown that the high molecular weight species disappeared from the zymographic gels when samples were pre-treated with APMA alone or in combination with reduction and alkylation (Guo *et al.*, 1999; Lim *et al.*, 1997). This procedure was repeated to confirm that the high molecular weight species could be fragmented. Next, an attempt was made to break up these species within a gel and then to separate the fragments so that individual components could be identified.

2.2.4.1 Activation of gelatinase species

Altogether, Bruch's-choroid preparations from 11 human donor eyes (age range 58-91 years) were macerated in a pestle and mortar and the suspension centrifuged at 10000g for 5 minutes to yield a MMP extract of 3.5 mls.

The following solutions were prepared for APMA activation, reduction and alkylation. A 20 mM solution of APMA was made by dissolving 0.07g in 0.1 ml DMSO and making up the volume to 10.0 mls with 0.1 N NaOH. Dithiothreitol (DTT, 20mM) was made by dissolving 0.03 g in 10.0 mls of Tris-HCl buffer. A 50 mM solution of iodoacetate (IAA) was made by dissolving 0.093 g in 10.0 mls of Tris-HCl buffer.

Two test tubes, each containing 0.75mls of tissue extract were pre-incubated at 37^{o}C for 15 minutes. 0.25 mls of Tris-HCl buffer was added to one of the tubes to act as control. APMA activation was initiated in the other tube by the addition of 0.05mls of 20mM APMA solution (final concentration 1mM). Following an incubation period of 1 hour, 0.1ml DTT solution was added to reduce the sample giving a final concentration of 2.0mM. After an incubation period of 30 minutes, 0.1 ml IAA (final concentration, 5mM) was added with a further incubation of 30 minutes.

At the end of the incubation period, both tubes were placed in an ice-bath for further processing. Each sample (40µl) was added to 40µl of SDS sample buffer and 15µl of this mixture was applied to a gel lane. Gels were then processed for zymography.

2.2.4.2 Fragment analysis using double electrophoretic separation

Activation by APMA results in the dissolution of the high molecular weight species as observed by gelatin zymography. If these complexes break up into their respective monomeric species, then it should be possible to identify the resulting species.

A single lane zymographic gel was prepared and 200µl of tissue extract was mixed with 200µl of non-reducing SDS sample buffer and the whole mixture layered into the single lane. Electrophoresis was carried out and the MMP enzymes re-natured by incubation in 2.5% Triton X-100 for 1 hour. The gel was then cut in two, one-half acting as control and the other half activated/reduced/alkylated as described in section 2.2.4.1. Thus the control half should have intact high molecular weight complexes whilst in the other half, the regions normally occupied by high molecular weight species should now contain the constituent monomeric species.

Thin slithers of the gel (40mm x 5mm) containing all the gelatinase species were cut out and mixed with non-reducing SDS buffer for 10 minutes (Figure 2.1). These were loaded onto a gelatin zymography gel containing only the separating layer. Electrophoresis was performed a second time and the gel processed for zymography to identify the resulting gelatinase species in the activated sample.

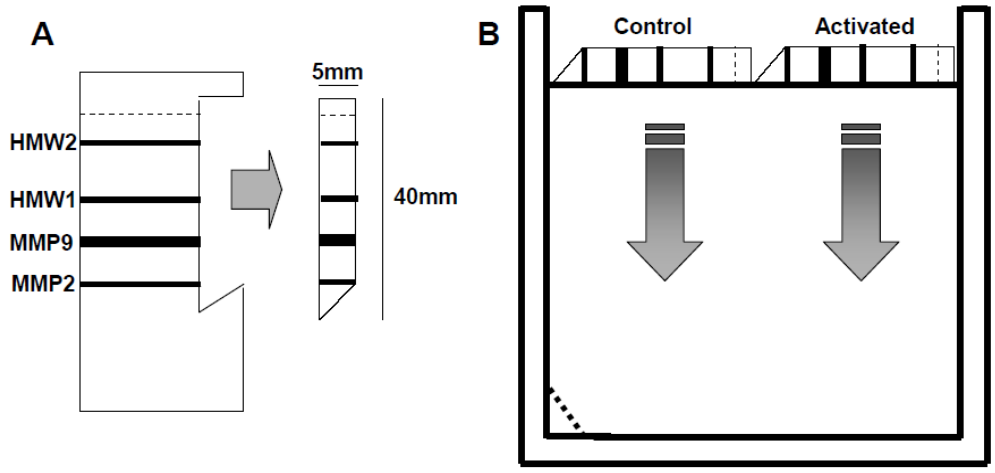

Figure 2.1 Schematic representation of the double electrophoretic procedure.

2.2.5 Subunit characterisation of high molecular weight species by Western blots

Four 8 mm peripheral trephines from each eye were pooled and homogenized in Tris-HCl buffer. They were centrifuged at 10,000 rpm for 30 minutes at 4 °C and supernatant was collected for analysis. The samples were subjected to SDS-PAGE. 10 % SDS-PAGE gels (1 mm thick) containing a 4 % stacking layer were prepared. Samples were loaded into lanes with ColorBurst Markers (Invitrogen, UK). Electrophoresis was performed for 1 hour at 150 V using the X Cell SureLock mini-Cell system (Invitrogen). Following electrophoresis, the gels were removed from their cassettes and rinsed in distilled water.

Proteins within the gel were transferred to nitrocellulose sheets by the iBlot Dry blotting system (Invitrogen, UK). The iBlot Anode Stack was placed in the bottom

and the pre-run gel was put on the transfer membrane of the anode stack. A water soaked iBlot sheet of filter paper was placed on top of the gel. Air bubbles present between the membrane and gel were removed by the Blotting Roller. The iBlot Cathode Stack was placed on top of the filter paper with the copper electrode sheet facing uppermost. Good electrical contact was again achieved by use of the roller. To remove extra solution during the performance, an iBlot disposable sponge was placed on the inner side of the lid.

Pilot experiments with transfer of FCS proteins carried out at 20 V running voltage had shown the time required for efficient transfer was about 6-8 minutes. Thus for extracts of Bruch's-choroid, a time of 7 minutes was chosen to carry out the transfer.

After the electrophoretic transfer, sponge and cathode stacks were discarded and the gel and filter paper carefully removed. The underlying nitrocellulose membrane was carefully removed and used for immunodetection or staining of proteins.

2.2.6 Ageing changes in the gelatinase system of Bruch's membrane

Free and bound pools of gelatinases of peripheral Bruch's-choroid were obtained as follows. The 8mm diameter sample of Bruch's-choroid was placed in an Eppendorf tube and 100 µl PBS added. The tube was vortexed every 5 minutes five times for a period of one minute. Tubes were then centrifuged for 5 minutes at 10,000 g and the supernatant removed. Twenty microliters of the supernatant

representing the free pool of MMPs was mixed with 40 µl of non reducing SDS sample buffer and 20 µl of this mixture was loaded onto zymographic gels.

The remaining tissue button was washed several times with 1.0 ml aliquots of PBS and pilot analysis (not reported) did not show any further release of MMPs. After washing and a final centrifugation procedure, the pellet of tissue was reconstituted with 20 µl water and 40 µl non-reducing SDS sample buffer. Then samples were vortexed for five minutes and centrifuged as described above. Finally, 20 µl of the supernatant, representing the bound or SDS-extracted fraction, was loaded onto zymographic gels. After controlling for gel-to-gel variation, the band areas for individual gelatinase species were plotted against the age of the corresponding donor.

2.2.7 Statistical analysis

Standard linear and non-linear regression analysis was applied using a commercial statistical package (Fig-Sys, Biosoft, Cambridge, UK) that utilised the Marquardt-Levenberg algorithm. Statistical significance of the Pearson's correlation coefficient were obtained by the t-statistic with N-2 degrees of freedom.

2.3 RESULTS

2.3.1 Gelatinase species of human Bruch's membrane

A zymogram of the releasable pool of gelatinase species extracted from Bruch's-choroid preparations from two donors aged 75 and 83 years is shown in Figure 2.2. Altogether, six gelatinase species were discernable. Logarithmic plots of migratory distance versus molecular weight were used to characterise individual species (Figure 2.2B). As shown in several other studies, pro- and active forms of MMP9 were characterised by molecular weights of 92 and 84 kDa respectively. Active MMP9 was just about discernable in the releasable pool of MMPs in these donors. This releasable species was found to be absent in most donors assessed. Pro and active forms of MMP2 were characterised by molecular weights of 65 and 58 kDa respectively. In addition, two high molecular weight species were routinely observed, running in these preparations with molecular weights of 150 and 348 kDa and now termed HMW1 and HMW2 respectively. A more comprehensive analysis of molecular weights determined individually and in pooled samples from several donors has provided molecular weights for HMW1 & 2 of 122 ± 9kDa and 344 ± 22kDa (Mean±SD(n), n=24) respectively.

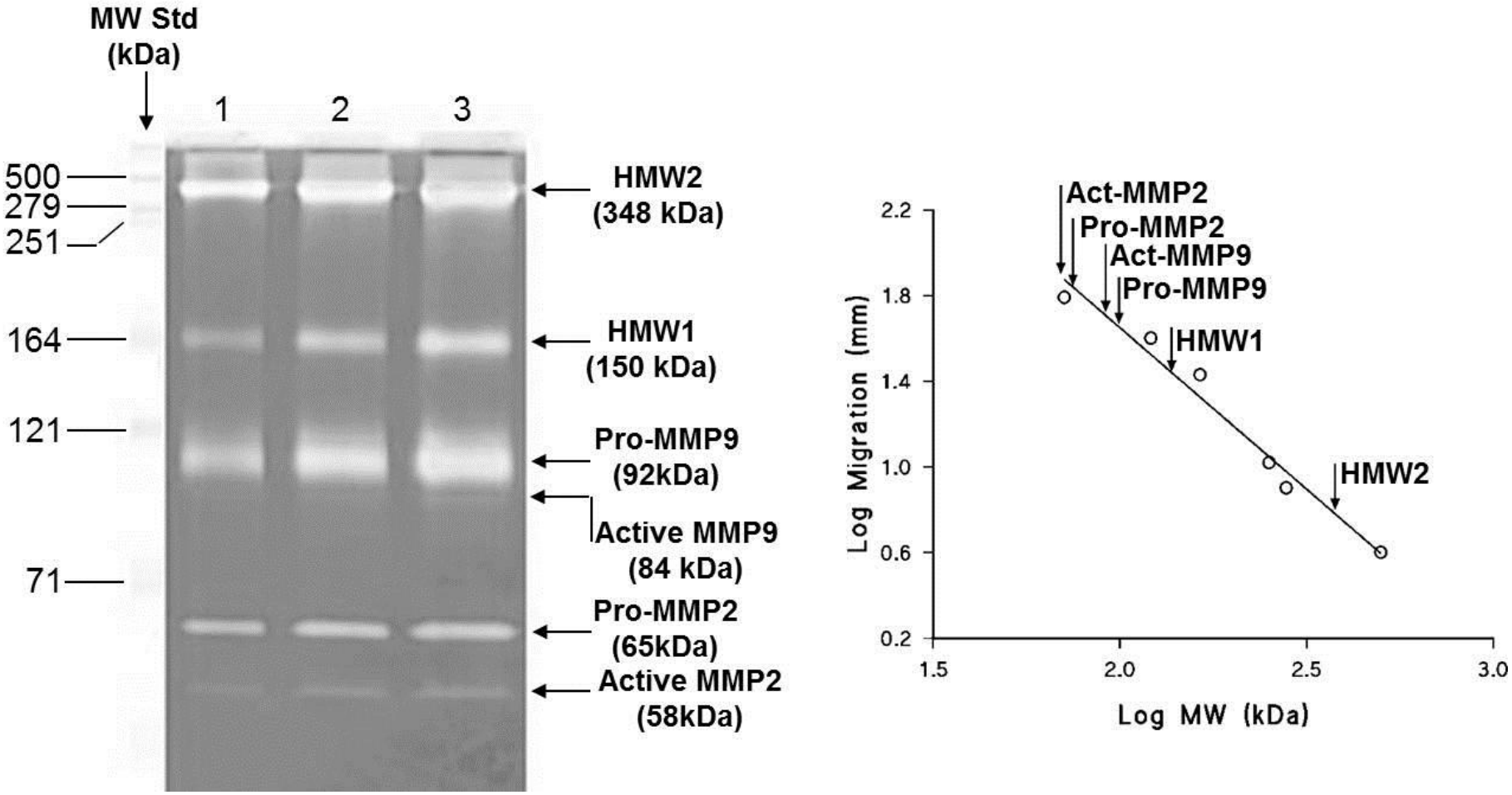

Figure 2.2 The releasable pool of gelatinase species of Bruch's membrane.

Bruch's-choroid was isolated from two pair of eyes (donor ages 75 & 83 years). After mixing with an equal volume of SDS sample buffer, 10, 15 and 20 ul were loaded into lanes 1, 2 &3 respectively. Altogether five gelatinase species were clearly identifiable. Log plots were used to calculate the molecular weights of HMW1 and HMW2 as 150 and 348 kDa respectively.

The characteristic feature of matrix metalloproteinase is that they are Mn^{2+} containing, Ca^{2+} dependent proteases. Thus the removal of divalent ions results in inhibition of MMP activity. Incubation of gels in 10mM EDTA, to remove metal ions, confirmed that the high molecular weight species identified on zymographic gels of human Bruch's-choroid extracts were indeed MMPs (Figure 2.3).

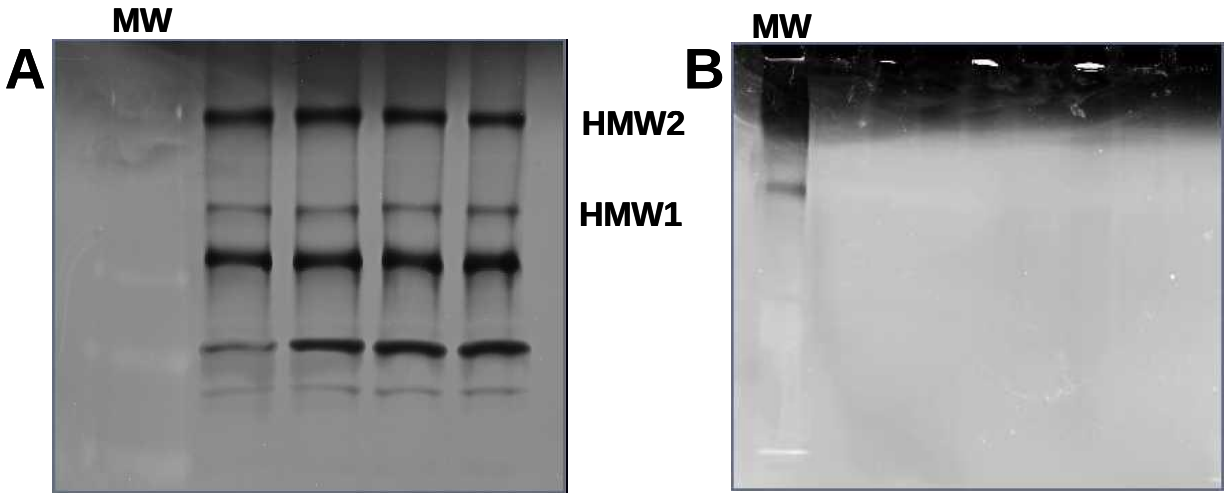

Figure 2.3 Effect of 10mM EDTA on the proteolytic activity of extracts of Bruch's-choroid.

A tissue extract of Bruch's-choroid was prepared from two eyes of a donor aged 72 years. The normal zymogram in (A) showed the presence of high molecular weight species, HMW1 &2. Incubation in the absence of divalent ions (B) resulted in loss of all gelatinolytic activity confirming the high molecular weight species as belonging to the gelatinase family of proteolytic enzymes.

2.3.2 Parameters of quantitative zymography

The stability of MMP activity in SDS containing buffers, the relationship between enzyme activity and area under corresponding zymographic bands and the importance of including an internal standard to normalise for gel-to-gel variation has been addressed.

2.3.2.1 MMP stability in SDS buffers

An MMP extract was obtained from frozen quadrants of Bruch's-choroid from 21 donors (age range 51-87 years). Aliquots were incubated with non-reducing SDS sample buffer for various periods in the range 0-2 hours. Triplicate zymographic gels were then run to assess the effect of exposure to SDS on enzyme activity (Figure 2.4). The results show that the activity of all six gelatinase species was not altered up to a SDS exposure period of 2 hours (Figure 2.4B).

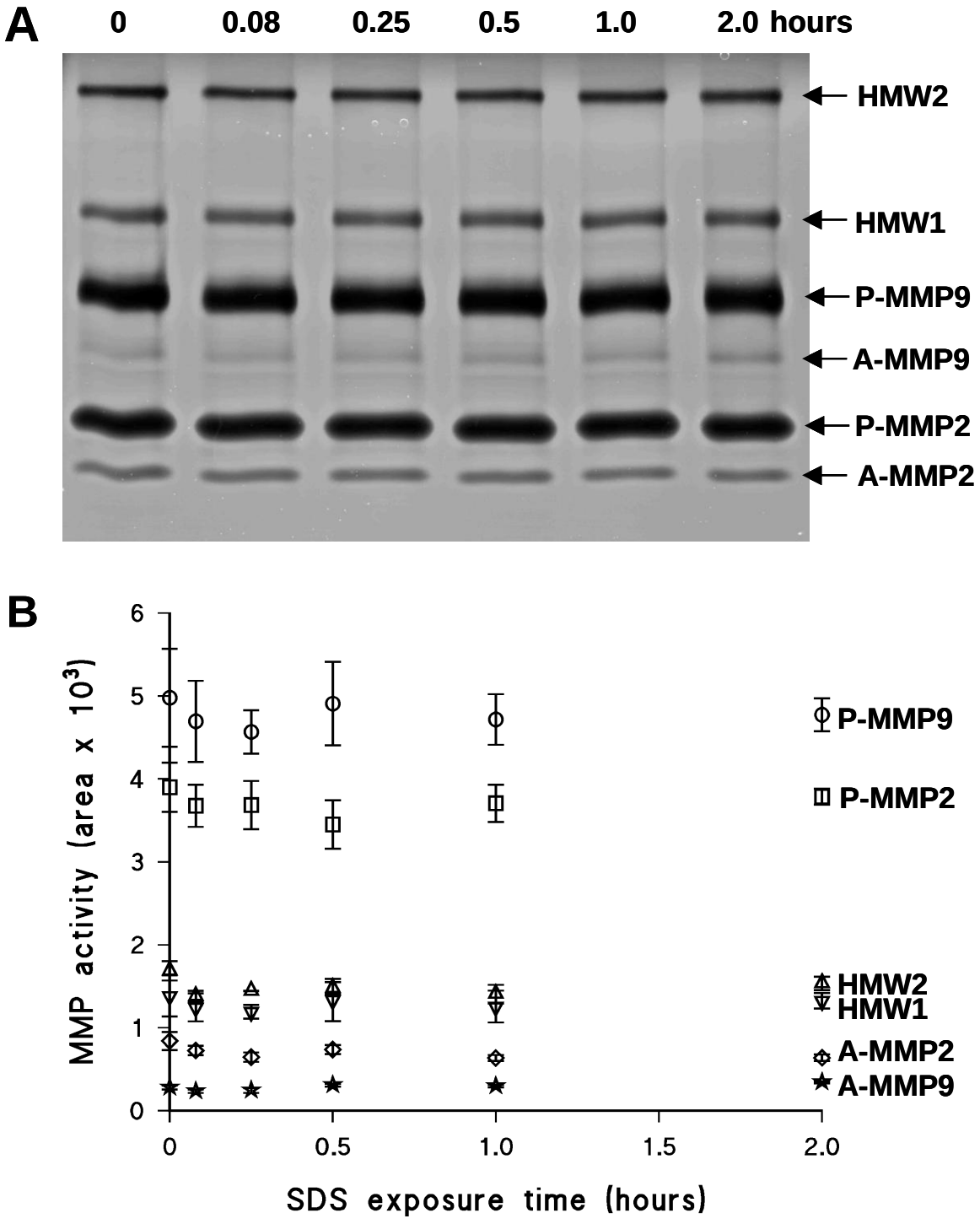

Figure 2.4 Effect of exposure period to SDS buffers on the proteolytic activity of MMPs extracted from human Bruch's-choroid.

(A) All six gelatinase species are clearly delineated on the zymograms. (B) Quantitative analysis of data obtained from three gels showing little (if any) variation in enzyme activity demonstrating stability of activity up to the 2 hours of exposure assessed.

2.3.2.2 Relationship between enzyme levels and band areas on zymography

Demonstrating a relationship (linear or non-linear) between the amount of enzyme and the resulting densitometric area under the zymographic band is an essential requirement prior to use of the technique for quantitative zymography. It is also necessary to define the limits of enzyme activity over which a quantitative approach can be entertained. In the present study, FCS pro-MMP 2 & 9 enzymes were used as test probes. Pilot work varying the amount of FCS applied had shown that amounts greater than 1.5µl resulted in gross distortion and streaking of the pro-MMP2 band. For quantitative purposes therefore, the amount of FCS applied was varied between 0 and 1.5 µl. A representative zymogram and quantitative analysis is depicted in Figure 2.5. The results show the potential for the use of zymography for quantitative applications. In all subsequent analyses, quantification was only undertaken if bands were free from distortion or streaking effects.

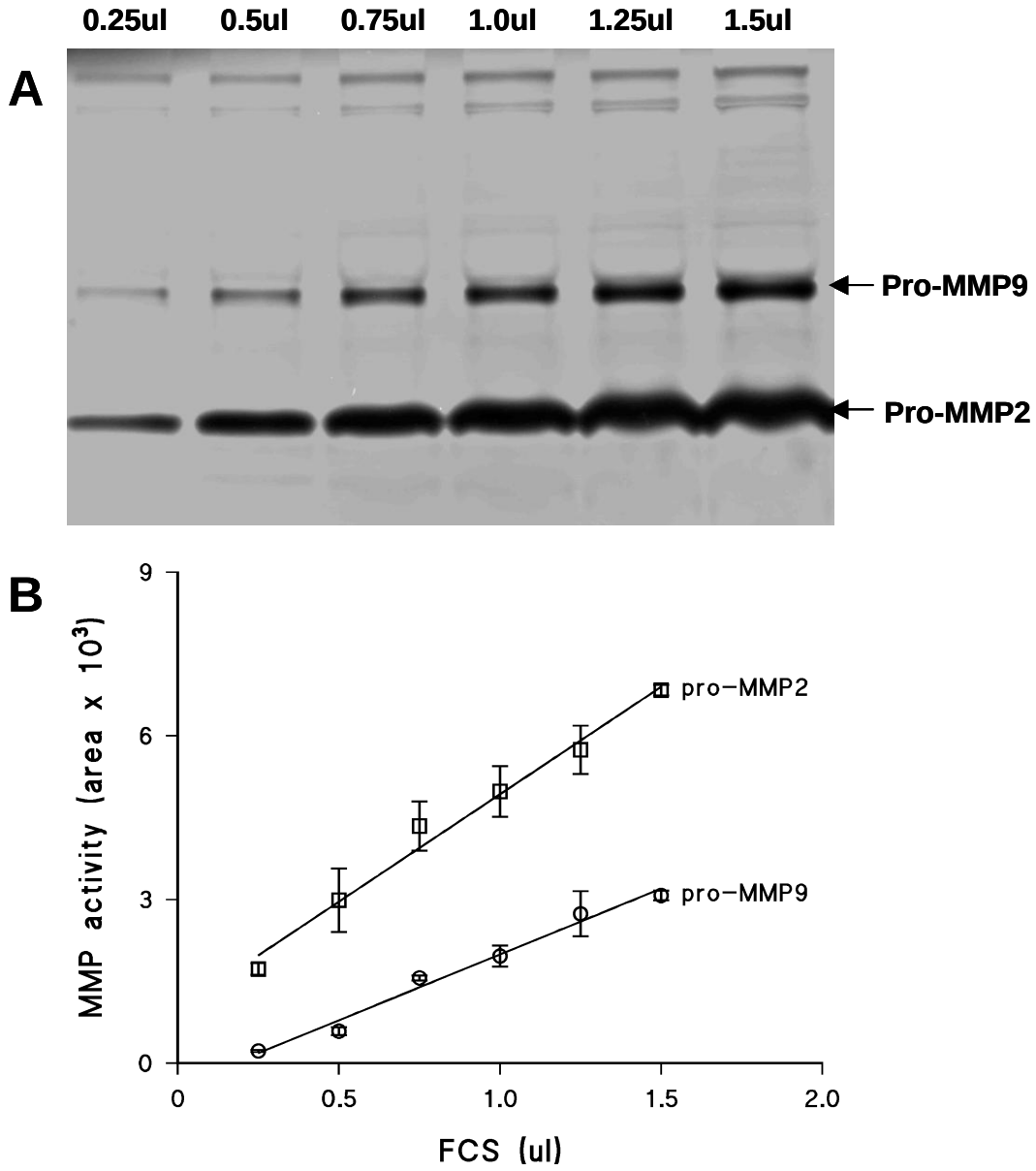

Figure 2.5 Quantitative relationship between the amount of enzyme applied and the resulting band area on densitometric analysis for MMPs in FCS.

(A) Zymogram showing progressive darkening of the pro-MMP9 band whereas the high levels of pro-MMP2 lead to considerable distortion. (B) Within the FCS range of 0-1.5µl, a linear relationship was observed between enzyme level and corresponding band area. Mean ± SD, n=3.

2.3.2.3 FCS as internal standard to correct for gel-to-gel variation

The use of commercially available (and therefore standardized) ready-made gels and staining solutions minimizes the likelihood of gel-to-gel variation in staining of background and gel bands. Nevertheless, variations in incubation solutions, temperature fluctuations, extent of SDS removal during incubation with 2.5% Triton X-100, etc., can lead to gel-to-gel variations and must be taken into account if data from several gels is to be compared. The use of an internal standard to cater for such fluctuations is always recommended.

FCS, incorporating pro-MMPs 2&9 is often used because of the stability and reproducibility of its MMP bands. To assess its usefulness, four gels were prepared each containing the same amount of FCS and a tissue extract (from 11 eyes, age range 67-82 years). After electrophoresis, gels were developed in zymographic buffer for periods of 13, 16, 18 and 22 hours and destained for various times to induce variability in both background and gel band staining intensity. The resulting zymograms are depicted in Figure 2.6. The zymogram labelled number 5 is identical to zymogram number 4 but has been scanned on a different scanner (Biorad).

As expected, band intensities have varied considerably because of the different incubation times. Within a given gel, the variation in intensity of MMP2 or MMP9 bands (run in triplicate lanes) in the FCS solutions was observed to be about 4.7 ± 1.7%. In tissue samples, this variability was 6.6 ± 2%.

Development of zymograms is normally carried with an incubation period of 18 hours. Thus, gel 3 (incubation time 18 hours) was selected as standard for comparison with the other gels. The raw data for levels of pro-MMPs 2&9 (after subtracting for background staining intensity) in the various gels is represented in

Figure 2.7A and as expected shows much variation between gels. Note also that the gel scanned on a different scanner (Biorad) showed abnormally low values.

The average area under the FCS MMP9 band (A_{std}) in gel 3 was taken as standard and the area under the gelanolytic bands in the other gels corrected as follows:

$A_{corrected} = [(A_{std}) / A_{test}) \times (\text{area under gel band})]$

where A_{test} represents the area under the FCS pro-MMP9 band in the test gel. The resulting corrections have been applied and are represented in Figure 2.7B. Following the corrections, the level of pro-MMP 2&9 activity is found to be similar in all the gels. Thus, despite variations in staining intensity/incubation conditions, the inclusion of FCS can assist in controlling gel variability. After correction, the gel to gel variability in the level of pro-MMP9 was determined to be 2.4%, due likely to the higher level and therefore accuracy in determining its area under the bands. With the low levels of pro-MMP2, errors increase in the accurate determination of areas, and correspondingly, inter gel variability was 19.5%.

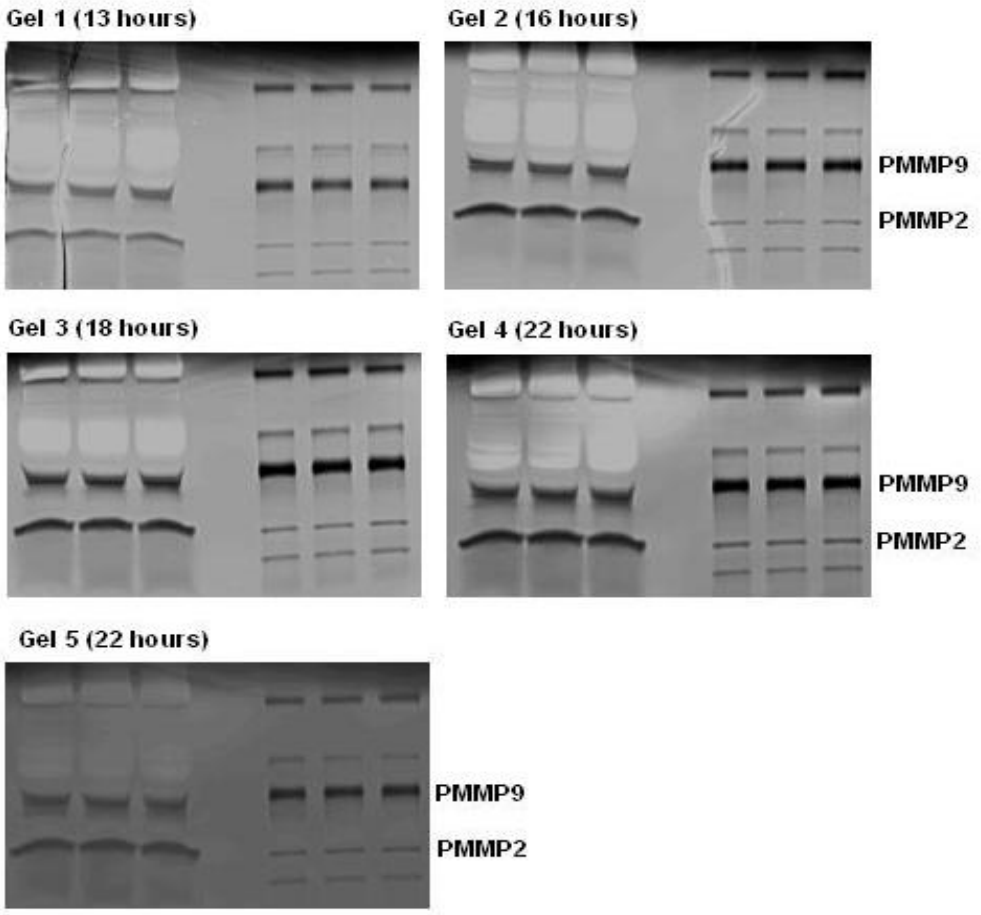

Figure 2.6 Zymograms of FCS and Bruch's-choroid tissue extracts developed for various times to induce variability in background and gel band staining.

Gel 5 is a scan of gel 4 but carried out on a different scanner to that for gels 1-4.

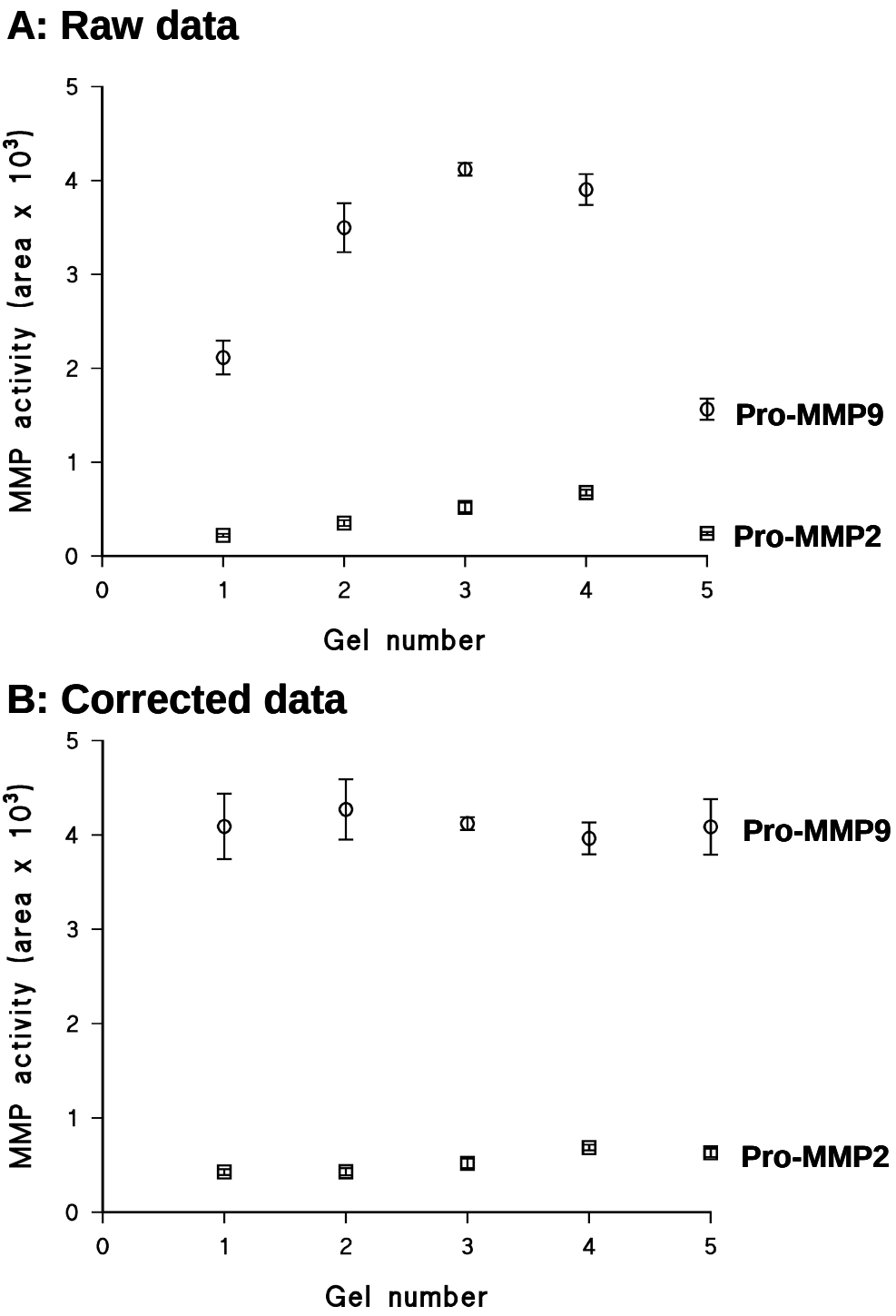

Figure 2.7 Raw and corrected data for pro-MMP2&9.

(A) Areas under the pro-MMP 2&9 bands were determined by Quantiscan analysis software (correcting for background intensity) for gels 1-5 of Figure 2.6.

(B) Using the pro-MMP9 band of the FCS sample of Gel 3 as standard, all other gelatinase activities have been corrected accordingly as explained in the text.

2.3.3 HMW1 and HMW2 fragment analyses

2.3.3.1 Activation of gelatinase species

A tissue extract was prepared from 11 donor eyes (age range 58-91 years) and aliquots were APMA activated, reduced and alkylated. The resulting zymograms and densitometric scans of individual lanes are depicted in Figure 2.8. Activation resulted in the complete loss of the HMW1 band and considerable loss of the HMW2 band. These changes were associated with increases in the level of active MMPs 2&9.

The increased levels of active enzymes could be due to conversion of endogenous pro-MMPs and from released monomers arising from the breakdown of HMW1 & 2. It could also be argued that these active forms arise from endogenous monomeric MMPS without much contribution from HMW1 & 2. Since activated forms should display increased gelatinase activity, the increased banding intensity may simply be a reflection of this process. Activation of a sample that does not contain much HMW1 & 2 would indicate how the monomeric species behave after activation.

Thus a sample of FCS was activated with APMA and the resulting zymogram is displayed in Figure 2.9. Although activation did not lead to the complete removal of pro-enzymes, partial conversion to activated forms is clearly discernable. In the case of pro-MMP2, loss of activity in the latent form does not appear to be fully translated into the activated form. Thus the large increase in activated MMPs 2 & 9 in Figure 2.8 may well reflect a contribution from the loss of HMW1 & 2.

Further work to identify the components of the high molecular weight species has utilised fragment analysis after activation and the technique of Western blotting.

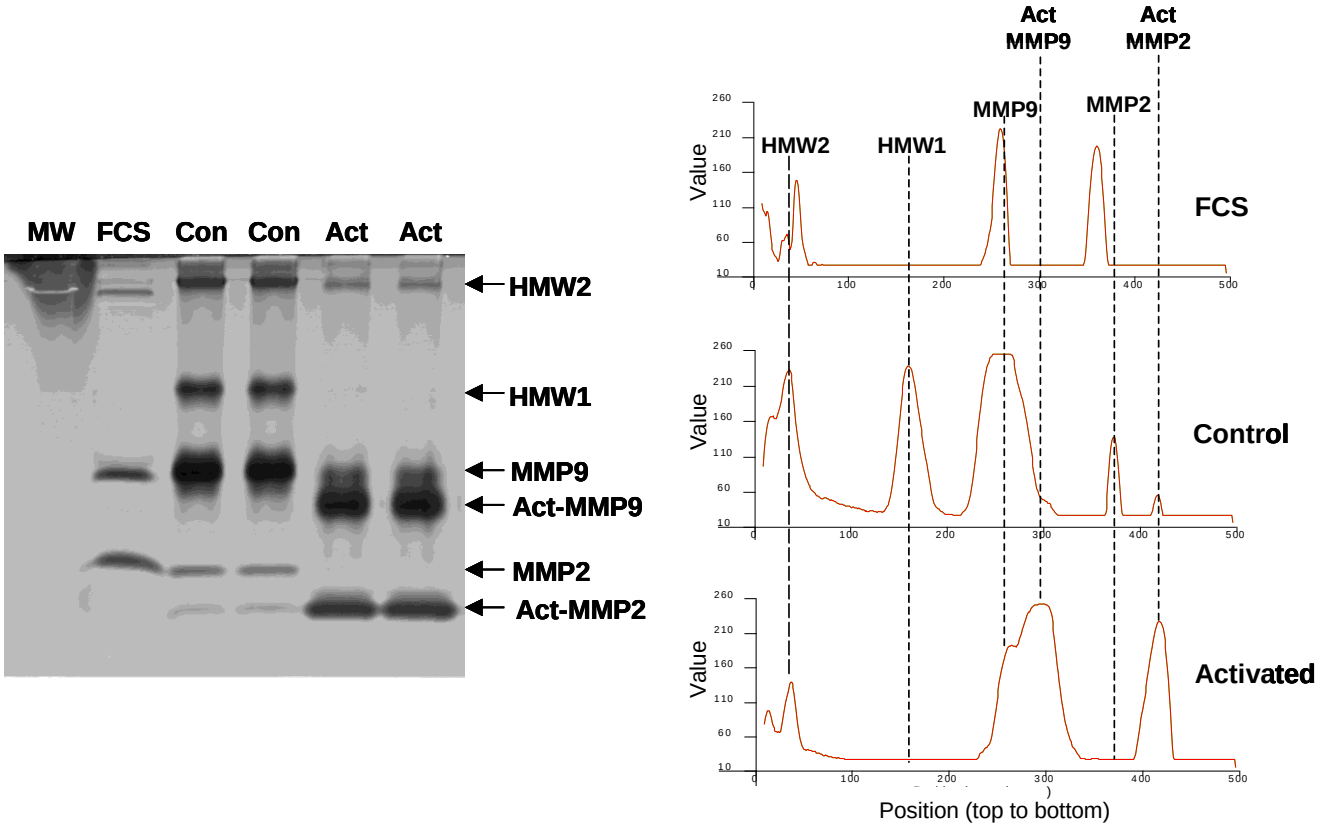

Figure 2.8 Activation of gelatinase species.

A concentrated extract was obtained from 11 eyes (donor age range 58-91 years) and on zymography showed the ample presence of all gelatinase species except active MMP9 (Con lanes). Activation resulted in the complete loss of HMW1 with a major reduction in the intensity of the HMW2 band. These changes were accompanied with an increase in the levels of activated MMPs2&9.

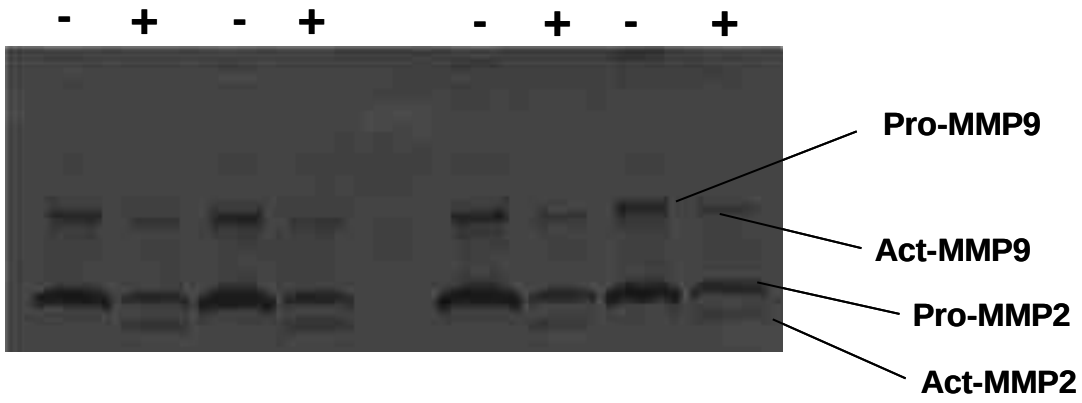

Figure 2.9 APMA activation of FCS pro-MMPs 2 & 9.

The (-) and (+) symbols represent samples as controls or APMA activated respectively. The procedure resulted in partial activation since some pro-MMP activity remained after the incubation. Nevertheless, the increased banding intensity of the activated forms was lower than the intensity loss of the pro-MMP bands.

2.3.3.2 HMW fragment analysis using double electrophoretic separations

In the previous section, APMA activation resulted in the removal of the HMW species with an increase in the level of active MMPs 2&9. However, it was not certain how much of this increase was due to activation of HMW derived MMP species and how much due to activation of endogenous free pro-MMPs.

An alternate method to assess the contribution would be to separate the individual gelatinases species in a single lane gel by electrophoretic means. Then activating the HMW species whilst within the gel would be expected to release the monomeric species in the locality of the HMW regions within the gel. Removing a slither of the activated gel (as diagrammed in Figure 2.1) and running it in the

dimension shown, should separate the individual components released on activating the HMW species.

Tissue extract from 11 donor eyes (section 2.3.3.1) was utilised in these studies. Initially, the gelatinase extract was separated by standard SDS-PAGE (i.e., without gelatin substrate) and following activation/reduction/alkylation, a slither of the gel containing all of the MMP species was loaded for zymographic analysis (Figure 2.10A).

In the control half of the gel (with a slither that was not activated), the lengthy electrophoretic procedure resulted in partial breakdown of both HMW2 to yield pro-MMP9 and in the case of HMW1, yielded both pro- and active MMP9 species. In addition, both pro-MMPs 2 & 9 were also activated. In the activated portion of the gel, gelanolytic activity was considerably subdued. However, HMW1 & 2 were removed leading to the presence of activated MMP9 in both cases.

Subsequently, the primary separation of the gelatinases was undertaken in the presence of gelatin substrate (Figure 2.10B). Under these conditions, APMA activation resulted in more stable preservation of activated MMP9 monomers. The presence of MMP9 in the HMW species was therefore confirmed. Activity of pro and active MMP2 was better preserved when the primary separation was undertaken in the presence of gelatin substrate (Figure 2.10B). Nevertheless, activation resulted in considerable loss of this species and in the activated portion of the gel, some active conversion of endogenous pro-MMP2 can just be discerned. Because of the labile nature of active MMP2 under the conditions employed, the likelihood of detecting released MMP2 from HMW1&2 (if any) was minimal under the conditions utilised.

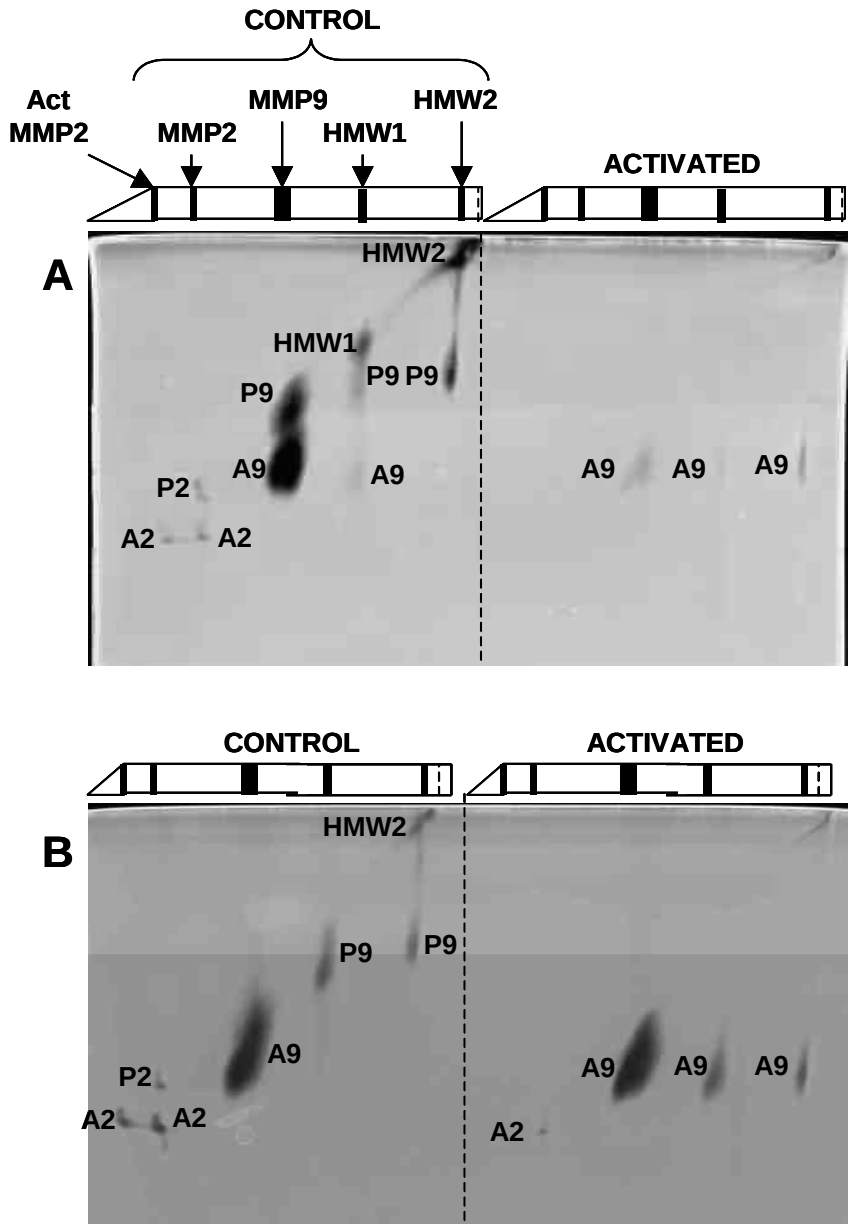

Figure 2.10 Compositional analysis of the breakdown products of HMW1&2 following activation.

Gel A: The initial separation of the various gelatinase was performed by standard SDS-PAGE under on-reducing conditions. Gel slithers were obtained from control and activated gels and place on top of a gelatin separating gel, electrophoresed and subjected to standard zymography. In the control portion, there is evidence of partial breakdown of HMW1&HMW2 and activation of MMPs 2&9. Activation in the absence of gelatin (and under the conditions utilised) resulted in marked loss of gelatinase activity. Nonetheless, activation resulted in the release of MMP9 species from both HMW1& HMW2.

Gel:B The initial separation was performed on a gelatin zymography gel and resulted in better preservation of gelatinase activities (control section). Activation resulted in breakdown of HMW1&2 giving rise to activated MMP9 species.

P9 & A9, pro- and active MMP9 respectively.

P2 & A2, pro- and active MMP2 respectively.

2.3.4 Component analysis of HMW species by Western blots

Pilot experiments were carried out to ensure that the Western transfer procedure was sufficiently optimised to ensure the transfer of the high molecular weight species to the nitrocellulose membranes. Several batches of antibodies to MMPs 2 & 9 were obtained but nearly all showed some degree of cross-reactivity between the species.

Probing the nitrocellulose membranes with antibodies directed towards MMP9 showed positive reactivity against pro-MMP9, HMW1 and HMW2 (Figure 2.11). These results showing the presence of pro-MMP9 in the high molecular weight complexes corroborates the evidence from zymographic studies described earlier.

Antibodies raised against MMP2 were positive towards pro-MMP2 and active forms of the enzyme, as expected. But they also reacted against pro-MMP9. This cross-reactivity against pro-MMP9 should have also resulted in cross-reactivity against HMW1 & 2 since pro-MMP9 has been localised to these species. However, only HMW1 was occasionally picked up but reactivity towards HMW2 was never observed (Figure 2.12)

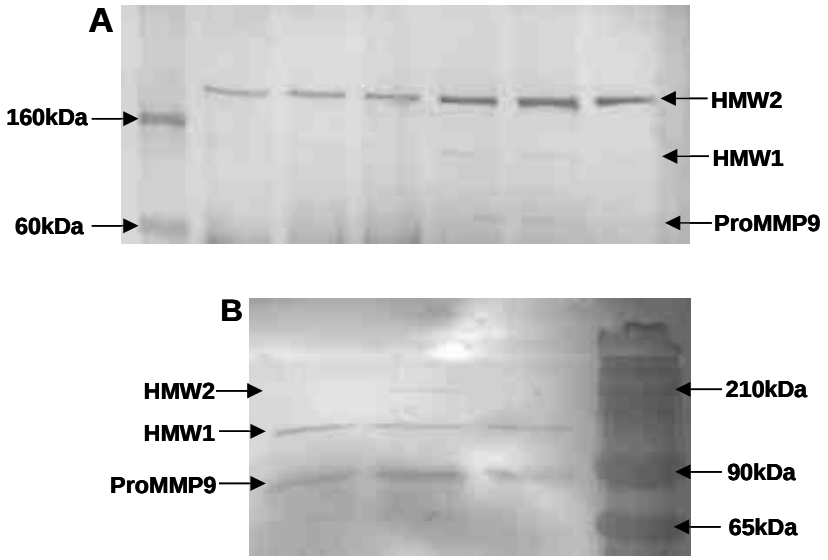

Figure 2.11 Representative Western blots with antibodies directed towards proMMP9.

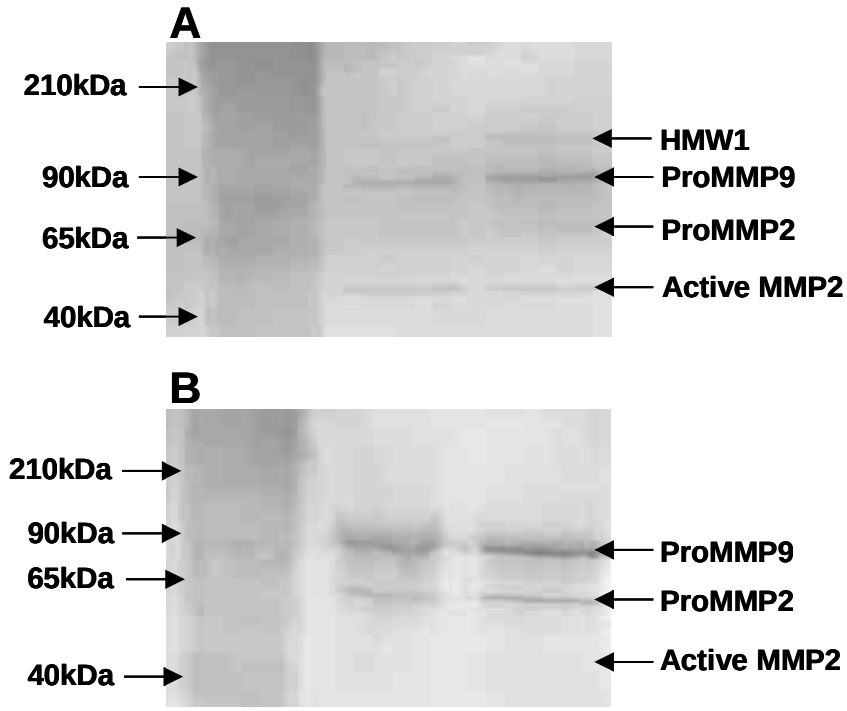

Figure 2.12 Representative Western blots with antibodies directed towards pro-MMP2.

2.3.5 Age related changes in the gelatinase system of human Bruch's membrane

The effect of ageing on the gelatinase components of Bruch's membrane was investigated in 29 donor eyes in the age range 21 to 99 years. Vigorous agitation of 8mm disc samples in PBS was used to obtain the free pool of gelatinases with subsequent extraction of the washed sample with non-reducing SDS sample buffer to provide the bound pool.

Zymographic gels of the free and bound fractions for a donor subset in the age range 22-87 years are shown in Figure 2.13. Visual inspection of gels clearly shows the variation in level of individual gelatinase species between donors.

The free pool of gelatinases was dominated by the presence of pro-MMP9 but its activated form (active MMP9) was not observed in any of the samples analysed. Active MMP2, on the other hand was observed in the soluble fraction in 48% of donor samples. High molecular weight species were also observed in the soluble fraction but with very much diminished levels compared to pro-MMP9.

The bound pool was dominated by HMW2 and pro-MMP9 and active MMP9 was observed to be present in 45% of the donors examined. Active MMP2 was present in the bound fraction of all donors.

For normalisation of data between gels, densitometric scans with software assisted background subtraction and corrections for gel-to-gel variation with FCS as internal standard were undertaken. Further calculations were made to take into account the volumes of the extracted samples and gelatinase activity of bands was expressed as densitometric area per 8 mm disc of tissue. The resulting activities for

the various gelatinase species of Bruch's membrane are presented as function of donor age in Figure 2.14-Figure 2.16.

Aging of Bruch's membrane was associated with an increase in the amount of bound pro-MMP9 ($p<0.05$) but with a decrease in the free pool ($p<0.05$). In comparison to pro-MMP9, levels of activated MMP9 were very low or absent. Given the very low level of this species, the validity of attempting a correlation with age must remain questionable. Bound and free levels of pro-MMP2 did not appear to change with age of donor. Levels of active MMP2 were higher in the bound pool compared to the free pool but an ageing relationship was not observed for this species.

Aging of Bruch's membrane resulted in increased levels of total and bound HMW2 ($P < 0.005$). Level of HMW1 showed considerable variation between donors and ageing was associated with an increase in both total and bound levels ($P < 0.05$ and $P < 0.01$, respectively). Most of the HMW1 and HMW2 species was found in the bound fraction of the membrane and constituted 87 % ± 10 % and 80 % ± 20 % (mean ± SD) of individual levels respectively. The combined gelatinase activity of HMW1 and HMW2 was responsible for 23 % ± 20% of overall gelatinase activity in the releasable pool and 43 % ± 8 % in the bound pool.

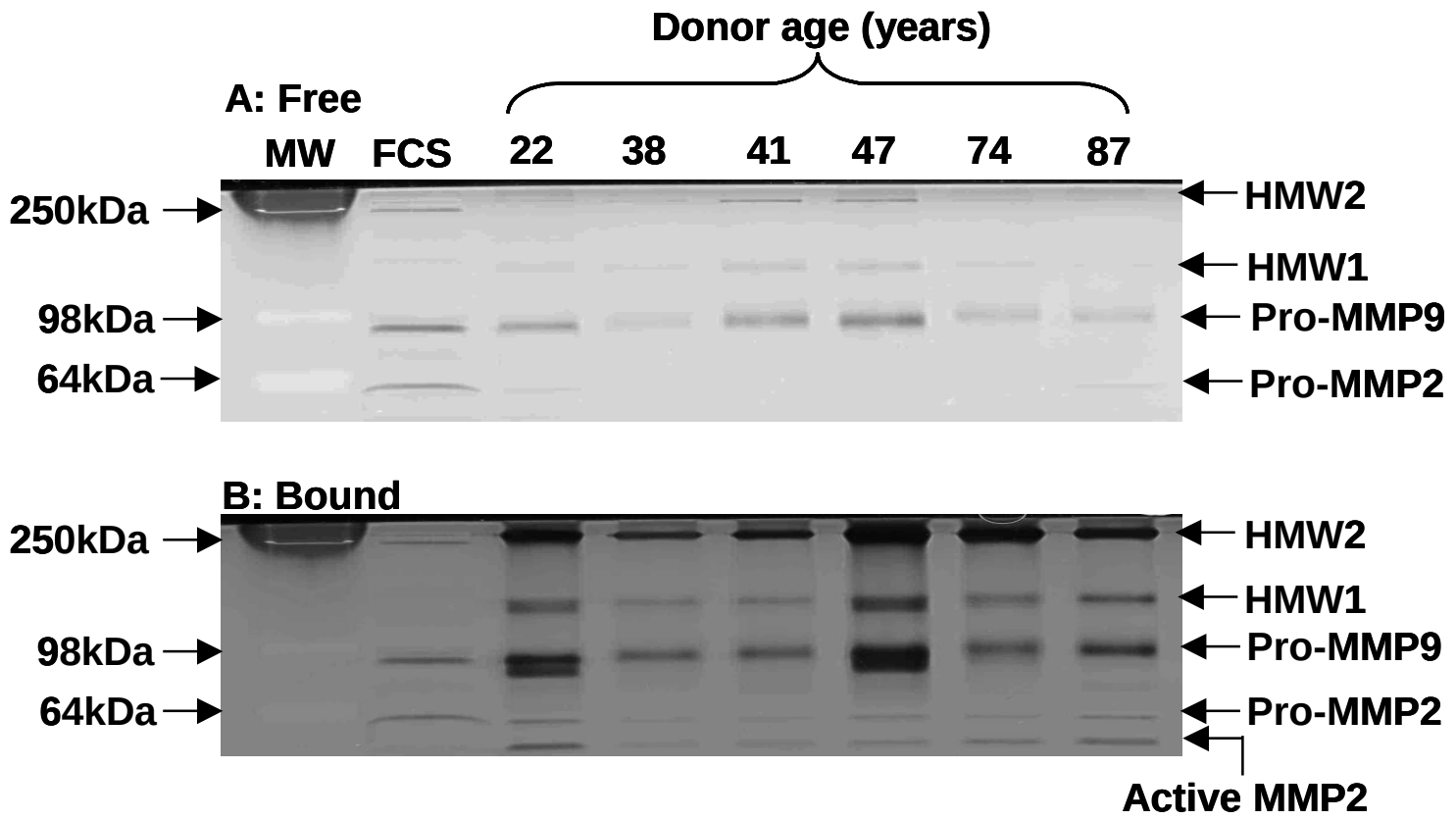

Figure 2.13 Zymograms for quantification of free and bound gelatinase activity of Bruch's membrane.

A: Eight millimeter tissue discs were vortexed in PBS for 5 minutes, spun at 10,000 g and supernatant containing released enzymes removed and processed for zymography.
B: Remaining tissue disc was washed several times with PBS and then extracted with non-reducing SDS extraction buffer to obtain the extracted fraction.
MW, molecular weight standards; FCS, foetal calf serum.

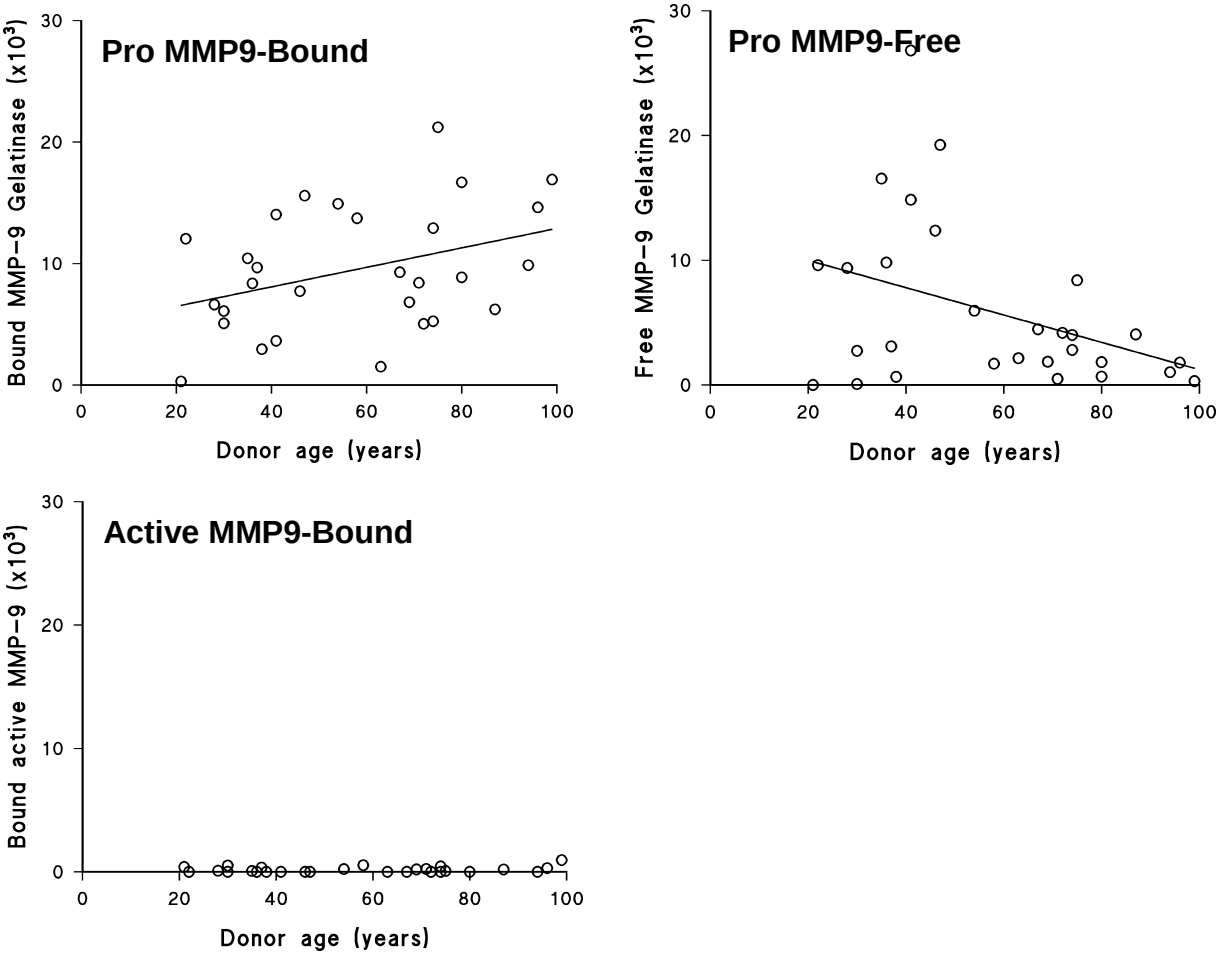

Figure 2.14 Age-related variation in variation in bound and free levels of the MMP9 species in Bruch's membrane.

The peripheral fundus was sampled in 29 donor eyes, age range 21-99 years and gelatinase activity is expressed as the area under the corresponding zymographic bands. Ageing was associated with an increase in the amount of bound pro-MMP9 ($p<0.05$) but a decrease in the level of free ($p<0.05$). Active MMP9 was only present in the bound fraction.

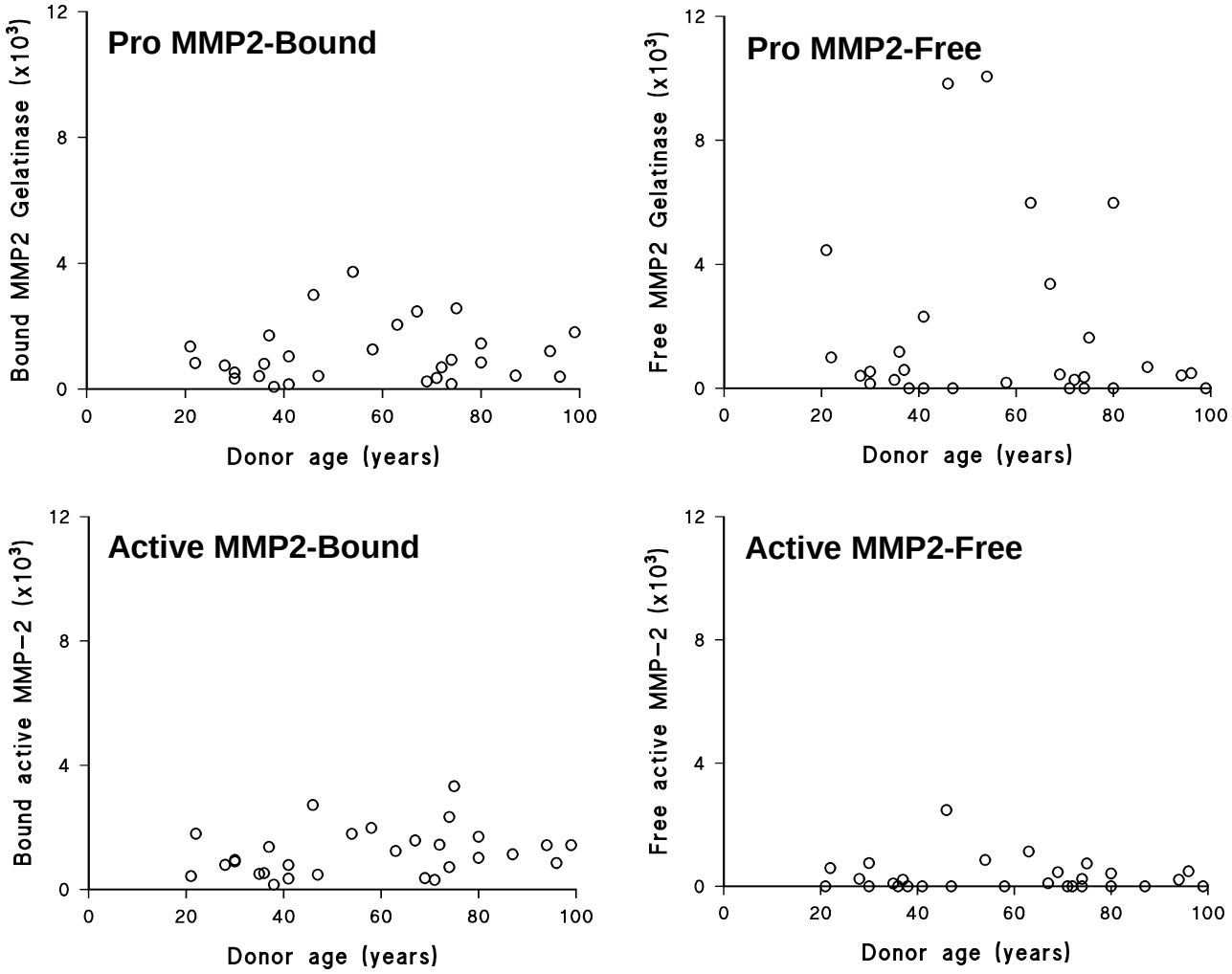

Figure 2.15 Age-related variation in bound and free levels of the MMP2 species in Bruch's membrane.

Ageing did not result in any significant alterations in the levels of latent or active MMP species.

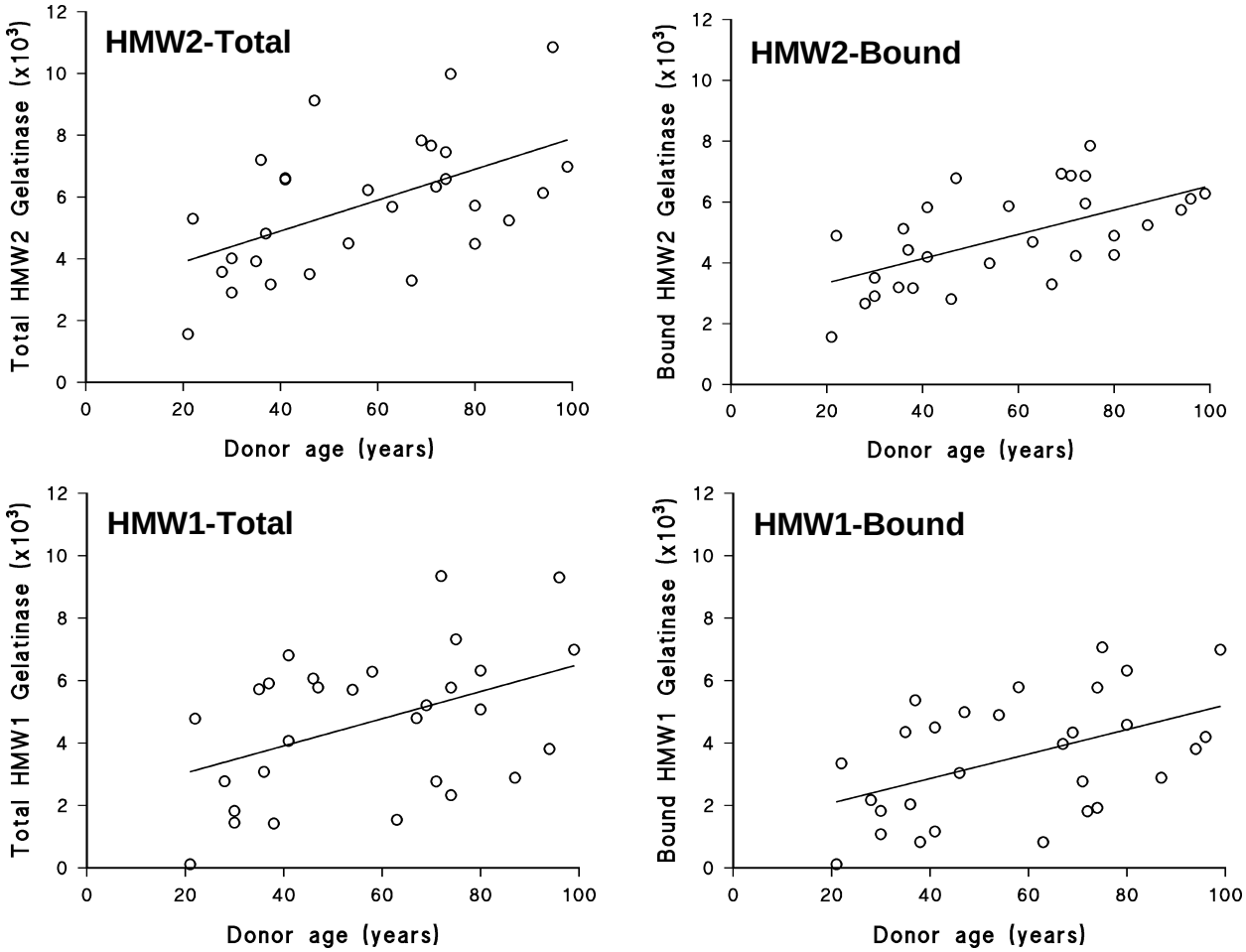

Figure 2.16 Age-related variation in the total and bound level of high molecular weight gelatinase species of Bruch's membrane.

Total and bound levels of HMW2 species were observed to increase linearly with age of ($p<0.005$). Despite the large scatter in the data, total and bound levels of HMW1 also showed an age-related increase ($p<0.05$ & $p<0.01$ respectively).

The age related variations between bound and free compartments were investigated by plotting the percentage of bound MMP species versus age of donor (Figure 2.17).

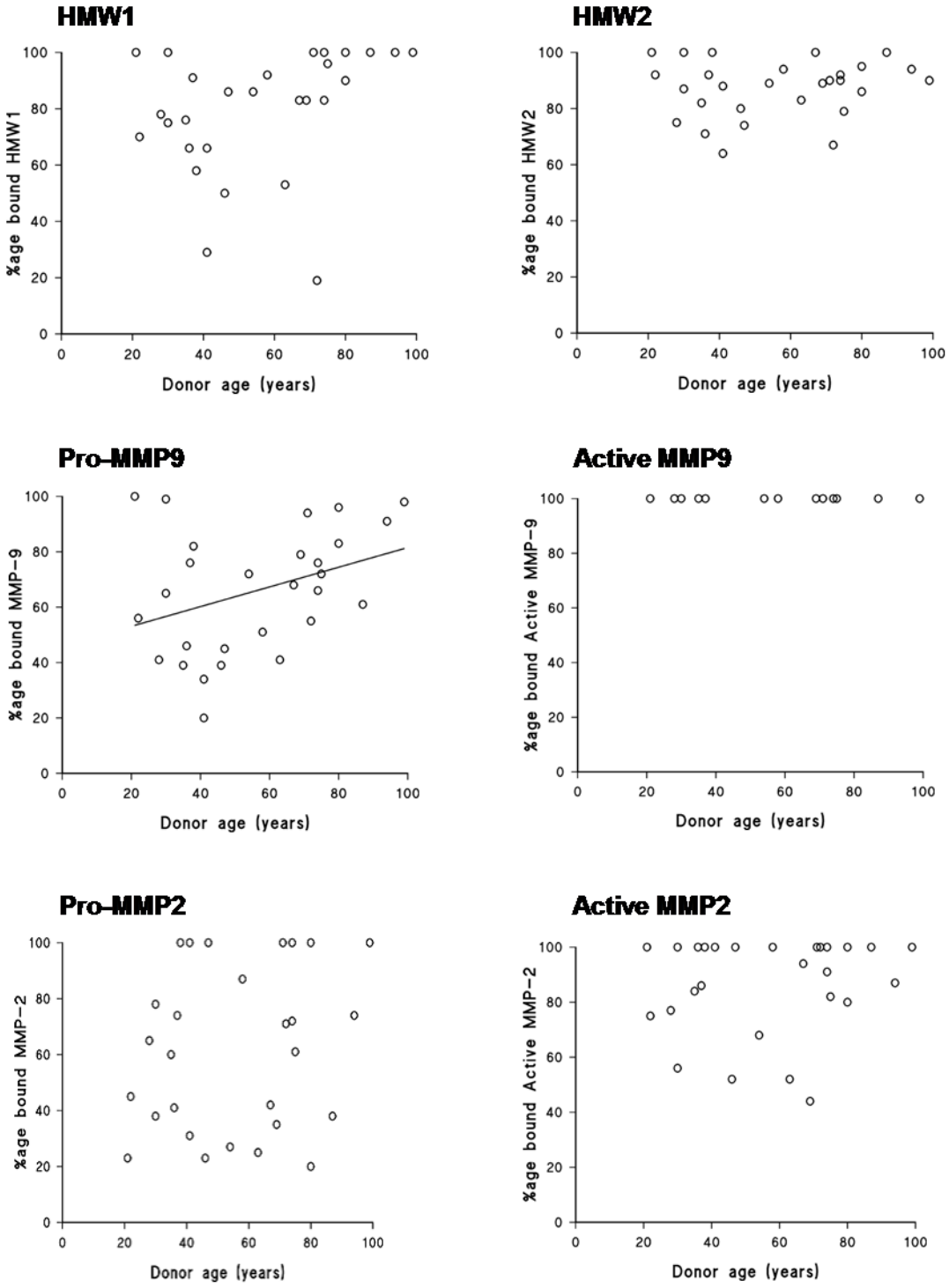

Figure 2.17 Age related variations in the percentage of bound gelatinase species.

Of all the gelatinase species, pro-MMP9 was the only one that showed a significant increase in binding to the matrix with age ($p<0.05$). In the absence of statistical significance, the data for the other gelatinases has been grouped to provide an average value for the percentage bound to the matrix of Bruch's membrane (Table 2.1).

Gelatinase species	Percentage bound
HMW1	80 ± 21
HMW2	87 ± 10
Pro-MMP9	**
Pro-MMP2	62 ± 29
Active MMP9	100 ± 0
Active MMP2	87 ± 17

Table 2.1 The percentage of total gelatinase species found in the bound compartment of Bruch's membrane.

** Not calculated because of the presence of an ageing relationship. Mean ± SD.

2.4 DISCUSSION

The importance of the MMP system lies in its ability to degrade extracellular matrices so as to allow the migration of phagocytic and endothelial cells in the processes of inflammatory response and new blood vessel growth. Their involvement in tumour cell invasion and in choroidal neovascularisation has been well documented.

Proteolytic activity of MMPs is also required for the normal maintenance of extracellular matrices. The tightly coupled processes of degradation and synthesis provide a mechanism for continual rejuvenation of matrices throughout life. This is particularly important for Bruch's membrane for several reasons. Firstly, it houses high-traffic transport pathways for exchange of nutrients and waste products to and from a photoreceptor layer that maintains one of the highest rates of oxidative metabolism of any cell type in the body. Secondly, it is situated at a location with an elevated risk of oxidative and free-radical mediated damage. Thirdly, it has to deal with highly damaged and potentially damaging phagocytic 'debris' that has been extruded onto its surface by the overlying RPE. Hence Bruch's requires efficient regenerative mechanisms to maintain its structural and functional characteristics.

Ageing of Bruch's suggests that these regenerative mechanisms are not fully operational in that nearly 50% of the collagen content in aged specimens was shown to exist in an oxidatively damaged state (Karwatowski *et al.*, 1995). The presence within a tissue of active forms of MMPs is an indicator of an attempt at proteolysis. Active forms of gelatinases MMPs 2&9 have previously been demonstrated in aged

human Bruch's membrane (Ahir *et al.*, 2002; Guo *et al.*, 1999). It is possible that the MMP system remains at an operational state but that the highly damaged and cross-linked nature of the collagen molecule prevents effective degradation. The level of active MMPs is another consideration that will dictate the degree of degradation. Interestingly, Guo et al., 1999 showed that active MMPs were frequently present in the more slowly ageing peripheral region and only occasionally in the faster ageing macular region.

Preliminary assessment of the gelatinase system of ageing Bruch's membrane requires identification and characterisation of individual species and their associated age-related changes (if any). In the present study, identification of gelatinases species was based on the technique of substrate gelatin zymography and the limitations imposed by this approach require some clarification.

The use of SDS buffers for preparing samples for SDS-PAGE (for Western blots) or zymography leads to the disassociation of dimers, trimers, tetramers or polymers if the monomeric units were initially held together by non-covalent bonds. Such complexes cannot be detected by zymography and the quantification of monomers would artificially elevate the levels found physiologically. With this caveat in mind, the analysis of Bruch's-choroid preparations showed the presence of six distinct gelatinase species on the zymograms: latent Pro- forms of MMPs 2 &9 of molecular weights 95 and 65 kDa respectively, their activated counter parts of molecular weights 84 and 58 kDa, and two additional high molecular weight species designated as HMW1 and HMW2 of molecular weights 122 and 344 kDa respectively.

Most publications only show the regions of zymograms housing the monomeric MMPs 2 &9, ignoring the high molecular weight components. Others have noted the presence of these species on their zymograms (Guo *et al.*, 1999; Lim *et al.*, 1997). In the present study, nearly 23% of the gelatinase activity found in the free compartment of the membrane was due to the presence of HMW1 and HMW2. Even greater amounts of these species (43%) were present in the bound fraction of the membrane. Previous studies have suggested that these high molecular weight species are most likely to be homo- and hetero polymers of pro-MMPs 2&9. If this were the case, then these HMW species would be responsible for sequestrating latent forms of MMPs 2&9, thereby diminishing the monomeric pool for activation. Moreover, the age related increase in HMW1 & 2 would serve to further sequester monomeric species in the elderly.

Activation of tissue extracts with APMA resulted in the disintegration of the HMW complexes with a concomitant increase in the level of activated MMPs 2 & 9. Although this result suggests that the HMW species contain both MMPs 2 & 9, the relative contribution from endogenous monomeric MMPs 2 & 9 complicates the analysis. APMA activation of FCS, that contains very little (if any) HMW species, resulted in the movement of the gelatinase bands towards lower molecular weights without an increase in staining intensity. Based on this result, the analysis shown in Figure 2.8 certainly supports the inclusion of MMPs 2&9 in the HMW complex. The double electrophoretic separations clearly demonstrated the presence of MMP9 in the HMW complexes and this was also supported by the Western blots. The age related increase in HMW1 & 2 would therefore imply greater sequestration of pro-MMPs 2&9 in ageing donors.

The high level of pro-MMP9 present in Bruch's samples allowed for greater accuracy in their quantification by gelatin zymography. The amount of pro-MMP9 in the bound compartment increased with ageing of donor ($p<0.05$) whilst that in the free compartment showed a decrease ($p<0.05$). Thus, greater binding to the membrane and incorporation into the HMW complexes would appear to result in decreased levels of free pro-MMP9. Active MMP9 was only found in the bound compartment of Bruch's membrane with levels very small compared to pro-MMP9. This species was present in 45% of the donors examined. Because levels were so low, and often near the detection limit, the scatter in the age-dependency analysis was considerably higher. The fact that all the active MMP species was bound to the matrix is perhaps not surprising. Pro-MMP9 binds to the damaged and hence uncoiled strands of the triple helix chain of the collagen molecule (Rosenblum *et al.*, 2010). This binding results in conformational changes that lead to activation and auto-catalytic removal of the inhibitory pro-peptide. Once activated, the activated MMP9 remains bound to the uncoiled chain and has translational capability along the collagen molecule. Thus, activated molecules of MMP9 would be expected to be bound to the matrix.

Levels of pro-MMP2 were somewhat evenly distributed between bound and free compartments and did not show alterations with age. Active MMP2 was present in the bound fraction of all donors examined. It was also present in the free compartment in 48% of donors. Again, the presence of active MMP2 in the free compartment is not surprising. Pro-MMP2 is activated on the basolateral surface of the RPE cell (section 1.3.3.3.3) and the activated form must then diffuse through the matrix of the membrane to interact with its substrate. Unlike active MMP9, levels of

active MMP2 were found to be very high, about 50% of the level of pro-MMP2. This high level is in keeping with its role as a constitutive MMP in the homeostatic regulation of matrix maintenance.

In the case of MMP9, the age related increase in binding and incorporation into the HMW species explains the observed lower level of pro-MMP9 in the free pool. A lowered free pool of pro-MMP9 would be expected to impact on the pool of activated MMP9 but this analysis is hampered by the low sensitivity of the zymographic technique for such quantification. This ageing process has been shown as a pathway in Figure 2.18. Similar considerations should also apply to the pools of MMP2 but the present results clearly show that the free levels of pro-MMP2 are not reduced. One possible explanation for this anomaly may be that the free pool of pro-MMPs 2&9 has been overestimated. This could arise if the tissue housed polymeric forms that were non-covalently bound leading to their dissolution in SDS buffers, resulting in artificially elevating the free pool of pro-MMPs. This aspect is addressed in the following chapter.

Figure 2.18 Pathway regulating the free level of pro-MMPs in Bruch's membrane.

CHAPTER 3

STRUCTURAL CONFIGURATION OF GELATINASE SPECIES OF BRUCH'S MEMBRANE

3 STRUCTURAL CONFIGURATION OF GELATINASE SPECIES OF BRUCH'S MEMBRANE

3.1 INTRODUCTION

The technique of substrate zymography has been used extensively in the analysis MMPs. Gelatin and the milk protein casein have been used as substrates for the detection of MMPs 2&9 and MMPs 1&3 respectively (Guo *et al.*, 1999). Pro-MMPs are latent enzymes that require the removal of an inhibitory pro-peptide for activation. Thus under normal circumstances and in the presence of substrate, these latent enzymic forms would not show any proteolytic activity. However, during preparation of samples for electrophoresis, an anionic detergent, sodium dodecyl sulphate (SDS) is used to solubilise the proteins. The binding of SDS with the latent MMPs causes conformational alterations that lead to partial activation without cleavage of the inhibitory pro-peptide. Hence, the process of zymography allows the detection of 'latent' forms of MMPs. Since physiological activation of MMPs results in species of lower molecular weight, both latent and activated MMPs can be identified and quantified by zymography.

There is one major drawback to zymography. The SDS used to solubilise proteins (and to partially activate latent MMPs) also disassociates macromolecular complexes that are held together by hydrophobic and/or electrostatic interactions. Thus, zymographic analyses only allow the detection and quantification of

monomeric or covalently bounded multi-meric MMP species. Physiologically, the presence of loosely or non-covalently bound multi-meric species may be more important in the assessment of biological activity.

Techniques that do not break up the non-covalently bonded macromolecular complex are required to verify and characterise such species. Size-exclusion gel filtration chromatography can separate such macromolecular complexes in an intact configuration. The availability of different grades of gel material means that a suitable preparation can be chosen to fractionate complexes within a certain molecular weight range.

As shown previously (Chapter 2), the gelatinase species of human Bruch's membrane exist in bound and free compartments. Since SDS buffers can extract most of the bound form, the interaction that keeps the gelatinase species bound must entail hydrophobic and/or electrostatic bonding. In the present analysis, only the soluble pool of gelatinases has been examined for the presence of high molecular weight complexes.

Gel filtration chromatography has been used to fractionate the free pool of gelatinase species of human Bruch's membrane according to size and molecular weight of individual species. The presence of gelatinase activity in each of the elution fractions of the chromatographic run was determined by gelatin zymography. Column calibration with proteins of known molecular weight allowed the assignment of specific molecular weights to the gelatinase species identified. The fractionation scheme also provided elution fractions that were predominantly enriched in HMW2 species. Thus it was possible to fragment this complex (free of contaminating pro-

MMP2 that is normally present in crude extracts) with APMA and assess its composition regarding the presence of pro-MMP2.

3.2 METHODS

3.2.1 Sample preparation

Gel filtration chromatography requires much larger samples than zymography because of the inherent dilution due to the elution process. Thus tissue samples from several eyes were combined for a given preparation. Altogether eight preparations were obtained from a total of 29 donor eyes (age range 65-90 years).

The anterior portion of the globe was removed followed by the vitreous and retina. The remaining globe was 'opened' in the shape of a Maltese cross and each of the quadrants transferred to phosphate buffered saline (PBS, Sigma-Aldrich, UK). RPE layer was removed by gently brushing away with a Camel hair brush. The Bruch's-choroid layer was removed from the sclera by blunt dissection. Following a quick rinse in PBS, samples were either used immediately or stored at –70ºC for future use. Pooled samples from several eyes were macerated with a pestle and mortar in Tris-HCl buffer (100 mM Tris, 0.15 M NaCl, 10 mM $CaCl_2$, 0.02 % sodium azide, pH 7.5) and centrifuged at 10,000 rpm for five minutes. Supernatant volumes obtained ranged between 1.2 and 3.0mls depending on the amount of tissue used.

3.2.2 Gel filtration chromatography

Sepharose CL-6B separating media (delivered as a suspension in distilled water) was obtained from Sigma-Aldrich, UK. The distilled water was decanted and replaced with Tris-HCl buffer and mixed on a magnetic stirrer for about 1 hour. The process was repeated a further six times. Finally, the mixture was degassed and the Sepharose CL-6B packed into a filtration column (30 cm x 1.5 cm i.d). A reservoir of Tris-HCl buffer was attached to the top of the column and flow maintained overnight to allow tight packing of the gel material. Flow rate through the column was adjusted to 0.6-1.0mls per minute.

3.2.2.1 Determination of column void volume, v_o

The void volume of the column (v_o) was determined using Blue dextran of molecular weight 2000 kDa. A solution of blue dextran (prepared in Tris-HCl buffer) was run on the chromatography column and the absorbance of the resulting fractions was read at 610nm. A plot of the absorbance against cumulative fraction volume allowed the determination of the void volume of the column. This void volume was determined regularly to ensure stability of the column.

3.2.2.2 Molecular weight calibration

All proteins used for calibrating the column were obtained from Sigma-Aldrich (UK). These included: Carbonic anhydrase MW 29 kDa; albumin, MW 66 kDa; alcohol dehydrogenase MW 150 kDa; β-amylase, MW 200 kDa; apoferritin, MW 443 kDa; and thyroglobulin, MW 669 kDa. All protein samples were prepared in Tris-HCl

buffer and run individually on the column. The absorbance of the fractions was read at 280nm. A plot of absorbance versus the ve/vo ratio was used to determine the ve/vo of the peak of the individual protein. Peak ve/vo (volume $_{eluant}$ /volume $_{void\ volume}$) ratios for individual proteins were plotted against their respective logarithmic molecular weights to obtain the calibration curve.

3.2.2.3 Gel filtration chromatography of gelatinases

Supernatants from the tissue extracts (volume 0.6mls) were applied to the column and the chromatographic run instigated. Eluant aliquots were collected every 1.5 to 2.0 minutes using a LKB (Sweden) fraction collector. The protein profile of the chromatography run was obtained by measuring the absorbance of the fractions at a wavelength of 280nm. The gelatinase components in each fraction were determined by gelatin zymography as previously described (section 2.2.2). Areas under individual gelatinase species were plotted as a function of gel fraction. The intensity of the bands with proteolytic activities of gelatinases was plotted as a function of fraction number to determine their mobility on the column.

3.2.3 Fragment analysis of HMW2

In the previous studies of chapter 2, uncertainties remained as to the inclusion of pro-MMP2 in the HMW2 polymeric species. Clarification could be obtained if a purer source of HMW2 was available without any contaminating pro-MMP2 in the sample. On gel filtration chromatography, such a sample with trace amounts of

HMW1 and pro-MMP9 was available and was therefore fragmented by APMA activation (2.2.4.1) and the breakdown products analysed.

3.3 RESULTS

3.3.1 Gel filtration chromatography of gelatinase species

The analysis was undertaken with the free gelatinase extracts from pooled donor eyes. Following gel filtration chromatography, individual fractions were subjected to gelatin zymography to identify the presence of various gelatinase species. Representative gels showing the distribution of MMPs in the chromatographic run for two extracts are shown in Figure 3.1. Figure 3.1A was obtained from an extract from 3 eyes, donor ages 71, 73 & 84 years and Figure 3.1B from 8 eyes, donor age range 69-84 years. In gel filtration chromatography, larger species are eluted early followed by species of progressively decreasing molecular weight.

These zymograms show that fractions could be categorised into four groups. The first group collected at early stage (fraction numbers 15-20) contained high levels of HMW2 and lesser amounts of HMW1 and MMP9 and traces of MMP2. Group 2 contained traces of HMW2. All the major species of gelatinases were present in Group 3 with Group 4 containing primarily MMP2 and MMP9.

The Group 1 region of the chromatographic run represents the elution of very large complexes that could not enter the spaces within the gel beads and have been

'voided' from the column. Thus the presence of HMW2, HMW1, pro-MMP9 together with trace amounts of pro-MMP2 in this region implies that all these species must have run as one large macromolecular weight MMP complex, now termed 'LMMC'.

All four of the above mentioned gelatinase species were also present in Group 3 fractions but they could not have run as a complex since this would have shifted their elution to the void volume region (Group 1). It seems odd that despite the different molecular weights (as determined by zymographic methods), HMW1, HMW2 and pro-MMP9 appear to be present in the same elution fractions. It is likely that under gel filtration conditions, the individual species may be migrating as loosely bound polymers and therefore the molecular weights assigned by zymography would not be valid. The situation can be resolved by determining the molecular weight of the eluting species and will be addressed later. Another possibility that must be entertained to explain this anomaly is that following elution, pro-MMP9 may have polymerised to the high molecular weight forms during the time between elution collection and the zymographic runs. This is perhaps not surprising since working solutions of FCS also tend to accumulate HMW1 & 2 over time.

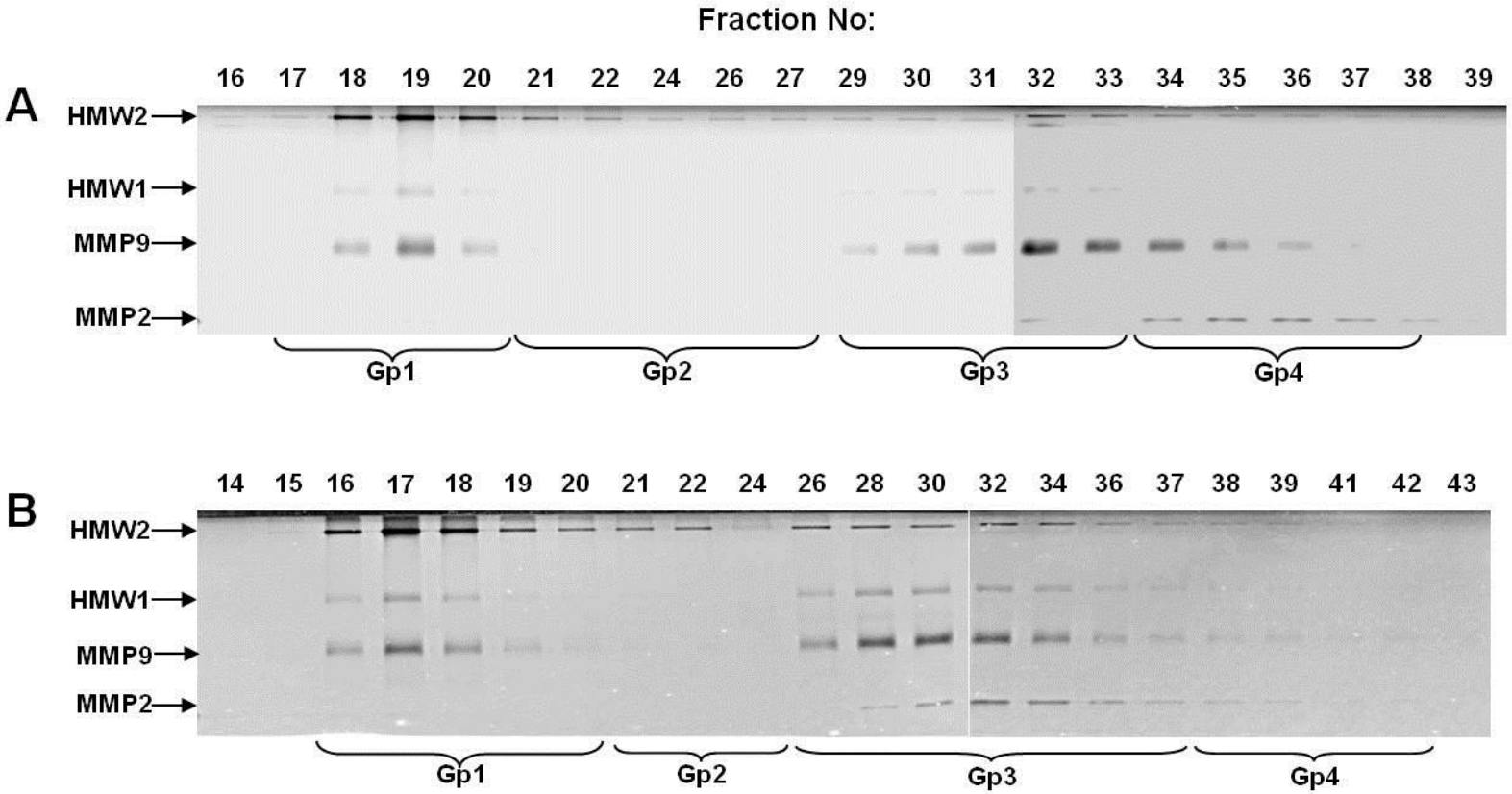

Figure 3.1 Gel filtration chromatography of the free gelatinase pool of Bruch's membrane.

After gel filtration individual fractions were subjected to gelatin zymography. Highest levels of HMW2 were present in the early fractions together with the presence of HMW1 and MMP9. This was followed by fractions containing very little gelatinase activity except for traces of HMW2. MMP9 together with some HMW1/HMW2 was then released accompanied in later fractions with MMP2.
A: Extract from three eyes (5mls), donor ages 71, 73, and 84 years; applied 0.6ml to column
B: Extract from 8 eyes (2.0mls), donor age range 69-84 years; applied 0.8mls to column

The gels were subjected to densitometry and the distribution of individual gelatinases in the chromatographic fractions is shown for four preparations in Figure 3.2. In every preparation examined, the earliest group of gelatinases eluted contained a mixture of HMW2, HMW1, high levels of pro-MMP9 together with the trace amounts of pro-MMP2. The peak of these MMP species corresponded to fractions 17-20 with an elution volume of about 17-18 mls i.e., at the void volume of the column (described later). Thus these four MMP species at the forefront of the elution profile must have moved as a single macromolecular MMP complex (designated earlier as LMMC).

Pro-MMP9 was present in two discreet peaks along the chromatographic run. The first peak corresponded to the species complexed in the LMMC particle whilst the later eluted species corresponded to the free form. It should also be pointed out that in preparations 2, 3 & 4, peaks for non-LMMC derived HMW1 & 2 corresponded to the peaks of pro-MMP9, i.e., they appeared to run in the same fractions but not as a complex since this would have shifted their elution profiles towards the void volume of the run. Running together would suggest that under the conditions of the gel filtration process, these various species appear to display similar molecular weights.

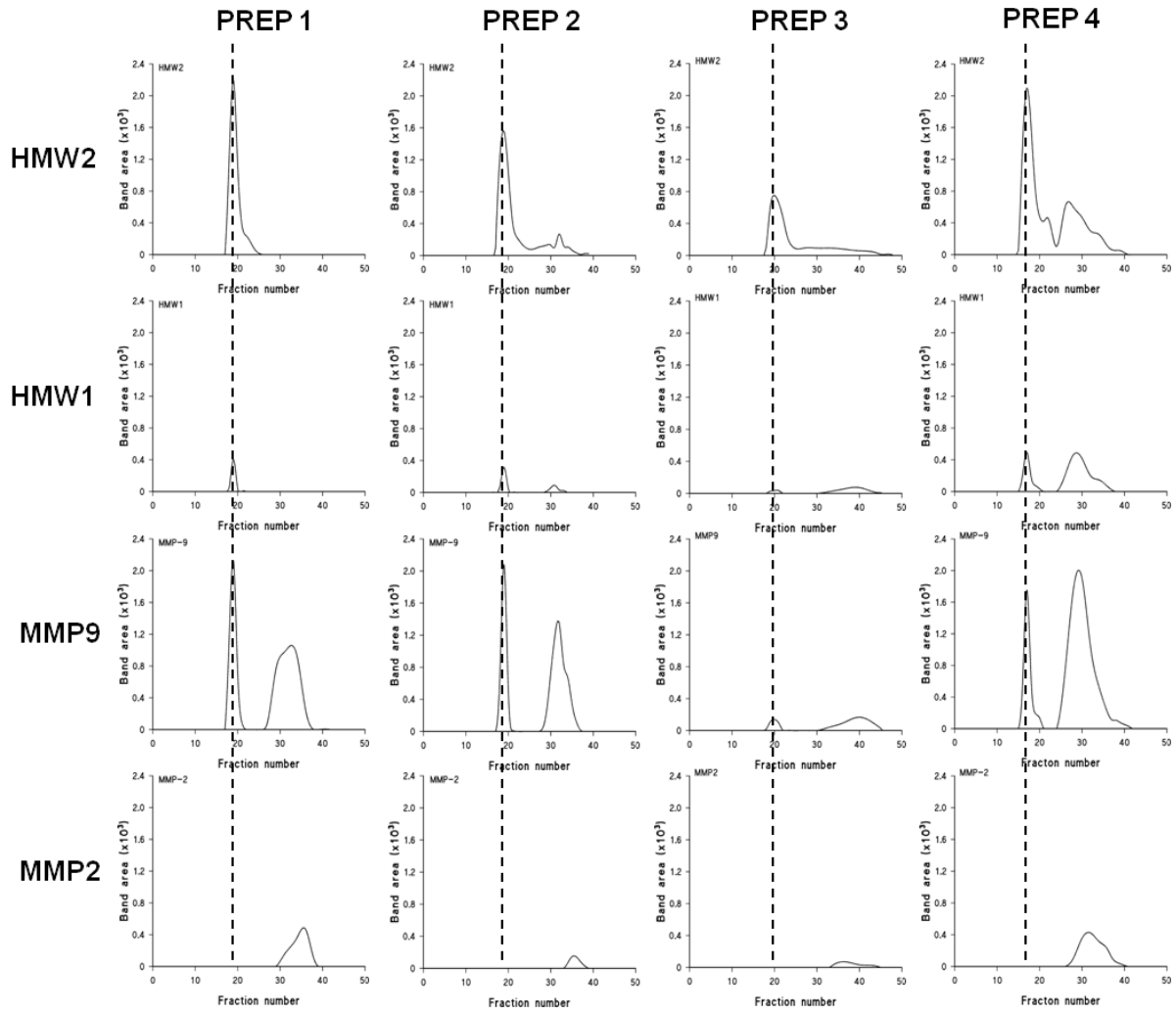

Figure 3.2 Gel filtration chromatography of the free gelatinase pool of Bruch's membrane.

Band intensities corresponding to the various gelatinase species have been plotted as a function of fraction number. In every preparation examined, the earliest fractions corresponding to the highest molecular weight species always contained a mixture of HMW2, HMW1 and MMP9 indicative of the fact that these species moved as one complexed macromolecular entity. Three of the four preparations displayed also showed that the free MMP9 fractions were also associated with some degree of HMW1 & HMW2. MMP2, being the smallest species, was eluted last but with considerable overlap with the slightly larger MMP9 species.
Prep 1: extract from two eyes (donor ages 72&79 years); Prep 2: extract from 3 eyes (donor ages 71, 73 & 84 years, Gel A of Fig.1); Prep 3: extract from two donor eyes (ages 67 & 81 years); Prep 4: extract from 8 eyes (donor age range 69-84 years; Gel B of Fig.1).

3.3.2 Molecular weights of gelatinase species by gel filtration

3.3.2.1 Determination of void volume of column

The void volume (vo) is the elution volume of molecules that are excluded from the gel filtration medium because they are larger than the largest pores in the matrix and pass straight through the gel bed. In the case of Sepharose CL-6B, Blue dextran of MW 2000 kDa is too large and will be completely excluded from the matrix. This dextran was therefore run on the column to determine the void volume. Any gelatinase species appearing close to this void volume would have also been excluded because of its very large size.

Two separate runs with Blue dextran are shown in Figure 3.3 allowing the determination of void volume of the column as 17.25 mls. Void volumes for different columns were within the range 16-18mls.

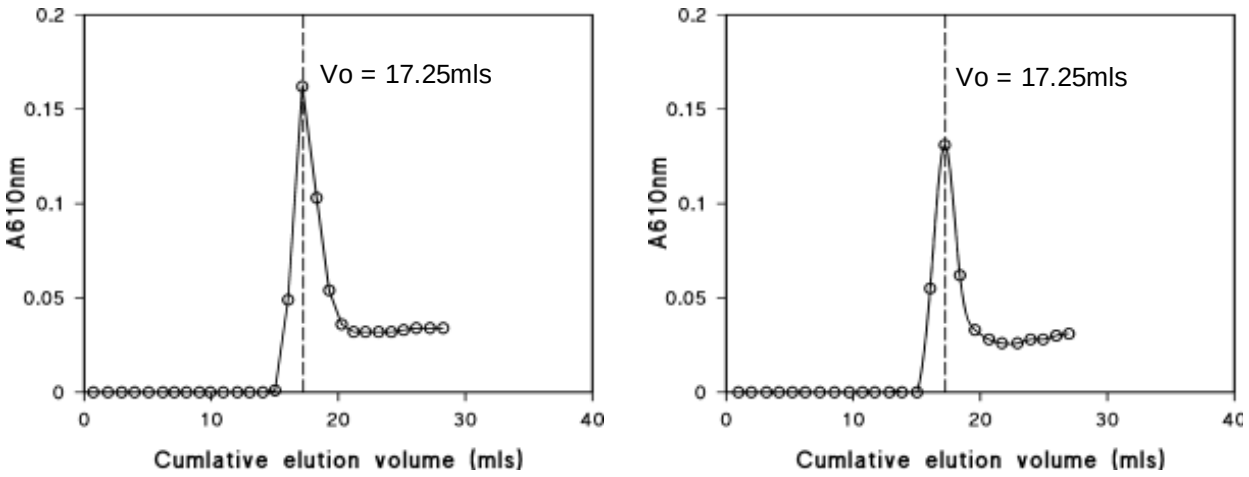

Figure 3.3 Determination of the void volume of the column.

3.3.2.2 Protein calibration curve for determination of molecular weights

Proteins of various molecular weights in the range 29 – 669 kDa were run individually and the ve/vo ratios of the elution peaks were determined (Figure 3.4). Elution profiles for carbonic anhydrase, albumin and beta-amylase were characterised by a single peak. However, the commercial samples of alcohol dehydrogenase and apoferritin showed two peaks with the smaller molecular component being a breakdown product. In the case of thyroglobulin, polymerisation was noted with one of the peaks coinciding with the void volume.

The ve/vo ratios for the various protein markers were plotted against their respective logMW to obtain a calibration plot (Figure 3.5). The relationship between ve/vo and logMW was described by the equation:

$$\text{LogMW} = -2.14 * (ve/vo) + 8.89.$$

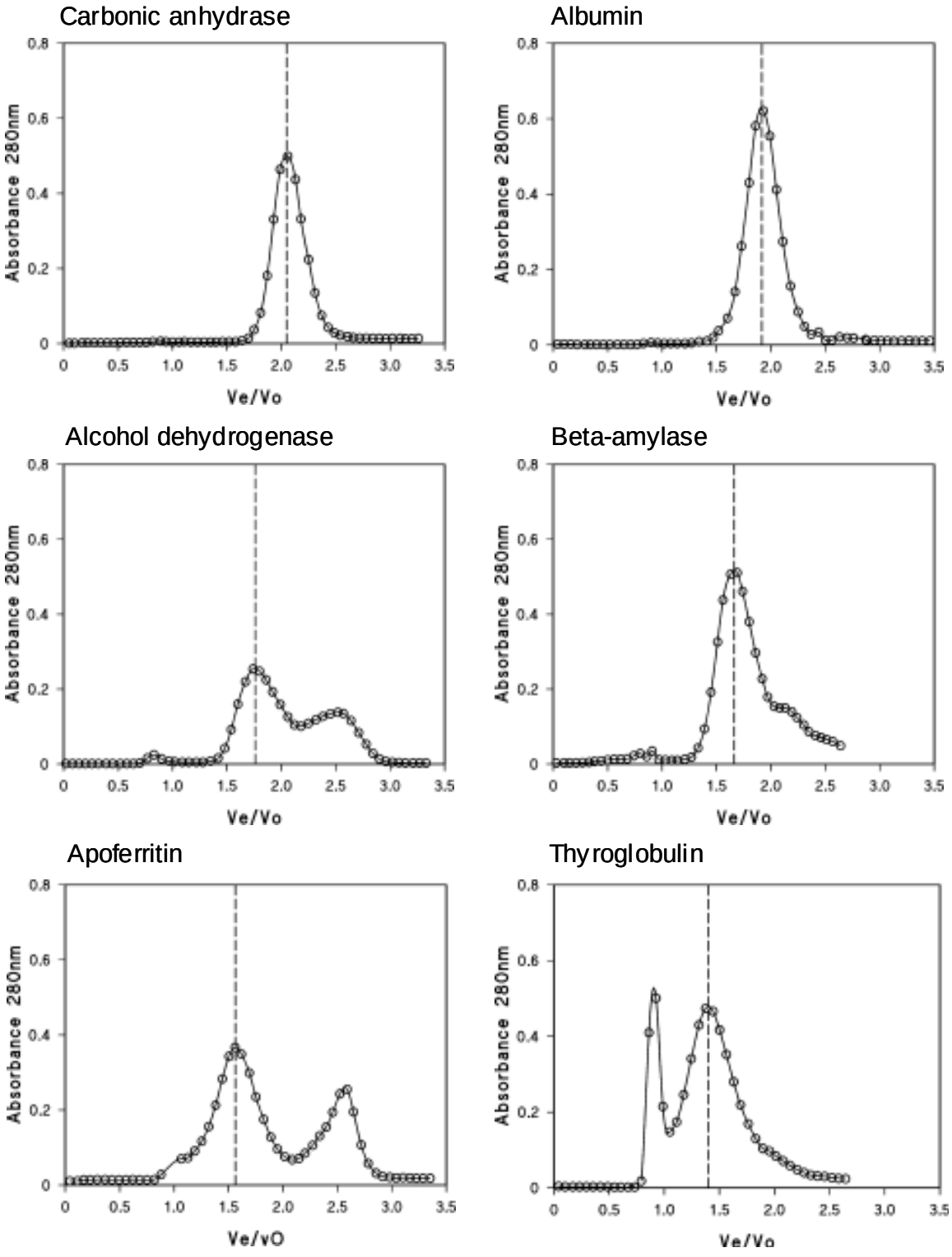

Figure 3.4 Elution profiles of protein molecular weight standards used in the construction of a calibration curve.

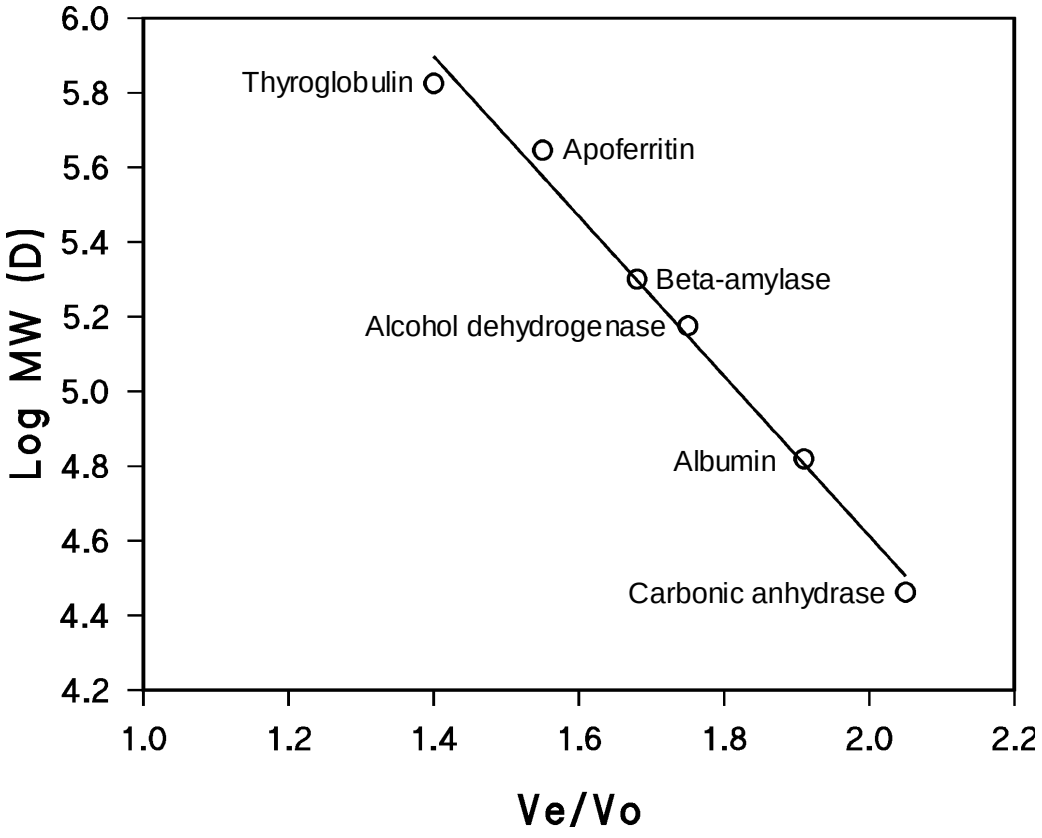

Figure 3.5 Calibration curve for determination of molecular weights of MMP species by gel filtration chromatography.

3.3.3 Molecular weights of gelatinase species of Bruch's membrane

The elution profiles of MMP extracts of Bruch's membrane were normalised with respect to ve/vo ratios and a representative plot is given in Figure 3.6. The peak ve/vo for individual species was determined and with reference to the calibration plot of Figure 3.5, the relevant molecular weight of the gelatinase was calculated.

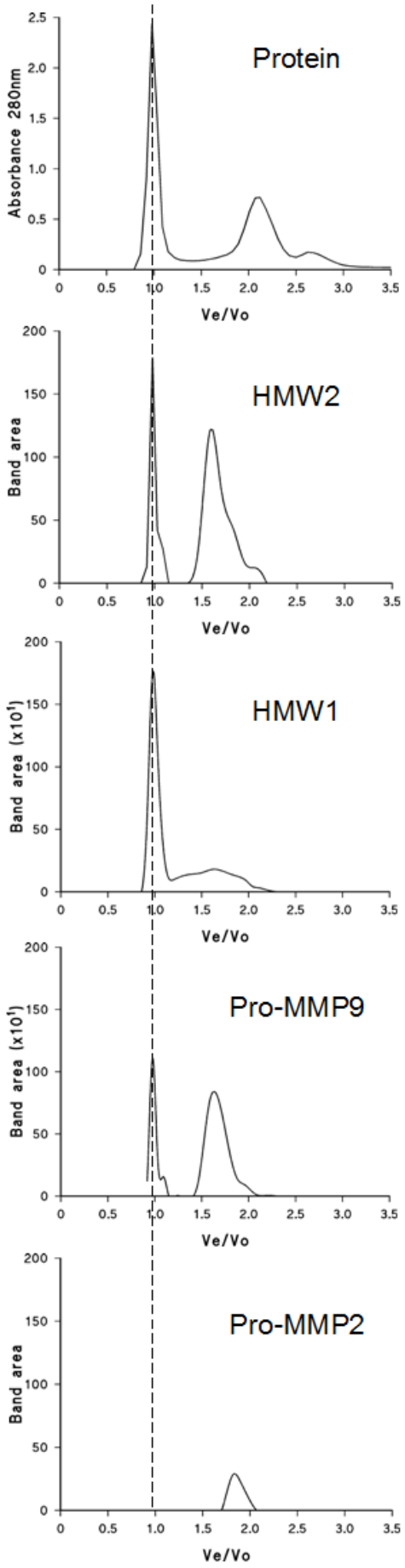

Figure 3.6 Gel filtration chromatography and analysis of various gelatinase species in the eluant fractions.

The extract was obtained from four eyes of donors aged 86-95 years. The cumulative fraction volumes were converted to ve/vo ratios by dividing by the void volume of the column, determined in this run as 17.25mls. The elution profiles show the presence of HMW1, HMW2, and Pro-MMP9 in the void volume region of the run. Pro-MMP2 was also visibly present as a faint band in this region but levels were below the detection limits of densitometry. These gelatinases represent the contribution of the LMMC complex. The later fractions constitute the free, uncomplexed gelatinase species. In this particular run, the HMW1 fraction showed a broad profile. From the peak ve/vo ratios and with reference to the protein calibration plot (Figure 3.5), the molecular weights of HMW2, HMW1, Pro-MMP9, and Pro-MMP2 were calculated as 292, 218, 240 and 94 kDa respectively.

The molecular weights of individual gelatinase species obtained from 6-8 fractionations have been tabulated in Table 3.1. Also shown are the molecular weights derived from zymography. Molecular weights derived from gel filtration represent the 'true' configuration of the gelatinase species whereas those derived from zymography represent the monomers in the loosely bound complex.

The data shows that in the free pool of Bruch's membrane, pro-MMP2 and HMW2 exist as monomers, and pro-MMP9 and HMW1 exist as dimers. Since in this configuration, the molecular weights of pro-MMP9, HMW1 and HMW2 are similar, their elution profiles were also similar giving rise to the distribution observed in Group 3 of the gel profiles in Figure 3.1.

	Zymography (Z)	Gel Filtration (GF)	Ratio (GF/Z)	State in tissue
Pro-MMP2	65 ± 1 kDa*	88 ± 14 kDa	1.3	Monomer
Pro-MMP9	95 ± 2 kDa*	191 ± 35 kDa	2.0	Dimer
HMW1	122 ± 9 kDa	208 ± 19 kDa	1.7	Dimer
HMW2	344 ± 22 kDa	307 ± 17 kDa	0.9	Monomer

Table 3.1 Comparison of molecular weights of gelatinase species determined by gel filtration and zymography.

The ratio of molecular weights by the two techniques was also calculated (GF/Z) and rounding up to whole numbers allowed for designation of species in the free pool as either monomer or dimer. Data has been presented as Mean ± SD (n) where n= 6-8. *data from chapter 2.

3.3.4 Fragment analysis of HMW2.

An eluant fraction (fraction 20, preparation 3, Figure 3.2) containing predominantly HMW2 species with some contamination with pro-MMP9 but with no pro-MMP2 was activated/reduced/alkylated to obtain fragments for analysis of released MMPs (Figure 3.7). Fragmentation of HMW2 resulted in the release of the MMP2 species and therefore this complex is a co-polymer of pro-MMPs 2 & 9

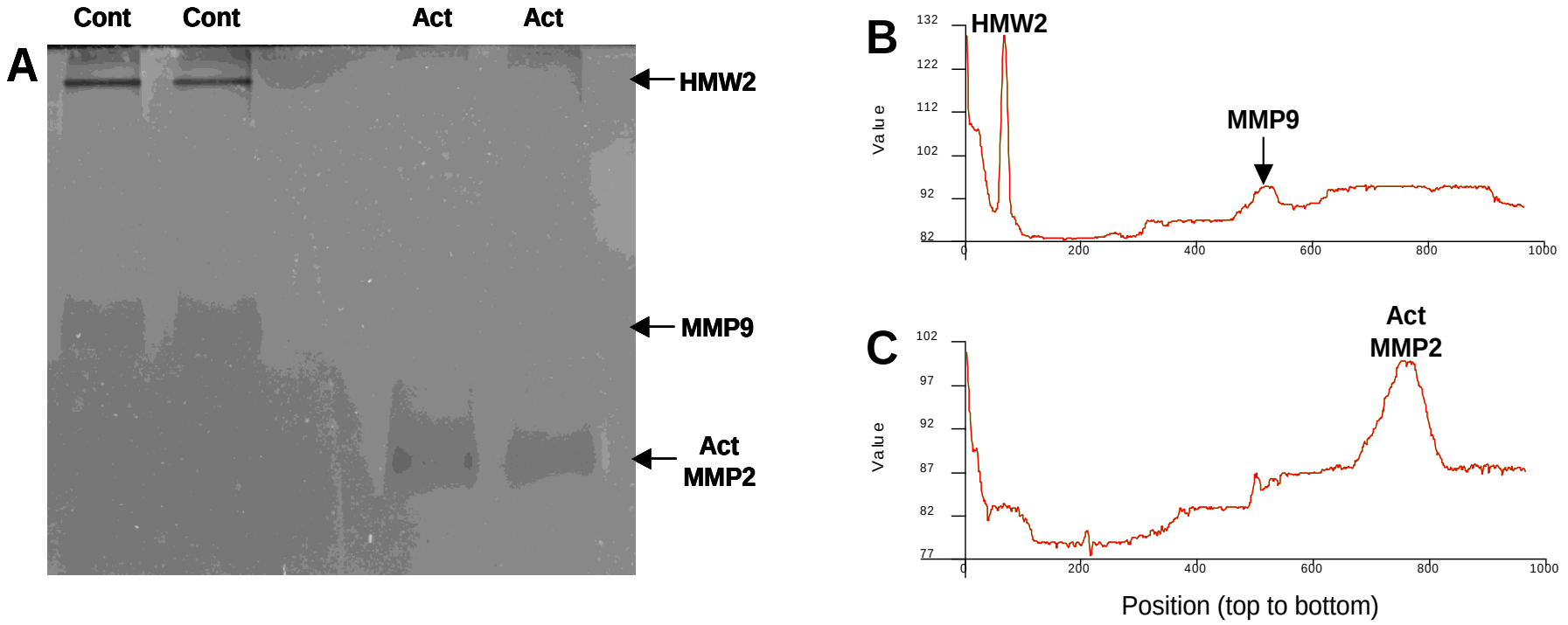

Figure 3.7 Activation of gelatinases in the HMW2 enriched fraction.

Fraction 20 of Preparation 3 (Figure 3.2) that contained predominately HMW2 and some MMP9 was activated and the resulting zymogram is shown in A. The HMW2 band was lost with a concomitant increase in levels of activated MMP2. The underlying changes are made more clear in the scans of B and C. Scan B shows the presence of HMW2 and MMP9 but no HMW1 or MMP2 species. Activation (Scan C) shows loss of HMW2, increase in the region of active and inactive MMP9 and a prominent increase in the level of active MMP2.

3.4 DISCUSSION

Previous studies using zymography have identified the presence of pro-and active forms of MMP9 (MW 95 & 84 kDa respectively) and MMP2 (MW 65 & 58 kDa respectively) in human Bruch's membrane (Ahir *et al.*, 2002; Guo *et al.*, 1999). The present study has confirmed the existence of two further MMP species, termed HMW1 & 2 of molecular weights 122 ± 9 and 344 ± 22 kDa respectively (Chapter 2, (Kumar *et al.*, 2010). Thus six gelatinase species have now been identified in human Bruch's membrane.

Fragment and Western blot analyses have demonstrated the presence of pro-MMP9 in HMW1 & 2 and therefore these high molecular weight species are most likely to be homo or hetero polymers of MMPs 2 & 9. Confirming the presence of pro-MMP2 within these complexes has proved difficult. However, the present gel filtration analysis allowed the isolation of a fraction enriched in HMW2 without contamination from pro-MMP2. Fragment analysis of such a preparation showed that the HMW2 species also contained MMP2. Thus the HMW2 complex must be a co-polymer of pro-MMPs 2 & 9.

The zymographic techniques have successfully demonstrated the unitary presence of various components of the MMP system in Bruch's. However our knowledge of higher order structures formed through non-covalent interactions between monomeric units has been rudimentary. Gel filtration chromatography has allowed the analysis of MMP species in their native configuration. Thus, pro-MMP2 and HMW2 species were observed to exist as monomers whilst pro-MMP9 and

HMW1 circulated within Bruch's as dimers. The relative equivalence of molecular weights of Pro-MMP9, HMW1 and HMW2 in their native configurations meant that they were eluted roughly within the same fractions of the chromatographic run.

The most reproducible finding in the gel filtration profile was the presence of HMW2, HMW1 and high levels of pro-MMP9 at the elution front in the void volume. Such a grouping travelling at the elution front can only occur if the components were bound together in a complex, now termed the large macromolecular MMP complex (LMMC). Pro-MMP2 was just detectable in the LMMC region of the fractionation regime.

The HMW2 species sequesters pro-MMPs 2 & 9 and the LMMC complex sequesters HMW2, HMW1 and a lot of pro-MMP9. Such sequestration is expected to reduce the level of free pro-MMPs for activation and may impact on the MMP-mediated turnover of Bruch's membrane. The inter-relationships between the six gelatinase species and the LMMC complex can be used to construct a working model of the MMP pathway that can be used to predict the effect of age and age-related diseases on the operation of the renewal system of Bruch's membrane (Figure 3.8).

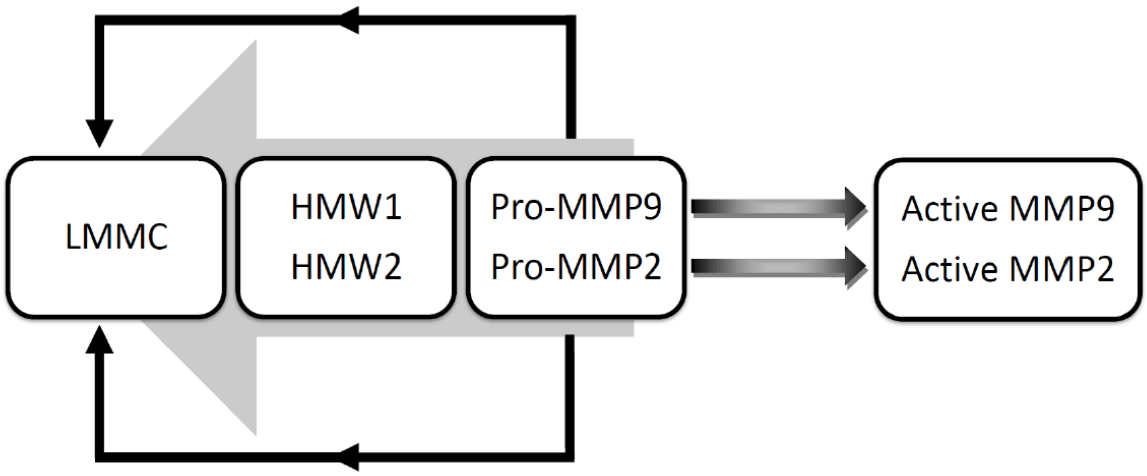

Figure 3.8 The MMP pathway in human Bruch's membrane.

The level of MMPs 2 & 9 in the free pool will regulate the rate of activation of these enzymes. In the case of pro-MMP2, previous studies have already demonstrated the rate of activation being dependent on optimum levels of both pro-MMP2 and TIMP2 near the basolateral surfaces of the RPE (Butler *et al.*, 1998; Strongin *et al.*, 1995). Little is known of the activation mechanism of pro-MMP9 in an extracellular compartment, but as suggested by several reports, if activation is dependent on binding of the molecule to damaged portions of the collagen molecule, then the amount of activated MMP9 will depend on the available pool of pro-MMP9 for activation.

Ageing of Bruch's is associated with an increase in the levels of HMW1 & 2 and therefore increased sequestration of pro-MMPs 2&9. Such an increase will be expected to lead to greater formation of the LMMC complex further sequestrating pro-MMP9. A reduction in the level of free pro-MMPs will impact on the conversion to

activated form of MMPs. This may explain the reported scarcity of active forms at macular locations compared to peripheral locations in ageing human donor eyes (Guo *et al.*, 1999).

Experimental verification of the free levels of pro-MMPs 2&9 has not yet been undertaken. Measurements that utilise zymographic techniques are doomed to failure because the use of SDS buffers will release the large pool of pro-MMP9 from the LMMC complex leading to the artefactual elevation of pro-MMP9 levels. It may be possible to undertake such an analysis using high performance liquid chromatographic (HPLC) techniques using gel permeation columns.

The development of the above scheme for the MMP pathway was dependent on identifying and characterising the individual members of the gelatinase system in human Bruch's membrane and evaluating the age related changes in its components. In age-related macular degeneration (AMD), the advanced nature of the ageing changes would suggest that the MMP pathway may have been shifted far to the left. This has yet to be investigated.

CHAPTER 4

THE GELATINASE SYSTEM

IN AGE RELATED MACULAR DEGENERATION (AMD)

4 THE GELATINASE SYSTEM IN AGE RELATED MACULAR DEGENERATION (AMD)

4.1 INTRODUCTION

Age-related macular degeneration (AMD) remains the single largest cause of untreatable blindness in the elderly population (Klein *et al.*, 1992). The prevalence of the disease is age dependent with levels of 1.3%-3% in the young (<55 years) increasing to 28%-30% in those aged 75 years and older (Friedman *et al.*, 2004; Klein *et al.*, 1992). Clinically, AMD is divided into early and late forms. Early AMD is characterised by the presence of drusen and retinal pigmentary abnormalities such as hypo- or hyperpigmentation (Nowak, 2006). Drusen are dome shaped deposits lying between the basal lamina of the retinal pigment epithelium (RPE) and inner collagenous layer of Bruch's membrane. Although the presence of drusen remains a hallmark of AMD, they are also present in normal advanced ageing. It is the size, number and degree of confluency of druse that determines the risk of AMD (Pauleikhoff et al., 1990; Ambati et al., 2003). Early AMD progression to the late type is associated with two specific phenotypes; the 'dry' form, present in about 13% of all AMD patients showing geographic atrophy of the RPE and photoreceptors whilst the 'wet' form (comprising 10-20%) is associated with additional neovascular complications (Friedman *et al.*, 2004).

The aetiological mechanisms underlying the development and progression of AMD remain uncertain. Epidemiological studies have shown AMD to be a highly

complex, multi-factorial disease that has both a genetic disposition and considerable gene-environmental interactions (Hawkins *et al.*, 1999; VanNewkirk *et al.*, 2000). A genetic predisposition has been indicated from studies of familial aggregation, twin studies and classical linkage analysis (Klaver *et al.*, 1998; Majewski *et al.*, 2003). The diverse genetic associations with AMD best reflect the complex nature of the disease process. These genetic variations associated with AMD include several members of the complement pathway, components in lipid metabolism (cholesterylester transfer protein (CETP), hepatic lipase (LIPC), apolipoprotein E), heat shock serine protease (Htra1) and polymorphisms in the satellite promoter region of the matrix metalloproteinase-9 gene (MMP9) (Cameron *et al.*, 2007; Chen *et al.*, 2010; Edwards *et al.*, 2005; Fiotti *et al.*, 2005; Neale *et al.*, 2010; Thakkinstian *et al.*, 2006)

Despite the complexities of the mechanisms involved, the underlying changes in Bruch's membrane of AMD donors show clear signs of advanced ageing (Dorey *et al.*, 1989; Sarks *et al.*, 1999). Thus normal ageing changes such as increased thickness of Bruch's (Okubo *et al.*, 1999; Ramrattan *et al.*, 1994), deposition of normal and abnormal ECM material (Karwatowski *et al.*, 1995), increased cross-link formation (oxidative and non-enzymic glycosylation leading to advanced glycation end-products, AGEs and ALEs) (Handa *et al.*, 1999) and the accumulation of lipid-rich debris (Holz *et al.*, 1994; Pauleikhoff *et al.*, 1990) are further exaggerated in AMD.

The gross structural changes in AMD impact on the functional competence of Bruch's membrane. Transport functions such as movement of fluids and diffusional delivery of macromolecules across the membrane are further reduced (Hussain *et al.*,

2010; Hussain *et al.*, 2004). Clinically, reduced transport status is often indicated by reduced scotopic thresholds in the elderly and in those with early maculopathy due to reduced efficiency in the transport of vitamin A (Chen *et al.*, 1992; Owsley *et al.*, 2001; Owsley *et al.*, 2006; Steinmetz *et al.*, 1993). In AMD, diminished metabolic support may therefore be the initial insult that progresses to the death of RPE and photoreceptors, recruiting additional inflammatory or neovascular episodes.

The important role of the MMP degradation system in maintaining the structural and functional characteristics of normal ageing Bruch's membrane has previously been stressed. It would appear to be even more important in the case of AMD where gross abnormalities have been identified. Thus not surprisingly, the MMP system has begun to attract attention. TIMP3 levels of Bruch's membrane were considerably elevated in AMD donors compared to age-matched controls with the consensus being that elevated TIMP3/MMP ratios may underlie the increased thickening of Bruch's in this condition (Fariss *et al.*, 1998; Kamei *et al.*, 1999). Involvement of the MMP system in the aetiology of AMD has also been inferred from the raised levels of plasma pro-MMP9 in these patients (Chau *et al.*, 2008). This increased expression of pro-MMP9 may be related to polymorphisms in the promoter region of the MMP9 gene since this appears to dictate the transcription activity for this enzyme (Peters *et al.*, 1999; Shimajiri *et al.*, 1999; Ye, 2000). Thus in mesanglial cells of mice, 24 repeats of the cytosine-adenine (CA) sequence in the promoter region was associated with 20 times higher expression of pro-MMP9 compared to strains with 20 CA repeats (Fornoni *et al.*, 2002). An association between the length of the MMP9 promoter microsatellites and choroidal neovascularisation has been

documented and alleles with 22 or more CA repeats were more often found in AMD patients (Fiotti *et al.*, 2005).

The present investigation was therefore designed to 'screen' donor tissue and clarify any disturbance (if present) in the gelatinase component of the MMP degradation system of Bruch's membrane from donors with AMD. It would have been ideal to examine macular regions but tissue samples were only available from aged donors and the highly degenerative state and scar formation meant that isolation of intact samples was very difficult. Previous studies have shown that similar ageing changes occur across the entire fundus but that the macular region ages at a faster rate. With this in mind, peripheral samples of Bruch's-choroid were obtained from six AMD (age range 71-95 years) and thirteen control donors (age range 71-99 years) and the level of the different gelatinase species in the free and bound fractions was quantified by zymographic methods.

4.2 METHODS

4.2.1 Tissue preparation

Human donor eyes, with consent granted for research, (13 pairs, age range, 71-99 years and post-mortem times 24-48 hours) were obtained from the Bristol Eye Bank, U.K. In addition, six AMD donor eyes (ages 71, 79, 81, 83, 87 and 95 years) were obtained through the Macular Disease Society Eye Donor Scheme, UK. Clinical data sheets accompanied AMD donor eyes and their status was confirmed by fundus examination during the dissection procedure. The corneas were removed for use in transplantation surgery and the remaining globes were transported to the laboratory on saline moistened pads in an icebox.

The methodology for obtaining peripheral samples was identical to that described previously (section 2.2.1). Briefly, the tissue sample (8mm disc) was taken from the peripheral region of the fundus along an imaginary line joining the optic disc, fovea and the cut edge of the anterior globe.

4.2.2 Sample preparation for zymography

Methodology was as described in the ageing study described previously (section 2.2.6). Briefly, for extraction of free and bound pools of gelatinase species, 100µl of PBS was added to each sample and the tubes voxtexed five times for periods of one minute each. Samples were then centrifuged for 5 minutes at 10,000g and the supernatant, representing the free pool of MMPs removed. Twenty micro-

litres of the supernatant was mixed with 40µl of non-reducing SDS sample buffer (Invitrogen, UK) and 20µl of this mixture applied to zymographic gels.

The pellet from the above centrifugation was washed several times with 1.0mls aliquots of PBS and reconstituted with 20µl water and 40µl non-reducing SDS sample buffer. Samples were vortexed as before, spun at 10,000g for five minutes and 20µl of the supernatant representing the bound or SDS-extracted fraction applied to zymographic gels.

4.2.3 Zymography

Zymographic analysis was identical to that previously described (section 2.2.2). Protein molecular weight standards were included in each gel to allow determination of the molecular weights of individual gelatinase species. For each gel, log plots of migratory distance versus molecular weight were constructed.

4.2.4 Statistical analysis

Data has been presented as Mean ± 1 SD. The Mann-Whitney test was employed to assess significant differences ($p<0.05$; $p<0.01$ or $p<0.005$) between control and AMD samples using the add-in XLSTAT statistical analysis software for Microsoft Excel.

4.3 RESULTS

Several zymographic gels were required to undertake this screening analysis and therefore special care was taken to ensure that all procedures remained identical. Thus times for incubation, staining and de-staining were strictly controlled to minimise variations between gels.

The resulting zymograms were scanned, grey scaled with colours inverted, and aligned with respect to the position of the molecular weight markers included in each gel. They were then collated from the different gels and have been presented in Figure 4.1. All gelatinase species normally present in control samples were also present in AMD donor samples.

The free pool of gelatinases released was marked by the absence of active MMP9 from both AMD and control donors (Figure 4.1A). A visual inspection of the gels showed levels of pro-MMP9 to be elevated in AMD donors whereas levels of pro-MMP2 were reduced. The migratory distances of HMW2, HMW1, Pro- and active MMP2 were virtually the same within and between donor subsets. However, the migratory distances of pro-MMP9 showed a detectable variation within each donor set.

In the bound pool, levels of HMW2, HMW1 and pro-MMP9 were greater in the AMD donor group in comparison to controls (Figure 4.1B). On the other hand, levels of pro- and active MMP2 species were generally lower in the AMD group.

The variability in the migratory distances of pro-MMP9 observed in the free pool was much clearer in the bound samples due to the higher level of enzymatic

activity present on these zymograms. Comparing the positions of the pro-MMP9 bands in AMD donors aged 71 and 83 years suggests the possible presence of two adjacent bands in the latter. The presence of two proteins running close to each other is also indicated on gels for the 87 year old AMD donor, and control donors aged 94, 80a and 71 years. The likelihood of two adjacent protein bands can also be inferred by comparing the 98-year-old control band with neighbouring lanes for the 80a and 99-year-old samples. In the present study, no attempt was made to separate these bands and the mid-point was used in determining molecular weights.

Furthermore, active MMP9 in the control bound pool was observed as a narrow distinct band but in AMD samples, such specific banding was less frequently encountered and replaced by a broader smear (Figure 4.1B). Representative densitometric gel scans of control samples show clearly identifiable active MMP9 peaks (Figure 4.2 a, b). Scans of AMD samples were generally dominated by a gradation of activated species that appeared as smears on the zymograms (Figure 4.2 c, d).

In the 95 year-old AMD donor, the gel scan of the bound fraction (Figure 4.2c) suggests that the pro-MMP9 band may actually house two gelatinase species since the scan profile for this species was not symmetric about the expected position for pro-MMP9 depicted in Figure 4.2a. The presence of a lower molecular weight pro-MMP9 species may also be responsible for the shift in the polymeric HMW1 form (compare Figure 4.2(c) with (a)). In other samples (Figure 4.2 (b) and (d)) the presence of a single pro-MMP9 species can be discerned since the scan profile remains symmetrically aligned around the expected position on the gel.

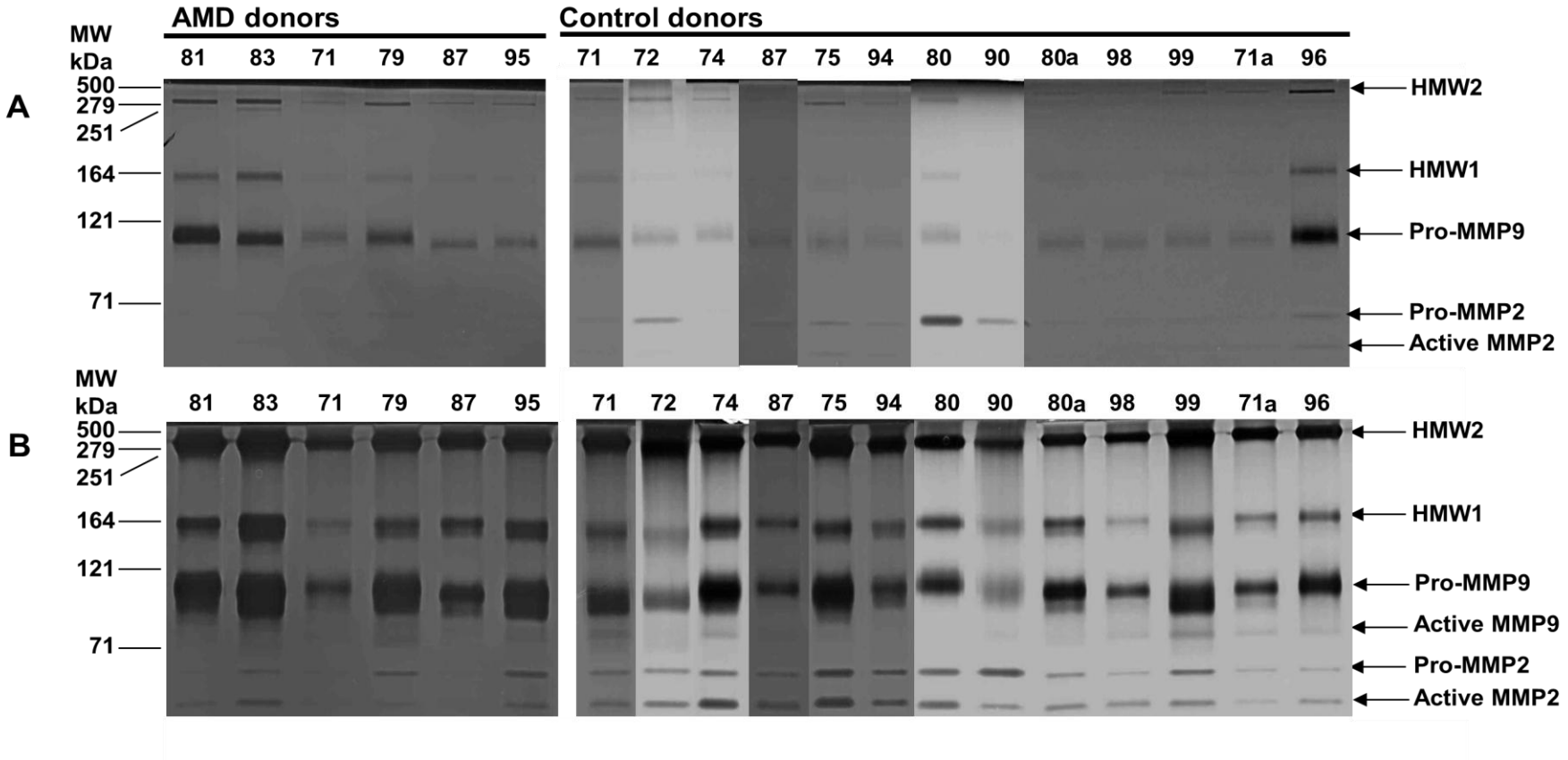

Figure 4.1 Zymographic analysis of the gelatinase component of Bruch's-choroid preparations.

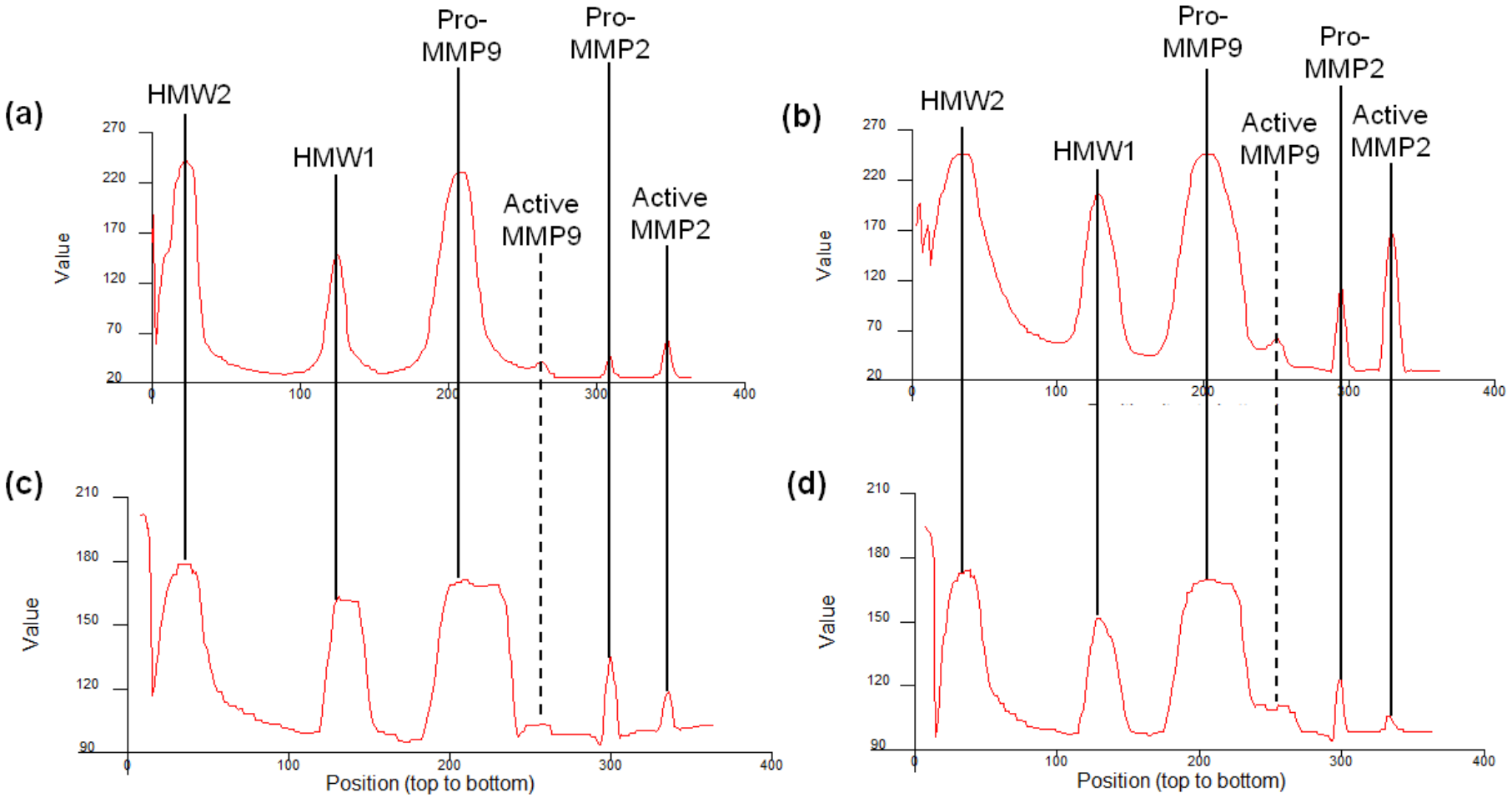

Figure 4.2 Densitometric scans of zymographic lanes in the bound fraction analysis of Panel B, Figure 4.1.

Scans (a) and (b) were from control donors (96 and 74 years old respectively).

Scans (c) and (d) were from AMD donors (95 and 79 years old respectively).

The molecular weight of individual gelatinase species was compared between controls and AMD donors. Each gel had its own molecular weight standards and logarithmic plots of relative migratory distance vs. molecular weight were used to calculate respective weights. The plot of Figure 4.3 was constructed by combining the molecular weight calibration standards from eight gels superimposing the mean molecular weights of the various gelatinase species found in the control bound fraction. Statistical analysis showed that there was no significant difference in the molecular weights of the various gelatinase species in the free and bound fractions between controls and AMD donors (Table 4.1).

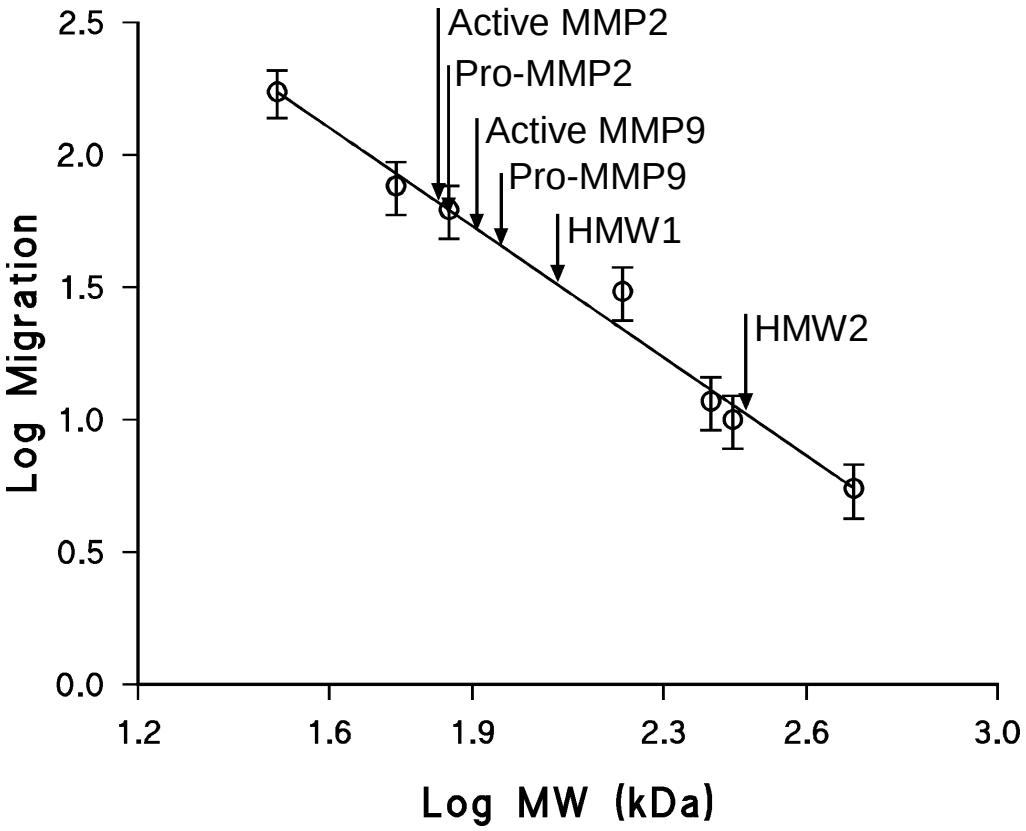

Figure 4.3 Calibration curve to measure the molecular weights of gelatinase species in Bruch's membrane.

The molecular weight standards were in the range of 31 to 500 kDa and their migration is given as Mean ± SD of data taken from eight gels. The molecular weights of the gelatinase species depicted refer to the control bound fraction.

	MMP Molecular weights (kDa)					
	HMW2	**HMW1**	**Pro-MMP9**	**Active MMP9**	**Pro-MMP2**	**Active MMP2**
FREE POOL						
Control	322 ± 40	162 ± 8	95 ± 2	-	65 ± 1	58 ± 1
AMD	338 ± 34	164 ± 3	97 ±3	-	66 ± 1	59 ± 1
BOUND POOL						
Control	323 ± 52	161 ± 7	92 ± 3	82 ± 2	65 ± 1	58 ± 1
AMD	327 ± 14	162 ± 5	94 ± 3	84 ± 2	65 ± 1	58 ± 1

Table 4.1 The molecular weight of gelatinases in the free and bound pools of Bruch's-choroid preparation.

A quantitative analysis of the level of individual gelatinase species of Bruch's-choroid preparations in terms of the free, bound and total pools is given in Table 4.2. There was considerable variation in levels within each donor group and this was reflected in the large standard deviations for a given species. A better representation of the variability in the data is provided by the Box and Whisker plots shown in Figure 4.4.

MMP species	Donor group	Gelatinase activity (area / 8mm disc)		
		Free	Bound	Total
HMW2	Control	1435 ± 1520	12702 ± 3940	14137 ± 4725
	AMD	6685 ± 5444*	15195 ± 3018	21880 ± 8182*
HMW1	Control	1335 ± 2470	5996 ± 2911	7331 ± 4040
	AMD	6327 ± 7064**	10480 ± 5616	16807 ± 11950*
Pro-MMP9	Control	9354 ± 11895	16068 ± 7692	25422 ± 16553
	AMD	33375 ± 25579***	22572 ± 7274	55947 ± 30662*
Pro-MMP2	Control	1567 ± 1753	1393 ± 964	2960 ± 2071
	AMD	379 ± 374*	674 ± 700	1053 ± 854*
Active MMP9	Control	NDet	517 ± 376	517 ± 376
	AMD	NDet	195 ± 80*	195 ± 80*
Active MMP2	Control	357 ± 428	1978 ± 1140	2336 ± 1257
	AMD	335 ± 519	614 ± 534***	949 ± 885*

Table 4.2 Gelatinase activity of peripheral Bruch's-choroid in control and AMD donors.

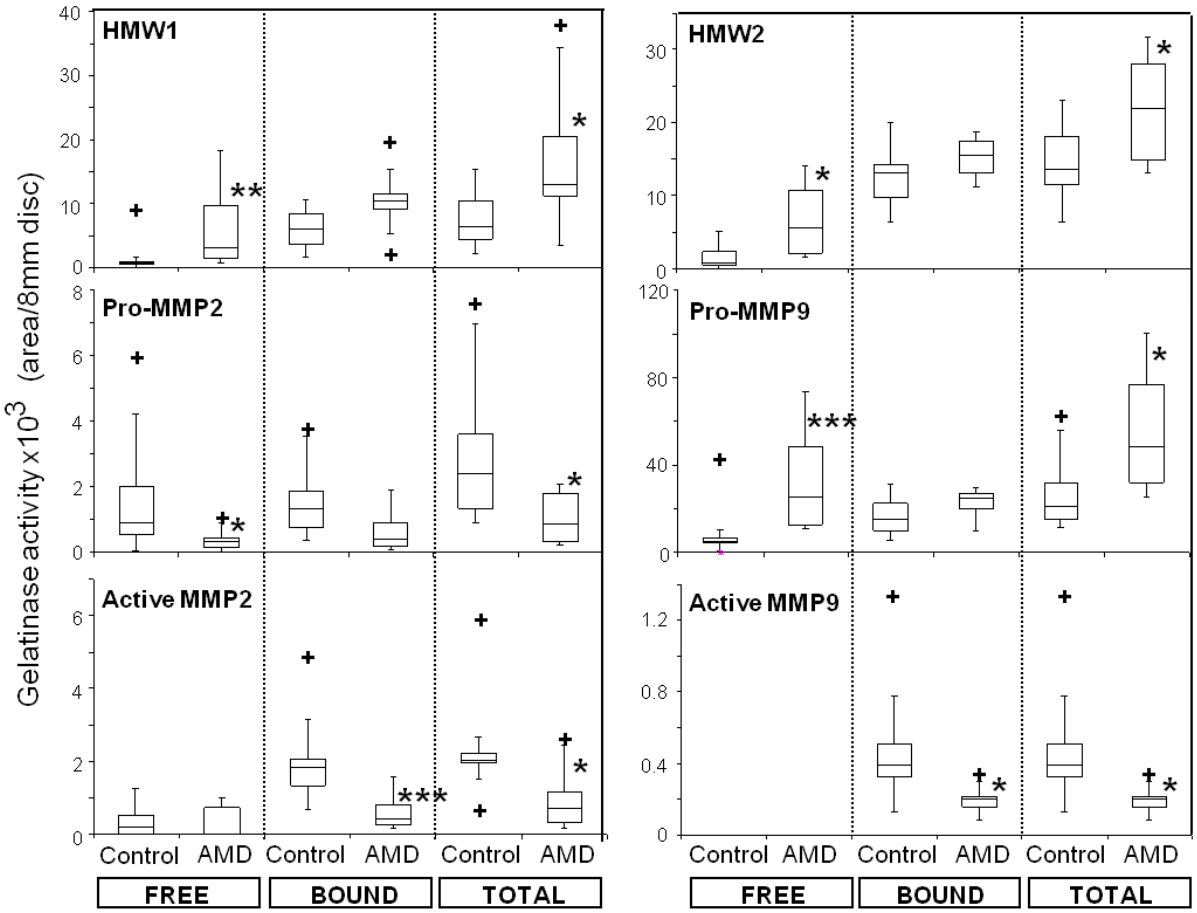

Figure 4.4 Box and Whisker plots of gelatinases in control and AMD Bruch's-choroid preparations.

Median, quartiles and inter-quartile ranges (IQR) were determined from the data of Table 2. The ends of the whiskers were set at 1.5 x IQR above the third quartile (Q3) and 1.5 x IQR below the first quartile (Q1). The maximum and minimum values, if outside the whisker range, are shown as crosses. * $p<0.05$; ** $p<0.01$; *** $p<0.005$.

The total level of high molecular weight gelatinases, HMW1 & HMW2, was significantly raised in donors with AMD ($p<0.05$). In the absence of a statistically significant increase in bound levels, the observed increase in total levels was due primarily to an increase in free levels of HMW1 and HMW2 ($p<0.01$ and $p<0.05$ respectively). The free level of HMW1 & 2 in AMD donors was about 4.8-fold higher than in controls. The percentage of total HMW1 & 2 that was in the bound fraction in controls was 82 and 90% respectively, whereas in AMD this was reduced to 62 and 69% respectively.

Levels of free pro-MMP9 were significantly raised in AMD donor tissue ($p<0.005$) doubling the total content of this MMP compared to controls ($p<0.05$). Despite this increase in the pro-form, bound and total active MMP9 levels were reduced ($p<0.05$).

The free and total levels of pro-MMP2 were reduced in AMD ($p<0.05$). Comparing means, the reduction in free and total amounted to 4- and 3-fold respectively. Also apparent in AMD samples was the reduction in bound and total levels of active MMP2 ($p<0.005$ and $p<0.05$ respectively).

In summary, in AMD donor samples of Bruch's membrane, levels of HMW1, HMW2 and pro-MMP9 were considerably raised. Levels of pro-MMP2, and active MMPs 2 & 9 were reduced.

4.4 DISCUSSION

The zymographic analysis has demonstrated a disturbance in the gelatinase machinery of Bruch's-choroid preparations from donors with AMD. More specifically, the total levels of active MMP2 and 9, enzymic forms responsible for proteolysis, were significantly reduced, diminishing the degradative capacity that is essential for maintaining the structural and functional characteristics of Bruch's membrane.

Lowered levels of active MMP2 may be a reflection of the lowered levels of the precursor, pro-MMP2. The activation mechanism for pro-MMP2 has been studied and is mediated by another metalloproteinase, a trans-membrane enzyme MMP14, in combination with TIMP2 (Alcazar *et al.*, 2007; Smine *et al.*, 1997; Strongin *et al.*, 1995). The activation takes place on the basolateral surface of the RPE and requires two molecules of MMP14. The first MMP14 molecule binds TIMP2 and this enables the formation of the ternary complex with pro-MMP2. A second MMP14 molecule then cleaves the pro-form to release active MMP2 (Butler *et al.*, 1998; Smine *et al.*, 1997; Strongin *et al.*, 1995). Thus, efficient activation requires the presence of MMPs and TIMPs in optimum concentrations near the basolateral surface of the RPE. The lowered levels of free pro-MMP2 ($p<0.05$) observed for donors with AMD would therefore reduce the rate of activation leading to a reduction in total active MMP2. Lowered levels of pro-MMP2 may be the consequence of greater sequestration by the increased levels of HMW1 & 2. These results support the proposal that decreased levels of active MMP2 contribute to the thickening of Bruch's membrane in the atrophic form of AMD (Guo *et al.*, 1999; Leu *et al.*, 2002; Marin-Castano *et al.*, 2005).

Regulatory mechanisms for the synthesis of pro-MMP9 and its activation are poorly understood. Current evidence suggests that the level of MMPs is dependent on transcriptional regulation since most MMP genes are expressed in response to active physiological or pathological tissue modelling (Fini *et al.*, 1995; Matrisian, 1992). In addition, basal levels of pro-MMP9 are determined by polymorphisms in the sequence of cytosine-adenine (CA) repeats in the promoter microsatellite region of the MMP9 gene (Shimajiri *et al.*, 1999). Increased CA repeats are associated with greater expression of pro-MMP9. Thus the higher number of CA repeats observed in AMD patients may explain both the higher levels of pro-MMP9 found in Bruch's membrane in the present study and the raised levels of plasma pro-MMP9 in patients with AMD (Chau *et al.*, 2008; Fiotti *et al.*, 2005).

The total amount (i.e., free + bound) of pro-MMP9 in Bruch's of donors with AMD was elevated nearly 2.2-fold compared to controls ($p<0.05$). But this only refers to the un-complexed pro-MMP9. The HMW1 and HMW2 species represent polymeric forms of pro-MMPs 2&9 (Kumar *et al.*, 2010) and since these levels were also elevated in AMD donors ($p<0.05$), the overall increase in pro-MMP9 must be much higher.

Despite the considerably elevated levels of pro-MMP9, active MMP9 levels were significantly reduced in AMD ($p<0.05$). The reduction in active MMP2 discussed above could be explained by the fact that levels of free pro-MMP2 were also decreased. In the case of active MMP9 however, the free levels of pro-MMP9 were actually raised nearly 3.5-fold ($p<0.005$). This discrepancy may be related to the fact that the measured 'free' pool of pro-MMP9 may not necessarily denote free. As shown previously (Chapter 3), HMW1 & 2 and pro-MMP9 aggregate to form large

macromolecular complexes termed ‘LMMC’ and this complex is released by PBS extraction into the ‘free’ pool. However, on solubilisation in SDS sample buffer for zymography, this complex breaks up releasing its content of pro-MMP9 molecules. Thus the ‘free’ pool of pro-MMP9 in Table 2 is an over-estimation. Further work is required to estimate the contribution of the LMMC species to the free pool of pro-MMP9.

The MMP pathway developed in the previous chapter and given again in Figure 4.5 is useful in understanding the nature of the gelatinase changes in Bruch’s membrane of AMD donors.

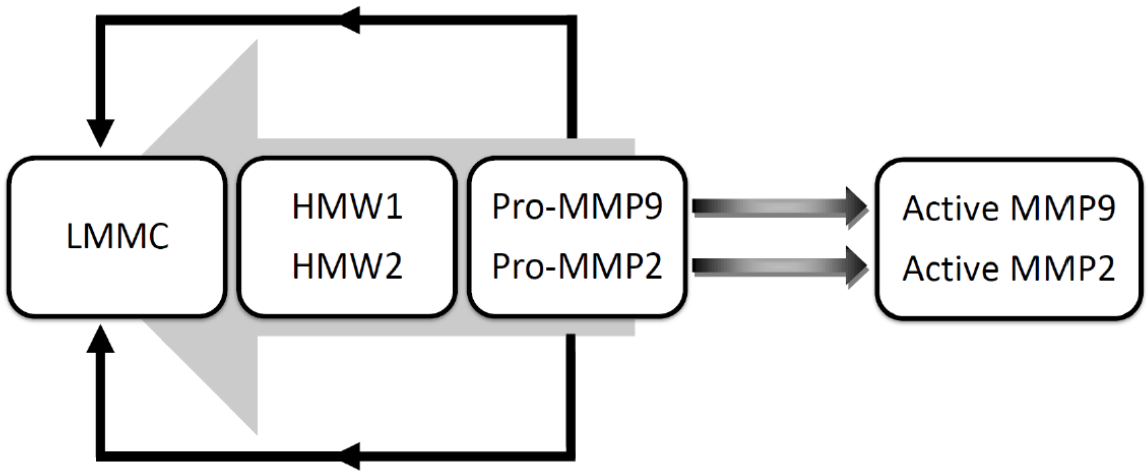

Figure 4.5 The MMP pathway in human Bruch’s membrane.

The formation and age-related increase of HMW1 and HMW2 is expected to diminish the free pool of pro-MMPs 2 & 9. The recruitment of pro-MMP9 in the formation of LMMC will further serve to diminish the pool of free pro-MMP9. The presence of polymorphisms with increased cytosine-adenine repeats in the promoter region in subjects with AMD will further serve (by increasing production of pro-MMP9) to drive the MMP pathway towards the left. This may or may not affect the level of free pro-MMP9 (because of the higher expression) but is expected to further decrease the level of free-MMP2. Further work is required to clarify the truly free pool of pro-MMP9 given the complication discussed earlier concerning release from LMMC during the zymographic assays. The ideal method would be to use short gel filtration columns (normally used for desalting purposes) to rapidly separate LMMC and then to quantify the isolated free pool of pro-MMP9. Thus the predicted reduction in levels of pro-MMPs 2 & 9 in AMD would impact on the conversion to activated forms and most likely explain the observed reduction of these species in AMD.

The study has also highlighted possible problems with the activation process for pro-MMP9 in donors with AMD. Normal activation of the 92kDa pro-MMP9 results in a partially active 88kDa transitional intermediate leading to the fully activated 84kDa MMP9 molecule (Ahir *et al.*, 2002). On the zymographic gels (Figure 4.1), this 84kDa-activated species was distinctly evident in control donors but in AMD donors was replaced by a broader smearing of the band. Densitometric scanning of electrophoretic bands due to a single protein species normally results in a Gaussian bell-shaped profile. In the active MMP9 region in AMD samples, the Gaussian profile

was absent suggesting the presence of several intermediates. Whereas the transition from inactive pro-MMP9 to the fully activated 84kDa MMP9 molecule was clearly apparent in the control samples, a more transitory presence was evident in the AMD samples, perhaps suggestive of problems with the activation process in these donors. Again, further work is required to activate MMP samples from AMD donors with perhaps aminophenylmercuric acetate (APMA) and follow the transitory conversion by zymography according to the methodology of Guo et al., 1999 (Guo *et al.*, 1999).

The present investigation was undertaken with samples derived from the peripheral fundus. Peripheral fundus was sampled because in AMD eyes, the presence of scar formation in the macular region due to the advanced nature of the disease in these aged donors made it virtually impossible to isolate intact specimens. In control donors, the ageing changes observed at macular locations were more advanced than at peripheral locations. Functional parameters of Bruch's membrane such as the hydraulic transport of fluids and the diffusional transport of high molecular weight dextrans declined at faster rates in the macular region (Hussain *et al.*, 2010; Moore *et al.*, 1995; Starita *et al.*, 1996). Similarly, whilst active MMP2 species were frequently observed in the periphery, they were only occasionally encountered at macular locations (Guo *et al.*, 1999). If the macular-peripheral difference in control donors also existed in AMD, then the changes in the gelatinase components in macular regions of these patients would be expected to be much more severe.

The physiological effects of a reduction in active MMPs -2 & -9 in Bruch's of AMD donors would be augmented by the increased levels of TIMP3 inhibitor (Kamei

et al., 1999), inhibition by increased levels of AGEs and ALEs (Nagai *et al.*, 2009) and the reduced susceptibility to proteolytic action by the highly cross-linked nature of the altered collagen molecule (Vater *et al.*, 1979). The resulting degenerative changes in Bruch's would be expected to initially impact on the metabolic exchange processes of the membrane. An early disturbance appears to be in the carrier mediated transport of vitamin A giving rise to reduced scotopic thresholds in the very elderly and early maculopathy (Chen *et al.*, 1992; Owsley *et al.*, 2001; Owsley *et al.*, 2006; Steinmetz *et al.*, 1993). A further compromise in the homeostatic mechanisms for exchange of nutritional and waste products across Bruch's is expected to impact initially on the RPE followed by deterioration in photoreceptor function.

The degenerative changes in functional parameters of Bruch's associated with normal ageing nevertheless maintain sufficient support so as not to impact on visual function during a normal life span (Hussain *et al.*, 2010; Moore *et al.*, 1995; Starita *et al.*, 1996). In AMD, the decreased degradative capacity documented in the present study due to lowered levels of active MMPs 2 & 9 may lead to the advanced ageing changes capable of providing the initial metabolic insult that can progress to pathology.

CHAPTER 5

MODULATION OF THE GELATINASE SYSTEM BY METAL CHELATION:

IMPLICATIONS FOR TRANSPORT PROPERTIES OF BRUCH'S MEMBRANE

5 MODULATION OF THE GELATINASE SYSTEM BY METAL CHELATION: IMPLICATIONS FOR TRANSPORT PROPERTIES OF BRUCH'S MEMBRANE

5.1 INTRODUCTION

Ageing of Bruch's membrane has been shown to be associated with increased level of polymeric forms of the gelatinase MMPs 2&9. There was also an increased amount of bound or 'sequestrated' gelatinases within the matrix of the membrane. All these changes were much exaggerated in AMD leading to the construction of the MMP pathway to partly explain the observed reduction in active levels of MMPs 2&9 in this disease.

The mechanisms governing the polymerisation and/or sequestration of MMP species is not known. However, considerable insight has been gained from investigations of the polymerisation potential of the amyloid-beta protein (Aβ) that is thought to underlie the formation of senile plaques in Alzheimer's disease.

In most globular proteins, the hydrophobic amino acid chains are buried within the interior of the protein. Thermodynamic perturbations are thought to expose these hydrophobic regions allowing the possibility for dimerization and polymerization. This initial conformational alteration can also arise from various physiological and pathological insults. It has been suggested that complexation of metals may overcome the thermodynamic barrier to autopolymerisation of Aβ (Bush, 2003; Exley

et al., 2001) and may underlie the significant elevation in concentrations of Fe(3+), AL(3+), Cu (2+) and Zn (2+) found co-localised with Aβ in senile plaques (Beauchemin *et al.*, 1998).

Metal ions have been reported to significantly influence the processes of aggregation of Aβ protein (Huang *et al.*, 2004; Ricchelli *et al.*, 2005). In the case of aluminium and iron, this initial aggregation leads to the formation of higher order structures termed fibrils. With Zn, Aβ protein rapidly forms amorphous aggregates, most likely due to increased hydrophobic interactions that only slowly progress to fibrils (Bolognin *et al.,* 2011; Frederickson *et al.*, 2001; Noy *et al.*, 2008; Tougu *et al.*, 2009). Metal chelators such as EDTA or desferrioxamine were able to dissolve the aggregates and fibrils formed by Aβ protein polymerisation (Atwood *et al.*, 1998; House *et al.*, 2004; Huang *et al.*, 1997).

The initial conformational changes lead to non-covalent interactions between the monomeric protein subunits. However, these transitory changes may lead on to changes in the redox state of the metal involved, exposure of highly reactive groups on proteins, and metal mediated formation of reactive oxygen species (Hayashi *et al.*, 2007; Nakamura *et al.*, 2007). Such protein-metal interactions can lead to deleterious effects on enzymic activity (Cuajungco *et al.*, 2000; Duce *et al.*, 2010).

There are many similarities between the behaviour of Aβ protein and the gelatinase system of Bruch's membrane. Pro-MMP9 has been shown to exist in a dimer configuration, stabilised by non-covalent linkages. Both pro-MMPs 2&9 undergo co-polymerisation by way of disulphide bridging to yield the high molecular weight structures HMW1 &2. Progress to higher order structures occurs via the incorporation of HMW1, HMW2, pro-MMP9 and some pro-MMP2 to yield the

supramolecular entity LMMC. This age-related structural shift towards high molecular weight complexes is exemplified by the MMP pathway established in chapter 3.

A question however remains regarding the likely involvement of metals in the polymerisation and sequestration process of gelatinases of Bruch's membrane. An age-related increase in metal deposition within Bruch's has been reported with considerably elevated levels in donors with AMD (Dentchev *et al.*, 2005; Dunaief, 2006). If these metals were to participate in protein polymerisation and deposition, the ensuing high molecular weight structures would be expected to interfere with the transport pathways of the membrane. Metals also bind to the phosphate polar heads of phospholipids stabilising them in their micellar or membraneous location. This would also aid in the entrapment and stabilisation of the lipid-rich debris observed in ageing Bruch's membrane. Metals would also be expected to participate in the binding of proteins to structural and deposited elements of the membrane. Heavy metals such as zinc and iron, through redox reactions, can generate reactive oxygen species that will further increase the risk of oxidative damage to Bruch's leading to increased cross-link formation and oxidative damage to structural and transport proteins.

The present study was therefore designed to assess the effect of removing metals on (a) the gelatinase system and (b) on the transport properties of Bruch's membrane. Perfusion studies were undertaken to assess the degree of metal-mediated sequestration (if any) of gelatinase species by the structural components of Bruch's membrane. Similarly, incubation studies with metal chelators were undertaken to assess the potential for activation of the MMP system. Effect of metal

chelation on the transport system was studied by determining the hydraulic conductivity of Bruch's membrane during the perfusion process with EGTA.

5.2 METHODS

5.2.1 Human Tissue Preparation

As previously, all human eyes utilised in this study were obtained with corneas removed from the Bristol Eye Bank (UK). Whole globes were dissected in a Petri dish lined with filter paper (Grade50 Whatman, Maidstone, UK) moistened in 0.1 M phosphate buffered saline (PBS) with an antibiotic/antimycotic mixture (Sigma-Aldrich, UK). The globes were hemisected by a circumferential incision at the pars plana, and the remaining anterior segment, lens, and vitreous discarded. The posterior globe was then opened in the form of a Maltese cross and the four quadrants separated. Overlying neural retina was gently peeled away exposing the underlying RPE cells. These were gently brushed away with a fine camel hairbrush. The Bruch's membrane-choroid complex was carefully separated from the sclera using blunt dissection and floated onto a moistened nylon (8µm-mesh) filter with Bruch's membrane facing uppermost.

5.2.2 Chamber Assembly for Perfusion with PBS and EGTA

A modified open-type Ussing chamber was used for the elution studies (Figure 5.1 to 5.3). It consisted of two half chambers that could be clamped together with the aid of guiding pins. The bottom plate had a central aperture of 6mm diameter with an entry port for perfusion medium and an exit port that was connected to a pressure transducer. The top unit had a central 8 mm diameter aperture with a 1 mm lip near the surface adjacent to the mounted tissue sample. Thus only 6mm diameter of the tissue preparation was exposed and the lip facilitated the retrieval of the eluted sample without risking damage to the preparation since the pipette tip would be rested on the lip during elution collection.

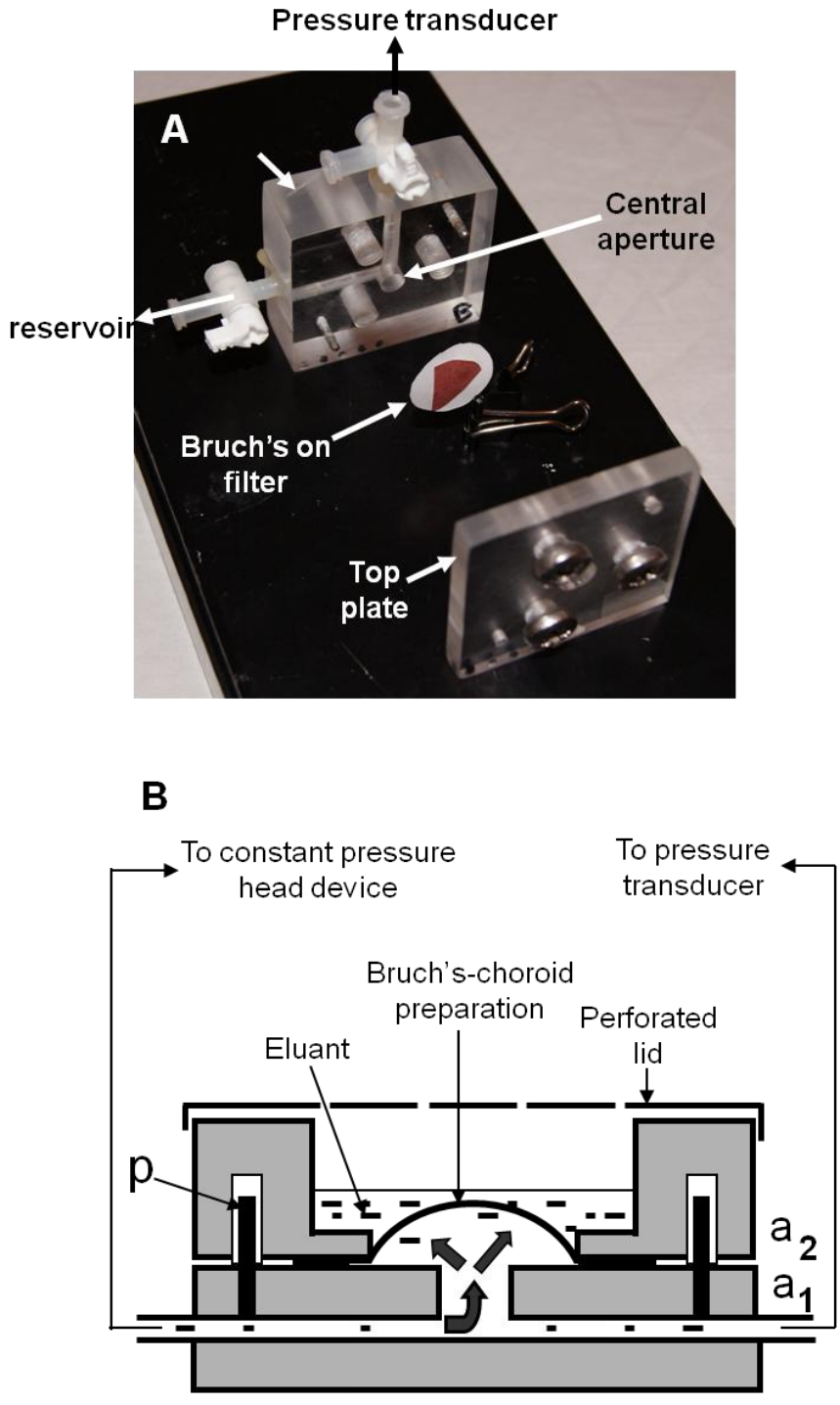

Figure 5.1 Open-type Ussing chamber used in the perfusion studies.

A. Photograph showing the components of the chamber. Tissue samples held on nylon filters are clamped between the two half-compartments.

B. Schematic of the operation of the perfusion chamber. A2 & a1 are the top and bottom half chambers; p, guiding pin. The lip in the upper plate allowed removal of eluant without risk of damaging the preparation. (From Kumar et al., 2011)

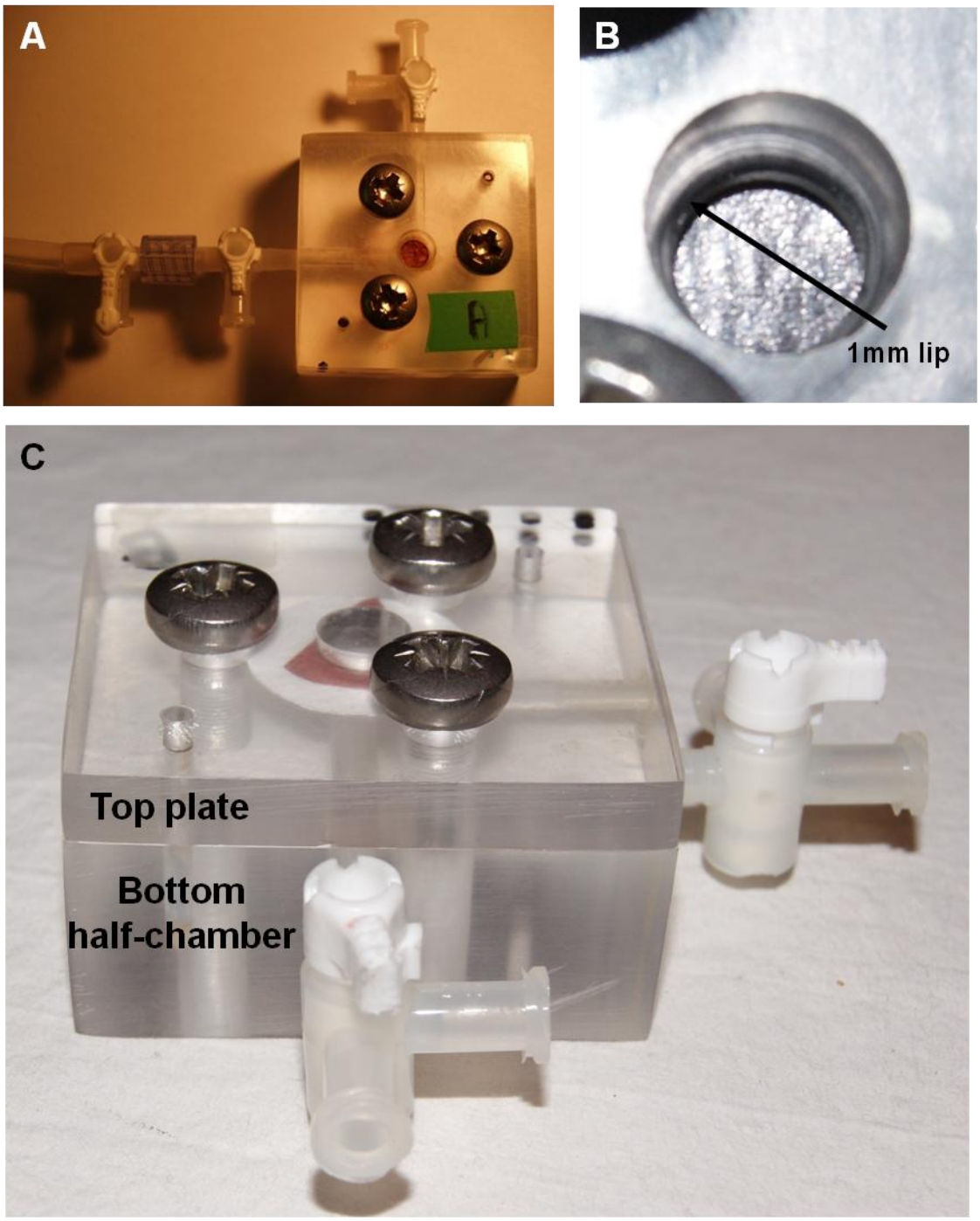

Figure 5.2 Assembled Ussing chamber.

A,C: Top and side views of the clamped chamber. B, Higher magnification photograph of the top plate aperture showing the lip at the bottom interface of the top plate.

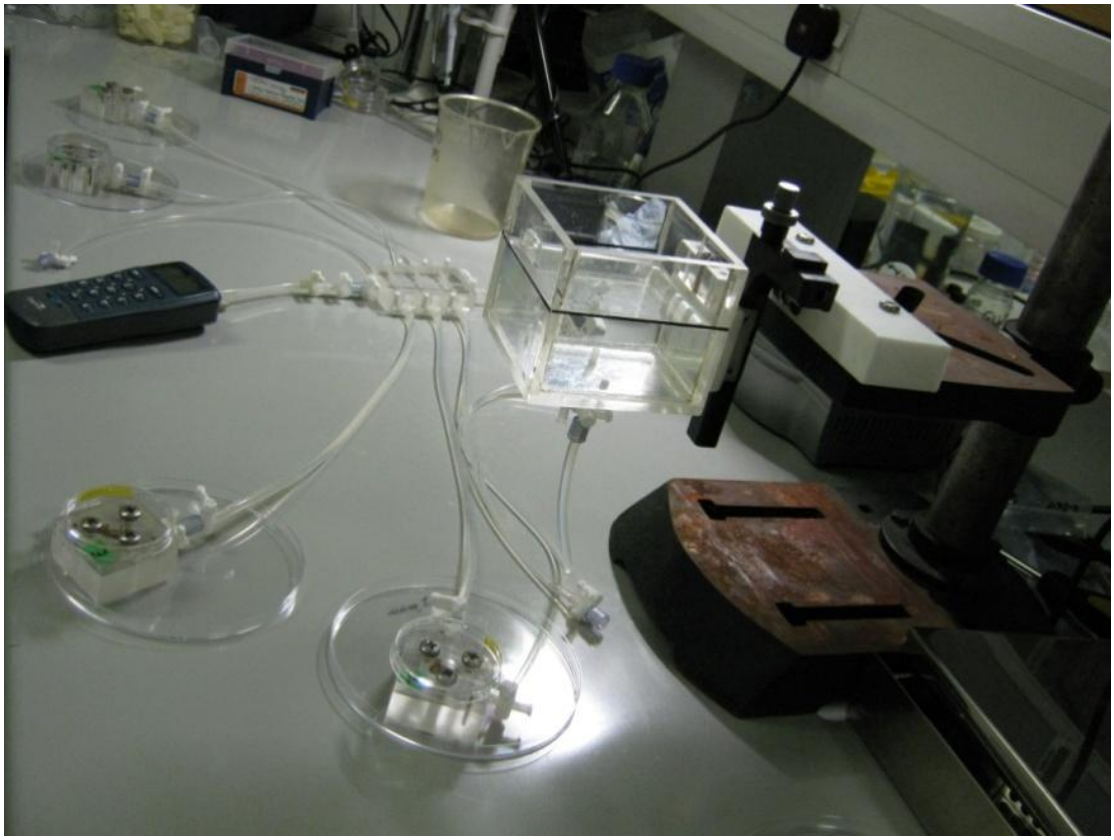

Figure 5.3 The complete perfusion apparatus showing reservoir and pressure transducer connections.

Tissue mounting was carried out as follows. The 8 mm Bruch's-choroid-nylon filter preparation (with Bruch's membrane facing upwards) was mounted over the aperture of the bottom unit of the chamber. With the aid of the locating pins, the top plate was lowered gently onto the preparation and the chamber clamped by applying a torque of 70cN to the three screws. Using a syringe, PBS was introduced into the bottom half-chamber and all trapped air bubbles were removed by carefully tilting the chamber. Eluant reservoir and transducer lines were connected to the chamber and

the hydrostatic pressure was adjusted to 200 mmH_2O. A water moistened filter pad was placed near the open aperture of the top plate and covered by a petri dish to maintain a humidified atmosphere so as to reduce eluant losses from evaporation.

Fluid eluted across the membrane preparation and entering the upper half-chamber was collected every hour and weighed to calculate its volume. After 6-8 hours perfusion, the perfusate was switched to 10 mM EGTA (Ethylene glycol tetraacetic acid) prepared in PBS and pH adjusted to 7.4. Further timed eluant collections were taken and at the end of the experiment, the chamber was dismantled and a central 6mm diameter tissue trephine was removed. Eluted fractions and tissue samples were subjected to gelatin zymography for MMP analysis.

5.2.3 Effect of metal chelation on the gelatinase system of Bruch's membrane

The perfusion experiments were designed to assess the likelihood of metal involvement in the sequestration or binding of MMP species to the structural elements of Bruch's membrane. Possible changes in the polymeric configuration of gelatinases on exposure to metal chelators was studied in both intact preparations and isolated free compartments of Bruch's membrane. In the former, 8mm discs of Bruch's-choroid were incubated with 10mM EGTA, pH 7.4 for one hour followed by zymographic analysis. In the latter, extracted fractions from Bruch's membrane were incubated with EGTA and effects on the gelatinase pool characterised by zymography.

5.2.4 Gelatin zymography for metalloproteinase activity

Zymography was performed as described previously (section 2.2.2). Briefly, 10% SDS-PAGE gels (1.0 mm thick) containing 4 % stacking layer and 0.1 % gelatin in the separating layer were utilised (Novex gels, Invitrogen, UK). Aliquots of the eluant were loaded into lanes with pre-stained molecular weight standards (Invitrogen, UK) and 20% foetal calf serum (FCS, Sigma-Aldrich UK) as an internal standard to correct for variations between gels in background staining. After electrophoresis, gels were incubated twice in 2.5 % Triton X-100 for half an hour each to remove SDS and renature the proteins. Then they were then incubated with reaction buffer (50 mM Tris-HCl, 10 mM $CaCl_2$, 75 mM NaCl, and 0.02 % NaN_3, pH 7.4) for 18 hours at 37 ºC to allow proteolytic digestion of gelatin. After incubation, gels were rinsed 3 times with distilled water for 5 min periods and stained with SimplyBlue SafeStain (Invitrogen, UK) containing Coomassie G-250 for 2 hours on an orbital shaker. Gels were destained with distilled water for 1 hour.

5.2.5 Calculation of hydraulic conductivity

The perfusion of the samples was carried out under a hydrostatic pressure of 200mmH_2O (1962 Pa). The eluant collected over a time t (sec) was weighed and assuming a density of 1g/ml, its volume (Vm^3) was calculated. The exposed area of the preparation was 2.83 x 10^{-5} m^2 (6mm diameter disc). Thus the hydraulic conductivity of the preparation was calculated as (m/sec/Pa):

$$HC = \frac{\text{Flow}}{\text{Pressure}} = \frac{\text{Volume } (m^3)}{\text{Time (t sec)} \times \text{Area (A)} \times \text{Pressure (Pa)}}$$

The tissue preparations were initially perfused with PBS for a period of 8 hours. Hydraulic conductivity was determined at various periods to obtain a base-line. At the 8-hour mark, PBS was replaced with 10mM EGTA. Fluid collections were taken every hour and thus the hydraulic conductivity determined was an average over that period. This hydraulic conductivity point was assigned as the value representing the mid-point of the fluid collection period.

5.3 RESULTS

5.3.1 Elution of MMPs from Bruch's membrane

The rate at which MMPs are eluted from the membrane preparation will be dependent on the applied hydrostatic pressure and the age of the donor. Although elution profiles could have been conducted at a faster rate by employing a high hydrostatic pressure, the risk of damage to the preparation would have been substantial. For this reason, a hydrostatic pressure of 200mmH_2O was chosen to mimic intra-ocular pressure resulting in elution periods of 8-12 hours over the donor age-range examined.

A representative zymogram of the composition of the eluant obtained in a Bruch's-choroid preparation from a 59 year-old donor is given in Figure 5.4.

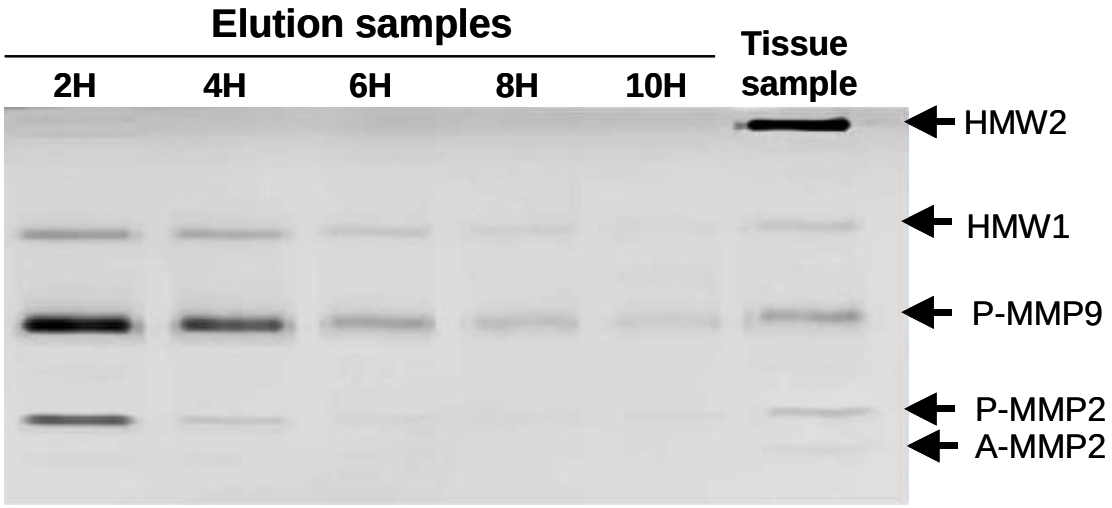

Figure 5.4 PBS elution of Bruch's membrane from a donor aged 59 years.

Elution was undertaken for 10 hours with sample collections every 2 hours. At termination of experiment, the 6mm diameter exposed sample of Bruch's-choroid was removed and together with the eluant samples, processed for zymography.

The elution samples showed the presence of all gelatinase species with the notable exception of active MMP9 and this species was also absent from the tissue sample analysed. Most of the releasable pool of MMPs was eluted within the first two hours of perfusion, with decreasing amounts being released thereafter. After 8 hours elution, release of MMPs was considerably reduced and at the limit of visual detection. Examination of the tissue sample after the elution procedure showed the presence of a substantial amount of MMPs. Thus the pool of MMPs of Bruch's membrane exists in bound and free compartments.

The elution profiles for the various gelatinase species were examined in 12 donor preparations (age range 65-84 years). For a given MMP species, total activity

in the preparation was calculated by adding activity in the various elution fractions plus that present in the tissue after the elution procedure. Then the amount released was expressed as a percentage of total activity (Figure 5.5).

Elution release profiles were different for the different MMP species. The amount of HMW2 released accounted for no more than 10% of the total content in the preparation. Release of HMW1 showed a hyperbolic profile diminishing the total pool by about 50% over an elution time of 12-14 hours. By contrast, the elution of pro-MMP2 was rapid with release of 80-90% of total activity within 4 hours of elution. The amount remaining bound was calculated to be about 10-20% of total activity. Since the molecular weights of active and pro-MMP2 are similar (58 & 65 kDa respectively), their elution profiles would be expected to be similar. However, active MMP2 was released much more slowly than pro-MMP2. This difference in elution profiles suggests that active MMP2 most probably exists in dynamic equilibrium between free and bound forms so that as the free species is removed by the elution process, more of the bound form is released. A similarly sustained release was also observed for pro-MMP9. Levels of active MMP9 were low or absent in the tissue samples and appeared to be below the detection limit in the eluted fractions.

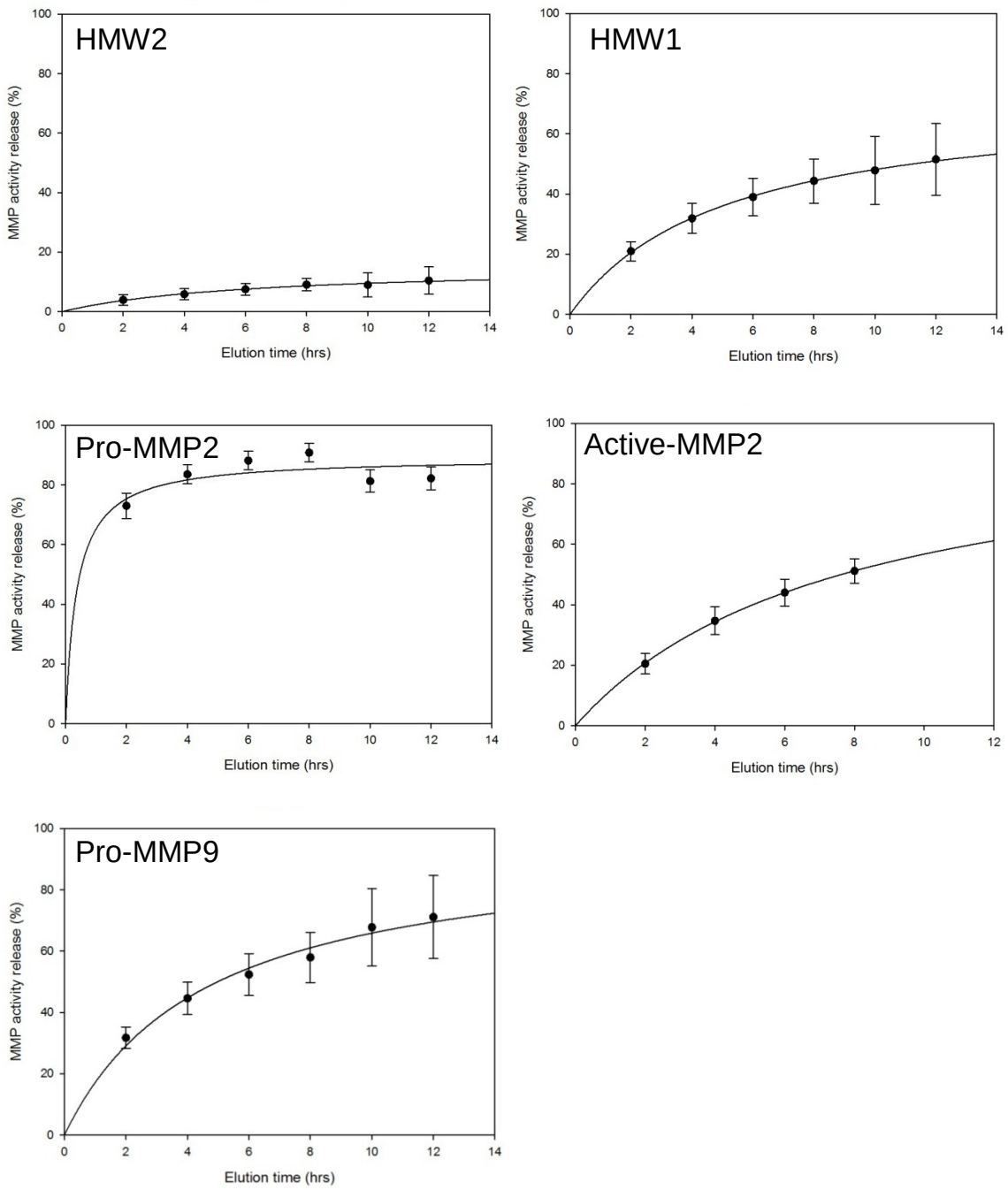

Figure 5.5 Elution profiles of the various gelatinase species of Bruch's membrane.

Data is plotted as Mean ± SD from 12 donor preparations (age-range 65-84 years).

5.3.2 Effect of EGTA on elution profiles of MMPs

Duplicate preparations were obtained for six of the donors utilised in the study of Figure 5.5. PBS elution was undertaken in one set for a period of 12 hours, contributing to the elution profiles presented in Figure 5.5. The other set was used to compare the effects of EGTA on the latter aspects of the elution profiles, i.e., at a stage when most of the free MMPs had been eluted out.

Standard PBS elution was started in the experimental set and maintained for 8 hours. This period of perfusion would have been sufficient to remove most of the free and mobile gelatinase component of the membrane (compare profile of pro-MMP2 in Figure 5.5). The continued release of other gelatinase species at or beyond 8 hours perfusion was most likely due to slow release from bound stores. After the eluant collection at 8 hours, the perfusing solution was switched to 10mM EGTA (prepared in PBS and pH adjusted to 7.4) and subsequent eluant aliquots collected. A representative zymogram of the eluant fractions under these experimental conditions for a donor of age 68 years is shown in Figure 5.6.

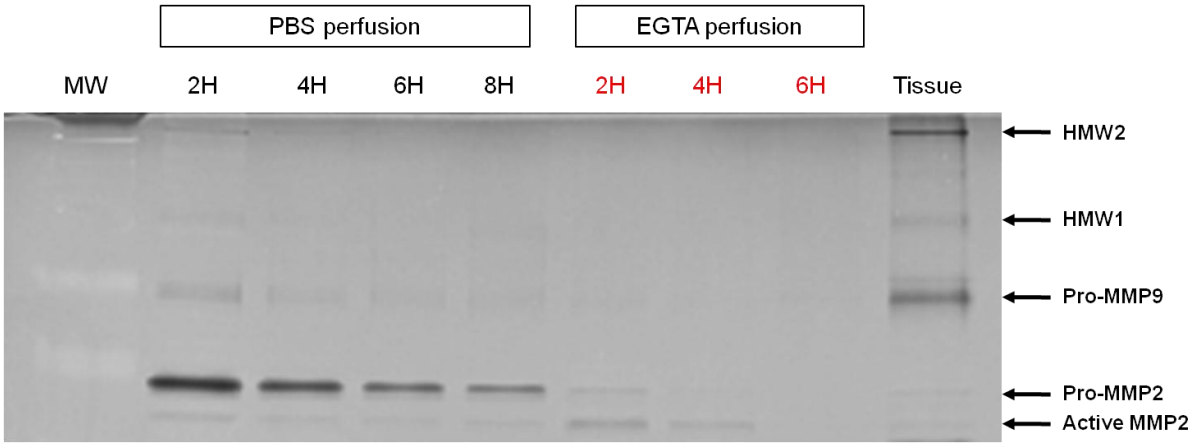

Figure 5.6 Effect of EGTA on the elution of MMPs from Bruch's membrane of a donor aged 68 years.

PBS was perfused for 8 hours and then switched to 10mM EGTA and perfusion continued for another 6 hours. At the end of the perfusion, the tissue sample and eluant fractions were processed for zymography.

Switching to 10mM EGTA after the preliminary elution with PBS had little affect (if any) on the elution of all the gelatinase species except active MMP2. The first two hours of EGTA elution were marked by increased release of active MMP2. The tissue sample (assessed at the end of the EGTA perfusion) contained very little pro- and active MMP2 species. The loss of pro-MMP2 is understandable given the overall duration of 14 hours elution.

The amount of gelatinase species released was quantified to allow comparisons between PBS and EGTA perfusion. The amount of individual gelatinase species in the eluant fraction 2-hours prior to the switch to EGTA (expressed as a percentage of total) was compared to the level obtained 2 hours after initiation of EGTA (Figure 5.7).

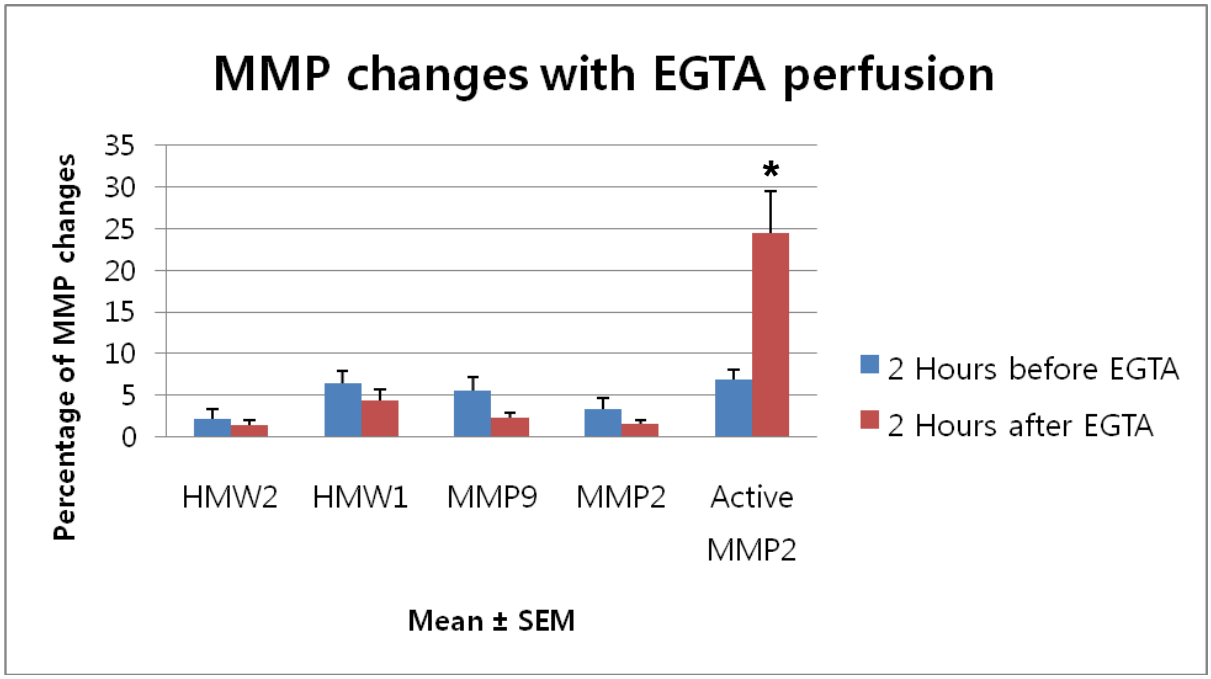

Figure 5.7 Effect of EGTA on the elution profiles of MMPs. Donor set of 6 eyes, age-range 65-84 years. Data given as Mean ± SEM. (*p<0.05)

The amount of HMW1, HMW2, pro-MMP9 and pro-MMP2 released after introduction of EGTA was lower than in the previous 2-hour period (with PBS) and is consistent with the diminishing release established earlier in Figure 5.5. However, EGTA considerably increased the amount of active MMP2 released ($p<0.05$).

The time course of release of active-MMP2 following application of EGTA has also been plotted (Figure 5.8):

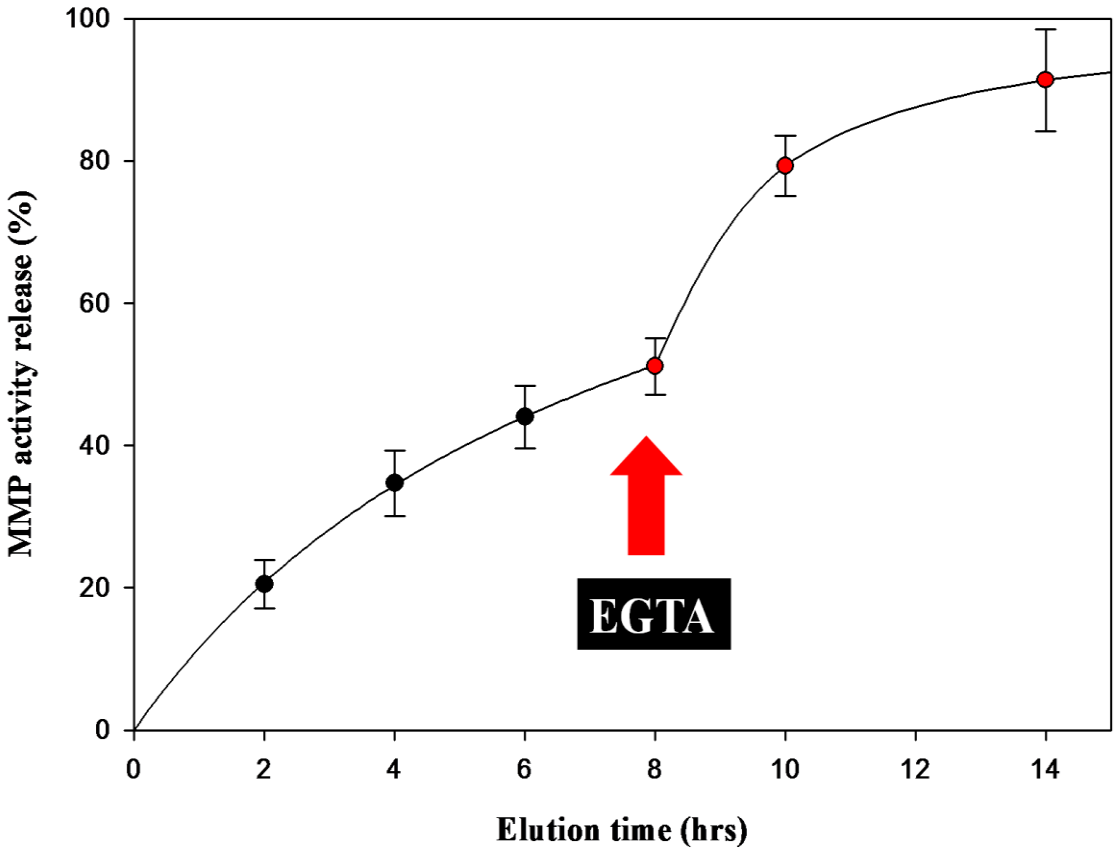

Figure 5.8 Effect of EGTA on the rate of release of active MMP2 from Bruch's membrane. Data given as Mean ± SD (n), n=6.

PBS elution showed the release of active MMP2 up to the 8 hours of elution. Introduction of EGTA accelerated this release so that virtually all of the endogenous active MMP2 was removed from the bound fraction.

Unlike Pro-MMP9 and HMW 1&2, pro-MMP2 is eluted out rapidly from the membrane preparation suggesting that if it binds to the matrix, it does so with very little affinity. Active MMP2 on the other hand appears to be bound and is released

slowly, this release being accelerated in the presence of EGTA. The corresponding change in the ratio of active to total MMP2 species ([active MMP2 / (active + latent)] in the combined eluant fractions (8-12 hour collections) and in the tissue preparation at the end of elution was determined (Figure 5.9).

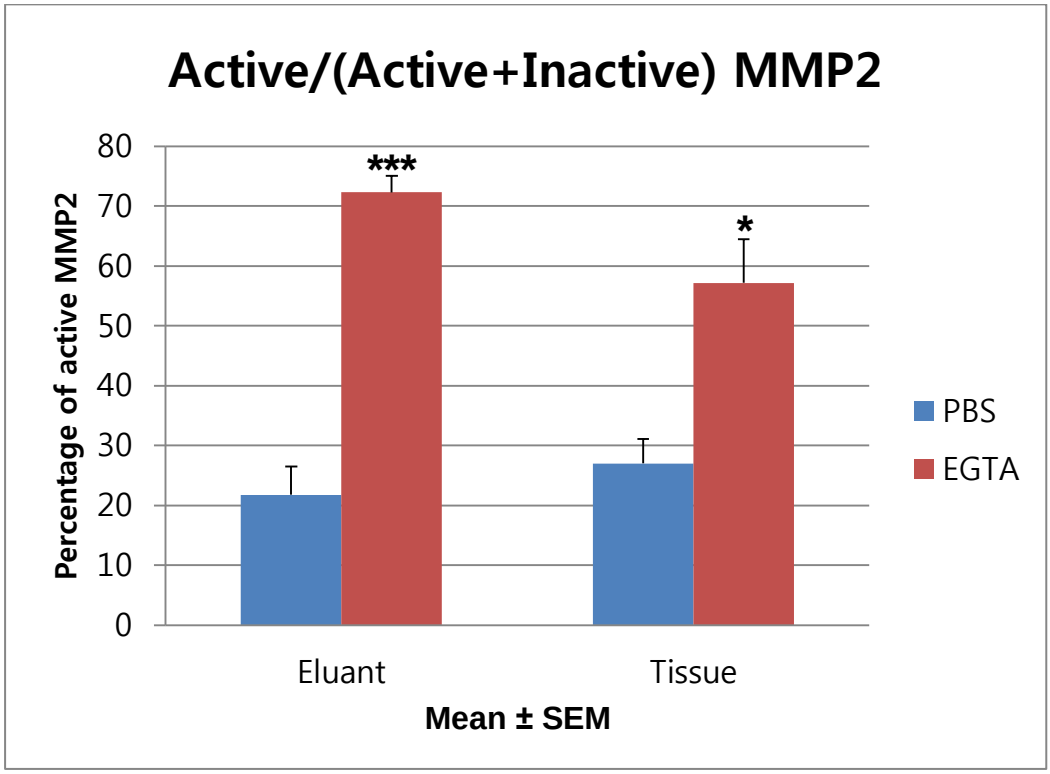

Figure 5.9 Alterations in the ratio of active over total MMP2 species in response to metal chelation by EGTA. (*p<0.05; ***p<0.001)

Six donors, age range 65-84 years.

The greater release of active MMP2 in comparison to pro-MMP2 following application of EGTA resulted in an increase of active MMP2 from 21 to 72% of total gelatinase species in the eluted volume ($p<0.001$). Despite the increased release of

active MMP2, tissue samples still contained a higher percentage of active MMP2 after exposure to EGTA ($p<0.05$). The latter result implies that tissue pro-MMP2 levels after EGTA must have also been reduced. Since most of pro-MMP2 was released by 8 hours of incubation, further release due to EGTA would have been very low and beyond the detection limits of zymography.

Eyes from young donors were rare. Elution experiments were undertaken in three young donor eyes (age 21-28 years) and the basal release of active MMP2 (determined as the ratio of active MMP2 to total MMP2 species) increased from 27% with PBS to 71% after perfusion with EGTA ($p<0.01$), a finding consistent with the results from the elderly donors. (Data not shown)

5.2.3. Effect of EGTA on the activity of MMPs of Bruch's membrane

The effect of EGTA on the stability of various gelatinases species was assessed in isolated MMP extracts and in intact tissue. Eyes of donors of age 83 and 79 years were used to obtain the required MMP fractions. One quadrant was homogenised and spun at 10000g to obtain the soluble fraction. One aliquot was incubated with PBS and the other with 10mM EGTA. Two adjacent 8mm trephines were also obtained from the peripheral fundus and one incubated in PBS and the other in 10 mM EGTA. Following incubation for 1 hour at 37°C, the incubation buffer and the tissue were processed for zymography. The resulting zymograms are shown in Figure 5.10.

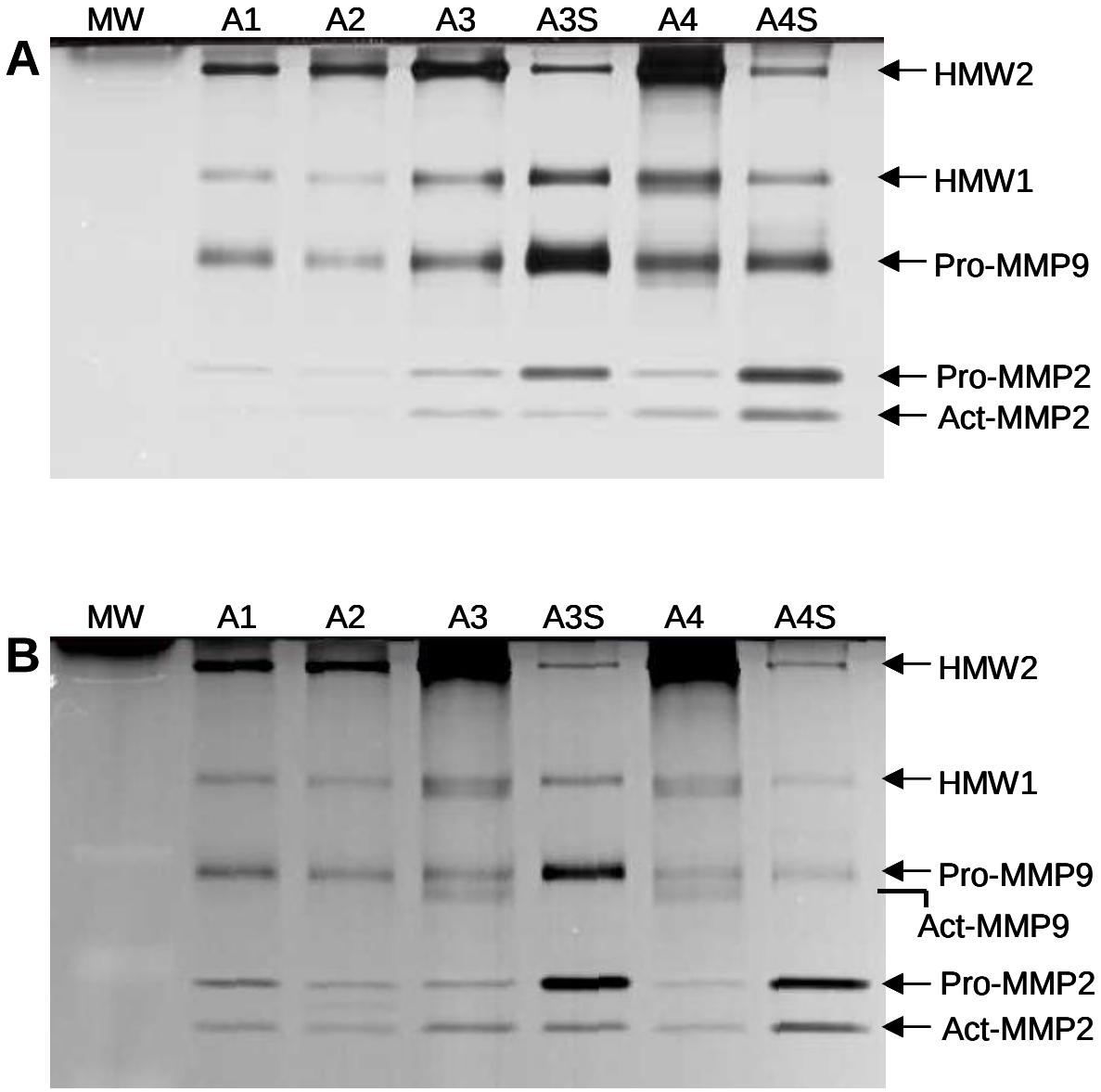

Figure 5.10 Effect of EGTA on stability and binding of MMP species of Bruch's membrane.

Samples A1 and A2 represent the soluble extract, incubated in PBS and EGTA respectively. Samples A3 and A4 represent 8mm diameter tissue discs incubated in PBS and EGTA respectively. The incubation medium overlying these tissue disc samples is represented by A3S and A4S respectively. Gel A and B represent 83 and 79 year old donors respectively.

In the soluble extract, activities of HMW1 and Pro-MMPs 2&9 were slightly reduced after incubation with EGTA for 1 hour in comparison to incubation with PBS.

Incubation of tissue discs with PBS showed some release of HMW species 1&2 and considerable release of pro-MMPs 2&9. Whereas active MMP2 was also released, active MMP9 remained bound to the membrane. Incubation with EGTA resulted in considerable loss of the pro-MMP9 signal. The reduction in the release of this species was not the result of greater amounts being bound to the tissue. Although some pro-MMP9 may be lost due to the action of EGTA (compare A1 with A2), the major fraction of the 'lost' enzyme appears to have been polymerised to high molecular weight forms (lane A4). EGTA was without affect on the release of pro-MMP2 but considerably increased the release of active MMP2.

5.2.4. Effect of EGTA on the hydraulic conductivity of Bruch's membrane.

Hydraulic conductivity was determined in 20 donors age-range 58-93 years using PBS over a period of 8 hours and there were no statistical differences between the early measurements and those near the 8-hour perfusion period. In pilot experiments, there was no change in basal hydraulic conductivity when the perfusion period was extended to 24 hours (data not shown). In seven donor preparations (age range 59-84 years), the 8-hour PBS perfusion was followed with an exposure to 10mM EGTA for a period of 3 hours. EGTA resulted in an increase in hydraulic conductivity of 2.3-fold over the first hour ($p<0.05$), 3.2-fold over the second hour ($p<0.05$), and 7.2-fold ($p<0.005$) over the third hour of perfusion compared to values at 8-hour with PBS (Figure 5.11).

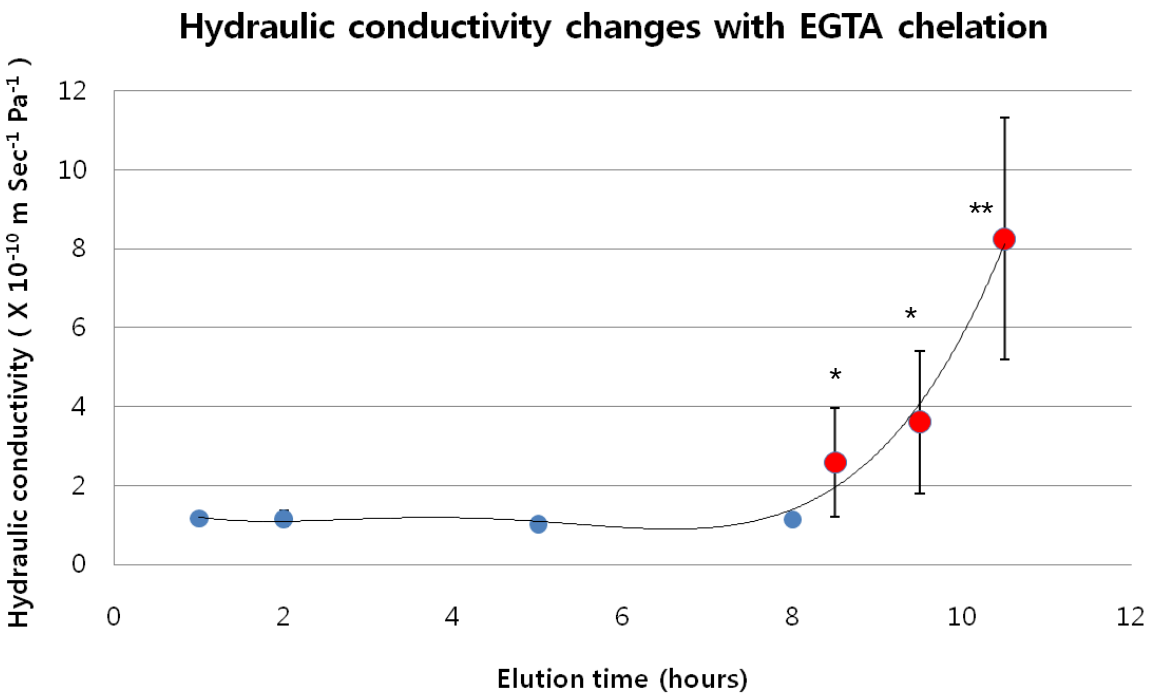

Figure 5.11 Effect of EGTA on the hydraulic conductivity of human Bruch's membrane.

Bruch's choroid preparations from 20 donors (age-range 58-93 years) were perfused with PBS for a period of 8 hours. In seven of these preparations (age range 59-84 years), EGTA was then substitited for PBS and perfusion continued for another 3 hours. Measurement of eluted volumes over a given time period were used to calculate the hydraulic conductivity at several intervals. Data is given as Mean ± SEM. *p<0.05; **p<0.005.

5.4 DISCUSSION

The elution studies with PBS provide an insight as to the level of bound and free gelatinases species and the ease with which they can be eluted from Bruch's membrane. HMW2, being the largest gelatinase species (apart from LMMC) remains tightly bound and elution over 12 hours resulted at most in loss of about 10% of the species. Pro-MMP2 on the other hand was rapidly eluted out and this free fraction accounted for nearly 90% of the total pool, the remaining 10% being tightly bound or trapped within the membrane complex. For quantitative purposes, it is important that dissection times are minimised so that release of pro-MMP2 into the dissection medium is minimised.

Although active MMP2 has a similar molecular weight to pro-MMP2, its behaviour in the elution profiles was very different. There was a slow and sustained release of this species over the time course of the elution procedure. The hyperbolic elution profile suggests a shift in the bound/free pool as the elution medium removes the released species. Similar hyperbolic plots were also obtained for HMW1 and pro-MMP9 and therefore these species must also exist largely in the bound form. A similar situation may also exist with HMW2 but the binding constants must be very high since so little was released over the 12-hour elution scheme employed in the present study.

Several mechanisms may be involved in the binding of proteins to the interior of extracellular matrices. In the case of the gelatinase species examined in the present study, elution would signify that these are not covalently bound. Similarly,

SDS extraction of the bound fraction also supports this conclusion. Non-covalent binding can occur via hydrophobic and/or hydrophilic interactions. The latter would include ionic interactions between the charged groups on proteins and the charged surfaces on matrix proteins such as the sulphated proteoglycans. Metal ions, by providing coordination points could also serve to anchor proteins to the matrix.

Metal chelators would therefore be expected to 'break' such interactions either directly or by modifying the structural matrix to release proteins. EGTA chelation was particularly effective in releasing active MMP2 species from Bruch's membrane.

Chelation of metals by EGTA was without effect on the activity of active-MMP9 or on its removal from the bound compartment. However, under static conditions, i.e., when the tissue was simply incubated and not perfused, in the presence of EGTA, very little pro-MMP9 was actually released into the medium. The amount bound was also reduced. There was evidence that EGTA diminished the activity of pro-MMP9 (Figure 5.10, Lanes A vs. B). This was only a minor reduction and cannot explain the major loss of this species on incubating the tissue with EGTA. It would appear that the released pro-MMP9 species rapidly polymerises to form HMW2 since the level of this species was raised (Figure 5.10, Lanes A4).

Perfusion of tissue samples with EGTA resulted in marked improvement in the hydraulic conductivity of Bruch's membrane. Whether this was due to enhanced release of active MMP2 or to the release and removal of proteo-lipid debris within the membrane requires further investigation. It could be argued that with PBS perfusion, there is release of active MMP2 (Figure 5.5) but without alterations in hydraulic conductivity over the first 8-hours of perfusion (Figure 5.11). On the other hand, the PBS mediated release of active MMP2 was slow and its removal by the perfusing

medium may not have allowed sufficient time for proteolytic activity. With EGTA, there was a large increase in active MMP2, elevating local concentrations, and therefore the likelihood of proteolytic action may have been enhanced. Introducing activated MMP2 into Bruch's has previously been shown to improve the hydraulic conductivity of the membrane (Ahir *et al.*, 2002). Therefore, metal chelation that can raise the free-pool of active MMP2 would be beneficial in improving the transport characteristics of Bruch's membrane. In the present modality of the perfusion procedure, released active MMP2 had diminished 'dwell' times within the membrane since it was removed by the pressure induced flow of fluid. Despite this, considerable improvement in hydraulic conductivity was obtained. Experimental designs that introduce EGTA into the membrane and then stop flow through the preparation would be expected to produce a larger effect on hydraulic conductivity. Metal chelation therapy would therefore appear to be a valid avenue for addressing the advanced ageing associated with AMD since, as indicated earlier, this disease is characterised by diminished transport pathways and considerably reduced levels of active MMPs 2&9.

EGTA would not be a good candidate for such a therapeutic approach since it may also result in polymerisation of pro-MMP9. Alternative metal chelators such as desferroximine and its analogues require further investigation.

CHAPTER 6

DISCUSSION

6 DISCUSSION

Extracellular matrices (ECMs) play important roles that are crucial to the survival of adjacent cellular elements. Structural and functional modifications of ECMs are associated with both pathological and physiological situations. In neovascular processes, extracellular matrix in front of the leading edge of the growing capillary tube needs to be ‘dissolved’ allowing growth and expansion of the capillary bed. This ‘clearing’ of ECM is attributed to the release of activated MMPs by endothelial cells at the growing end of the capillary tube. Under inflammatory conditions, macrophage invasion also requires the release of active MMPs to clear a pathway through the matrix. Similarly in the wound healing process, cells detaching and migrating to close the wound also release activated MMPs. Under normal physiological conditions, the most important process is the homeostatic turnover of the extracellular matrix. By tightly coupling the degradative (mediated by MMPs) and synthetic pathways, the matrix can be ‘rejuvenated’ thereby maintaining its structural and functional characteristics.

In the case of Bruch’s membrane, the homeostatic turnover of the matrix is particularly important. Its location in a highly oxidative environment, the presence of damaged but highly reactive outer segment debris discarded by the RPE, and the very high metabolic traffic through it all make Bruch’s highly susceptible to damage and therefore the requirement for continuous remodelling throughout the life of an individual.

As such, the presence of the MMP machinery has previously been demonstrated in Bruch's membrane (Alexander et al., 1990; Guo et al., 1999; Hunt et al., 1993; Vranka et al., 1997). However, several studies have shown that despite the presence of a rejuvenation potential, ageing of Bruch's leads to deterioration in structural and functional parameters (Moore *et al.*, 1995; Sarks, 1976). Thus, ageing of Bruch's is associated with thickening and accumulation of debris enriched in lipids (Okubo *et al.*, 1999; Ramrattan *et al.*, 1994). Functional parameters of hydraulic conductivity and protein diffusion also show deterioration and this change was beyond that predicted by the changes in thickness of the membrane (Hussain *et al.*, 2010; Moore *et al.*, 2001; Moore *et al.*, 1995; Starita *et al.*, 1996). Nonetheless, despite the severity of these changes, sufficient functional integrity was maintained to support photoreceptor function throughout the life-time of an individual although scotopic thresholds in the very elderly were indeed affected (Owsley *et al.*, 2006; Steinmetz *et al.*, 1993). In advanced ageing, associated with age-related macular degeneration, the changes in Bruch's are therefore expected to impact on the functional support provided to the RPE and photoreceptor layer.

The work of Karwatowski et al., (1995) on the nature of collagenous changes in ageing Bruch's membrane provided an insight into the status of the MMP machinery. These workers showed considerable oxidative damage and denaturation of collagen molecules with levels approaching 50% of the total collagen content in the very elderly. Thus, despite the presence of substrates, MMP activity appeared to be considerably subdued. In support was the observation that active MMP 2&9 species were rarely encountered in Bruch's membrane from macular regions (Guo *et al.*, 1999). The level of the natural MMP inhibitor, TIMP3 was also elevated with

ageing and some authors have suggested that the increased TIMP3/MMP level may be responsible for the reduction in proteolytic activity (Kamei *et al.*, 1999). However, this is unlikely since levels of pro-MMPs were also increased in ageing Bruch's (Guo *et al.*, 1999).

The level of latent MMPs does not reflect on the proteolytic activity within Bruch's membrane. It is the level of active-enzymes that dictates the degree of proteolytic hydrolysis. Nonetheless, the free level of latent or pro-MMPs may govern the rate of conversion to activated forms and this is best illustrated with regards to pro-MMP2. Pro-MMP2 is activated on the basolateral surfaces of the RPE. The first step in the activation process requires the formation of a ternary complex between MMP14, TIMP2 and pro-MMP2 on the surface of the RPE. The final step is the cleavage of the pro-peptide on pro-MMP2 by MMP14. Thus the free concentration of pro-MMP2 is vital in the initial formation of the primary ternary complex. Determining total levels of pro-MMP2 does not provide an assessment of the potential for activation; free levels need to be determined.

Activation mechanisms for pro-MMP9 are not clear. Certainly pro-MMP9 can be activated within the RPE cell and released onto Bruch's membrane but the pro-form within Bruch's can also be activated. Current work suggests that activation can occur following interaction with damaged substrate collagen molecules (Overall *et al.*, 2007; Rosenblum *et al.*, 2010). Following activation, the molecule remains bound to the substrate and this may be the reason why active MMP9 is only found bound to the matrix of the membrane. Active MMP9 has translational freedom and can therefore move along the collagen molecule during its proteolytic action.

In the present study, active levels of MMP9 were found in elderly donors and this would appear to contradict the results of Karwatowski et al., 1995 since elderly donors showed the large presence of abnormal collagen. One possibility to explain this anomaly is that highly damaged collagen molecules may not allow translational movement of active MMP9 and thus, although present, active MMP9 remains functionally inactive. This is supported by studies where addition of exogenously activated MMP9 resulted in marked improvement in the transport properties of Bruch's from elderly donors (Ahir *et al.*, 2002). This study also suggests the possibility that pro-MMP9 may not be accessible to altered collagen but that the addition of activated species does result in proteolytic hydrolysis.

Understanding the factors that regulate the free level of pro-MMPs 2&9 is therefore very important in determining the potential for activation and the subsequent proteolytic activity of the MMP system. Initial screening of Bruch's showed the presence of other gelatinase activities in addition to those expected from pro- and active forms of MMPs 2&9. Further analyses of these 'unknown' species showed them to be homo- and/or hetero polymers of pro-MMPs 2&9 and were named as HMW1 and HMW2 with molecular weights of 122 ± 9kDa and 344 ± 22kDa (Mean ± SD(n), n=24) respectively. Their presence in SDS-zymographic gels was indicative of covalent bonding between the monomers and the disulphide-mediated bonding was confirmed by hydrolysis with thiol reacting agents (APMA).

Gel filtration chromatography allows the analysis of non-covalently bonded complexes and this approach has identified the presence of a much larger MMP complex termed LMMC that incorporated HMW1, HMW2, pro-MMP9 and traces of pro-MMP2. A knowledge of the different gelatinase species and their age-related

changes in levels has allowed the formulation of the MMP pathway (reproduced below) to explain the observed alterations in the level of active species present in ageing Bruch's membrane.

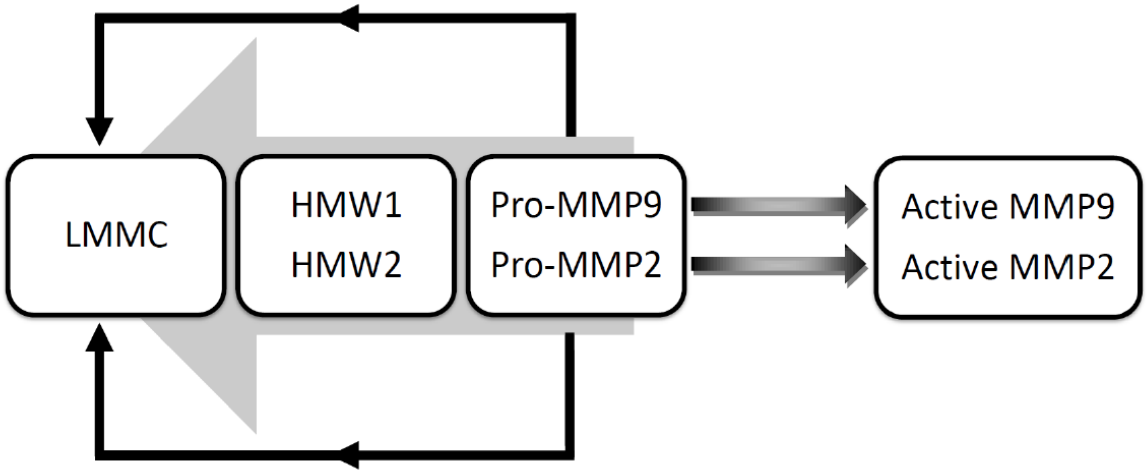

Figure 6.1 The MMP pathway in Bruch's membrane.

Figure 6.1 describes the interrelationships between the various gelatinase species in their free form within Bruch's membrane. To this, another layer of complexity must be added i.e., the equilibrium that these species have with respect to free and bound forms. The conversion of pro-MMPs 2&9 to high molecular species effectively sequesters these species from the activation process. Ageing of Bruch's leads to increased levels of HMW1 & 2 and therefore greater sequestration of pro-MMP9. In addition to this conversion, there is also binding of these species to the matrix of the membrane.

Ageing was associated with increased binding of pro-MMP9 and a decrease in the free pool. The currently measured 'free' pool of pro-MMP9 may not necessarily reflect the true value because on SDS solubilisation, pro-MMP9 released from LMMC would also add to the free pool. Thus ageing of Bruch's leads to greater sequestration of latent monomers of pro-MMPs 2&9 diminishing the availability for activation. Overall, ageing drives the MMP pathway towards the left and may account for the reduced gelatinase activity in aged tissue.

The potential for shifting the equilibrium between bound and free forms of gelatinase species was assessed by perfusing tissue samples with PBS. Within the first 2-4 hours of perfusion, most of the pro-MMP2 content was eluted out indicative of a low binding affinity for this species. The other species were eluted out very slowly suggestive of a shift between bound and free stores but the amount of HMW2 released was very low suggesting this species to be tightly bound.

In AMD, the ageing changes in the MMP system were advanced. Levels of HMW1 & 2 were much increased the sequestration of pro-MMPs 2&9. The greater shift towards the left in the MMP pathway was associated with very much reduced levels of free and bound pro-MMP2. However, the apparent free level of pro-MMP9 was very elevated. As indicated earlier, this apparent increase may be misleading since the contribution of pro-MMP9 from the LMMC pool has not been taken into account.

Increased levels of pro-MMP9 may be an important factor in the pathogenesis of AMD. Increased levels are more likely to drive the MMP pathway towards the left. Raised levels of pro-MMP9 are not restricted to ocular tissues since raised levels were also noted in the plasma of these patients (Chau *et al.*, 2008). These raised

levels may be the result of the polymorphisms in the micro-satellite promoter region of the MMP9 gene. The length of the cytosine-adenine (CA) repeats in this region appears to regulate the expression of the MMP9 pool and longer repeats (with greater expression of pro-MMP9) have been associated with patients with AMD (Fiotti *et al.*, 2005).

The most significant finding in donors with AMD was the reduced level of active MMPs 2&9 in Bruch's membrane, a result that could be predicted by a shift of the MMP pathway towards the left. The severely diminished levels of active MMPs may therefore explain the reduced degradative capacity in AMD that leads to the observed changes in structural and functional parameters of Bruch's membrane in this disease. Such a reduction in active MMPs is further complicated by the increased presence of AGEs and ALEs that are also known to inhibit the proteolytic activity of MMPs (Haas *et al.*, 1998; Howard *et al.*, 1996; Rittie *et al.*, 1999; Scott *et al.*, 1998).

The MMP pathway described above offers possible therapeutic strategies for intervention in AMD. The primary goal of any interventionist procedure would be to shift the pathway towards the right. The shift in the equilibrium between bound and free levels of active enzymes is one possibility. These active forms may be bound to the matrix by hydrophobic, ionic or metal-mediated interactions. If metal mediated entrapment is operative in the membrane, then the increased deposition of divalent metals in both ageing and AMD samples of Bruch's could be a contributory factor in active enzyme sequestration. Removal of divalent metals using the chelator EGTA was associated with release of active MMP2 from the bound fraction of the

membrane. Effect on active MMP9 could not be assessed due to the very low levels of this species and low sensitivity for detecting with zymography.

The EGTA mediated release of active MMP2 was also associated with improvements in the hydraulic conductivity of Bruch's membrane. These results suggest that bound active MMP2 was trapped and unable to participate in the proteolytic process but that on 'freeing' was able to act on substrates. The improvement in transport occurred despite the fact that most of the released active species was lost due to the perfusion process. A greater improvement would be expected if the membrane preparation was simply incubated in EGTA. EGTA is not suitable as a therapeutic agent since it also appeared to promote the polymerisation of pro-MMP9, a side-effect that must be avoided given the above discussion. Alternative metal chelators need to be assessed for their therapeutic potential.

Therapeutic intervention dictates that the MMP pathway must be shifted to the right. Improved knowledge of the biophysical and biochemical properties of the high molecular weight species and the potential for drug-mediated dissolution will in the future assist in developing novel strategies for this avenue for intervention in AMD. If the pathway cannot be shifted to the right, an alternative strategy would be to directly increase the levels of active MMPs. This means inducing the release of these species from the RPE.

The wound healing process provides just such a strategy. Proliferating RPE cells are known to release copious amounts of activated MMPs 2&9 in a cell-cycle dependent manner (Ahir *et al.*, 2002). Thus a small lesion that damages RPE cells will result in a wound healing response with RPE cells on the margins of the lesion migrating to fill the vacant spaces. In so doing they would release active MMPs as

they migrate and thereby ‘clean’ underlying Bruch’s membrane. In pan-retinal photocoagulation (argon blue-green laser at 250mW, 100msec duration, 200µm spot size) applied to human RPE explants in culture, the wound healing response was associated with increased expression of MMPs 2&3 by migrating/dividing RPE cells (Flaxel *et al.*, 2007). Several groups using conventional retinal lasers have shown partial removal of drusen in AMD patients (Cleasby *et al.*, 1979; Figueroa *et al.*, 1994; Ho *et al.*, 1999; Owens *et al.*, 1999).

With the newly introduced short pulse lasers, microbubble formation around melanosomes within the RPE leads to disintegration of cellular architecture and cell death without any acute effects on Bruch’s or photoreceptors (Brinkmann *et al.*, 2000; Framme *et al.*, 2009; Roegener *et al.*, 2004; Roider *et al.*, 1993). The laser-mediated lesions therefore induce expression and release of active MMPs. Increased presence of active MMPs has already been shown to improve the functional characteristics of Bruch’s membrane (Ahir *et al.*, 2002).

In AMD patients, RPE cells are already under stress and the active MMP release following laser lesions may not be as robust as in healthy RPE cells. Thus supplementation of this procedure with metal chelating agents that release bound active forms would supplement the therapeutic procedure.

REFERENCES

REFERENCES

Adorante, JS, Miller, SS (1990) Potassium-dependent volume regulation in retinal pigment epithelium is mediated by Na,K,Cl cotransport. *J Gen Physiol* 96(6): 1153-1176.

Ahir, A, Guo, L, Hussain, AA, Marshall, J (2002) Expression of metalloproteinases from human retinal pigment epithelial cells and their effects on the hydraulic conductivity of Bruch's membrane. *Invest Ophthalmol Vis Sci* 43(2): 458-465.

Ahmed, J, Braun, RD, Dunn, R, Jr., Linsenmeier, RA (1993) Oxygen distribution in the macaque retina. *Invest Ophthalmol Vis Sci* 34(3): 516-521.

Alberts, B, Bray, D, Lewis, J, Raff, M, Roberts, K, Watson, JD (1994) Cell junctions, cell adhesion, and the extracellular matrix. In: *Molecular Biology of the Cell*, 3 edn, pp 949-1010.

Alcazar, O, Cousins, SW, Marin-Castano, ME (2007) MMP-14 and TIMP-2 overexpression protects against hydroquinone-induced oxidant injury in RPE: implications for extracellular matrix turnover. *Invest Ophthalmol Vis Sci* 48(12): 5662-5670.

Alexander, JP, Bradley, JM, Gabourel, JD, Acott, TS (1990) Expression of matrix metalloproteinases and inhibitor by human retinal pigment epithelium. *Invest Ophthalmol Vis Sci* 31(12): 2520-2528.

Alm, A, Bill, A (1973) Ocular and optic nerve blood flow at normal and increased intraocular pressures in monkeys (Macaca irus): a study with radioactively labelled microspheres including flow determinations in brain and some other tissues. *Exp Eye Res* 15(1): 15-29.

Atwood, CS, Moir, RD, Huang, X, Scarpa, RC, Bacarra, NM, Romano, DM, Hartshorn, MA, Tanzi, RE, Bush, AI (1998) Dramatic aggregation of Alzheimer abeta by Cu(II) is induced by conditions representing physiological acidosis. *J Biol Chem* 273(21): 12817-12826.

Aumailley, M, Gayraud, B (1998) Structure and biological activity of the extracellular matrix. *J Mol Med* 76(3-4): 253-265.

Basset, P, Bellocq, JP, Wolf, C, Stoll, I, Hutin, P, Limacher, JM, Podhajcer, OL, Chenard, MP, Rio, MC, Chambon, P (1990) A novel metalloproteinase gene specifically expressed in stromal cells of breast carcinomas. *Nature* 348(6303): 699-704.

Bauer, EA, Kronberger, A, Stricklin, GP, Smith, LT, Holbrook, KA (1985) Age-related changes in collagenase expression in cultured embryonic and fetal human skin fibroblasts. *Exp Cell Res* 161(2): 484-494.

Bauer, EA, Silverman, N, Busiek, DF, Kronberger, A, Deuel, TF (1986) Diminished response of Werner's syndrome fibroblasts to growth factors PDGF and FGF. *Science* 234(4781): 1240-1243.

Bavik, CO, Busch, C, Eriksson, U (1992) Characterization of a plasma retinol-binding protein membrane receptor expressed in the retinal pigment epithelium. *J Biol Chem* 267(32): 23035-23042.

Beauchemin, D, Kisilevsky, R (1998) A method based on ICP-MS for the analysis of Alzheimer's amyloid plaques. *Anal Chem* 70(5): 1026-1029.

Beck, RE, Schultz, JS (1972) Hindrance of solute diffusion within membranes as measured with microporous membranes of known pore geometry. *Biochim Biophys Acta* 255(1): 273-303.

Bellovino, D, Morimoto, T, Tosetti, F, Gaetani, S (1996) Retinol binding protein and transthyretin are secreted as a complex formed in the endoplasmic reticulum in HepG2 human hepatocarcinoma cells. *Exp Cell Res* 222(1): 77-83.

Berg, JM, Shi, Y (1996) The galvanization of biology: a growing appreciation for the roles of zinc. *Science* 271(5252): 1081-1085.

Bhutto, IA, Uno, K, Merges, C, Zhang, L, McLeod, DS, Lutty, GA (2008) Reduction of endogenous angiogenesis inhibitors in Bruch's membrane of the submacular region in eyes with age-related macular degeneration. *Arch Ophthalmol* 126(5): 670-678.

Bialek, S, Miller, SS (1994) K+ and Cl- transport mechanisms in bovine pigment epithelium that could modulate subretinal space volume and composition. *J Physiol* 475(3): 401-417.

Bicknell, IR, Darrow, R, Barsalou, L, Fliesler, SJ, Organisciak, DT (2002) Alterations in retinal rod outer segment fatty acids and light-damage susceptibility in P23H rats. *Mol Vis* 8: 333-340.

Bill, A (1970) Ocular circulation. In: *Adler's physiology of the Eye* Vol. 5, pp 278-296: The C.V. Mosby Co.

Bird, AC, Marshall, J (1986) Retinal pigment epithelial detachments in the elderly. *Trans Ophthalmol Soc U K* 105 (Pt 6): 674-682.

Birdwell, CR, Gospodarowicz, D, Nicolson, GL (1978) Identification, localization, and role of fibronectin in cultured bovine endothelial cells. *Proc Natl Acad Sci U S A* 75(7): 3273-3277.

Birkedal-Hansen, H, Moore, WG, Bodden, MK, Windsor, LJ, Birkedal-Hansen, B, DeCarlo, A, Engler, JA (1993) Matrix metalloproteinases: a review. *Crit Rev Oral Biol Med* 4(2): 197-250.

Biswas, C, Zhang, Y, DeCastro, R, Guo, H, Nakamura, T, Kataoka, H, Nabeshima, K (1995) The human tumor cell-derived collagenase stimulatory factor (renamed EMMPRIN) is a member of the immunoglobulin superfamily. *Cancer Res* 55(2): 434-439.

Bjorklund, M, Heikkila, P, Koivunen, E (2004) Peptide inhibition of catalytic and noncatalytic activities of matrix metalloproteinase-9 blocks tumor cell migration and invasion. *J Biol Chem* 279(28): 29589-29597.

Bobbink, IW, Tekelenburg, WL, Sixma, JJ, de Boer, HC, Banga, JD, de Groot, PG (1997) Glycated proteins modulate tissue-plasminogen activator-catalyzed plasminogen activation. *Biochem Biophys Res Commun* 240(3): 595-601.

Bode, W, Maskos, K (2003) Structural basis of the matrix metalloproteinases and their physiological inhibitors, the tissue inhibitors of metalloproteinases. *Biol Chem* 384(6): 863-872.

Bok, D (1990) Processing and transport of retinoids by the retinal pigment epithelium. *Eye (Lond)* 4 (Pt 2): 326-332.

Bok, D (1985) Retinal photoreceptor-pigment epithelium interactions. Friedenwald lecture. *Invest Ophthalmol Vis Sci* 26(12): 1659-1694.

Bok, D (1994) Retinal photoreceptor disc shedding and pigment epithelial phagocytosis. In: *Retina*, Ryan, S (ed) Vol. 2, pp 81-94. St Louis, USA: Mosby.

Bok, D, Young, RW (1979) Phagocytic properties of the retinal pigment epithelium. In: *The Retinal Pigment Epithelium*, pp 148-174. Cambridge, MA: Harvard University Press.

Bolognin, S, Messori, L, Drago, D, Gabbiani, C, Cendron, L, Zatta, P Aluminum, copper, iron and zinc differentially alter amyloid-Abeta(1-42) aggregation and toxicity. *Int J Biochem Cell Biol* 43(6): 877-885.

Boulton, M, McKechnie, NM, Breda, J, Bayly, M, Marshall, J (1989) The formation of autofluorescent granules in cultured human RPE. *Invest Ophthalmol Vis Sci* 30(1): 82-89.

Boulton, M, Rozanowska, M, Rozanowski, B (2001) Retinal photodamage. *J Photochem Photobiol B* 64(2-3): 144-161.

Brinkmann, R, Huttmann, G, Rogener, J, Roider, J, Birngruber, R, Lin, CP (2000) Origin of retinal pigment epithelium cell damage by pulsed laser irradiance in the nanosecond to microsecond time regimen. *Lasers Surg Med* 27(5): 451-464.

Brown, D, Hamdi, H, Bahri, S, Kenney, MC (1994) Characterization of an endogenous metalloproteinase in human vitreous. *Curr Eye Res* 13(9): 639-647.

Bui, BV, Kalloniatis, M, Vingrys, AJ (2003) The contribution of glycolytic and oxidative pathways to retinal photoreceptor function. *Invest Ophthalmol Vis Sci* 44(6): 2708-2715.

Burns, RP, Feeney-Burns, L (1980) Clinico-morphologic correlations of drusen of Bruch's membrane. *Trans Am Ophthalmol Soc* 78: 206-225.

Bush, AI (2003) The metallobiology of Alzheimer's disease. *Trends Neurosci* 26(4): 207-214.

Butler, GS, Butler, MJ, Atkinson, SJ, Will, H, Tamura, T, Schade van Westrum, S, Crabbe, T, Clements, J, d'Ortho, MP, Murphy, G (1998) The TIMP2 membrane type 1 metalloproteinase "receptor" regulates the concentration and efficient activation of progelatinase A. A kinetic study. *J Biol Chem* 273(2): 871-880.

Cameron, DJ, Yang, Z, Gibbs, D, Chen, H, Kaminoh, Y, Jorgensen, A, Zeng, J, Luo, L, Brinton, E, Brinton, G, Brand, JM, Bernstein, PS, Zabriskie, NA, Tang, S, Constantine, R, Tong, Z, Zhang, K (2007) HTRA1 variant confers similar risks to geographic atrophy and neovascular age-related macular degeneration. *Cell Cycle* 6(9): 1122-1125.

Campbell, CE, Flenniken, AM, Skup, D, Williams, BR (1991) Identification of a serum- and phorbol ester-responsive element in the murine tissue inhibitor of metalloproteinase gene. *J Biol Chem* 266(11): 7199-7206.

Campochiaro, PA, Jerdon, JA, Glaser, BM (1986) The extracellular matrix of human retinal pigment epithelial cells in vivo and its synthesis in vitro. *Invest Ophthalmol Vis Sci* 27(11): 1615-1621.

Cha, H, Kopetzki, E, Huber, R, Lanzendorfer, M, Brandstetter, H (2002) Structural basis of the adaptive molecular recognition by MMP9. *J Mol Biol* 320(5): 1065-1079.

Chau, KY, Sivaprasad, S, Patel, N, Donaldson, TA, Luthert, PJ, Chong, NV (2008) Plasma levels of matrix metalloproteinase-2 and -9 (MMP-2 and MMP-9) in age-related macular degeneration. *Eye (Lond)* 22(6): 855-859.

Chen, JC, Fitzke, FW, Pauleikhoff, D, Bird, AC (1992) Functional loss in age-related Bruch's membrane change with choroidal perfusion defect. *Invest Ophthalmol Vis Sci* 33(2): 334-340.

Chen, W, Stambolian, D, Edwards, AO, Branham, KE, Othman, M, Jakobsdottir, J, Tosakulwong, N, Pericak-Vance, MA, Campochiaro, PA, Klein, ML, Tan, PL, Conley, YP, Kanda, A, Kopplin, L, Li, Y, Augustaitis, KJ, Karoukis, AJ, Scott, WK, Agarwal, A, Kovach, JL, Schwartz, SG, Postel, EA, Brooks, M, Baratz, KH, Brown, WL, Brucker, AJ, Orlin, A, Brown, G, Ho, A, Regillo, C, Donoso, L, Tian, L, Kaderli, B, Hadley, D, Hagstrom, SA, Peachey, NS, Klein, R, Klein, BE, Gotoh, N, Yamashiro, K, Ferris Iii, F, Fagerness, JA, Reynolds, R, Farrer, LA, Kim, IK, Miller, JW, Corton, M, Carracedo, A, Sanchez-Salorio, M, Pugh, EW, Doheny, KF, Brion, M, Deangelis, MM, Weeks, DE, Zack, DJ, Chew, EY, Heckenlively, JR, Yoshimura, N, Iyengar, SK, Francis, PJ, Katsanis, N, Seddon, JM, Haines, JL, Gorin, MB, Abecasis, GR, Swaroop, A (2010) Genetic variants near TIMP3 and high-density lipoprotein-associated loci influence susceptibility to age-related macular degeneration. *Proc Natl Acad Sci U S A* 107(16): 7401-7406.

Chevion, M (1988) A site-specific mechanism for free radical induced biological damage: the essential role of redox-active transition metals. *Free Radic Biol Med* 5(1): 27-37.

Chihara, E, Nao-i, N (1985) Resorption of subretinal fluid by transepithelial flow of the retinal pigment epithelium. *Graefes Arch Clin Exp Ophthalmol* 223(4): 202-204.

Chong, NH, Keonin, J, Luthert, PJ, Frennesson, CI, Weingeist, DM, Wolf, RL, Mullins, RF, Hageman, GS (2005) Decreased thickness and integrity of the macular elastic layer of Bruch's membrane correspond to the distribution of lesions associated with age-related macular degeneration. *Am J Pathol* 166(1): 241-251.

Chowers, I, Wong, R, Dentchev, T, Farkas, RH, Iacovelli, J, Gunatilaka, TL, Medeiros, NE, Presley, JB, Campochiaro, PA, Curcio, CA, Dunaief, JL, Zack, DJ (2006) The iron carrier transferrin is upregulated in retinas from patients with age-related macular degeneration. *Invest Ophthalmol Vis Sci* 47(5): 2135-2140.

Chung, L, Dinakarpandian, D, Yoshida, N, Lauer-Fields, JL, Fields, GB, Visse, R, Nagase, H (2004) Collagenase unwinds triple-helical collagen prior to peptide bond hydrolysis. *EMBO J* 23(15): 3020-3030.

Clark, SD, Kobayashi, DK, Welgus, HG (1987) Regulation of the expression of tissue inhibitor of metalloproteinases and collagenase by retinoids and glucocorticoids in human fibroblasts. *J Clin Invest* 80(5): 1280-1288.

Cleasby, GW, Nakanishi, AS, Norris, JL (1979) Prophylactic photocoagulation of the fellow eye in exudative senile maculopathy. A preliminary report. *Mod Probl Ophthalmol* 20: 141-147.

Cohen, LH, Noell, WK (1960) Glucose catabolism of rabbit retina before and after development of visual function. *J Neurochem* 5: 253-276.

Corcoran, ML, Hewitt, RE, Kleiner, DE, Jr., Stetler-Stevenson, WG (1996) MMP-2: expression, activation and inhibition. *Enzyme Protein* 49(1-3): 7-19.

Cowan, SW, Newcomer, ME, Jones, TA (1990) Crystallographic refinement of human serum retinol binding protein at 2A resolution. *Proteins* 8(1): 44-61.

Cringle, SJ, Yu, DY, Yu, PK, Su, EN (2002) Intraretinal oxygen consumption in the rat in vivo. *Invest Ophthalmol Vis Sci* 43(6): 1922-1927.

Cuajungco, MP, Faget, KY, Huang, X, Tanzi, RE, Bush, AI (2000) Metal chelation as a potential therapy for Alzheimer's disease. *Ann N Y Acad Sci* 920: 292-304.

Cunha-Vaz, JG, Shakib, M, Ashton, N (1966) Studies on the permeability of the blood-retinal barrier. I. On the existence, development, and site of a blood-retinal barrier. *Br J Ophthalmol* 50(8): 441-453.

Curcio, CA, Millican, CL, Bailey, T, Kruth, HS (2001) Accumulation of cholesterol with age in human Bruch's membrane. *Invest Ophthalmol Vis Sci* 42(1): 265-274.

Curry, FE (1984) Mechanics and thermodynamics of transcapillary exchange. In: *Handbook of Physiology*, pp 309-374: American Physiological Society.

Das, A, Frank, RN, Zhang, NL, Turczyn, TJ (1990) Ultrastructural localization of extracellular matrix components in human retinal vessels and Bruch's membrane. *Arch Ophthalmol* 108(3): 421-429.

De Clerck, YA, Yean, TD, Ratzkin, BJ, Lu, HS, Langley, KE (1989) Purification and characterization of two related but distinct metalloproteinase inhibitors secreted by bovine aortic endothelial cells. *J Biol Chem* 264(29): 17445-17453.

De La Paz, MA, Pericak-Vance, MA, Lennon, F, Haines, JL, Seddon, JM (1997) Exclusion of TIMP3 as a candidate locus in age-related macular degeneration. *Invest Ophthalmol Vis Sci* 38(6): 1060-1065.

DeClerck, YA, Yean, TD, Lee, Y, Tomich, JM, Langley, KE (1993) Characterization of the functional domain of tissue inhibitor of metalloproteinases-2 (TIMP-2). *Biochem J* 289 (Pt 1): 65-69.

Dentchev, T, Hahn, P, Dunaief, JL (2005) Strong labeling for iron and the iron-handling proteins ferritin and ferroportin in the photoreceptor layer in age-related macular degeneration. *Arch Ophthalmol* 123(12): 1745-1746.

Dollery, CM, McEwan, JR, Henney, AM (1995) Matrix metalloproteinases and cardiovascular disease. *Circ Res* 77(5): 863-868.

Donoso, LA, Kim, D, Frost, A, Callahan, A, Hageman, G (2006) The role of inflammation in the pathogenesis of age-related macular degeneration. *Surv Ophthalmol* 51(2): 137-152.

Donovan, A, Brownlie, A, Zhou, Y, Shepard, J, Pratt, SJ, Moynihan, J, Paw, BH, Drejer, A, Barut, B, Zapata, A, Law, TC, Brugnara, C, Lux, SE, Pinkus, GS, Pinkus, JL, Kingsley, PD, Palis, J, Fleming, MD, Andrews, NC, Zon, LI (2000) Positional cloning of zebrafish ferroportin1 identifies a conserved vertebrate iron exporter. *Nature* 403(6771): 776-781.

Dorey, CK, Wu, G, Ebenstein, D, Garsd, A, Weiter, JJ (1989) Cell loss in the aging retina. Relationship to lipofuscin accumulation and macular degeneration. *Invest Ophthalmol Vis Sci* 30(8): 1691-1699.

Duce, JA, Tsatsanis, A, Cater, MA, James, SA, Robb, E, Wikhe, K, Leong, SL, Perez, K, Johanssen, T, Greenough, MA, Cho, HH, Galatis, D, Moir, RD, Masters, CL, McLean, C, Tanzi, RE, Cappai, R, Barnham, KJ, Ciccotosto, GD, Rogers, JT, Bush, AI (2010) Iron-export ferroxidase activity of beta-amyloid precursor protein is inhibited by zinc in Alzheimer's disease. *Cell* 142(6): 857-867.

Dunaief, JL (2006) Iron induced oxidative damage as a potential factor in age-related macular degeneration: the Cogan Lecture. *Invest Ophthalmol Vis Sci* 47(11): 4660-4664.

Edwards, AO, Ritter, R, 3rd, Abel, KJ, Manning, A, Panhuysen, C, Farrer, LA (2005) Complement factor H polymorphism and age-related macular degeneration. *Science* 308(5720): 421-424.

Edwards, DR, Rocheleau, H, Sharma, RR, Wills, AJ, Cowie, A, Hassell, JA, Heath, JK (1992) Involvement of AP1 and PEA3 binding sites in the regulation of murine tissue inhibitor of metalloproteinases-1 (TIMP-1) transcription. *Biochim Biophys Acta* 1171(1): 41-55.

Elkins, PA, Ho, YS, Smith, WW, Janson, CA, D'Alessio, KJ, McQueney, MS, Cummings, MD, Romanic, AM (2002) Structure of the C-terminally truncated human ProMMP9, a gelatin-binding matrix metalloproteinase. *Acta Crystallogr D Biol Crystallogr* 58(Pt 7): 1182-1192.

Emi, K, Pederson, JE, Toris, CB (1989) Hydrostatic pressure of the suprachoroidal space. *Invest Ophthalmol Vis Sci* 30(2): 233-238.

Esterbauer, H, Schaur, RJ, Zollner, H (1991) Chemistry and biochemistry of 4-hydroxynonenal, malonaldehyde and related aldehydes. *Free Radic Biol Med* 11(1): 81-128.

Evans, GW (1986) Zinc and its deficiency diseases. *Clin Physiol Biochem* 4(1): 94-98.

Exley, C, Korchazhkina, OV (2001) The association of aluminium and beta-amyloid in Alzheimer's disease. In: *Aluminium and Alzheimer's disease*, pp 421-434. Amsterdam: Elsevier.

Fariss, RN, Apte, SS, Luthert, PJ, Bird, AC, Milam, AH (1998) Accumulation of tissue inhibitor of metalloproteinases-3 in human eyes with Sorsby's fundus dystrophy or retinitis pigmentosa. *Br J Ophthalmol* 82(11): 1329-1334.

Fariss, RN, Apte, SS, Olsen, BR, Iwata, K, Milam, AH (1997) Tissue inhibitor of metalloproteinases-3 is a component of Bruch's membrane of the eye. *Am J Pathol* 150(1): 323-328.

Farkas, RH, Chowers, I, Hackam, AS, Kageyama, M, Nickells, RW, Otteson, DC, Duh, EJ, Wang, C, Valenta, DF, Gunatilaka, TL, Pease, ME, Quigley, HA, Zack, DJ (2004) Increased expression of iron-regulating genes in monkey and human glaucoma. *Invest Ophthalmol Vis Sci* 45(5): 1410-1417.

Farkas, TG, Sylvester, V, Archer, D (1971) The ultrastructure of drusen. *Am J Ophthalmol* 71(6): 1196-1205.

Feeney-Burns, L (1980) The pigments of the retinal pigment epithelium. *Curr Top Eye Res* 2: 119-178.

Feeney-Burns, L, Ellersieck, MR (1985) Age-related changes in the ultrastructure of Bruch's membrane. *Am J Ophthalmol* 100(5): 686-697.

Feeney-Burns, L, Hilderbrand, ES, Eldridge, S (1984) Aging human RPE: morphometric analysis of macular, equatorial, and peripheral cells. *Invest Ophthalmol Vis Sci* 25(2): 195-200.

Figueroa, MS, Regueras, A, Bertrand, J (1994) Laser photocoagulation to treat macular soft drusen in age-related macular degeneration. *Retina* 14(5): 391-396.

Fini, ME, Girard, MT, Matsubara, M, Bartlett, JD (1995) Unique regulation of the matrix metalloproteinase, gelatinase B. *Invest Ophthalmol Vis Sci* 36(3): 622-633.

Finnemann, SC, Leung, LW, Rodriguez-Boulan, E (2002) The lipofuscin component A2E selectively inhibits phagolysosomal degradation of photoreceptor phospholipid by the retinal pigment epithelium. *Proc Natl Acad Sci U S A* 99(6): 3842-3847.

Fiotti, N, Pedio, M, Battaglia Parodi, M, Altamura, N, Uxa, L, Guarnieri, G, Giansante, C, Ravalico, G (2005) MMP-9 microsatellite polymorphism and susceptibility to exudative form of age-related macular degeneration. *Genet Med* 7(4): 272-277.

Fisher, RF (1987) The influence of age on some ocular basement membranes. *Eye (Lond)* 1 (Pt 2): 184-189.

Flaxel, C, Bradle, J, Acott, T, Samples, JR (2007) Retinal pigment epithelium produces matrix metalloproteinases after laser treatment. *Retina* 27(5): 629-634.

Fornoni, A, Wang, Y, Lenz, O, Striker, LJ, Striker, GE (2002) Association of a decreased number of d(CA) repeats in the matrix metalloproteinase-9 promoter with glomerulosclerosis susceptibility in mice. *J Am Soc Nephrol* 13(8): 2068-2076.

Foulds, WS (1990) The choroidal circulation and retinal metabolism--an overview. *Eye (Lond)* 4 (Pt 2): 243-248.

Frambach, DA, Marmor, MF (1982) The rate and route of fluid resorption from the subretinal space of the rabbit. *Invest Ophthalmol Vis Sci* 22(3): 292-302.

Framme, C, Walter, A, Prahs, P, Regler, R, Theisen-Kunde, D, Alt, C, Brinkmann, R (2009) Structural changes of the retina after conventional laser photocoagulation and selective retina treatment (SRT) in spectral domain OCT. *Curr Eye Res* 34(7): 568-579.

Frederickson, CJ, Bush, AI (2001) Synaptically released zinc: physiological functions and pathological effects. *Biometals* 14(3-4): 353-366.

Friedman, DS, O'Colmain, BJ, Munoz, B, Tomany, SC, McCarty, C, de Jong, PT, Nemesure, B, Mitchell, P, Kempen, J (2004) Prevalence of age-related macular degeneration in the United States. *Arch Ophthalmol* 122(4): 564-572.

Geurts, N, Martens, E, Van Aelst, I, Proost, P, Opdenakker, G, Van den Steen, PE (2008) Beta-hematin interaction with the hemopexin domain of gelatinase B/MMP-9 provokes autocatalytic processing of the propeptide, thereby priming activation by MMP-3. *Biochemistry* 47(8): 2689-2699.

Gioia, M, Monaco, S, Fasciglione, GF, Coletti, A, Modesti, A, Marini, S, Coletta, M (2007) Characterization of the mechanisms by which gelatinase A, neutrophil collagenase, and membrane-type metalloproteinase MMP-14 recognize collagen I and enzymatically process the two alpha-chains. *J Mol Biol* 368(4): 1101-1113.

Glatt, H, Machemer, R (1982) Experimental subretinal hemorrhage in rabbits. *Am J Ophthalmol* 94(6): 762-773.

Gold, B, Merriam, JE, Zernant, J, Hancox, LS, Taiber, AJ, Gehrs, K, Cramer, K, Neel, J, Bergeron, J, Barile, GR, Smith, RT, Hageman, GS, Dean, M, Allikmets, R (2006) Variation in factor B (BF) and complement component 2 (C2) genes is associated with age-related macular degeneration. *Nat Genet* 38(4): 458-462.

Goldberg, GI, Marmer, BL, Grant, GA, Eisen, AZ, Wilhelm, S, He, CS (1989) Human 72-kilodalton type IV collagenase forms a complex with a tissue inhibitor of metalloproteases designated TIMP-2. *Proc Natl Acad Sci U S A* 86(21): 8207-8211.

Goldberg, GI, Strongin, A, Collier, IE, Genrich, LT, Marmer, BL (1992) Interaction of 92-kDa type IV collagenase with the tissue inhibitor of metalloproteinases prevents dimerization, complex formation with interstitial collagenase, and activation of the proenzyme with stromelysin. *J Biol Chem* 267(7): 4583-4591.

Gomez, DE, Alonso, DF, Yoshiji, H, Thorgeirsson, UP (1997) Tissue inhibitors of metalloproteinases: structure, regulation and biological functions. *Eur J Cell Biol* 74(2): 111-122.

Gordiyenko, N, Campos, M, Lee, JW, Fariss, RN, Sztein, J, Rodriguez, IR (2004) RPE cells internalize low-density lipoprotein (LDL) and oxidized LDL (oxLDL) in large quantities in vitro and in vivo. *Invest Ophthalmol Vis Sci* 45(8): 2822-2829.

Grahn, BH, Paterson, PG, Gottschall-Pass, KT, Zhang, Z (2001) Zinc and the eye. *J Am Coll Nutr* 20(2 Suppl): 106-118.

Grant, ME, Heathcote, JG, Orkin, RW (1981) Current concepts of basement-membrane structure and function. *Biosci Rep* 1(11): 819-842.

Green, WR, Enger, C (1993) The 1992 Lorenz E Zimmerman Lecture. Age related macular degeneration: Histopathologic studies. *Ophthalmol* 100: 1519-1535.

Green, WR, Key, SN, 3rd (1977) Senile macular degeneration: a histopathologic study. *Trans Am Ophthalmol Soc* 75: 180-254.

Grindle, CF, Marshall, J (1978) Ageing changes in Bruch's membrane and their functional implications. *Trans Ophthalmol Soc U K* 98(1): 172-175.

Guo, L, Hussain, AA, Limb, GA, Marshall, J (1999) Age-dependent variation in metalloproteinase activity of isolated human Bruch's membrane and choroid. *Invest Ophthalmol Vis Sci* 40(11): 2676-2682.

Guymer, R, Luthert, P, Bird, A (1999) Changes in Bruch's membrane and related structures with age. *Prog Retin Eye Res* 18(1): 59-90.

Haas, TL, Davis, SJ, Madri, JA (1998) Three-dimensional type I collagen lattices induce coordinate expression of matrix metalloproteinases MT1-MMP and MMP-2 in microvascular endothelial cells. *J Biol Chem* 273(6): 3604-3610.

Hageman, GS, Anderson, DH, Johnson, LV, Hancox, LS, Taiber, AJ, Hardisty, LI, Hageman, JL, Stockman, HA, Borchardt, JD, Gehrs, KM, Smith, RJ, Silvestri, G, Russell, SR, Klaver, CC, Barbazetto, I, Chang, S, Yannuzzi, LA, Barile, GR, Merriam, JC, Smith, RT, Olsh, AK, Bergeron, J, Zernant, J, Merriam, JE, Gold, B, Dean, M, Allikmets, R (2005) A common haplotype in the complement regulatory gene factor H (HF1/CFH) predisposes individuals to age-related macular degeneration. *Proc Natl Acad Sci U S A* 102(20): 7227-7232.

Hageman, GS, Luthert, PJ, Victor Chong, NH, Johnson, LV, Anderson, DH, Mullins, RF (2001) An integrated hypothesis that considers drusen as biomarkers of immune-mediated processes at the RPE-Bruch's membrane interface in aging and age-related macular degeneration. *Prog Retin Eye Res* 20(6): 705-732.

Hageman, GS, Mullins, RF, Russell, SR, Johnson, LV, Anderson, DH (1999) Vitronectin is a constituent of ocular drusen and the vitronectin gene is expressed in human retinal pigmented epithelial cells. *FASEB J* 13(3): 477-484.

Hahn, P, Dentchev, T, Qian, Y, Rouault, T, Harris, ZL, Dunaief, JL (2004a) Immunolocalization and regulation of iron handling proteins ferritin and ferroportin in the retina. *Mol Vis* 10: 598-607.

Hahn, P, Qian, Y, Dentchev, T, Chen, L, Beard, J, Harris, ZL, Dunaief, JL (2004b) Disruption of ceruloplasmin and hephaestin in mice causes retinal iron overload and retinal degeneration with features of age-related macular degeneration. *Proc Natl Acad Sci U S A* 101(38): 13850-13855.

Haines, JL, Hauser, MA, Schmidt, S, Scott, WK, Olson, LM, Gallins, P, Spencer, KL, Kwan, SY, Noureddine, M, Gilbert, JR, Schnetz-Boutaud, N, Agarwal, A, Postel, EA, Pericak-Vance, MA (2005) Complement factor H variant increases the risk of age-related macular degeneration. *Science* 308(5720): 419-421.

Hammes, HP, Hoerauf, H, Alt, A, Schleicher, E, Clausen, JT, Bretzel, RG, Laqua, H (1999) N(epsilon)(carboxymethyl)lysin and the AGE receptor RAGE colocalize in age-related macular degeneration. *Invest Ophthalmol Vis Sci* 40(8): 1855-1859.

Handa, JT, Verzijl, N, Matsunaga, H, Aotaki-Keen, A, Lutty, GA, te Koppele, JM, Miyata, T, Hjelmeland, LM (1999) Increase in the advanced glycation end product pentosidine in Bruch's membrane with age. *Invest Ophthalmol Vis Sci* 40(3): 775-779.

Hawkins, BS, Bird, A, Klein, R, West, SK (1999) Epidemiology of age-related macular degeneration. *Mol Vis* 5: 26.

Hayashi, T, Shishido, N, Nakayama, K, Nunomura, A, Smith, MA, Perry, G, Nakamura, M (2007) Lipid peroxidation and 4-hydroxy-2-nonenal formation by copper ion bound to amyloid-beta peptide. *Free Radic Biol Med* 43(11): 1552-1559.

Hayes, KC, Lindsey, S, Stephan, ZF, Brecker, D (1989) Retinal pigment epithelium possesses both LDL and scavenger receptor activity. *Invest Ophthalmol Vis Sci* 30(2): 225-232.

Hazlett, LD, Meyer, DB (1974) Ferritin uptake in the Japanese quail retina. *Exp Eye Res* 19(4): 303-309.

He, X, Hahn, P, Iacovelli, J, Wong, R, King, C, Bhisitkul, R, Massaro-Giordano, M, Dunaief, JL (2007) Iron homeostasis and toxicity in retinal degeneration. *Prog Retin Eye Res* 26(6): 649-673.

Heller, J (1975) Interactions of plasma retinol-binding protein with its receptor. Specific binding of bovine and human retinol-binding protein to pigment epithelium cells from bovine eyes. *J Biol Chem* 250(10): 3613-3619.

Heller, J, Bok, D (1976) Transport of retinol from the blood to the retina: involvement of high molecular weight lipoproteins as intracellular carriers. *Exp Eye Res* 22(5): 403-410.

Hicks, M, Delbridge, L, Yue, DK, Reeve, TS (1989) Increase in crosslinking of nonenzymatically glycosylated collagen induced by products of lipid peroxidation. *Arch Biochem Biophys* 268(1): 249-254.

Ho, AC, Maguire, MG, Yoken, J, Lee, MS, Shin, DS, Javornik, NB, Fine, SL (1999) Laser-induced drusen reduction improves visual function at 1 year. Choroidal Neovascularization Prevention Trial Research Group. *Ophthalmology* 106(7): 1367-1373; discussion 1374.

Holz, FG, Schutt, F, Kopitz, J, Eldred, GE, Kruse, FE, Volcker, HE, Cantz, M (1999) Inhibition of lysosomal degradative functions in RPE cells by a retinoid component of lipofuscin. *Invest Ophthalmol Vis Sci* 40(3): 737-743.

Holz, FG, Sheraidah, G, Pauleikhoff, D, Bird, AC (1994) Analysis of lipid deposits extracted from human macular and peripheral Bruch's membrane. *Arch Ophthalmol* 112(3): 402-406.

Honda, S, Farboud, B, Hjelmeland, LM, Handa, JT (2001) Induction of an aging mRNA retinal pigment epithelial cell phenotype by matrix-containing advanced glycation end products in vitro. *Invest Ophthalmol Vis Sci* 42(10): 2419-2425.

Hoppe, G, Marmorstein, AD, Pennock, EA, Hoff, HF (2001) Oxidized low density lipoprotein-induced inhibition of processing of photoreceptor outer segments by RPE. *Invest Ophthalmol Vis Sci* 42(11): 2714-2720.

Hornebeck, W, Tixier, JM, Robert, L (1986) Inducible adhesion of mesenchymal cells to elastic fibers: elastonectin. *Proc Natl Acad Sci U S A* 83(15): 5517-5520.

House, E, Collingwood, J, Khan, A, Korchazkina, O, Berthon, G, Exley, C (2004) Aluminium, iron, zinc and copper influence the in vitro formation of amyloid fibrils of Abeta42 in a manner which may have consequences for metal chelation therapy in Alzheimer's disease. *J Alzheimers Dis* 6(3): 291-301.

Howard, EW, Benton, R, Ahern-Moore, J, Tomasek, JJ (1996) Cellular contraction of collagen lattices is inhibited by nonenzymatic glycation. *Exp Cell Res* 228(1): 132-137.

Huang, X, Atwood, CS, Moir, RD, Hartshorn, MA, Tanzi, RE, Bush, AI (2004) Trace metal contamination initiates the apparent auto-aggregation, amyloidosis, and oligomerization of Alzheimer's Abeta peptides. *J Biol Inorg Chem* 9(8): 954-960.

Huang, X, Atwood, CS, Moir, RD, Hartshorn, MA, Vonsattel, JP, Tanzi, RE, Bush, AI (1997) Zinc-induced Alzheimer's Abeta1-40 aggregation is mediated by conformational factors. *J Biol Chem* 272(42): 26464-26470.

Hughes, BA, Miller, SS, Machen, TE (1984) Effects of cyclic AMP on fluid absorption and ion transport across frog retinal pigment epithelium. Measurements in the open-circuit state. *J Gen Physiol* 83(6): 875-899.

Hunt, RC, Dewey, A, Davis, AA (1989) Transferrin receptors on the surfaces of retinal pigment epithelial cells are associated with the cytoskeleton. *J Cell Sci* 92 (Pt 4): 655-666.

Hunt, RC, Fox, A, al Pakalnis, V, Sigel, MM, Kosnosky, W, Choudhury, P, BIack, EP (1993) Cytokines cause cultured retinal pigment epithelial cells to secrete metalloproteinases and to contract collagen gels. *Invest Ophthalmol Vis Sci* 34(11): 3179-3186.

Hussain, AA, Starita, C, Hodgetts, A, Marshall, J (2010) Macromolecular diffusion characteristics of ageing human Bruch's membrane: implications for age-related macular degeneration (AMD). *Exp Eye Res* 90(6): 703-710.

Hussain, AA, Starita, C, Marshall, J (2004) Transport Characteristics of Ageing Human Bruch's Membrane. In: *Focus on Macular Degeneration Research*, Ioseliani, OR (ed), pp 59-113: Nova Science Publishers.

Hussain, AA, Voaden, MJ (1985) Postenucleation survival of taurine uptake by pigment epithelium and choroid of the baboon eye. *Exp Eye Res* 40(4): 643-646.

Ishibashi, T, Murata, T, Hangai, M, Nagai, R, Horiuchi, S, Lopez, PF, Hinton, DR, Ryan, SJ (1998) Advanced glycation end products in age-related macular degeneration. *Arch Ophthalmol* 116(12): 1629-1632.

Ishibashi, T, Patterson, R, Ohnishi, Y, Inomata, H, Ryan, SJ (1986) Formation of drusen in the human eye. *Am J Ophthalmol* 101(3): 342-353.

Johnson, LV, Leitner, WP, Staples, MK, Anderson, DH (2001) Complement activation and inflammatory processes in Drusen formation and age related macular degeneration. *Exp Eye Res* 73(6): 887-896.

Joseph, DP, Miller, SS (1991) Apical and basal membrane ion transport mechanisms in bovine retinal pigment epithelium. *J Physiol* 435: 439-463.

Kamei, M, Hollyfield, JG (1999) TIMP-3 in Bruch's membrane: changes during aging and in age-related macular degeneration. *Invest Ophthalmol Vis Sci* 40(10): 2367-2375.

Karwatowski, WS, Jeffries, TE, Duance, VC, Albon, J, Bailey, AJ, Easty, DL (1995) Preparation of Bruch's membrane and analysis of the age-related changes in the structural collagens. *Br J Ophthalmol* 79(10): 944-952.

Kennedy, CJ, Rakoczy, PE, Constable, IJ (1995) Lipofuscin of the retinal pigment epithelium: a review. *Eye (Lond)* 9 (Pt 6): 763-771.

Kikugawa, K, Beppu, M (1987) Involvement of lipid oxidation products in the formation of fluorescent and cross-linked proteins. *Chem Phys Lipids* 44(2-4): 277-296.

Kimura, E, Kikuta, E (2000) Why zinc in zinc enzymes? From biological roles to DNA base-selective recognition. *J Biol Inorg Chem* 5(2): 139-155.

Kirchheimer, JC, Remold, HG (1989) Functional characteristics of receptor-bound urokinase on human monocytes: catalytic efficiency and susceptibility to inactivation by plasminogen activator inhibitors. *Blood* 74(4): 1396-1402.

Klaver, CC, Wolfs, RC, Assink, JJ, van Duijn, CM, Hofman, A, de Jong, PT (1998) Genetic risk of age-related maculopathy. Population-based familial aggregation study. *Arch Ophthalmol* 116(12): 1646-1651.

Klein, R, Klein, BE, Linton, KL (1992) Prevalence of age-related maculopathy. The Beaver Dam Eye Study. *Ophthalmology* 99(6): 933-943.

Klein, RJ, Zeiss, C, Chew, EY, Tsai, JY, Sackler, RS, Haynes, C, Henning, AK, SanGiovanni, JP, Mane, SM, Mayne, ST, Bracken, MB, Ferris, FL, Ott, J, Barnstable, C, Hoh, J (2005) Complement factor H polymorphism in age-related macular degeneration. *Science* 308(5720): 385-389.

Klenotic, PA, Munier, FL, Marmorstein, LY, Anand-Apte, B (2004) Tissue inhibitor of metalloproteinases-3 (TIMP-3) is a binding partner of epithelial growth factor-containing fibulin-like extracellular matrix protein 1 (EFEMP1). Implications for macular degenerations. *J Biol Chem* 279(29): 30469-30473.

Kliffen, M, de Jong, PT, Luider, TM (1995) Protein analysis of human maculae in relation to age-related maculopathy. *Lab Invest* 73(2): 267-272.

Korshunov, SS, Skulachev, VP, Starkov, AA (1997) High protonic potential actuates a mechanism of production of reactive oxygen species in mitochondria. *FEBS Lett* 416(1): 15-18.

Krishnamurti, U, Rondeau, E, Sraer, JD, Michael, AF, Tsilibary, EC (1997) Alterations in human glomerular epithelial cells interacting with nonenzymatically glycosylated matrix. *J Biol Chem* 272(44): 27966-27970.

Kumar, A, El-Osta, A, Hussain, AA, Marshall, J (2010) Increased sequestration of matrix metalloproteinases in ageing human Bruch's membrane: implications for ECM turnover. *Invest Ophthalmol Vis Sci* 51(5): 2664-2670.

Kundaiker, S, Hussain, AA, Marshall, J (1996) Component characteristics of the vectorial transport system for taurine in isolated bovine retinal pigment epithelium. *J Physiol* 492 (Pt 2): 505-516.

Labat-Robert, J, Bihari-Varga, M, Robert, L (1990) Extracellular matrix. *FEBS Lett* 268(2): 386-393.

Leco, KJ, Khokha, R, Pavloff, N, Hawkes, SP, Edwards, DR (1994) Tissue inhibitor of metalloproteinases-3 (TIMP-3) is an extracellular matrix-associated protein with a distinctive pattern of expression in mouse cells and tissues. *J Biol Chem* 269(12): 9352-9360.

Leu, ST, Batni, S, Radeke, MJ, Johnson, LV, Anderson, DH, Clegg, DO (2002) Drusen are Cold Spots for Proteolysis: Expression of Matrix Metalloproteinases and Their Tissue Inhibitor Proteins in Age-related Macular Degeneration. *Exp Eye Res* 74(1): 141-154.

Leung, KW, Liu, M, Xu, X, Seiler, MJ, Barnstable, CJ, Tombran-Tink, J (2008) Expression of ZnT and ZIP zinc transporters in the human RPE and their regulation by neurotrophic factors. *Invest Ophthalmol Vis Sci* 49(3): 1221-1231.

Levi, S, Corsi, B, Bosisio, M, Invernizzi, R, Volz, A, Sanford, D, Arosio, P, Drysdale, J (2001) A human mitochondrial ferritin encoded by an intronless gene. *J Biol Chem* 276(27): 24437-24440.

Li, M, Atmaca-Sonmez, P, Othman, M, Branham, KE, Khanna, R, Wade, MS, Li, Y, Liang, L, Zareparsi, S, Swaroop, A, Abecasis, GR (2006) CFH haplotypes without the Y402H coding variant show strong association with susceptibility to age-related macular degeneration. *Nat Genet* 38(9): 1049-1054.

Liles, MR, Newsome, DA, Oliver, PD (1991) Antioxidant enzymes in the aging human retinal pigment epithelium. *Arch Ophthalmol* 109(9): 1285-1288.

Lim, GP, Russell, MJ, Cullen, MJ, Tokes, ZA (1997) Matrix metalloproteinases in dog brains exhibiting Alzheimer-like characteristics. *J Neurochem* 68(4): 1606-1611.

Lin, WL (1989) Immunogold localization of extracellular matrix molecules in Bruch's membrane of the rat. *Curr Eye Res* 8(11): 1171-1178.

Liotta, LA, Steeg, PS, Stetler-Stevenson, WG (1991) Cancer metastasis and angiogenesis: an imbalance of positive and negative regulation. *Cell* 64(2): 327-336.

Loffler, KU, Lee, WR (1986) Basal linear deposit in the human macula. *Graefes Arch Clin Exp Ophthalmol* 224(6): 493-501.

Majewski, J, Schultz, DW, Weleber, RG, Schain, MB, Edwards, AO, Matise, TC, Acott, TS, Ott, J, Klein, ML (2003) Age-related macular degeneration--a genome scan in extended families. *Am J Hum Genet* 73(3): 540-550.

Malek, G, Li, CM, Guidry, C, Medeiros, NE, Curcio, CA (2003) Apolipoprotein B in cholesterol-containing drusen and basal deposits of human eyes with age-related maculopathy. *Am J Pathol* 162(2): 413-425.

Malik, N, Greenfield, BW, Wahl, AF, Kiener, PA (1996) Activation of human monocytes through CD40 induces matrix metalloproteinases. *J Immunol* 156(10): 3952-3960.

Maller, J, George, S, Purcell, S, Fagerness, J, Altshuler, D, Daly, MJ, Seddon, JM (2006) Common variation in three genes, including a noncoding variant in CFH, strongly influences risk of age-related macular degeneration. *Nat Genet* 38(9): 1055-1059.

Marin-Castano, ME, Csaky, KG, Cousins, SW (2005) Nonlethal oxidant injury to human retinal pigment epithelium cells causes cell membrane blebbing but decreased MMP-2 activity. *Invest Ophthalmol Vis Sci* 46(9): 3331-3340.

Marmor, MF, Abdul-Rahim, AS, Cohen, DS (1980) The effect of metabolic inhibitors on retinal adhesion and subretinal fluid resorption. *Invest Ophthalmol Vis Sci* 19(8): 893-903.

Marmorstein, LY, Munier, FL, Arsenijevic, Y, Schorderet, DF, McLaughlin, PJ, Chung, D, Traboulsi, E, Marmorstein, AD (2002) Aberrant accumulation of EFEMP1 underlies drusen formation in Malattia Leventinese and age-related macular degeneration. *Proc Natl Acad Sci U S A* 99(20): 13067-13072.

Marshall, GE, Konstas, AG, Lee, WR (1993) Collagens in ocular tissues. *Br J Ophthalmol* 77(8): 515-524.

Marshall, GE, Konstas, AG, Reid, GG, Edwards, JG, Lee, WR (1994) Collagens in the aged human macula. *Graefes Arch Clin Exp Ophthalmol* 232(3): 133-140.

Marshall, GE, Konstas, AG, Reid, GG, Edwards, JG, Lee, WR (1992) Type IV collagen and laminin in Bruch's membrane and basal linear deposit in the human macula. *Br J Ophthalmol* 76(10): 607-614.

Marshall, JH, A. A. Starita, C. (1998) Retinal Pigment Epithelium: Function and Disease. *Oxford University Press*: 669-692.

Matrisian, LM (1992) The matrix-degrading metalloproteinases. *Bioessays* 14(7): 455-463.

Matrisian, LM (1990) Metalloproteinases and their inhibitors in matrix remodeling. *Trends Genet* 6(4): 121-125.

Maurice, DM, Salmon, J, Zauberman, H (1971) Subretinal pressure and retinal adhesion. *Exp Eye Res* 12(2): 212-217.

Melhus, H, Nilsson, T, Peterson, PA, Rask, L (1991) Retinol-binding protein and transthyretin expressed in HeLa cells form a complex in the endoplasmic reticulum in both the absence and the presence of retinol. *Exp Cell Res* 197(1): 119-124.

Miceli, MV, Liles, MR, Newsome, DA (1994) Evaluation of oxidative processes in human pigment epithelial cells associated with retinal outer segment phagocytosis. *Exp Cell Res* 214(1): 242-249.

Michel, CC, Curry, FE (1999) Microvascular permeability. *Physiol Rev* 79(3): 703-761.

Millis, AJ, Hoyle, M, McCue, HM, Martini, H (1992) Differential expression of metalloproteinase and tissue inhibitor of metalloproteinase genes in aged human fibroblasts. *Exp Cell Res* 201(2): 373-379.

Miyamoto, Y, Del Monte, MA (1994) Na(+)-dependent glutamate transporter in human retinal pigment epithelial cells. *Invest Ophthalmol Vis Sci* 35(10): 3589-3598.

Moiseyev, G, Chen, Y, Takahashi, Y, Wu, BX, Ma, JX (2005) RPE65 is the isomerohydrolase in the retinoid visual cycle. *Proc Natl Acad Sci U S A* 102(35): 12413-12418.

Moore, DJ, Clover, GM (2001) The effect of age on the macromolecular permeability of human Bruch's membrane. *Invest Ophthalmol Vis Sci* 42(12): 2970-2975.

Moore, DJ, Hussain, AA, Marshall, J (1995) Age-related variation in the hydraulic conductivity of Bruch's membrane. *Invest Ophthalmol Vis Sci* 36(7): 1290-1297.

Morgunova, E, Tuuttila, A, Bergmann, U, Isupov, M, Lindqvist, Y, Schneider, G, Tryggvason, K (1999) Structure of human pro-matrix metalloproteinase-2: activation mechanism revealed. *Science* 284(5420): 1667-1670.

Mullins, RF, Aptsiauri, N, Hageman, GS (2001) Structure and composition of drusen associated with glomerulonephritis: implications for the role of complement activation in drusen biogenesis. *Eye (Lond)* 15(Pt 3): 390-395.

Mullins, RF, Johnson, LV, Anderson, DH, Hageman, GS (1997) Characterization of drusen-associated glycoconjugates. *Ophthalmology* 104(2): 288-294.

Murate, T, Hayakawa, T (1999) Multiple functions of tissue inhibitors of metalloproteinases (TIMPs): new aspects in hematopoiesis. *Platelets* 10(1): 5-16.

Murphy, G, Knauper, V (1997) Relating matrix metalloproteinase structure to function: why the "hemopexin" domain? *Matrix Biol* 15(8-9): 511-518.

Murphy, G, Ward, R, Gavrilovic, J, Atkinson, S (1992) Physiological mechanisms for metalloproteinase activation. *Matrix Suppl* 1: 224-230.

Murphy, G, Willenbrock, F (1995) Tissue inhibitors of matrix metalloendopeptidases. *Methods Enzymol* 248: 496-510.

Murphy, GJ, Murphy, G, Reynolds, JJ (1991) The origin of matrix metalloproteinases and their familial relationships. *FEBS Lett* 289(1): 4-7.

Nagai, N, Klimava, A, Lee, WH, Izumi-Nagai, K, Handa, JT (2009) CTGF is increased in basal deposits and regulates matrix production through the ERK (p42/p44mapk) MAPK and the p38 MAPK signaling pathways. *Invest Ophthalmol Vis Sci* 50(4): 1903-1910.

Nagase, H (1996) *Zinc Metalloproteases in Health and Disease*. Taylor and Francis: London.

Nagase, H, Enghild, JJ, Suzuki, K, Salvesen, G (1990) Stepwise activation mechanisms of the precursor of matrix metalloproteinase 3 (stromelysin) by proteinases and (4-aminophenyl)mercuric acetate. *Biochemistry* 29(24): 5783-5789.

Nagase, H, Ogata, Y, Suzuki, K, Enghild, JJ, Salvesen, G (1991) Substrate specificities and activation mechanisms of matrix metalloproteinases. *Biochem Soc Trans* 19(3): 715-718.

Nakamura, M, Shishido, N, Nunomura, A, Smith, MA, Perry, G, Hayashi, Y, Nakayama, K, Hayashi, T (2007) Three histidine residues of amyloid-beta peptide control the redox activity of copper and iron. *Biochemistry* 46(44): 12737-12743.

Neale, BM, Fagerness, J, Reynolds, R, Sobrin, L, Parker, M, Raychaudhuri, S, Tan, PL, Oh, EC, Merriam, JE, Souied, E, Bernstein, PS, Li, B, Frederick, JM, Zhang, K, Brantley, MA, Jr., Lee, AY, Zack, DJ, Campochiaro, B, Campochiaro, P, Ripke, S, Smith, RT, Barile, GR, Katsanis, N, Allikmets, R, Daly, MJ, Seddon, JM (2010) Genome-wide association study of advanced age-related macular degeneration identifies a role of the hepatic lipase gene (LIPC). *Proc Natl Acad Sci U S A* 107(16): 7395-7400.

Negi, A, Marmor, MF (1986a) Mechanisms of subretinal fluid resorption in the cat eye. *Invest Ophthalmol Vis Sci* 27(11): 1560-1563.

Negi, A, Marmor, MF (1986b) Quantitative estimation of metabolic transport of subretinal fluid. *Invest Ophthalmol Vis Sci* 27(11): 1564-1568.

Newsome, DA, Huh, W, Green, WR (1987) Bruch's membrane age-related changes vary by region. *Curr Eye Res* 6(10): 1211-1221.

Nowak, JZ (2006) Age-related macular degeneration (AMD): pathogenesis and therapy. *Pharmacol Rep* 58(3): 353-363.

Noy, D, Solomonov, I, Sinkevich, O, Arad, T, Kjaer, K, Sagi, I (2008) Zinc-amyloid beta interactions on a millisecond time-scale stabilize non-fibrillar Alzheimer-related species. *J Am Chem Soc* 130(4): 1376-1383.

Okubo, A, Rosa, RH, Jr., Bunce, CV, Alexander, RA, Fan, JT, Bird, AC, Luthert, PJ (1999) The relationships of age changes in retinal pigment epithelium and Bruch's membrane. *Invest Ophthalmol Vis Sci* 40(2): 443-449.

Olson, MW, Bernardo, MM, Pietila, M, Gervasi, DC, Toth, M, Kotra, LP, Massova, I, Mobashery, S, Fridman, R (2000) Characterization of the monomeric and dimeric forms of latent and active matrix metalloproteinase-9. Differential rates for activation by stromelysin 1. *J Biol Chem* 275(4): 2661-2668.

Organisciak, DT, Darrow, RM, Barsalou, L, Darrow, RA, Kutty, RK, Kutty, G, Wiggert, B (1998) Light history and age-related changes in retinal light damage. *Invest Ophthalmol Vis Sci* 39(7): 1107-1116.

Overall, CM (2002) Molecular determinants of metalloproteinase substrate specificity: matrix metalloproteinase substrate binding domains, modules, and exosites. *Mol Biotechnol* 22(1): 51-86.

Overall, CM (1994) Regulation of tissue inhibitor of matrix metalloproteinase expression. *Ann N Y Acad Sci* 732: 51-64.

Overall, CM, Butler, GS (2007) Protease yoga: extreme flexibility of a matrix metalloproteinase. *Structure* 15(10): 1159-1161.

Overall, CM, Wrana, JL, Sodek, J (1991) Transcriptional and post-transcriptional regulation of 72-kDa gelatinase/type IV collagenase by transforming growth factor-beta 1 in human fibroblasts. Comparisons with collagenase and tissue inhibitor of matrix metalloproteinase gene expression. *J Biol Chem* 266(21): 14064-14071.

Owens, SL, Guymer, RH, Gross-Jendroska, M, Bird, AC (1999) Fluorescein angiographic abnormalities after prophylactic macular photocoagulation for high-risk age-related maculopathy. *Am J Ophthalmol* 127(6): 681-687.

Owsley, C, Jackson, GR, White, M, Feist, R, Edwards, D (2001) Delays in rod-mediated dark adaptation in early age-related maculopathy. *Ophthalmology* 108(7): 1196-1202.

Owsley, C, McGwin, G, Jackson, GR, Heimburger, DC, Piyathilake, CJ, Klein, R, White, MF, Kallies, K (2006) Effect of short-term, high-dose retinol on dark adaptation in aging and early age-related maculopathy. *Invest Ophthalmol Vis Sci* 47(4): 1310-1318.

Paci, E, Greene, LH, Jones, RM, Smith, LJ (2005) Characterization of the molten globule state of retinol-binding protein using a molecular dynamics simulation approach. *FEBS J* 272(18): 4826-4838.

Padgett, LC, Lui, GM, Werb, Z, LaVail, MM (1997) Matrix metalloproteinase-2 and tissue inhibitor of metalloproteinase-1 in the retinal pigment epithelium and interphotoreceptor matrix: vectorial secretion and regulation. *Exp Eye Res* 64(6): 927-938.

Pappenheimer, JR (1953) Passage of molecules through capillary wals. *Physiol Rev* 33(3): 387-423.

Pappenheimer, JR, Renkin, EM, Borrero, LM (1951) Filtration, diffusion and molecular sieving through peripheral capillary membranes; a contribution to the pore theory of capillary permeability. *Am J Physiol* 167(1): 13-46.

Pauleikhoff, D, Harper, CA, Marshall, J, Bird, AC (1990) Aging changes in Bruch's membrane. A histochemical and morphologic study. *Ophthalmology* 97(2): 171-178.

Pavloff, N, Staskus, PW, Kishnani, NS, Hawkes, SP (1992) A new inhibitor of metalloproteinases from chicken: ChIMP-3. A third member of the TIMP family. *J Biol Chem* 267(24): 17321-17326.

Pederson, JE (1994) Fluid physiology of the subretinal space. In: *Retina*, Ryan, SJ (ed) Vol. 2, pp 1955-1968: Mosby-Year Book Inc.

Peters, DG, Kassam, A, St Jean, PL, Yonas, H, Ferrell, RE (1999) Functional polymorphism in the matrix metalloproteinase-9 promoter as a potential risk factor for intracranial aneurysm. *Stroke* 30(12): 2612-2616.

Pino, RM, Essner, E (1981) Permeability of rat choriocapillaris to hemeproteins. Restriction of tracers by a fenestrated endothelium. *J Histochem Cytochem* 29(2): 281-290.

Pino, RM, Thouron, CL (1983) Vascular permeability in the rat eye to endogenous albumin and immunoglobulin G (IgG) examined by immunohistochemical methods. *J Histochem Cytochem* 31(3): 411-416.

Pluen, A, Netti, PA, Jain, RK, Berk, DA (1999) Diffusion of macromolecules in agarose gels: comparison of linear and globular configurations. *Biophys J* 77(1): 542-552.

Quinn, RH, Miller, SS (1992) Ion transport mechanisms in native human retinal pigment epithelium. *Invest Ophthalmol Vis Sci* 33(13): 3513-3527.

Ra, HJ, Parks, WC (2007) Control of matrix metalloproteinase catalytic activity. *Matrix Biol* 26(8): 587-596.

Ramrattan, RS, van der Schaft, TL, Mooy, CM, de Bruijn, WC, Mulder, PG, de Jong, PT (1994) Morphometric analysis of Bruch's membrane, the choriocapillaris, and the choroid in aging. *Invest Ophthalmol Vis Sci* 35(6): 2857-2864.

Redenti, S, Chappell, RL (2004) Localization of zinc transporter-3 (ZnT-3) in mouse retina. *Vision Res* 44(28): 3317-3321.

Refojo, MF (1982) Molecular shape and effective diffusion radius. *Invest Ophthalmol Vis Sci* 22(1): 129-130.

Reinboth, JJ, Gautschi, K, Munz, K, Eldred, GE, Reme, CE (1997) Lipofuscin in the retina: quantitative assay for an unprecedented autofluorescent compound (pyridinium bis-retinoid, A2-E) of ocular age pigment. *Exp Eye Res* 65(5): 639-643.

Renkin, EM (1954) Filtration, diffusion, and molecular sieving through porous cellulose membranes. *J Gen Physiol* 38(2): 225-243.

Renkin, EM, Gustafson-Sgro, M, Sibley, L (1988) Coupling of albumin flux to volume flow in skin and muscles of anesthetized rats. *Am J Physiol* 255(3 Pt 2): H458-466.

Ricchelli, F, Drago, D, Filippi, B, Tognon, G, Zatta, P (2005) Aluminum-triggered structural modifications and aggregation of beta-amyloids. *Cell Mol Life Sci* 62(15): 1724-1733.

Rittie, L, Berton, A, Monboisse, JC, Hornebeck, W, Gillery, P (1999) Decreased contraction of glycated collagen lattices coincides with impaired matrix metalloproteinase production. *Biochem Biophys Res Commun* 264(2): 488-492.

Robert, AM, Robert, L (1980) Biology and pathology of elastic tissues. In: *Frontiers of Matrix Biology* Vol. 8. Basel.

Robert, L, hornebeck, W (1986) Frontiers of Matrix Biology Vol. 11, pp 58-77. Basel.

Roegener, J, Brinkmann, R, Lin, CP (2004) Pump-probe detection of laser-induced microbubble formation in retinal pigment epithelium cells. *J Biomed Opt* 9(2): 367-371.

Roider, J, Hillenkamp, F, Flotte, T, Birngruber, R (1993) Microphotocoagulation: selective effects of repetitive short laser pulses. *Proc Natl Acad Sci U S A* 90(18): 8643-8647.

Rosenblum, G, Van den Steen, PE, Cohen, SR, Bitler, A, Brand, DD, Opdenakker, G, Sagi, I (2010) Direct visualization of protease action on collagen triple helical structure. *PLoS One* 5(6): e11043.

Ruberti, JW, Curcio, CA, Millican, CL, Menco, BP, Huang, JD, Johnson, M (2003) Quick-freeze/deep-etch visualization of age-related lipid accumulation in Bruch's membrane. *Invest Ophthalmol Vis Sci* 44(4): 1753-1759.

Sakai, N, Decatur, J, Nakanishi, K, Eldred, GE (1996) Ocular age pigment 'A2E': an unprecedented pyridinium bisretinoid. *J Am Chem Soc* 118: 1559-1560.

Sarks, SH (1976) Ageing and degeneration in the macular region: a clinico-pathological study. *Br J Ophthalmol* 60(5): 324-341.

Sarks, SH, Arnold, JJ, Killingsworth, MC, Sarks, JP (1999) Early drusen formation in the normal and aging eye and their relation to age related maculopathy: a clinicopathological study. *Br J Ophthalmol* 83(3): 358-368.

Sato, H, Takino, T, Okada, Y, Cao, J, Shinagawa, A, Yamamoto, E, Seiki, M (1994) A matrix metalloproteinase expressed on the surface of invasive tumour cells. *Nature* 370(6484): 61-65.

Sayre, LM, Sha, W, Xu, G, Kaur, K, Nadkarni, D, Subbanagounder, G, Salomon, RG (1996) Immunochemical evidence supporting 2-pentylpyrrole formation on proteins exposed to 4-hydroxy-2-nonenal. *Chem Res Toxicol* 9(7): 1194-1201.

Schmidt, A, Bunte, A, Buddecke, E (1987) Proliferation-dependent changes of proteoglycan metabolism in arterial smooth muscle cells. *Biol Chem Hoppe Seyler* 368(3): 277-284.

Schmidt, SY, Peisch, RD (1986) Melanin concentration in normal human retinal pigment epithelium. Regional variation and age-related reduction. *Invest Ophthalmol Vis Sci* 27(7): 1063-1067.

Scott, JE (1995) Extracellular matrix, supramolecular organisation and shape. *J Anat* 187 (Pt 2): 259-269.

Scott, KA, Wood, EJ, Karran, EH (1998) A matrix metalloproteinase inhibitor which prevents fibroblast-mediated collagen lattice contraction. *FEBS Lett* 441(1): 137-140.

Sethi, CS, Bailey, TA, Luthert, PJ, Chong, NH (2000) Matrix metalloproteinase biology applied to vitreoretinal disorders. *Br J Ophthalmol* 84(6): 654-666.

Shakib, M, Rutkowski, P, Wise, GN (1972) Fluorescein angiography and the retinal pigment epithelium. *Am J Ophthalmol* 74(2): 206-218.

Shapiro, SD, Kobayashi, DK, Welgus, HG (1992) Identification of TIMP-2 in human alveolar macrophages. Regulation of biosynthesis is opposite to that of metalloproteinases and TIMP-1. *J Biol Chem* 267(20): 13890-13894.

Sheraidah, G, Steinmetz, R, Maguire, J, Pauleikhoff, D, Marshall, J, Bird, AC (1993) Correlation between lipids extracted from Bruch's membrane and age. *Ophthalmology* 100(1): 47-51.

Shichi, H (1969) Microsomal electron transfer system of bovine retinal pigment epithelium. *Exp Eye Res* 8(1): 60-68.

Shimajiri, S, Arima, N, Tanimoto, A, Murata, Y, Hamada, T, Wang, KY, Sasaguri, Y (1999) Shortened microsatellite d(CA)21 sequence down-regulates promoter activity of matrix metalloproteinase 9 gene. *FEBS Lett* 455(1-2): 70-74.

Smine, A, Plantner, JJ (1997) Membrane type-1 matrix metalloproteinase in human ocular tissues. *Curr Eye Res* 16(9): 925-929.

Solomon, A, Akabayov, B, Frenkel, A, Milla, ME, Sagi, I (2007) Key feature of the catalytic cycle of TNF-alpha converting enzyme involves communication between distal protein sites and the enzyme catalytic core. *Proc Natl Acad Sci U S A* 104(12): 4931-4936.

Sottile, J, Mann, DM, Diemer, V, Millis, AJ (1989) Regulation of collagenase and collagenase mRNA production in early- and late-passage human diploid fibroblasts. *J Cell Physiol* 138(2): 281-290.

Sperti, G, van Leeuwen, RT, Quax, PH, Maseri, A, Kluft, C (1992) Cultured rat aortic vascular smooth muscle cells digest naturally produced extracellular matrix. Involvement of plasminogen-dependent and plasminogen-independent pathways. *Circ Res* 71(2): 385-392.

Starita, C, Hussain, AA, Pagliarini, S, Marshall, J (1996) Hydrodynamics of ageing Bruch's membrane: implications for macular disease. *Exp Eye Res* 62(5): 565-572.

Starita, C, Hussain, AA, Patmore, A, Marshall, J (1997) Localization of the site of major resistance to fluid transport in Bruch's membrane. *Invest Ophthalmol Vis Sci* 38(3): 762-767.

Steinmetz, RL, Haimovici, R, Jubb, C, Fitzke, FW, Bird, AC (1993) Symptomatic abnormalities of dark adaptation in patients with age-related Bruch's membrane change. *Br J Ophthalmol* 77(9): 549-554.

Steinmetz, RL, Polkinghorne, PC, Fitzke, FW, Kemp, CM, Bird, AC (1992) Abnormal dark adaptation and rhodopsin kinetics in Sorsby's fundus dystrophy. *Invest Ophthalmol Vis Sci* 33(5): 1633-1636.

Stricklin, GP, Welgus, HG (1983) Human skin fibroblast collagenase inhibitor. Purification and biochemical characterization. *J Biol Chem* 258(20): 12252-12258.

Strongin, AY, Collier, I, Bannikov, G, Marmer, BL, Grant, GA, Goldberg, GI (1995) Mechanism of cell surface activation of 72-kDa type IV collagenase. Isolation of the activated form of the membrane metalloprotease. *J Biol Chem* 270(10): 5331-5338.

Sundelin, S, Wihlmark, U, Nilsson, SE, Brunk, UT (1998) Lipofuscin accumulation in cultured retinal pigment epithelial cells reduces their phagocytic capacity. *Curr Eye Res* 17(8): 851-857.

Sunness, JS, Johnson, MA, Massof, RW, Marcus, S (1988) Retinal sensitivity over drusen and nondrusen areas. A study using fundus perimetry. *Arch Ophthalmol* 106(8): 1081-1084.

Tam, EM, Moore, TR, Butler, GS, Overall, CM (2004) Characterization of the distinct collagen binding, helicase and cleavage mechanisms of matrix metalloproteinase 2 and 14 (gelatinase A and MT1-MMP): the differential roles of the MMP hemopexin c domains and the MMP-2 fibronectin type II modules in collagen triple helicase activities. *J Biol Chem* 279(41): 43336-43344.

Taniquchi, Y (1976) Ultrastructure of newly formed vessels in diabetic retinopathy. *Jap J Ophthalmol* 20: 19-31.

Thakkinstian, A, Bowe, S, McEvoy, M, Smith, W, Attia, J (2006) Association between apolipoprotein E polymorphisms and age-related macular degeneration: A HuGE review and meta-analysis. *Am J Epidemiol* 164(9): 813-822.

Tian, SF, Toda, S, Higashino, H, Matsumura, S (1996) Glycation decreases the stability of the triple-helical strands of fibrous collagen against proteolytic degradation by pepsin in a specific temperature range. *J Biochem* 120(6): 1153-1162.

To, CH, Hodson, SA (1998) The glucose transport in retinal pigment epithelium is via passive facilitated diffusion. *Comp Biochem Physiol A Mol Integr Physiol* 121(4): 441-444.

Toris, CB, Pederson, JE, Tsuboi, S, Gregerson, DS, Rice, TJ (1990) Extravascular albumin concentration of the uvea. *Invest Ophthalmol Vis Sci* 31(1): 43-53.

Tornquist, P, Alm, A (1979) Retinal and choroidal contribution to retinal metabolism in vivo. A study in pigs. *Acta Physiol Scand* 106(3): 351-357.

Tougu, V, Karafin, A, Zovo, K, Chung, RS, Howells, C, West, AK, Palumaa, P (2009) Zn(II)- and Cu(II)-induced non-fibrillar aggregates of amyloid-beta (1-42) peptide are transformed to amyloid fibrils, both spontaneously and under the influence of metal chelators. *J Neurochem* 110(6): 1784-1795.

Tremble, P, Chiquet-Ehrismann, R, Werb, Z (1994) The extracellular matrix ligands fibronectin and tenascin collaborate in regulating collagenase gene expression in fibroblasts. *Mol Biol Cell* 5(4): 439-453.

Tserentsoodol, N, Gordiyenko, NV, Pascual, I, Lee, JW, Fliesler, SJ, Rodriguez, IR (2006) Intraretinal lipid transport is dependent on high density lipoprotein-like particles and class B scavenger receptors. *Mol Vis* 12: 1319-1333.

Tsuboi, S (1987) Measurement of the volume flow and hydraulic conductivity across the isolated dog retinal pigment epithelium. *Invest Ophthalmol Vis Sci* 28(11): 1776-1782.

Tsuboi, S, Pederson, JE (1988) Effect of plasma osmolality and intraocular pressure on fluid movement across the blood-retinal barrier. *Invest Ophthalmol Vis Sci* 29(11): 1747-1749.

Ugarte, M, Osborne, NN (2001) Zinc in the retina. *Prog Neurobiol* 64(3): 219-249.

Vaday, GG, Lider, O (2000) Extracellular matrix moieties, cytokines, and enzymes: dynamic effects on immune cell behavior and inflammation. *J Leukoc Biol* 67(2): 149-159.

Van den Steen, PE, Van Aelst, I, Hvidberg, V, Piccard, H, Fiten, P, Jacobsen, C, Moestrup, SK, Fry, S, Royle, L, Wormald, MR, Wallis, R, Rudd, PM, Dwek, RA, Opdenakker, G (2006) The hemopexin and O-glycosylated domains tune gelatinase B/MMP-9 bioavailability via inhibition and binding to cargo receptors. *J Biol Chem* 281(27): 18626-18637.

van der Schaft, TL, de Bruijn, WC, Mooy, CM, Ketelaars, DA, de Jong, PT (1991) Is basal laminar deposit unique for age-related macular degeneration? *Arch Ophthalmol* 109(3): 420-425.

van der Schaft, TL, Mooy, CM, de Bruijn, WC, Oron, FG, Mulder, PG, de Jong, PT (1992) Histologic features of the early stages of age-related macular degeneration. A statistical analysis. *Ophthalmology* 99(2): 278-286.

Van Wart, HE, Birkedal-Hansen, H (1990) The cysteine switch: a principle of regulation of metalloproteinase activity with potential applicability to the entire matrix metalloproteinase gene family. *Proc Natl Acad Sci U S A* 87(14): 5578-5582.

VanNewkirk, MR, Nanjan, MB, Wang, JJ, Mitchell, P, Taylor, HR, McCarty, CA (2000) The prevalence of age-related maculopathy: the visual impairment project. *Ophthalmology* 107(8): 1593-1600.

Vater, CA, Harris, ED, Jr., Siegel, RC (1979) Native cross-links in collagen fibrils induce resistance to human synovial collagenase. *Biochem J* 181(3): 639-645.

Vranka, JA, Johnson, E, Zhu, X, Shepardson, A, Alexander, JP, Bradley, JM, Wirtz, MK, Weleber, RG, Klein, ML, Acott, TS (1997) Discrete expression and distribution pattern of TIMP-3 in the human retina and choroid. *Curr Eye Res* 16(2): 102-110.

Warburg, O (1927) Uber die Klassifizierung tierischer Gerwbe nach ihrem Stoffwechsel. *Biochem Z* 184: 484.

Weber, BH, Vogt, G, Pruett, RC, Stohr, H, Felbor, U (1994) Mutations in the tissue inhibitor of metalloproteinases-3 (TIMP3) in patients with Sorsby's fundus dystrophy. *Nat Genet* 8(4): 352-356.

Wendt, RP, Klein, E, Bresler, EH, Holland, FF, Serind, RM, Villa, H (1979) Sieving properties of hemodialysis membranes. *J membr Sci* 5: 23-49.

Wiegand, RD, Giusto, NM, Rapp, LM, Anderson, RE (1983) Evidence for rod outer segment lipid peroxidation following constant illumination of the rat retina. *Invest Ophthalmol Vis Sci* 24(10): 1433-1435.

Wight, TN, Mecham, RP (1987) *Biology of Proteoglycans*. Academic Press: Orlando.

Wilcox, DK (1988) Vectorial accumulation of cathepsin D in retinal pigmented epithelium: effects of age. *Invest Ophthalmol Vis Sci* 29(8): 1205-1212.

Williams, JC, Jr., Mark, LA, Eichholtz, S (1998) Partition and permeation of dextran in polyacrylamide gel. *Biophys J* 75(1): 493-502.

Wilson, TM, Strang, R, Wallace, J, Horton, PW, Johnson, NF (1973) The measurement of the choroidal blood flow in the rabbit using 85-krypton. *Exp Eye Res* 16(6): 421-425.

Winkler, BS (1983) The intermediary metabolism of the retina: Biochemical and functional aspects. *American Academy of Ophthalmology*: 227.

Witz, G (1989) Biological interactions of alpha,beta-unsaturated aldehydes. *Free Radic Biol Med* 7(3): 333-349.

Woessner, JF, Jr. (1991) Matrix metalloproteinases and their inhibitors in connective tissue remodeling. *FASEB J* 5(8): 2145-2154.

Yau, KW, Baylor, DA (1989) Cyclic GMP-activated conductance of retinal photoreceptor cells. *Annu Rev Neurosci* 12: 289-327.

Ye, S (2000) Polymorphism in matrix metalloproteinase gene promoters: implication in regulation of gene expression and susceptibility of various diseases. *Matrix Biol* 19(7): 623-629.

Yefimova, MG, Jeanny, JC, Guillonneau, X, Keller, N, Nguyen-Legros, J, Sergeant, C, Guillou, F, Courtois, Y (2000) Iron, ferritin, transferrin, and transferrin receptor in the adult rat retina. *Invest Ophthalmol Vis Sci* 41(8): 2343-2351.

Young, RW (1982) The Bowman Lecture, 1982. Biological Renewal. Applications to the eye. *Trans Ophthalmol Soc U K* 102 (Pt 1): 42-75.

Young, RW (1976) Visual cells and the concept of renewal. *Invest Ophthalmol Vis Sci* 15(9): 700-725.

Zeng, G, Millis, AJ (1994) Expression of 72-kDa gelatinase and TIMP-2 in early and late passage human fibroblasts. *Exp Cell Res* 213(1): 148-155.